1992

Implementation of a mesoscale boundary layer wind model in the San Francisco Bay Area

Allen Jacob Becker
San Jose State University

Order Number 1348650

Implementation of a mesoscale boundary layer wind model in the San Francisco Bay Area

Becker, Allen Jacob, M.S.

San Jose State University, 1992

U·M·I

300 N. Zeeb Rd.
Ann Arbor, MI 48106

IMPLEMENTATION OF A MESOSCALE BOUNDARY LAYER WIND MODEL IN THE SAN FRANCISCO BAY AREA

A Thesis

Presented to

the Faculty of the Department of Meteorology

San Jose State University

In Partial Fulfillment

of the Requirements for the Degree

Master of Science

By

Allen Jacob Becker

May, 1992

APPROVED FOR THE DEPARTMENT OF METEOROLOGY

Alison F. C. Bridger

Alison F. C. Bridger

Francis L. Ludwig

Douglas M. Sinton

Douglas Sinton

APPROVED FOR THE UNIVERSITY

M. Lou Lewandowski

ABSTRACT

IMPLEMENTATION OF A MESOSCALE BOUNDARY LAYER
WIND MODEL IN THE SAN FRANCISCO BAY AREA

by Allen J. Becker

A mass consistent boundary layer wind flow model, named "Winds on Critical Streamline Surfaces" (WOCSS; Ludwig and Endlich, 1988), has been modified and extensively tested. Large observational data sets from the Bay Area Air Quality Management District and from an earlier field study of the marine atmospheric boundary layer were used to test model performance.

Real-time data was used to test the model for a variety of synoptic situations. WOCSS reproduces observed winds well, especially in stronger flow situations. Inversion topography data for the San Francisco Bay Area was incorporated into WOCSS, resulting in increased accuracy over higher terrain. The nested grid provisions in the model have been tested for the first time to address some problems noted by Tredo (1987), and also to focus on local, operationally significant areas. The nested grid feature is of limited utility; better results will be attained with increased model resolution.

Graphics routines have been developed to produce model output in the form of vector wind fields on either horizontal or flow-following surfaces, as well as isopleths of horizontal and vertical wind components.

ACKNOWLEDGMENTS

The author wishes to thank Alison F. C. Bridger for her patient help and valuable consultation throughout the course of this research. The generous advice and guidance from Francis L. Ludwig, Roy M. Endlich, Peter F. Lester, and Douglas Sinton are also greatly appreciated. Thanks also go to Bryan Logie for his assistance in reducing important data from the MABLES - WC project.

TABLE OF CONTENTS

TABLE OF CONTENTS
(continued)

LIST OF FIGURES

LIST OF TABLES

1. INTRODUCTION

The need for accurate boundary layer wind data is well established. For example, short range forecasting (nowcasting) depends on the ability to understand complex mesoscale wind circulations (McGinley, 1986; Mass and Dempsey, 1985). Detailed knowledge of the wind field enables real-time assessment of pollutant transport and diffusion (Anderson, 1971; Thuillier, 1987). An important example concerns the ability to respond rapidly and effectively to a radioactive release (Thuillier, 1987). Fire weather prediction requires accurate and rapid depiction of air flow over complex terrain. Other examples include forecasting for aviation terminals, military operations, oil spills, ice floe motions, and quantitative precipitation forecasting (Danard, 1977; Cionco, 1985; Ludwig, 1986).

The detailed description of a mesoscale wind field ideally requires a dense network of wind observation sites. Typically, however, wind reports are sparse, especially in regions where terrain is most complex. For applications such as those mentioned above, it is no longer sufficient to characterize airflow in the boundary layer with simple subjective analysis techniques using sparse observations.

In the last decade, mesoscale meteorological modelling schemes have made significant progress in providing improved analyses of local and regional wind flow patterns. These

models range in sophistication from complicated synoptic- and large-scale prognostic models, to simple diagnostic interpolation schemes. The large-scale prognostic models, however, cannot effectively resolve mesoscale circulations with sufficient temporal and spatial accuracy due to the enormous computing resources required. This problem can be overcome with prognostic limited-area mesoscale models. For example, Pielke (1974) used two- and three-dimensional primitive equation models to study the sea-breeze problem. These models adequately simulated the flow over south Florida, and predicted the locations of thunderstorm activity. He concluded that the three-dimensional model works best in fully simulating the sea-breeze. This class of model simulates the flow in complex terrain satisfactorily, but requires detailed input data (usually difficult to obtain) and large computing resources.

In order to circumvent the prohibitive computational requirements of the more sophisticated models, simplified diagnostic and prognostic models have become increasingly available in the last two decades. An example is the one-layer primitive equation model by Danard (1977) which divides the PBL into four sub-layers: a surface layer of constant stress, a well-mixed boundary layer (where mass is conserved), an inversion layer, and a free atmosphere above. Danard applied this model to the Juan de Fuca Straight area to study orographic channelling and sea-breeze circulations.

Compared to simpler models, there was a 10°-15° reduction in the difference between observed and computed winds.

A similar approach involves a one-level sigma-coordinate model developed by Mass and Dempsey (1985) which is suitable for diagnosing and forecasting surface winds in regions of complex terrain. This model incorporates parameterized diabatic forcing and boundary layer friction, but is not mass-conservative. It requires only modest computer time and limited initial data (e.g., 850 mb heights and temperatures, and the lapse rate at a single location). With isolated exceptions, Mass and Dempsey found very close correlation between calculated and observed wind patterns.

A third type of simplified model utilizes the principle of mass conservation (i.e., nondivergence) to deduce flow patterns in the lower atmosphere. Observed winds are interpolated to a two- or three-dimensional grid using an interpolation scheme (e.g., Cressman, 1959). The winds are then adjusted to fulfill the constraint of mass continuity. This adjustment has been shown to substantially improve the accuracy of the model wind field (Nitz, et al., 1985b). Physical processes such as nonlinear advection, diabatic forcing and adiabatic temperature change can only be included implicitly through the observed data. Therefore, in a region of strong gradients and sparse data, a mass-conservative model may not be very reliable. This type of

model does, however, have the advantage of requiring very modest computer resources and minimal input data.

Pielke (1984) emphasized that mass-conserving diagnostic models are very economical and effective in the analysis of mesoscale wind fields. He specified the following conditions for maximum model performance: 1) the terrain must provide the dominant forcing; 2) below the highest terrain, a strong, well-defined inversion should exist at the top of the boundary layer; and 3) sufficient observations should be available for model input. The San Francisco Bay Area (SFBA) satisfies these model requirements.

Early mass-conserving models required only surface temperature distribution and topography data (Anderson, 1971). Dickerson (1978) developed a mass-conserving model to provide input winds for air pollution models in the San Francisco Bay Area. The model requires the inversion base height (at one location) and mean winds within the mixed layer. Since observed data alone can induce erroneous mass loss or gain, Dickerson's model adjusts the product of the mean wind and inversion base height in such a way that the mass is conserved while observed data are changed only minimally. The model allows for flow around obstacles which protrude through the inversion base. Sherman (1978) designed a similar mass-conserving model to assess the regional environmental effects of toxic atmospheric

releases. This model produced winds which were input to a pollutant transport model. Sherman found that explicit incorporation of terrain significantly improved the representation of the output wind field.

Ludwig (1985) modified Sherman's handling of irregular terrain by replacing the rectangular coordinate system with terrain-following coordinates, based on the earlier work of Bhumralkar, et al.(1980) and Estoque (1973). Fosberg and Sestak (1986) utilized the new coordinate system, and made improvements allowing for compressible flow and mountain wave activity, making the model suitable for studying severe downslope winds in complex terrain. Fosberg and Sestak's model also used an improved method of interpolation (inverse squared distance) which needs only scattered surface and upper-air reports.

Over the past several years, a mass-conserving model (COMPLEX) was created by Ludwig and Endlich (1987) for use in regions of complex terrain. It requires few surface wind reports, one temperature sounding, and geostrophic winds computed from pressure observations. The Pacific Gas & Electric Co. sponsored the development of this scheme for real-time use at its Diablo Canyon Nuclear Power Plant (Thuillier, 1987; Nitz et al., 1985a, 1985b). COMPLEX calculates nondivergent winds using a procedure that iteratively makes local changes to u and v wind components until divergence is eliminated (Endlich, 1967). Methods for

incorporating the principle of energy conservation into the model were devised and discussed by Ludwig (1985). The methods were intended to account for the changes in potential energy with vertical motion in a stably-stratified atmosphere. In the method implemented by Ludwig (1986), the energy conservation principle determines the degree to which flow surfaces will follow the underlying terrain. The height of a flow surface in the model is the fractional distance between the ground and the top of the boundary layer domain (e.g., Ludwig and Endlich, 1988). The surfaces are generally terrain-following, but are allowed to intersect terrain under stable atmospheric conditions. Model theory is discussed in greater detail in Chapter 2.

COMPLEX has been used to examine the dispersion of pollutants in regions of complex terrain under variable meteorological conditions (Ludwig, 1986). It produces wind fields which can be input into transport and diffusion models, which can then provide estimates of pollutant concentrations.

Erasmus (1986a) applied COMPLEX (Endlich and Lee, 1983) to flow around the island of Oahu, Hawaii. He found that some details of the flow were not well reproduced by the model. For example, flow accelerated over sharply protruding ridges and separated in the lee of these ridges and in steep-sided valleys. Erasmus attempted to overcome these problems by incorporating parameterized surface

roughness, specifying valley flow separation circulations, and calculating an acceleration factor for flow over ridges. Erasmus' improved three-dimensional boundary layer flow model performed best in regions where terrain is most complex, apparently justifying his modifications to the model (Erasmus, 1986b).

Tredo (1987) adapted COMPLEX to run on a microcomputer, and tested the model's ability to reproduce observed winds in the SFBA. He used a large data set for the SFBA gathered during the Marine Atmospheric Boundary Layer Experiments - West Coast; MABLES-WC (Lester, 1979). The model produced wind fields which corresponded well to observations. Tredo (1987) suggested that model performance could be improved by more detailed specification of initial winds in regions of strong wind speed/direction gradients (e.g., the strong convergence zone near Morgan Hill in the southern end of the domain). He also recommended that COMPLEX be revised to accept more than one temperature sounding, especially near coastlines and complex terrain. Finally, Tredo recommended that experiments be conducted for the SFBA using (a) smaller grid-spacing for finer topographic resolution, and (b) the nested grid capabilities for increased wind field resolution.

Muranaka (1988) modified COMPLEX in a study of strong downslope windstorms in southern Alberta. Observations and simulations of such storms indicate that they are driven by

hydrostatic lee waves. Muranaka imposed an upper boundary topography (derived from observations) designed to simulate mountain lee waves. The model produced surface winds which were similar to observed surface winds, with a speed increase beneath the wave trough axis.

Additional modifications and improvements to COMPLEX were recommended by Ludwig and Endlich (1987a). For example, they suggested that the technique used to shape flow surfaces should be empirically adjusted to include the effects of stability. Other suggested improvements involved the way in which the underlying terrain influenced the shape of flow surfaces, and in the interpolation methods used to define the "first guess" wind field. Ludwig and Endlich also recommended that the model make more effective use of input data by using more than one temperature and wind profile. Multiple profiles could be used to calculate flow surface shapes, and would allow a spatially varying wind at the top of the domain (instead of a uniform wind). Finally, they suggested implementing existing provisions for using finer (nested) grids in areas of special interest, where results from a larger grid can be used to obtain first-guess winds for a smaller, nested grid.

Recently, Ludwig and Endlich (1987b) recommended further modifications to COMPLEX, including the use of more observations aloft, and limiting adjustments in the vicinity of observed winds during the mass balancing process. They

suggested testing the model with San Francisco Bay Area data, and adjusting the parameters (discussed more fully below) until the best results are achieved.

Based on the foregoing recommendations, Ludwig and Endlich (1988) developed a new version of the COMPLEX wind code, now named WOCSS (Winds on Critical Streamline Surfaces). WOCSS contains provisions for the inclusion of multiple temperature soundings, for incorporating inversion topography (which would be expected to determine flow surface shapes), and for the inclusion of nested grids. The latter two provisions are discussed in Chapter 4. A large part of the code has been rewritten and reorganized by Ludwig and Endlich (e.g., 1988) in an effort to make it easier for the user to understand and modify. The code is modular, allowing the user to make changes and recompile quickly, so that experimentation is facilitated. With the numerous improvements and modifications to WOCSS, the model is ideally suited for use in nowcasting and testing other wind field analysis applications.

The extensive modifications to WOCSS since the work of Tredo (1987) and Muranaka (1988) have necessitated extensive testing and verification of the model's new capabilities. This is a major goal of the present study. In addition, many of the new features are explored here, including the prescribed inversion topography option, and the nested grid provision. Tredo conducted preliminary tests for the San

Francisco Bay Area using a limited data set. Thorough testing with a richer data set is performed here. Additionally, while Tredo only looked at one common synoptic situation, all basic SFBA synoptic flows are examined here. The current study represents a more systematic testing of the WOCSS model for the San Francisco Bay Area.

The primary objectives of the current research are (1) to test WOCSS as a potential tool for real-time nowcasting in the SFBA, and (2) to conduct tests of the model incorporating Tredo's and Ludwig's recommendations.

The initial goal is to compare the performance of the current version of the WOCSS model to that used by Tredo (1987). Several changes have been made to the code, and, in order to provide confidence in model performance and continuity before more extensive experiments were conducted, comparisons were made between WOCSS and COMPLEX output using the same input data.

The model has no intrinsic graphical display capabilities. Using commercially available software (i.e., PLOT88), model output can now be clearly displayed and analyzed. In addition to the display of a vector wind field on either horizontal or flow surfaces, isopleths of horizontal wind speeds, and wind speed differences from case-to-case are presented.

Using real-time data provided by the Bay Area Air Quality Management District (BAAQMD), the operational

capabilities of the WOCSS model have been explored. BAAQMD data was used both in initializing the model, and in verifying the model output winds. Analyses of the SFBA wind field were made, with subsequent verification to assess accuracy in terms of the degree to which predicted flow field features are reproduced. Model output assessment was achieved by comparing observed winds and model output at eight stations from which data is used to initialize the model (Bethel Island, Napa, Petaluma, Union City, San Jose, San Martin, Benicia, and Oakland; see Appendix A-1 for complete listing). The same assessment was conducted using enhanced data (stations selectively added to the basic eight), and with reduced data (stations selectively deleted). Errors in model output (normal, enhanced, or reduced cases) are defined in two ways: (1) each station's observed wind direction and speed are compared to model output at (or near) that location, and (2) the ensemble average of all station observations are compared to model output averaged at all station locations.

While multiple soundings can provide improved resolution of the inversion and atmospheric conditions in the domain, it would be most desirable to know the actual topography of the inversion (if present). King (1980) pointed out that there are spatial and temporal variations in the height of the inversion base in the SFBA. Miller (1968) noted that a diurnal oscillation in inversion base

height at San Francisco is related to the seabreeze, with a maximum height at 2200 PST and a minimum at 1400 PST. The large height oscillations along the Pacific coast are in response to horizontal divergence and convergence patterns associated with the seabreeze within the marine layer. Based on extensive data gathered during the summers of 1964-66, Miller (1968) described the shape of the inversion in the SFBA as that of "an elongated bowl, with the lowest and most intense portion located near the Bay." Over the Bay, the inversion is lower and more stable, while over the surrounding hills, it is higher and less stable (Lester, 1985). West of the Bay, inversion heights climb gently upward over the ocean (Roope, 1980). Russell and Uthe (1978) produced several maps of mixing depth using a large network of 13 sodars (acoustic radars) in the SFBA, supporting Miller's conclusions about the inversion's structure and fluctuations.

Undoubtedly, the shape of the inversion plays a significant role in determining the distribution of surface winds in the SFBA. This role will be tested and examined using WOCSS and the inversion topography data set gathered during MABLES (which includes gridded inversion heights at 4 km resolution). Model results with and without the specified inversion shape will be compared, especially with respect to the effect of inversion topography on the distribution of surface wind speeds.

WOCSS calculations can be performed on coarse, medium, and fine grids. Each grid is contained completely within the next coarser grid (Ludwig and Endlich, 1988). Thus, coarse grid output can be used as input to the finer grid. The nested grid feature will be tested for special problem areas in the domain. For example, Tredo (1987) noted two areas where model winds poorly represented observed winds: near Morgan Hill and near the Golden Gate (see Fig. 1-1). Nested grids are focused on these areas to investigate the problem and improve model performance. In general, the finer grids could of course be applied in areas of special nowcasting concern (e.g., airports and wind power sites).

The effective implementation of WOCSS to the SFBA as a research and operational analysis tool requires the best available observational data. Therefore, experiments will be conducted to evaluate model performance using two SFBA data sources: (1) real-time data available from the Bay Area Air Quality Management District (BAAQMD) on a day-to-day basis, and (2) data gathered during an extensive observational program carried out in the summer of 1978 (MABLES-WC; Lester, 1979).

Real-time data is available from the BAAQMD on a regular basis, and is accessed through the San Jose State Meteorology Department's weather data network. While the amount of available data varies, it includes reports from a dense network of SFBA stations (including several coastal

stations), and a few wind and temperature profiles. This is discussed in more detail in Chapter 3b. A map of the BAAQMD stations is presented in Figure 1-1.

During the period July 31 - August 17, 1978 an extensive program of observations was conducted along the central California coast. This project, the Marine Atmospheric Boundary Layer Experiments--West Coast (MABLES-WC), resulted in a detailed boundary layer wind data set. This data set was used by Tredo (1987) to verify COMPLEX's ability to reproduce observed winds, and will be used in the current research because of its good quality and location within a complex terrain setting. Included are data from 30 surface observation sites, two vertical wind profile sites, and one temperature sounding site. Inversion base topography from this data has been extracted and has also been used here (discussed in detail in Chapter 4a). A map of the MABLES stations is presented in Figure 1-2. Samples of wind, temperature sounding, and terrain data files are presented in Appendices A-2, A-3, and A-4, respectively.

Sensitivity to model resolution will be examined. Tredo used SFBA terrain data with an 8 km resolution. Finer terrain data is available for this research. It is of 1 km resolution, and spans from west of Moss Landing (UTM {490,4090}) to near Sacramento (UTM {660,4286}). A program was written to read the 1 km resolution terrain dataset and

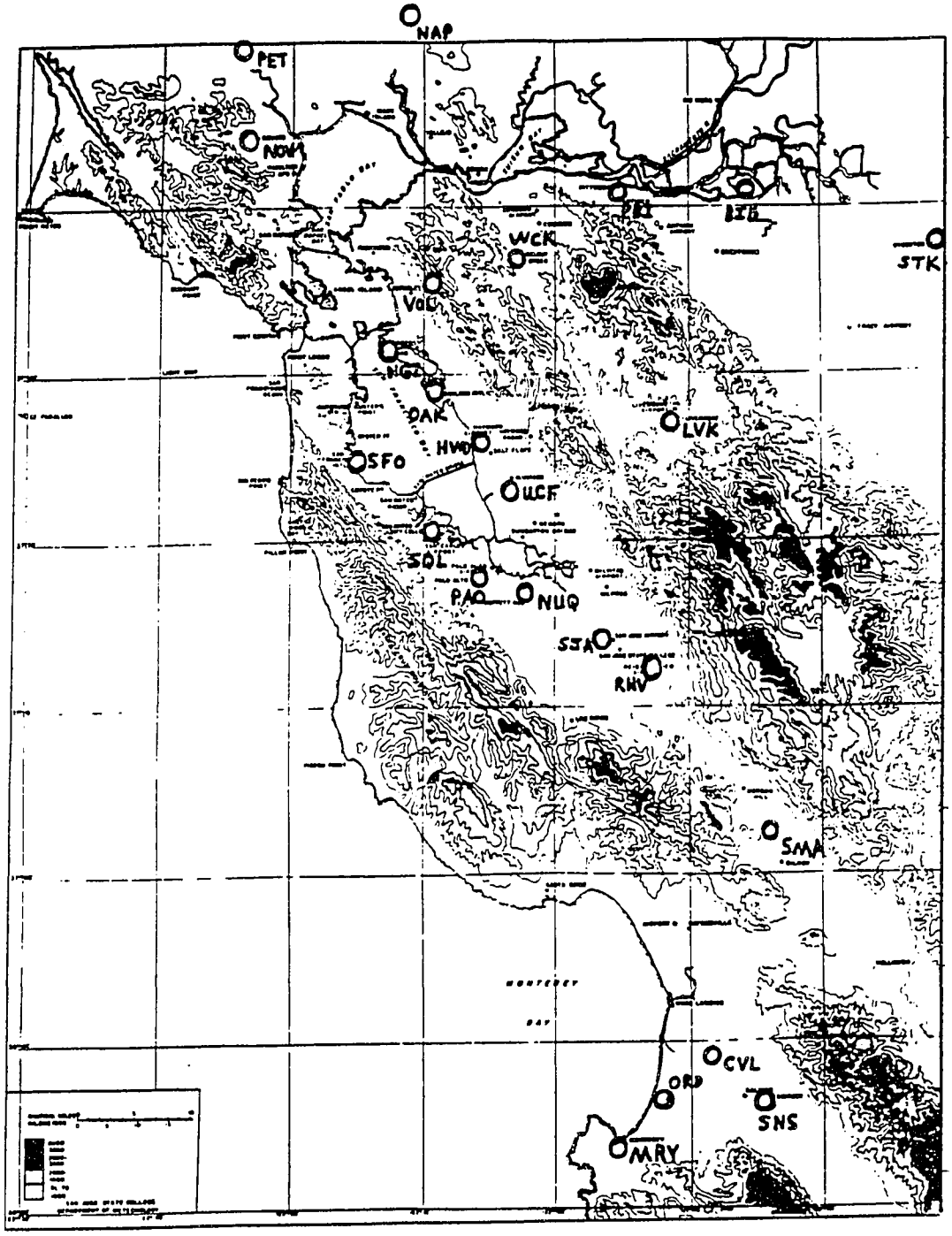

Figure 1-1 Map of Bay Area Air Quality Management District (BAAQMD) stations.

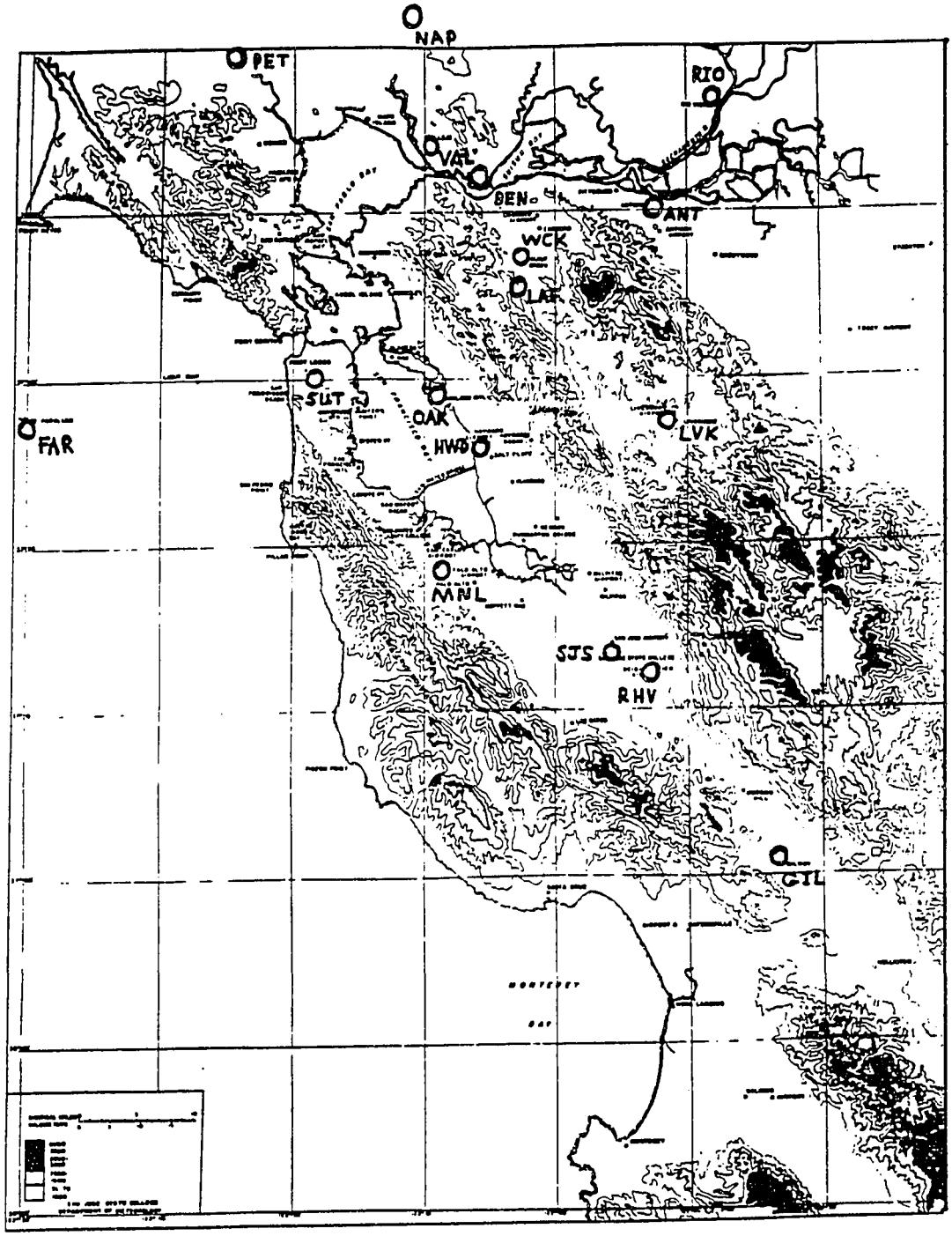

Figure 1-2 Map of Marine Atmospheric Boundary Layer Experiment (MABLES) stations.

create terrain data files covering any desired domain and resolution. The program is listed in Appendix B-1. It creates gridded terrain data for WOCSS at 1 to 10 km resolution, and also creates terrain data to be used with the PLOT88 plotting software.

2. MODEL DESCRIPTION

a. Critical Streamline Concept

When the atmosphere is neutral or unstable, WOCSS assumes that the flow parallels the underlying terrain surface. When the atmosphere is stable, the model employs a critical streamline concept, and assumes that atmospheric processes are adiabatic. The buoyant restoring force acting on a displaced parcel is proportional to the temperature difference between the atmosphere and the parcel, which in turn depends on the environmental lapse rate and parcel displacement distance. Since work is required to move air from its equilibrium position, potential energy is gained by the displaced air. The critical streamline height is the height to which a parcel of air must be lifted so that its initial kinetic energy equals the potential energy gained by the lifting. In the model this is determined by using average wind conditions at the lowest geometric altitudes. If the critical streamline height is lower than the top of a topographic barrier, flow in the model is directed around the obstacle. Otherwise, the air will flow over the obstacle (Ludwig and Endlich, 1988; Ludwig, 1986).

b. Flow Surface Determination

The model's coordinate system is flow-following. The actual configuration of the flow surfaces depends on terrain

variability and the height of the boundary layer top over the lowest terrain elevation (as defined by the user). The vertical domain of the model at this point is divided into several layers (not necessarily of equal depth). The temperature profile and interpolated wind field are then used to determine the critical streamline height for each flow surface; this is the highest elevation of each flow surface above the highest topographical point. The model makes subsequent passes throughout the domain to ensure that each surface does not approach too closely to the next higher surface. The height of each flow surface above the remaining grid points is determined by linear interpolation between the boundary layer top and the terrain. The model allows flow surfaces to intersect terrain, and at these locations the wind is set to zero. Mass conservation then requires flow around the obstacle encountered (see Fig. 2-1 for a depiction of flow surfaces relative to terrain).

A model option allows the user to specify some aspects of the shape of the flow surfaces instead of using the critical streamline formulations. For example, a slope factor specifies the extent to which the boundary layer top follows the shape of the underlying terrain (the factor equals 0 for a horizontal top and 1 for a terrain-following top). The user can adjust this factor so that diurnal stability variations can be accounted for. The boundary layer top can also be given a linear slope, corresponding to

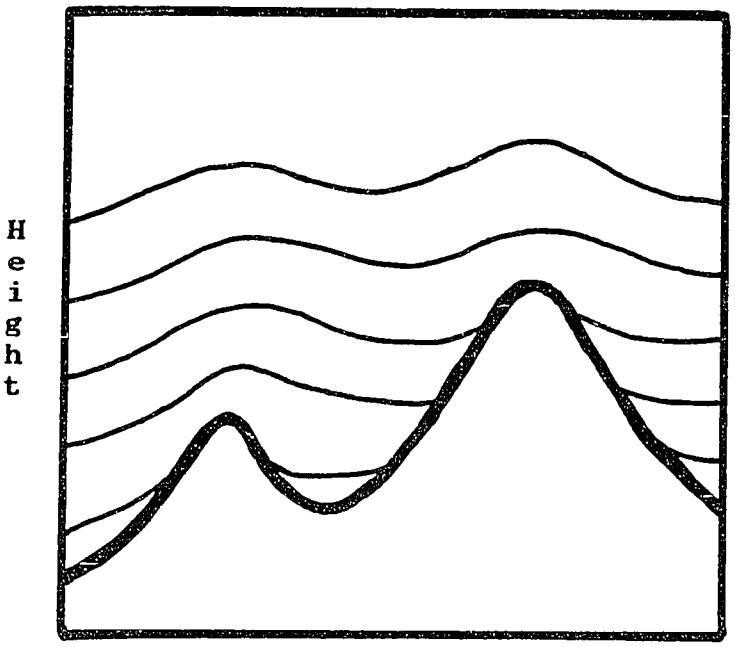

Figure 2-1 Schematic diagram showing flow surfaces (light curves) in the model domain, with the lower surfaces intersecting the higher terrain (heavy curve).

a synoptic gradient (Nitz, et al., 1985b; Ludwig, 1986).

c. Nondivergent Flow Fields and Mass Conservation

The heart of the mass-consistent wind model involves the balancing of mass by reducing the divergence of the wind field as much as possible. After the flow surfaces are determined, the interpolated wind components at each grid point are multiplied by the layer thickness at that point. Divergence of the mass-weighted wind is then reduced iteratively by sequential passes through the grid (Endlich, 1967). Horizontal wind components through the sides of volume elements (Fig. 2-2) are adjusted so that mass inflow balances mass outflow. Each adjustment changes the divergence values for adjacent volume elements. Thus, the procedure must be repeated several times (typically 20-30 iterations) for reduction of divergence to a level within a user-specified limit (Endlich, 1990). There are some situations where divergence cannot be eliminated (e.g., box canyons and convergence zones).

d. Model Operation

When operating the WOCSS model, the user can change various default parameters (e.g., number of grids, grid resolution, number of stations). Topographic and meteorological data are then input. The required data include station locations (UTM coordinates), surface wind

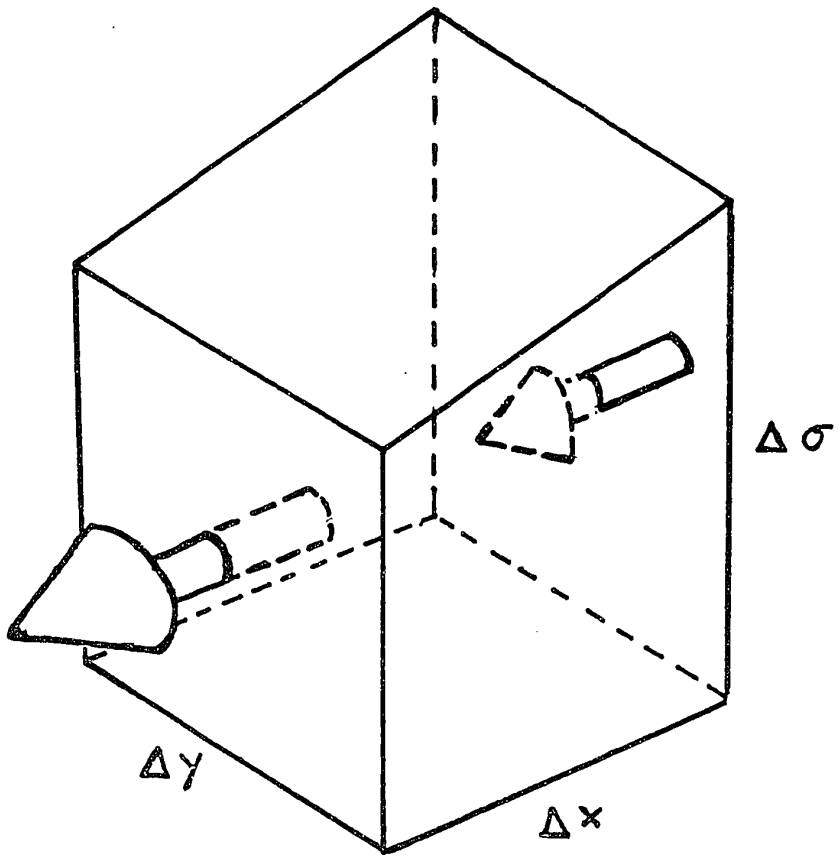

Figure 2-2 A volume element in the grid mesh.

and temperature data, and vertical profiles of wind direction, wind speed, and temperature at one or more locations. The input data is used to obtain a first guess wind field (using a distance-weighted interpolation) for determination of flow surface shapes. The first guess wind field is then adjusted toward mass-consistency (nondivergence), as discussed above. If nested grids are employed, the adjusted wind field is then used to provide a first-guess field for the next smaller grid, where the flow surfaces are again defined and mass-conserving winds attained. Finally, output wind speeds and directions on flow surfaces are used to estimate winds on constant elevation surfaces, and at anemometer level (10 m AGL).

3. ANALYSIS OF MODEL PERFORMANCE IN SAN FRANCISCO BAY AREA CASES

a. Comparison of COMPLEX and WOCSS Model Output

Tredo (1987) used an earlier version of WOCSS known as COMPLEX. The current study in some respects is a continuation and expansion of Tredo's work. Some general comparisons will be made between the two versions of the model, in an attempt to demonstrate the degree of continuity in the model and to verify that WOCSS is working properly. As noted before, Tredo recognized some problems with COMPLEX output in the San Francisco Bay Area. There was a problem with wind directions in Morgan Hill, an area of complex terrain features that tend to induce strong convergence patterns. The west-northwesterly model winds were apparently influenced by the Oakland sounding, and failed to reproduce the observed east-southeasterly winds. To remedy this difficulty near Morgan Hill, Tredo recommended that additional grid points be placed in this area (i.e., using the nested grid provision), and additional neighboring observations be included. Another problem found by Tredo was accelerated winds at isolated grid points located on the highest terrain. Tredo felt that the wind acceleration problem was terrain-induced, and recommended further experimentation.

In order to compare COMPLEX and WOCSS, Tredo's data from 00Z, 10 August, 1978 were used. His original model winds (at 4km resolution, with every other vector plotted)are shown in Fig. 3-1. The same output (using the current plotting scheme) is shown in Fig. 3-2. Throughout this thesis, all wind field plots will show observed winds as bold vectors, and model winds as regularly-spaced light vectors. The winds in Tredo's case were typical of an SFBA summer synoptic situation, with northwesterly winds channelled through valleys. Note the excessive winds on high terrain (for example, at UTM 624,4152).

The same original data were next input to WOCSS. The results are shown in Fig. 3-3. (Note that the domain used here is somewhat expanded over that used by Tredo). It is readily seen that in the new model formulation the excessive accelerations over higher terrain have been eliminated or smoothed. For example, the flow near Mt. Hamilton shows only a slight speed increase over the winds in the Livermore area. The flow appears to be more uniform in speed and direction over a large area, and agreement between observed winds and those modeled by WOCSS is much better than with COMPLEX (e.g., see Travis AFB and San Jose; all station UTM coordinates are listed in Appendix A-1). Fig. 3-4 shows a vector difference plot (Fig. 3-2 minus Fig. 3-3) and illustrates the changes between COMPLEX and WOCSS. The vectors indicate the overall stronger winds modeled by

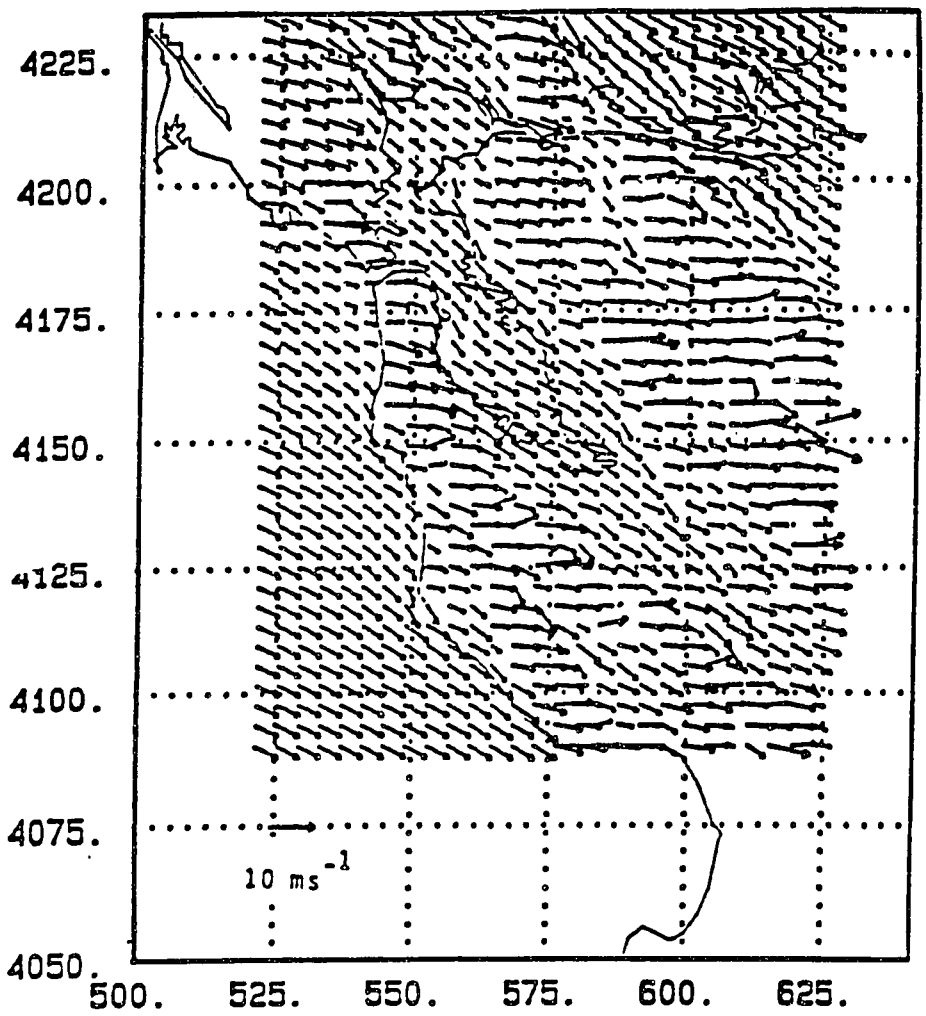

Figure 17c
Sub-set Model Surface Winds
for August 10, 1978, 00 GMT

Figure 3-1 Plot of full-set model surface winds for August 10, 1978, 00 GMT (from Tredo, 1987, using model CMPLX).

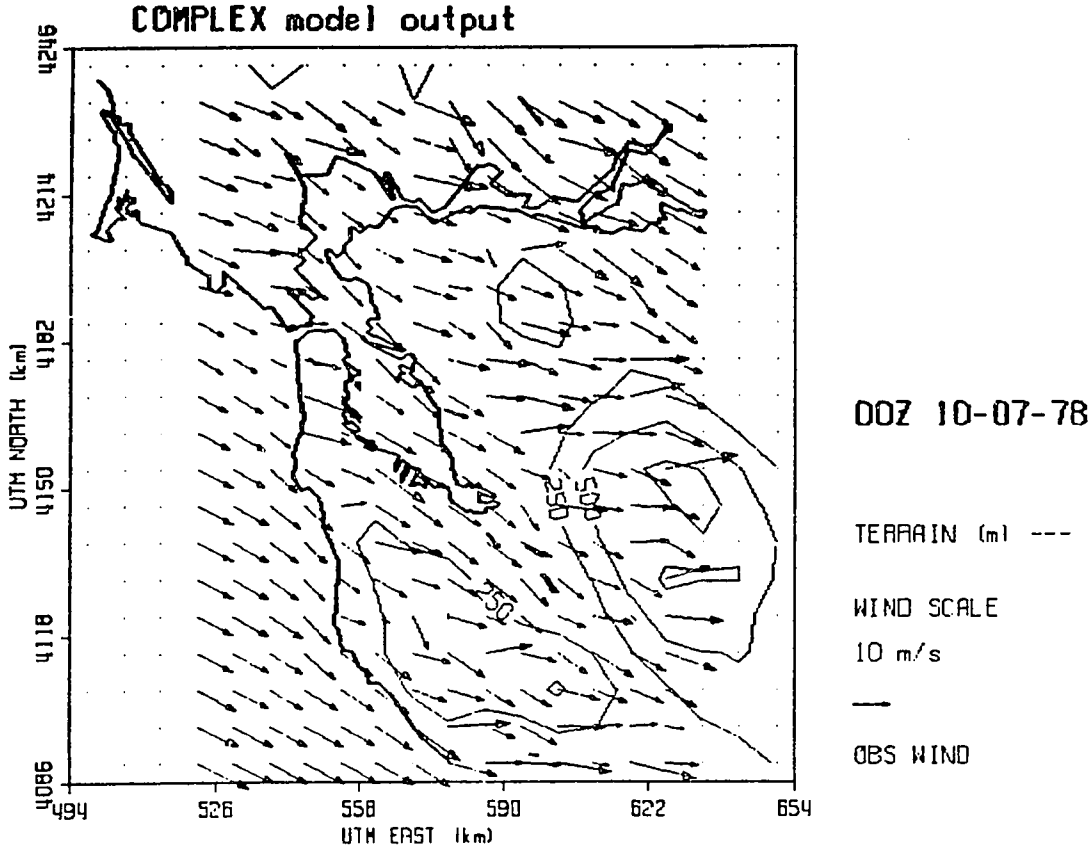

Figure 3-2 Same as Figure 3-1, but using current plotting scheme.

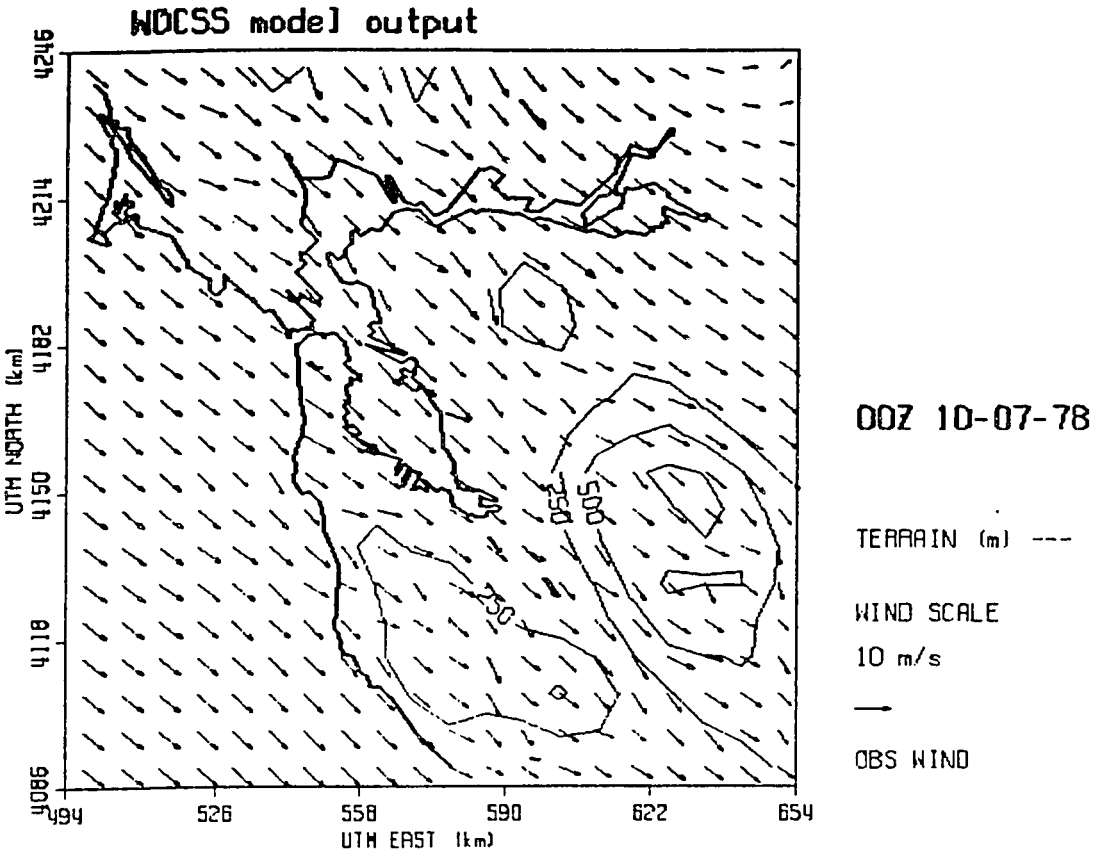

Figure 3-3 Plot of WOCSS model surface winds for August 10, 1978, 00 GMT.

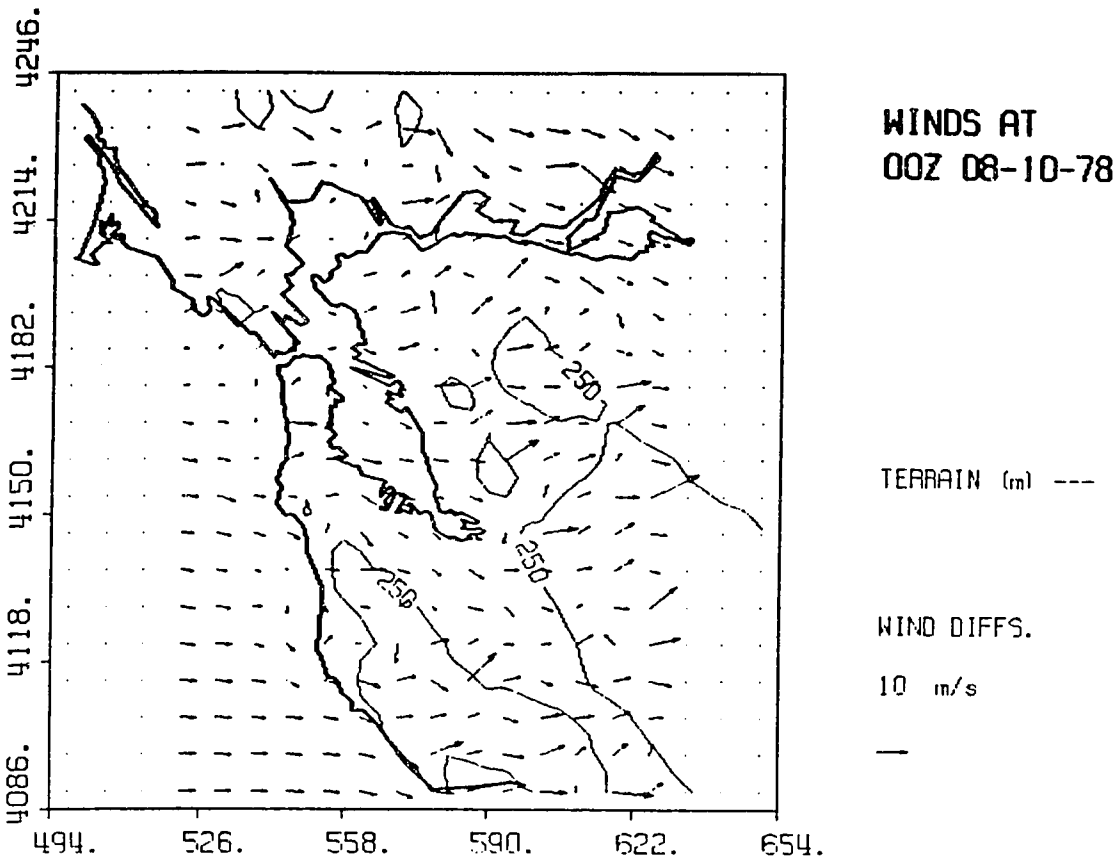

Figure 3-4 Vector difference plot of Figure 3-2 minus Figure 3-3.

COMPLEX (in this and all subsequent vector difference plots, the latter-mentioned run is always subtracted from the former-mentioned run, here COMPLEX minus WOCSS). The speeds in COMPLEX were generally higher by about 5-10 ms^{-1}, except windward of the coastal hills and inland mountains. COMPLEX also exhibits much more flow around terrain barriers. The difference plot clearly shows the irregular accelerations produced by COMPLEX over the higher terrain of the Santa Cruz and Hamilton ranges. Overall, WOCSS output speeds are more uniform and realistic than COMPLEX's.

The original COMPLEX run used observations from a basic set of stations (Travis AFB, Moffett NAS, Oakland Airport, Hayward Airport, San Francisco Airport, San Jose Airport, San Jose State University, Mt. Sutro tower, Salinas Airport, and Sacramento). As mentioned, the model did not produce accurate wind directions in the Morgan Hill area (UTM 620,4115). To explore this problem, data from both Morgan Hill and Gilroy were added to the basic run (Fig. 3-3); the results are shown in Fig. 3-5. Since both of the winds at the additional stations had a southerly component (probably a seabreeze effect from the Monterey Bay), the new run shows a marked directional shift in the southern end of the Santa Clara Valley. This is seen most clearly in Fig. 3-6, a vector difference plot (Fig. 3-3 minus Fig. 3-5); note that the difference vectors have been magnified. The principle

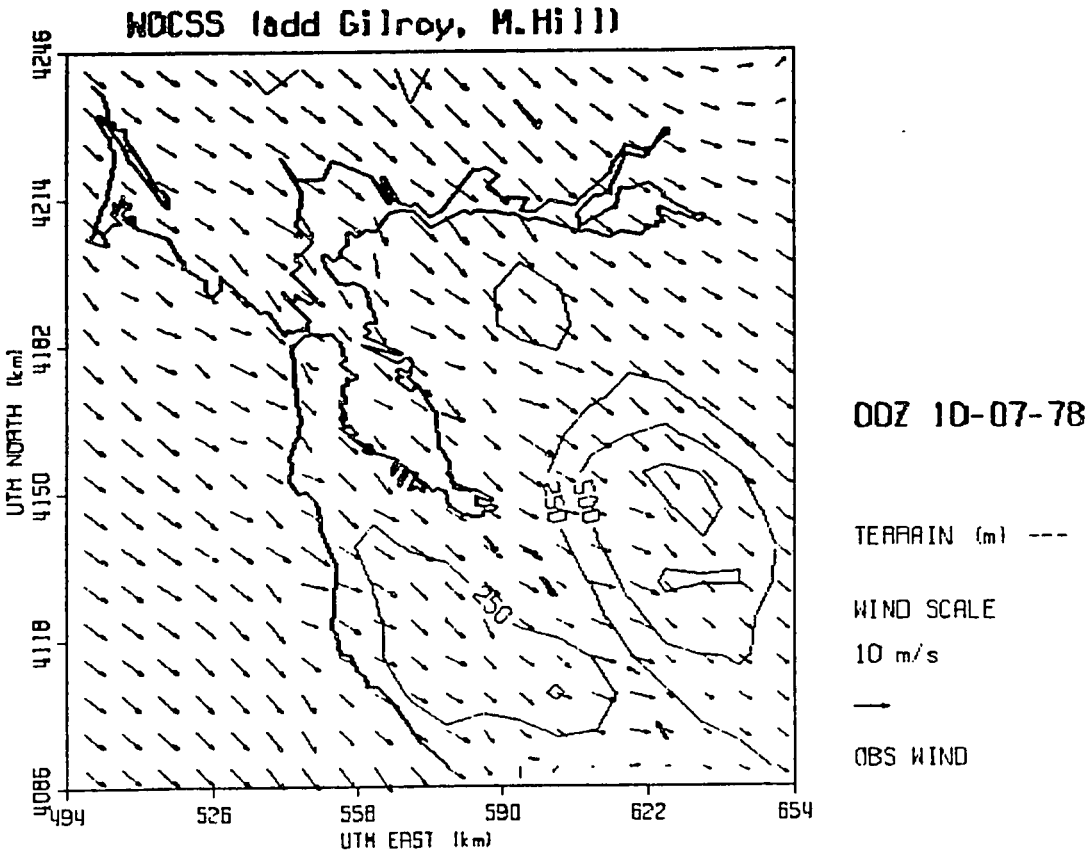

Figure 3-5 Same as Figure 3-3, but with Morgan Hill and Gilroy added to the station data set.

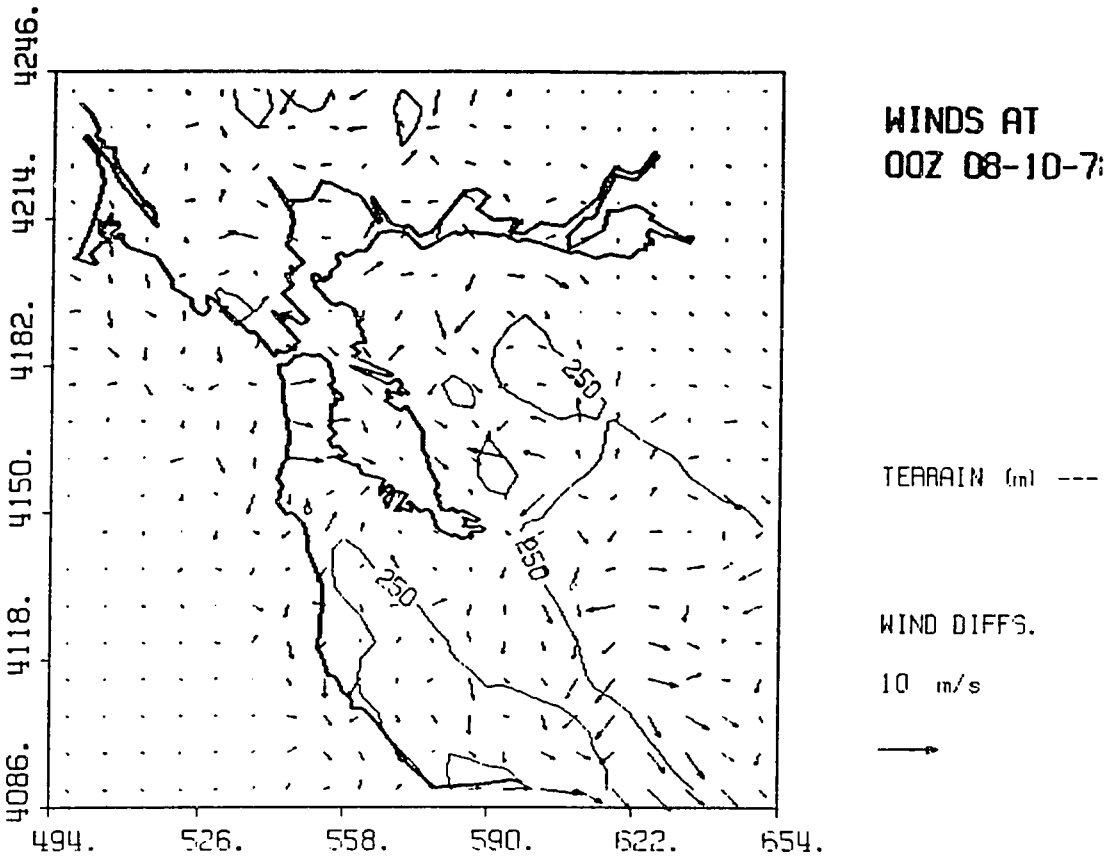

Figure 3-6 Vector difference plot of Figure 3-5 minus Figure 3-2.

effects are limited to the Morgan Hill valley area, although some effects are noted throughout the model domain. The effect on model output of adding the two stations appears to have spread upwind. By adding both Morgan Hill and Gilroy, WOCSS produced much more of the southerly flow that Tredo found to be lacking.

b. **Verification for San Francisco Bay Area under various synoptic conditions**

Introduction

To date, few evaluations of the model's performance and capabilities have appeared in the literature (an earlier incarnation of the model was discussed by Thuillier, 1987). The purpose of the work discussed in this section is to analyze the performance of WOCSS in generating gridded wind data for the SFBA for a variety of synoptic situations. Specifically, the model was run for a number of cases representative of the variety of synoptic flow patterns that characterize the region. In certain runs, one or more additional stations were included in the basic set of available wind observations used to initialize the model, while in other runs a reduced set of the wind data was used. Output winds were then compared with observed winds and also with climatological flow patterns. The purpose of these comparisons was to determine whether additional initial data might improve results, and also whether missing initial data might degrade results. A final test was conducted at 5 km resolution (instead of 8 km) to investigate what effect increased resolution may have on model output.

Description of Experiments

The results of a large number of tests with the model are reported below. These tests were conducted with three

basic goals in mind, and these define the structure of the following three sections. The basic format of each test was as follows: wind and temperature sounding data was available from one site (Oakland) in the domain. Surface wind data were extracted from the seven observing sites operated by the BAAQMD (see Fig. 1-2 for locations), together with the surface winds at Oakland (eight sites total). The only difference from one test to the next was the input wind and temperature data.

Hayes et al. (1984) showed seven surface flow patterns characteristic of the SFBA (Fig. 3-7). The northwesterly flow regimes are typical of summer, and are associated with the offshore Pacific High. This flow is often enhanced during the afternoon by the sea breeze. Southerly and southeasterly flows on the other hand are characteristic of the approach of synoptic storms during winter. The typical synoptic situation associated with each of the basic flow regimes is described in Table 1-1.

Having qualitatively matched flow patterns with synoptic climatology, several months of synoptic charts were examined to find examples of each pattern. Wind and temperature data from the selected dates were then obtained from the BAAQMD, and used for initialization and verification of WOCSS. The synoptic situation for each test is discussed briefly below. Comparisons between model and observed winds are discussed in Chapter 3c.

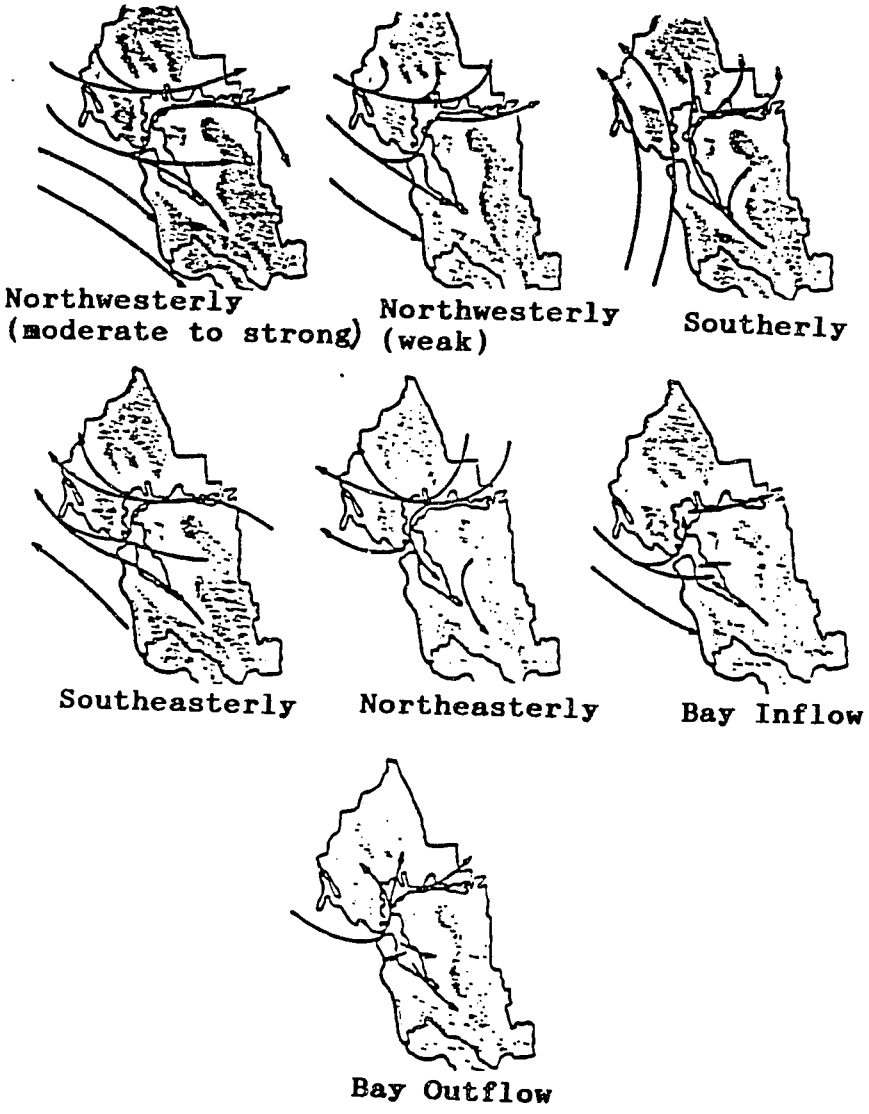

Figure 3-7 San Francisco Bay Area air flow pattern types (from Hayes et al., 1984).

Table 1-1 San Francisco Bay Area air basin flow types and associated typical synoptic situations.

FLOW TYPE	PRIME TIMES OF OCCURRENCE	SYNOPTIC CLIMATOLOGY
NW-Weak	Late nights in Spring, Summer, Fall; Winter afternoons.	Moderate Pacific High, weak interior Low.
NW-Moderate to Strong	Afternoons, especially Spring, Summer, Fall.	Strong Pacific High and interior Low.
Northeast	Winter afternoons (Oct.-April).	Great Basin High and offshore Pressure gradient.
South	Winter and Spring days, especially morning hours.	Synoptic storms, especially those approaching from the WNW.
Southeast	Winter, and Fall mornings.	Synoptic storms, especially those approaching from the WSW.
Bay Outflow	Mid-day throughout the year, especially Fall and Winter (absent in Summer).	Weak synoptic field and regional upslope.
Bay Inflow	Night-time throughout the year, especially Fall and Winter (absent in Summer).	Weak synoptic field and regional drainage.
Calm	Winter and & Fall; mostly at night.	Pressure gradient very weak.

Tests of the model were also conducted for a particular date when surface wind data were available from additional sites in the SFBA. For the case of weak northwesterly flow in particular, more detailed comparisons were made between model and observed winds. The additional input data enabled WOCSS to capture particular flow details, and identify sites where observed wind data may be of greater or lesser value in capturing flow patterns. These tests are discussed in Chapter 3d.

In Chapter 3e the sensitivity of the model to missing input data is discussed. The weak northwesterly flow case was again chosen, but with input data from each (or more) of the eight basic stations sequentially unused.

Finally, Chapter 3f examines the effect that finer resolution may have on model output.

c. Model performance in simulating climatological flow patterns

Northwesterly Flow Patterns

NW - Weak

Figure 3-8 shows the surface winds modeled for this late fall weak northwesterly case. There is a fairly good correspondence between observed and model winds in this case. Exceptions are noted at Napa (UTM 564,4230), where the model winds appear to be driven more by the westerly flow aloft, and not the observed southerly flow up the Napa

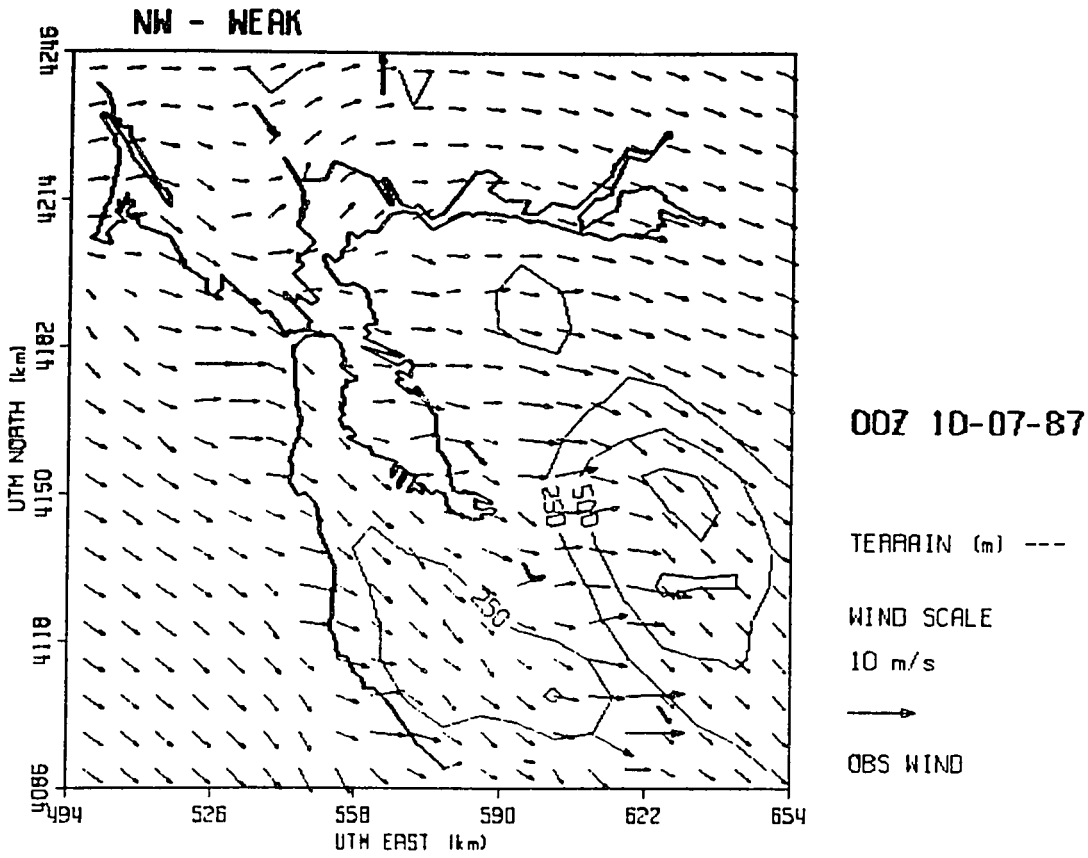

Figure 3-8 Plot of Weak Northwesterly case (October 7, 1987, 00 GMT).

valley. A similar feature is observed at San Jose, where again the observed winds fail to guide the model flow down the Santa Clara valley. Attention is directed to the windward side of elevated terrain, where winds are seen to be somewhat stronger than winds both upstream and downstream. This is due to the effect of the weak inversion (the base of the inversion at Oakland was at 827 feet). An earlier run of this same case, but using an erroneous Oakland sounding (with no inversion) produced a much smoother wind field without noticeable acceleration over the hills (Fig. 3-9). However, the model output speeds shown in Fig. 3-8 are better than those shown in Fig. 3-9. For tabulated comparison of model and observed winds at each station, and between the two runs mentioned, see Tables 3-1 and 3-2, Appendix C. These tables show output from the analysis procedure mentioned in Chapter 1c above (the source code is presented in Appendix B-2). Note that the table shows error percentages, defined as the smallest angle between model and observed winds, divided by 360°.

NW - Moderate

Figure 3-10 shows the surface winds for a case of moderate springtime northwesterly flow following the passage of a cold front. Notable features are the westerly flows at both Napa and Petaluma, again apparently responding to the flow aloft (as opposed to the observations). San Jose shows good agreement between model and observed winds, and a

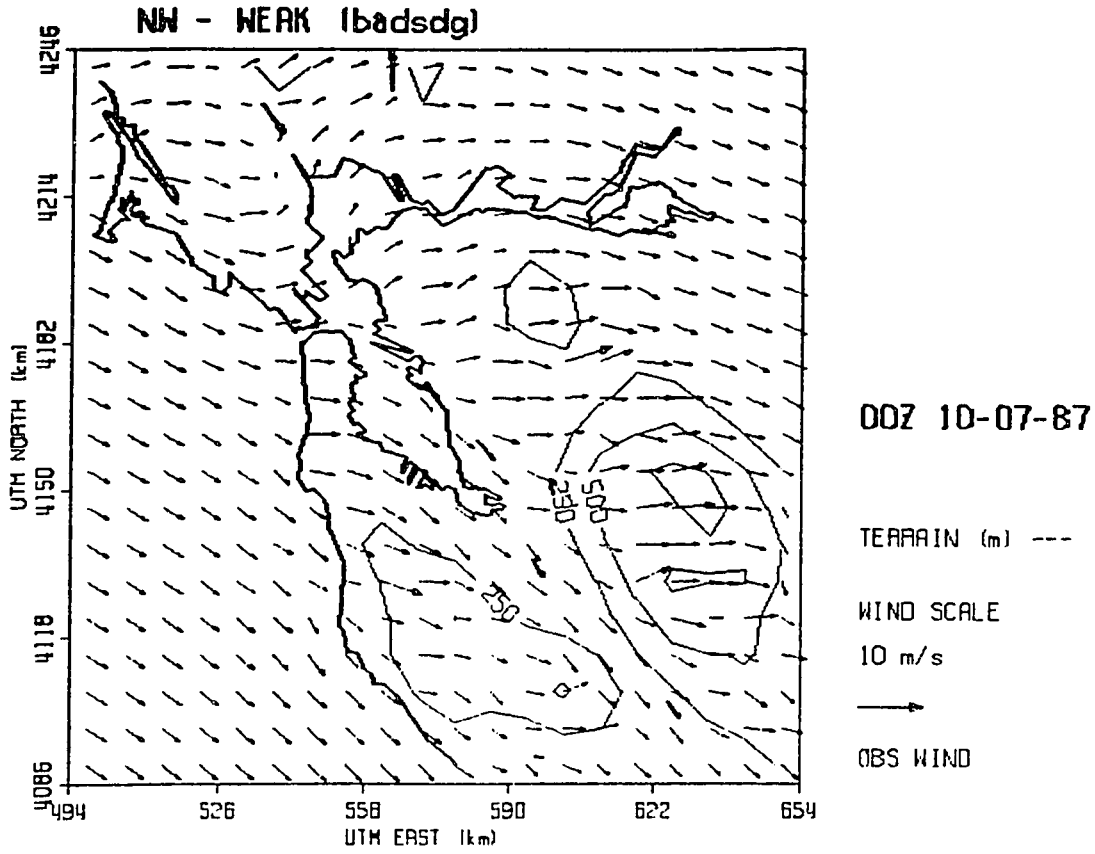

Figure 3-9 Same as Figure 3-8, but with erroneous Oakland sounding.

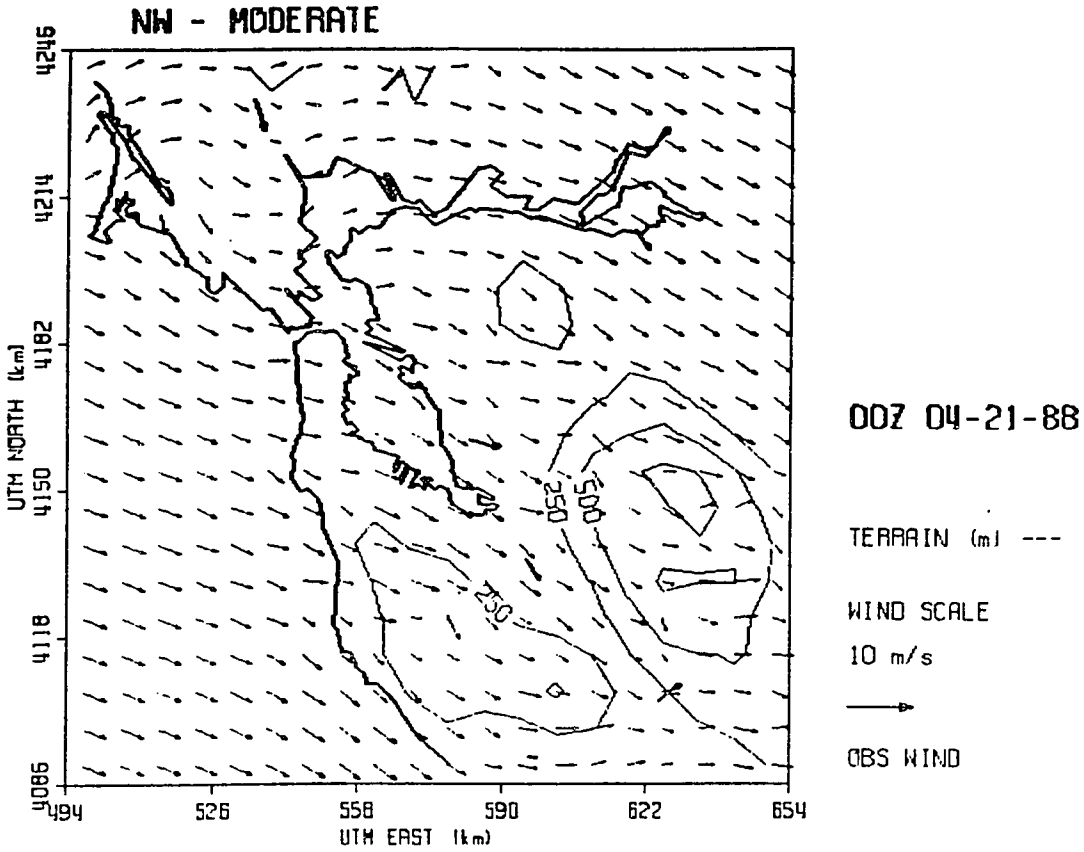

Figure 3-10 Plot of Moderate Northwesterly case (April 21, 1988, 00 GMT).

distinct flow is observed down the Santa Clara valley. However, San Martin's (UTM 625,4104) model wind (westerly) seems to be more influenced by the prevailing upstream flow than by the southwesterly winds observed. In general, the model does well in capturing observed flow details. For tabulated comparison of model and observed winds at each station, see Table 3-3, Appendix C.

NW - Strong

Figure 3-11 shows the surface winds for this strong northwesterly flow situation in late fall, again after the passage of a cold front. Observed and model winds are in exceptionally close agreement. Model speeds are 0.5% faster (on average) than observed wind speeds. See Table 3-4, Appendix C for tabulated comparison of model and observed winds at each station.

These three northwesterly cases suggest that the model is more accurate in response to a stronger flow pattern. However, the moderate flow case produced the worst model/observed speed ratio. The wind directions for the moderate and strong cases show excellent agreement between model and observations.

Northeasterly Flow Patterns

WOCSS was tested with a northeasterly flow condition. This flow pattern in the SFBA is typically associated with a surface high pressure area located northeast of the area,

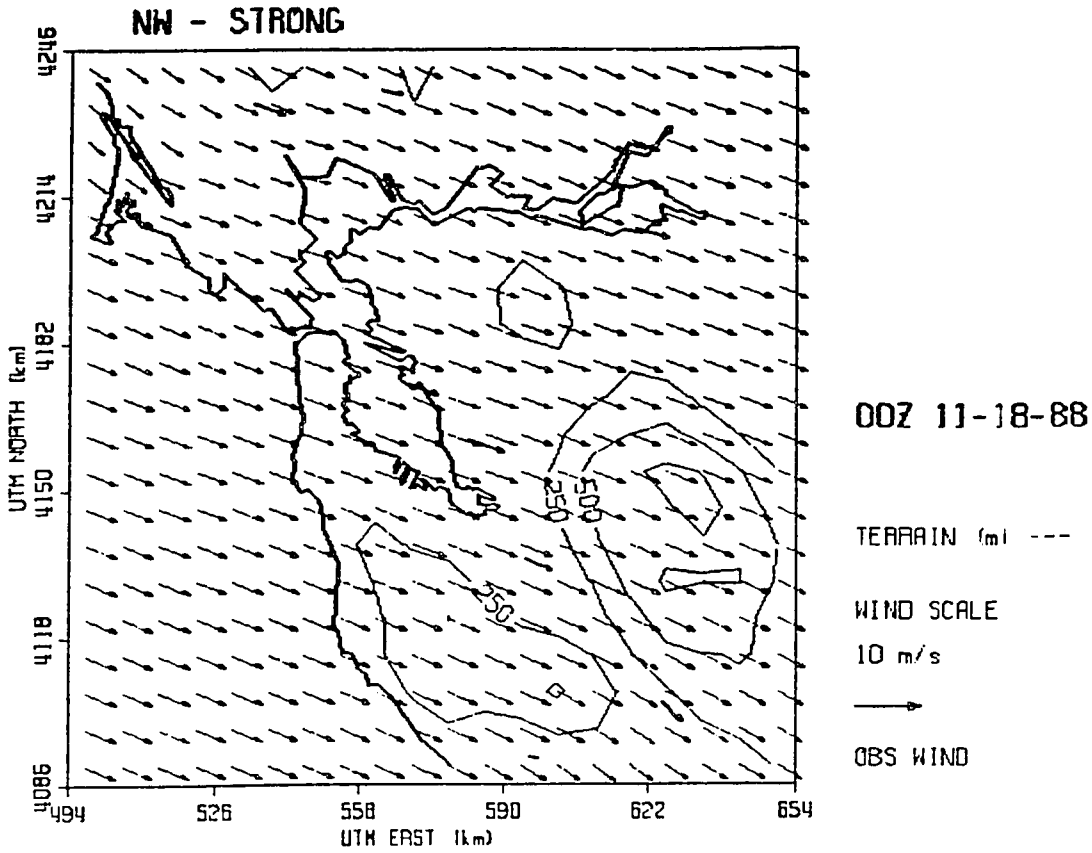

Figure 3-11 Plot of Strong Northwesterly case (November 18, 1988, 00 GMT).

with resulting offshore flow. The same conditions are often associated with the Santa Ana in Southern California.

Surface winds produced by the model for this case are shown in Fig. 3-12. In this run, additional observing sites were available and used (20 total) so that many smaller-scale flow features are discernible. Observed flow is fairly weak throughout the SFBA, with wind speeds at several of the stations under 4 ms^{-1}. Flow produced by WOCSS is also weak, with northeasterly flow through the center of the region. The offshore flow is disturbed in the vicinity of the Golden Gate. A closer inspection of the observed winds reveals that Vollmer Peak (in the Berkeley hills -- see Fig. 1-1 for location map) was reporting a wind directly opposed to the general flow. Vollmer Peak's elevation is 1906 feet MSL, and it is likely that it is capturing a return flow, or in any case is not representative of the boundary layer flow regime over the greater SFBA. Otherwise, model and observed winds are in good agreement. See Table 3-5 in Appendix C for a tabulated comparison.

The above discussion led to a test of the same case, but with Vollmer Peak data suppressed. The results show a dramatic improvement in the wind flow through the Golden Gate gap, now in good agreement with observations in that area (Fig. 3-13). Table 3-6 in Appendix C shows a marked improvement in the performance of the modeled wind speeds at several locations. These results suggest that including

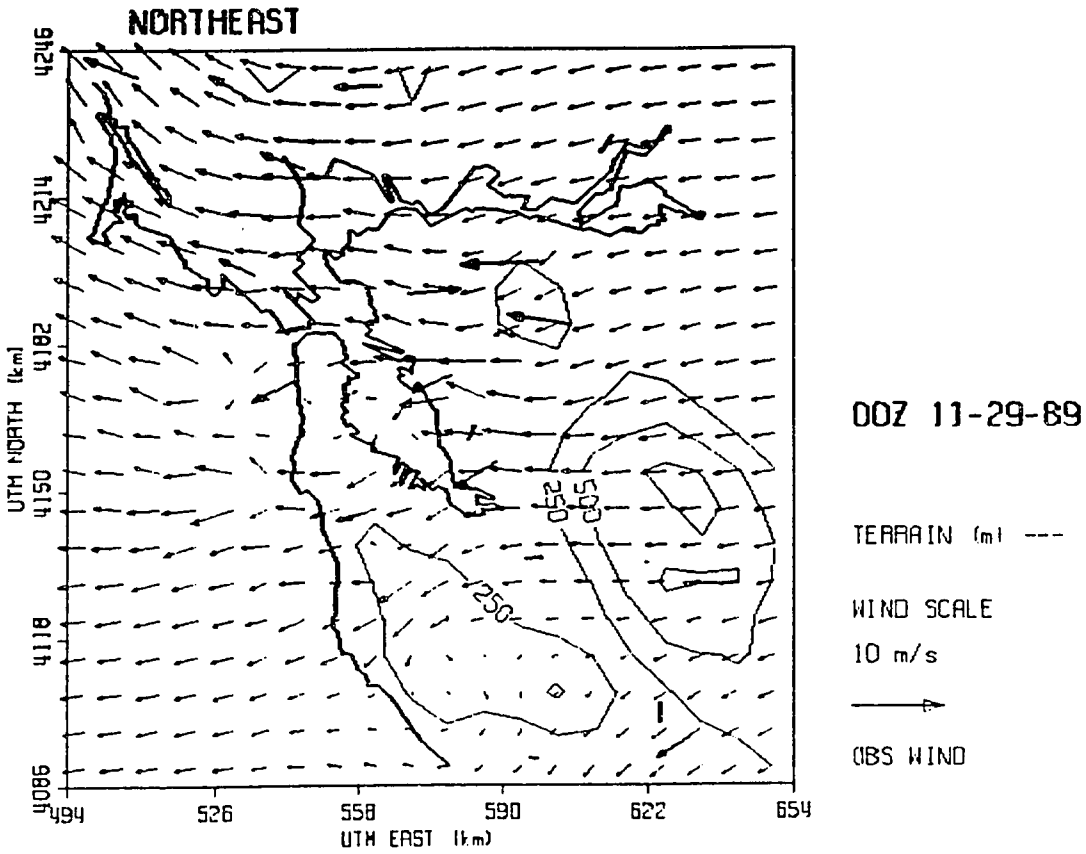

Figure 3-12 Plot of Northeasterly case (November 29, 1989, 00 GMT).

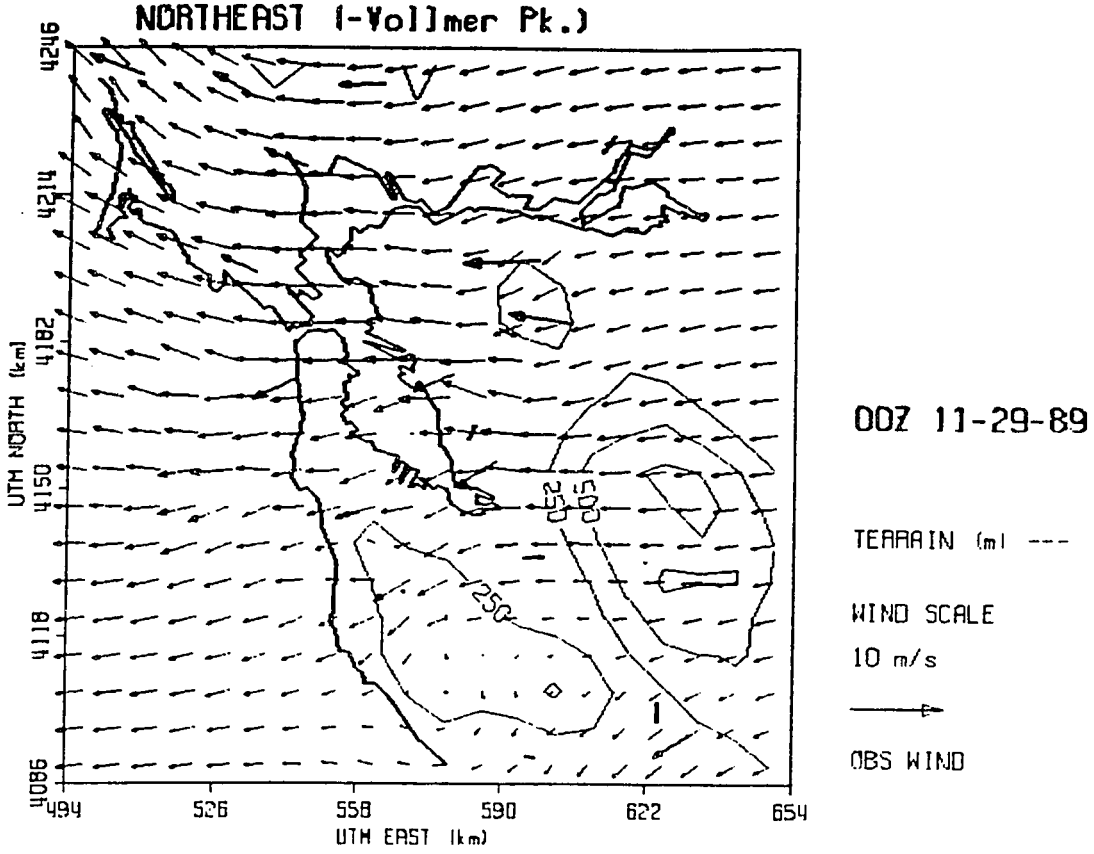

Figure 3-13 Same as Figure 3-12, but with Vollmer Peak data suppressed.

data from higher altitude stations (especially those above the inversion base) may lead to erroneous results. Table 3-6 does show that the average model wind has increased, but this is seen primarily in those stations reporting weak winds. Of note is Mt. Hamilton (altitude 4381 feet MSL) where the deletion of the Vollmer Peak observation have changed the model/observed speed ratio from 729% to 819%. This eight-fold speed increase is exceptional, and is due to the light winds and high altitude of Mt. Hamilton.

Southerly/Southeasterly Flow Patterns

WOCSS was next tested with winds from a southerly quadrant. The two cases considered here are 12 hours apart, and illustrate flows typically encountered in advance of an approaching synoptic storm.

Southerly

Figure 3-14 shows the surface flow for this case. Observed winds were generally south to southeasterly, ranging from 115° at Petaluma to 190° at Bethel Island. Modeled flow is also from the SE-SSE across the domain. There is generally good agreement between observed and model winds in this case (see Table 3-7, Appendix C).

Southeasterly

Figure 3-15 shows the surface winds for this case. The observed winds were more easterly, as the synoptic low pressure system was passing to the south of the SFBA.

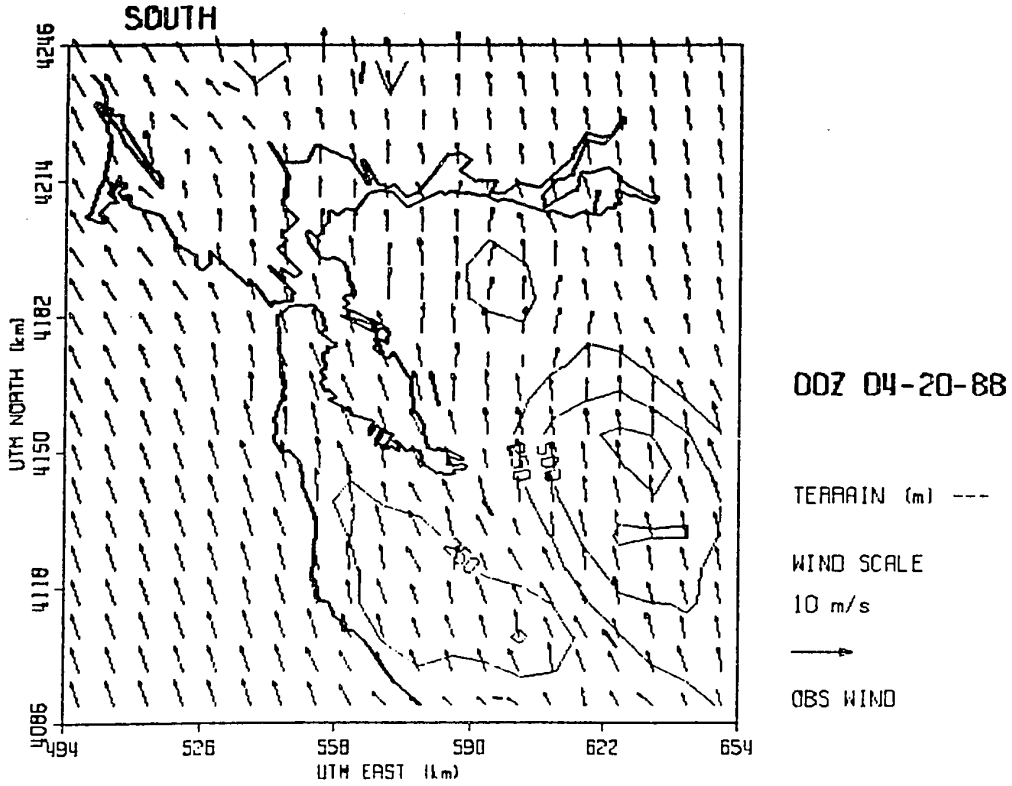

Figure 3-14 Plot of Southerly case (April 20, 1988, 00 GMT).

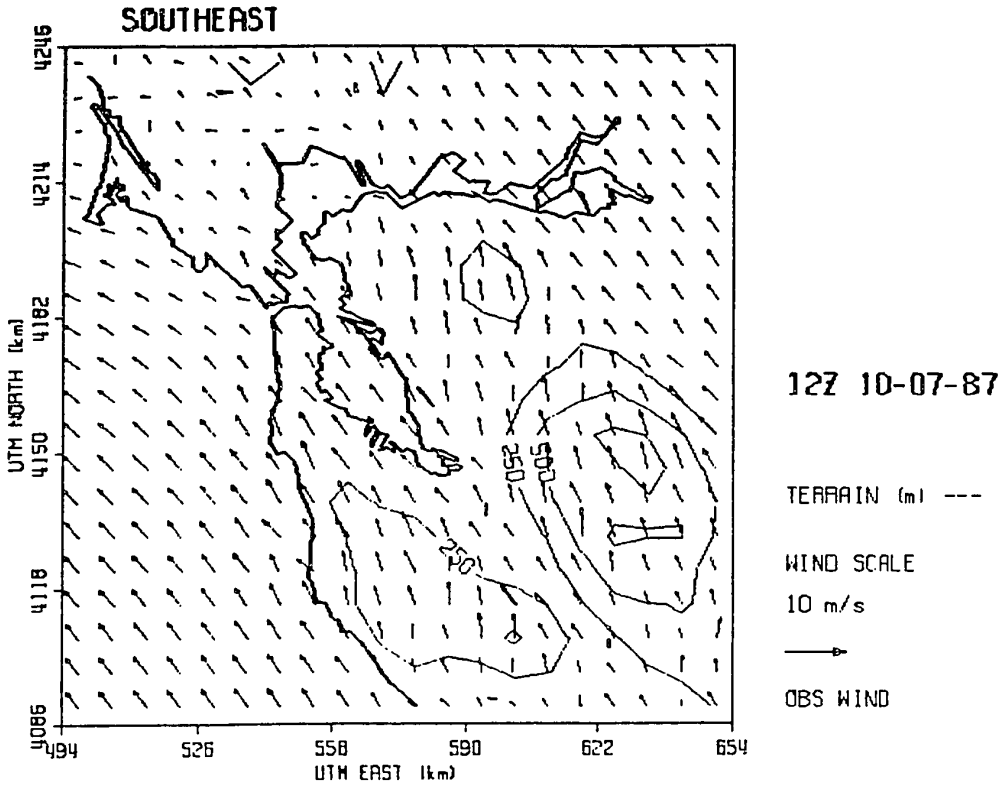

Figure 3-15 Plot of Southeasterly case (April 20, 1988, 12 GMT).

Observed and model winds are in good agreement (Table 3-8, Appendix C). However, Napa shows quite a directional error (both observed and modeled speeds are very light), while model speeds at Petaluma are somewhat reduced. It is likely that the very weak observed winds in the North Bay lead to poor model performance in that particular area. On the other hand, San Jose and San Martin exhibit good model directions, despite the weak flow in the Santa Clara valley.

Weak Inflow/Outflow Patterns

Finally we consider two tests on dates in December, 1988, characterized by weak surface flows into or out of the SFBA. The weak inflow/outflow patterns are typically associated with weak synoptic gradients, where local diurnal heating and cooling generate weak breezes.

Weak Outflow

Figure 3-16 shows the surface flow for this case. Flow is very weak through much of the region. Flow along the coast is offshore, and there is a general outflow from the SFBA. Surface winds at Oakland were 5.2 ms^{-1} from 50°, whereas those 18 km to the southeast at Union City were much weaker and from 238°. The modeled flow in this region is therefore dominated by the Oakland observation. Table 3-9, Appendix C shows that with this weak flow case, the model speeds are significantly slower than observed winds, probably influenced by the Oakland sounding (nearly calm in

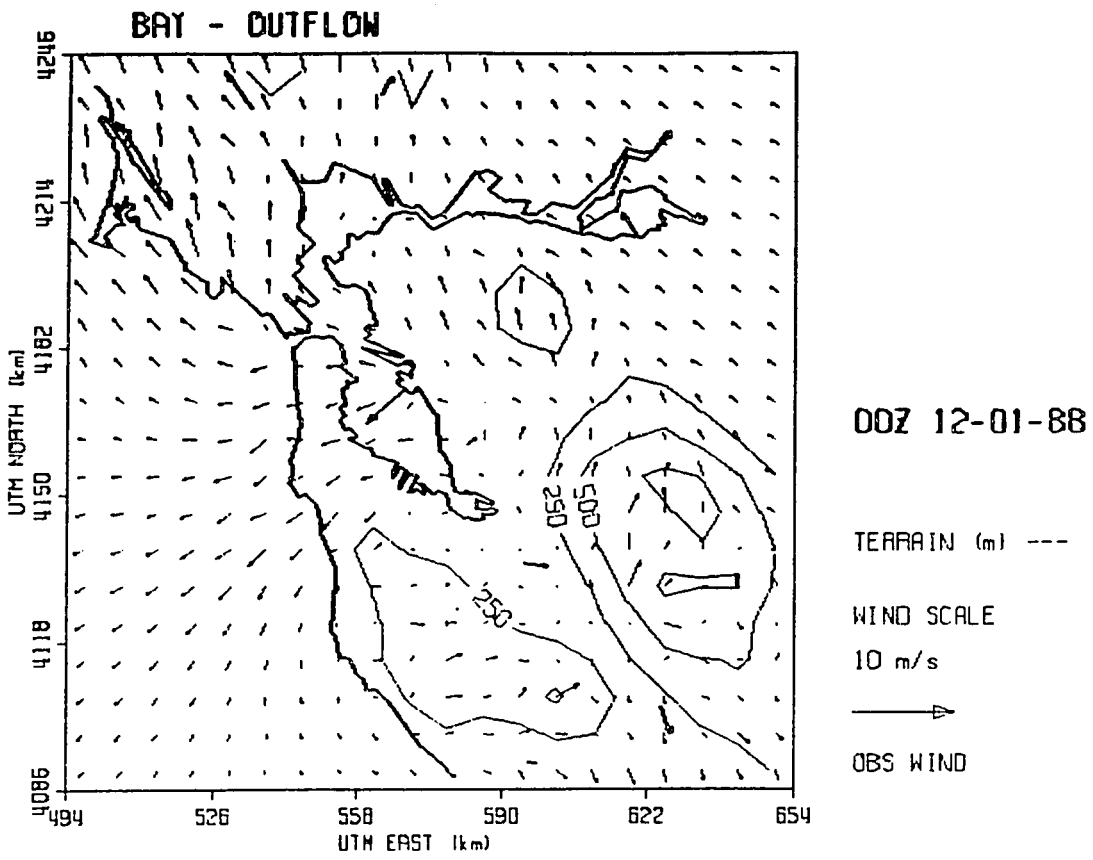

Figure 3-16 Plot of Weak Outflow case (December 1, 1988, 00 GMT).

the lower levels). Also, model and observed directions are not in good agreement (7.7% average error, worst of all the cases considered in this section). This is probably because of the strong divergence in the observed winds that cannot be completely removed without significant changes to the flow.

Weak Inflow

Figure 3-17 shows the surface flow for this case. Flow is weak again through much of the region, and flow along the coast is now alongshore. Unlike the outflow case discussed above, the modeled directions are in good agreement with observations, although the speeds still show a large discrepancy. Once again the speed discrepancy is likely due to the influence of the Oakland sounding (see tabulated comparison in Table 3-10, Appendix C).

Summary

In reviewing the synoptic climatology cases discussed above, the following statements can be made. With few exceptions, the model is seen to work very well in reproducing the basic SFBA climatological flow types. Model speed accuracy is diminished in weak flow situations, with modeled winds as much as 64% slower than observed speeds. Modeled wind directions appear best in northwest flow cases (particularly moderate and strong), perhaps due to the NW-SE orientation of the ridges/valleys in the SFBA region. In the northeasterly flow case, it was shown that selective

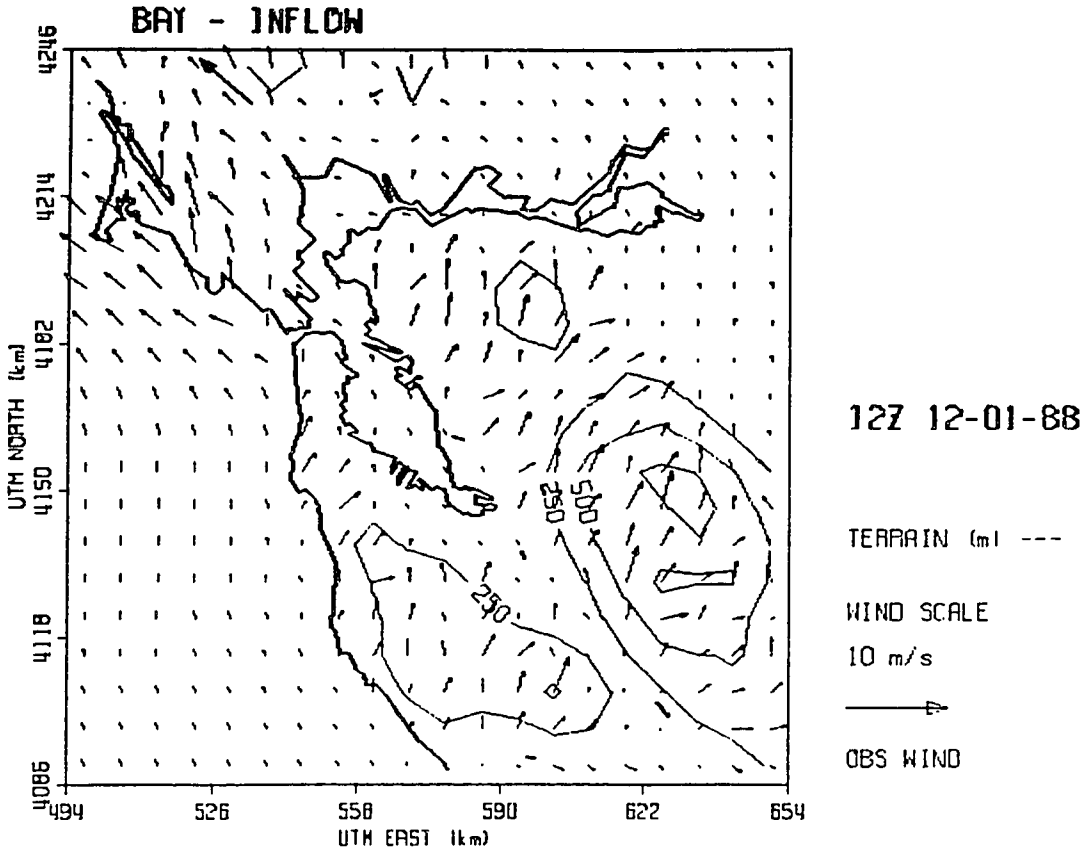

Figure 3-17 Plot of Weak Inflow case (December 1, 1988, 12 GMT).

disregard of certain stations can greatly improve the overall accuracy of modeled winds. This idea will be explored at length in Chapter 3e. A summary of all SFBA climatology case runs is found in Table 3-11, Appendix C.

d. Analysis of model performance during periods with additional input and verification data

The normal input data set used in the runs discussed in Chapter 3c consisted of eight surface wind observations, together with the Oakland sounding. This set was chosen since it was assumed that data from the seven BAAQMD sites and Oakland will almost always be available, while data from the other sites will be available occasionally. On some of the dates examined above, additional surface wind data were available. The additional data serves two purposes. First, it allows for a more detailed comparison between model and observed wind speeds and directions. Second, it enables the identification of sites where additional input data to WOCSS will improve modeled flow in the SFBA. Runs with additional input data are compared to the basic (weak northwesterly) case discussed above. The additional stations were chosen, in part, for their potential role in improving model handling of flow through the SFBA coastal gaps. The weak northwesterly case was chosen for these runs because of the availability of extra data, and because this flow pattern (the most prevalent of the basic flow types) is of particular interest in the SFBA.

Figure 3-8 showed the winds produced by the model using winds observed at the standard eight sites at 00Z on October 7, 1987. As discussed in Chapter 3c, the general flow pattern at this time was northwesterly due to high pressure

offshore and a thermal trough over the interior valleys. Figures 3-18 through 3-33 below will show model output using the 8 stations plus individual stations sequentially added to the data set.

Travis AFB added

In this test, wind data from Travis AFB (UTM coordinates 594,4235) were added to the standard data set. The resulting winds are shown in Fig. 3-18. A comparison of Fig. 3-18 and Fig. 3-8 shows that model winds are now much stronger in the delta region as a result of the strong winds (7.1 ms^{-1}) reported at Travis. Figure 3-19 shows the vector difference winds and contoured speed differences between runs with and without Travis, and shows an influence across an area 30-40 km in radius around Travis AFB. Note that in Fig. 3-19 and subsequent vector difference plots, the calculation reflects the difference between the run without Travis data, and the run with Travis data. The scale used for vector differences in this section is magnified 3-fold relative to that used in the wind plots. Table 3-12 in Appendix C shows the wind summary for this run; it indicates that the model winds are, on average, 16% slower than observed winds (compared to 19% with the basic run; see Tables 3-1 or 3-20, Appendix C). Note that Table 3-12 shows results from only eight stations, as Santa Rosa lies beyond the model domain. The directional error is slightly reduced to 5.4% (from 5.5%). Thus, adding Travis AFB has slightly

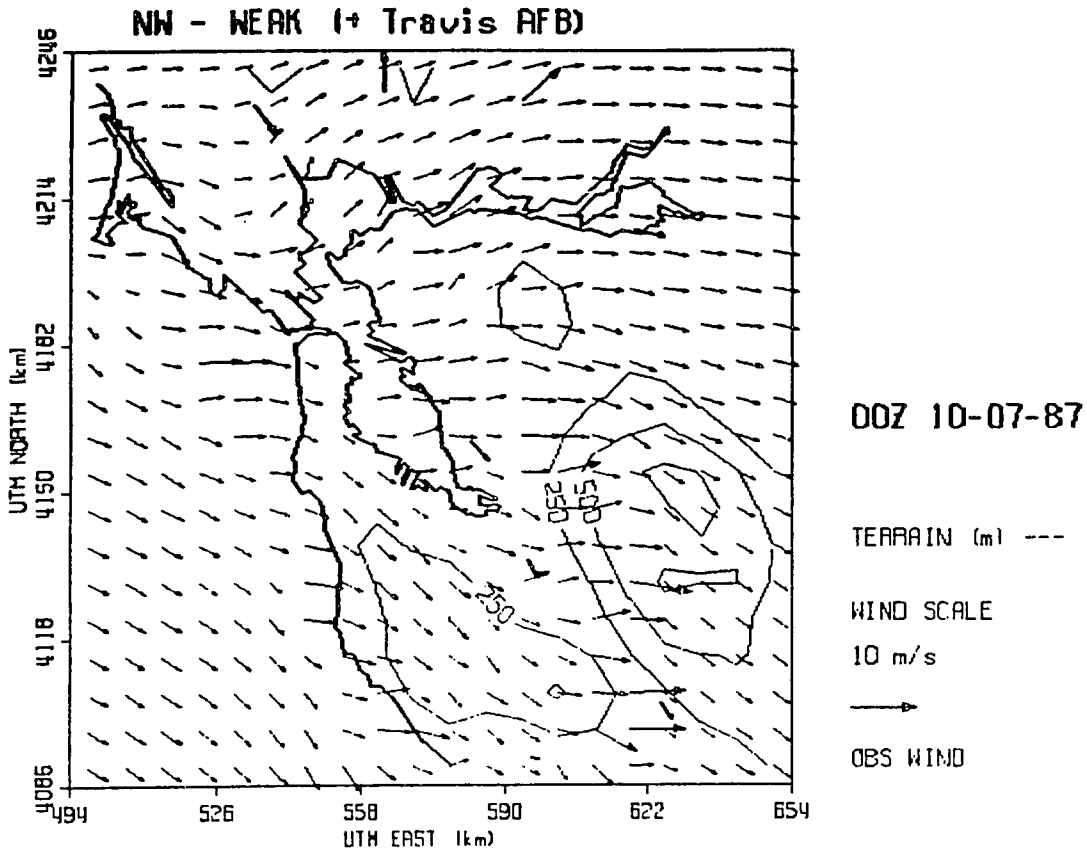

Figure 3-18 Plot of Weak Northwesterly case (as in Figure 3-8) but with Travis AFB added to station data set.

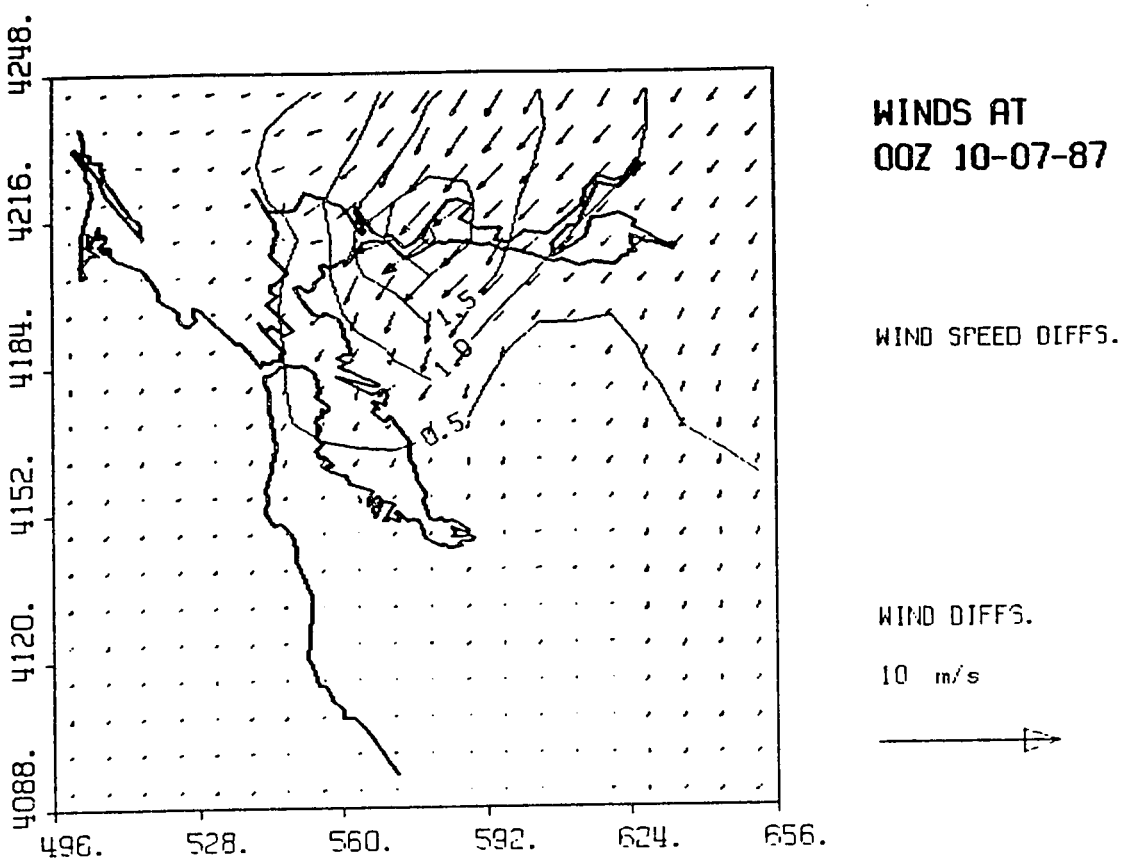

Figure 3-19 Vector difference plot of Figure 3-8 minus Figure 3-18.

improved overall model performance.

Pittsburg added

In this test, wind data from Pittsburg (UTM coordinates 595,4210) were added to the standard data set. The resulting winds are shown in Fig. 3-20. A comparison of Fig. 3-20 and Fig. 3-8 shows that winds are strengthened in the area around and to the northeast of Pittsburg, and westerly flow through the delta region is enhanced. Figure 3-21 shows that Pittsburg influences model winds over a large area. Tables 3-13 and 3-20 in Appendix C indicate speed and direction results slightly better than those for Travis AFB.

Alameda NAS added

In this test, wind data from Alameda NAS (UTM coordinates 561,4181) were added to the standard data set. The resulting winds are shown in Fig. 3-22. Winds here were reported at 360°, and thus a more northerly flow is generated across the bay in this area (compare with Fig. 3-8). The vector difference plot (Fig. 3-23) shows that Alameda's influence extends westward across the San Francisco peninsula. Tables 3-14 and 3-20 in Appendix C show that the addition of Alameda NAS reduces the model wind speeds to 75% of observed values, with slightly greater directional errors. Of all the cases considered in this section, the addition of Alameda NAS data degrades model

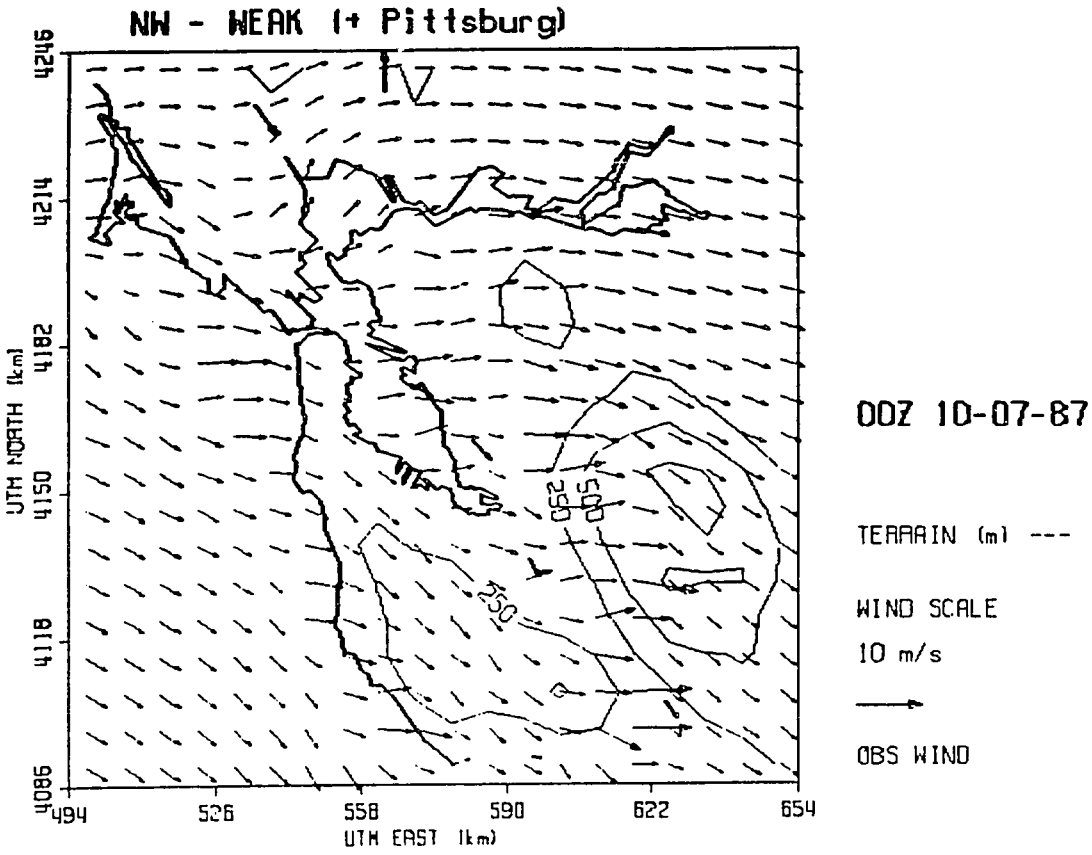

Figure 3-20 Same as Figure 3-18, but with Pittsburg added.

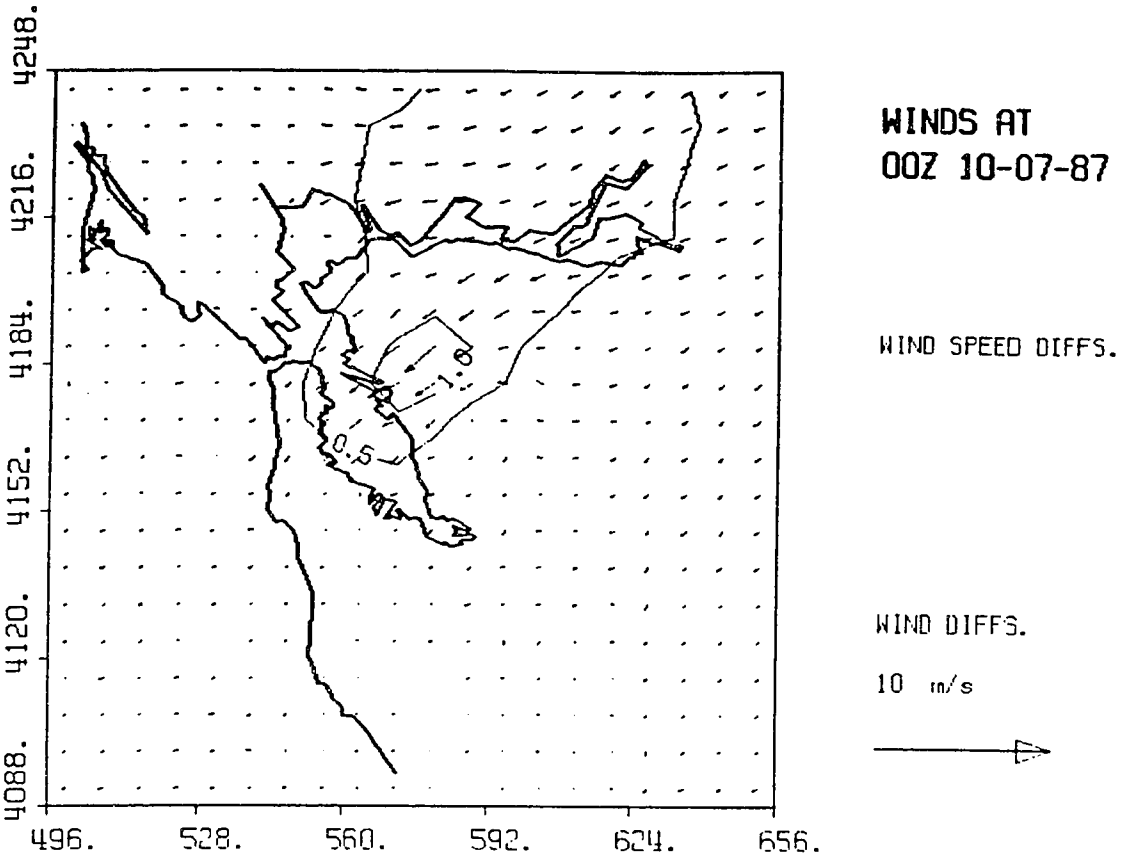

Figure 3-21 Vector difference plot of Figure 3-8 minus Figure 3-20.

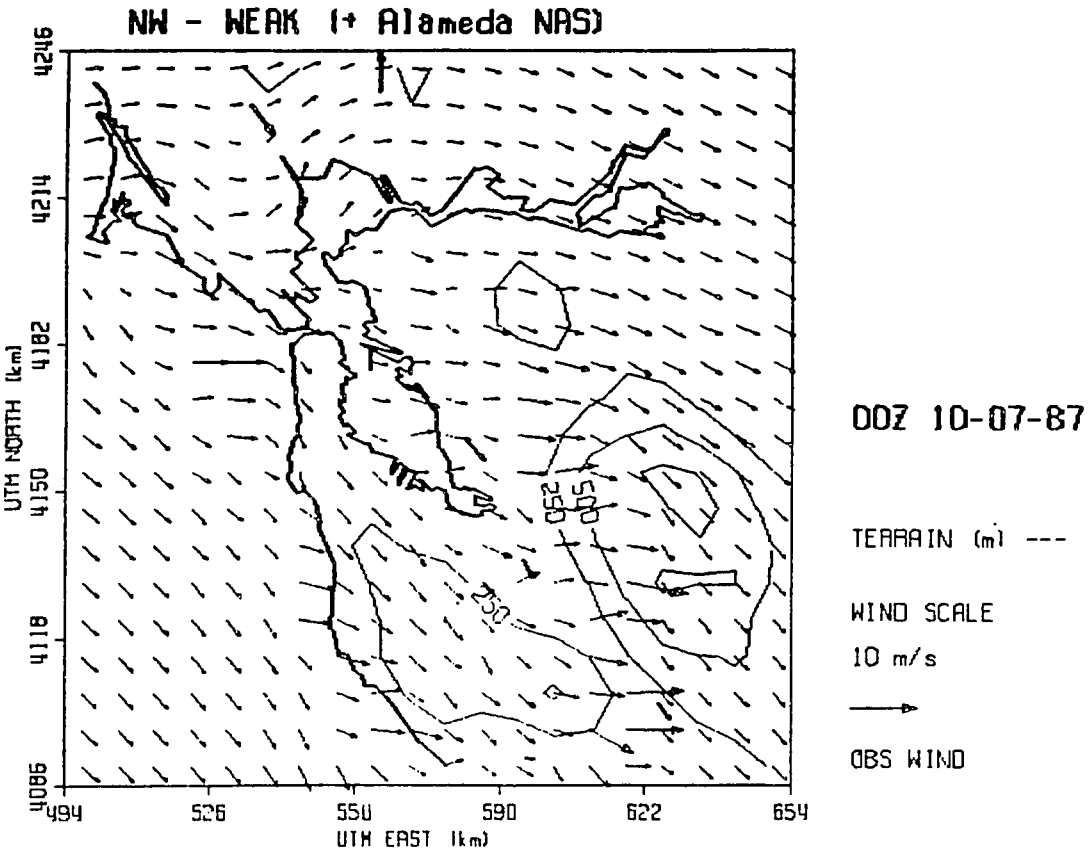

Figure 3-22 Same as Figure 3-18, but with Alameda added.

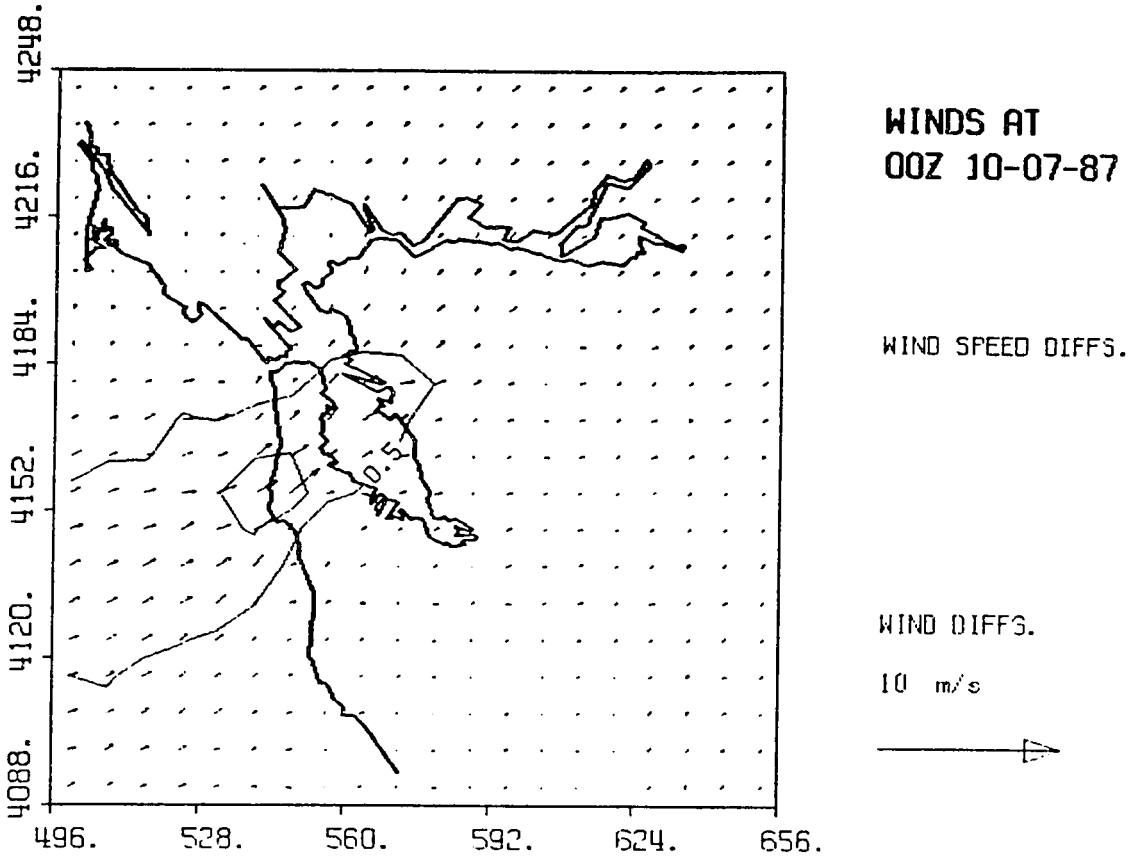

Figure 3-23 Vector difference plot of Figure 3-8 minus Figure 3-22.

output the most.

Benicia added

In this test, wind data from Benicia (UTM coordinates 574,4212) were added to the standard data set. The resulting winds are shown in Fig. 3-24. Although the observed wind at Benicia was light (1.8 ms^{-1}), an influence is noted from the Golden Gate to Oakland and Berkeley (see Fig. 3-25). Tables 3-15 and 3-20 in Appendix C show that model winds are 18% slower than observed winds, with a 6.2% directional error. This is comparable to the basic run, with only a slight reduction in directional accuracy. The effects are greatest where the nearby winds were strongest in the original analysis.

Vallejo added

In this test, wind data from Vallejo (UTM coordinates 567,4217) were added to the standard data set. The resulting winds are shown in Fig. 3-26. The observed wind at Vallejo was 4 ms^{-1} from 225°. With the addition of the data, model winds now have a more southerly component in the region from the Golden Gate to Vallejo. Changes are most apparent in the immediate vicinity of Vallejo (Fig. 3-27), but closer inspection shows that the influence extends from the western boundary of the domain over the ocean to the north delta area. It should be remembered that the overriding physical constraint operating in WOCSS is the principal of mass consistency, applied after an inverse

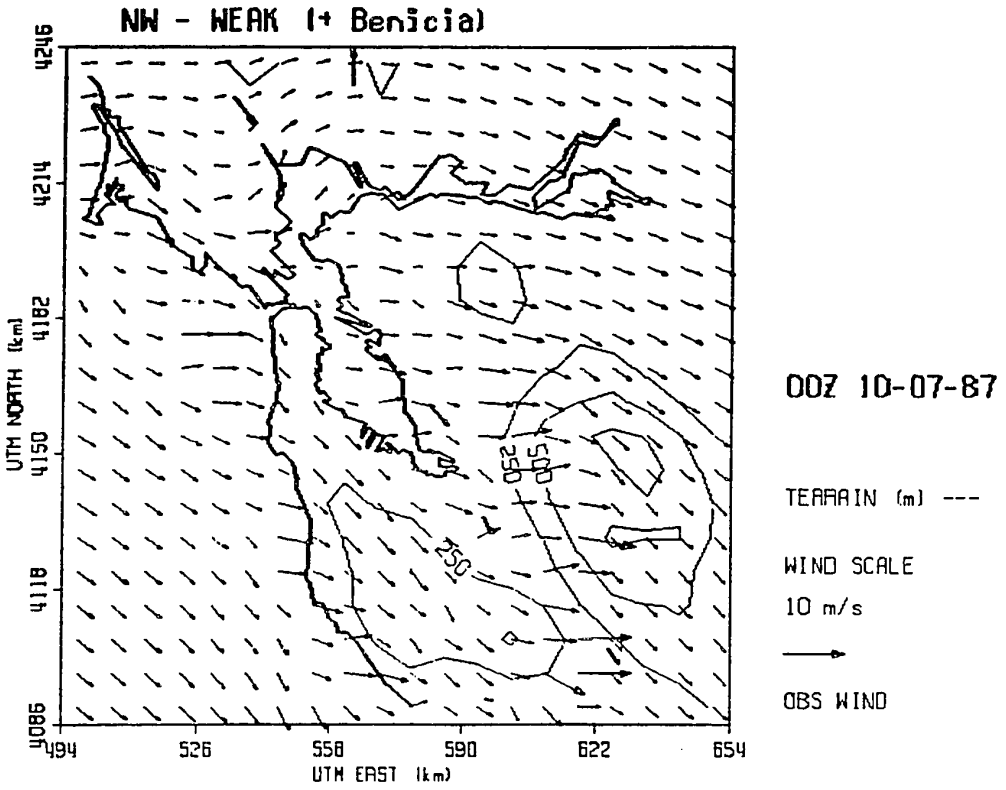

Figure 3-24 Same as Figure 3-18, but with Benicia added.

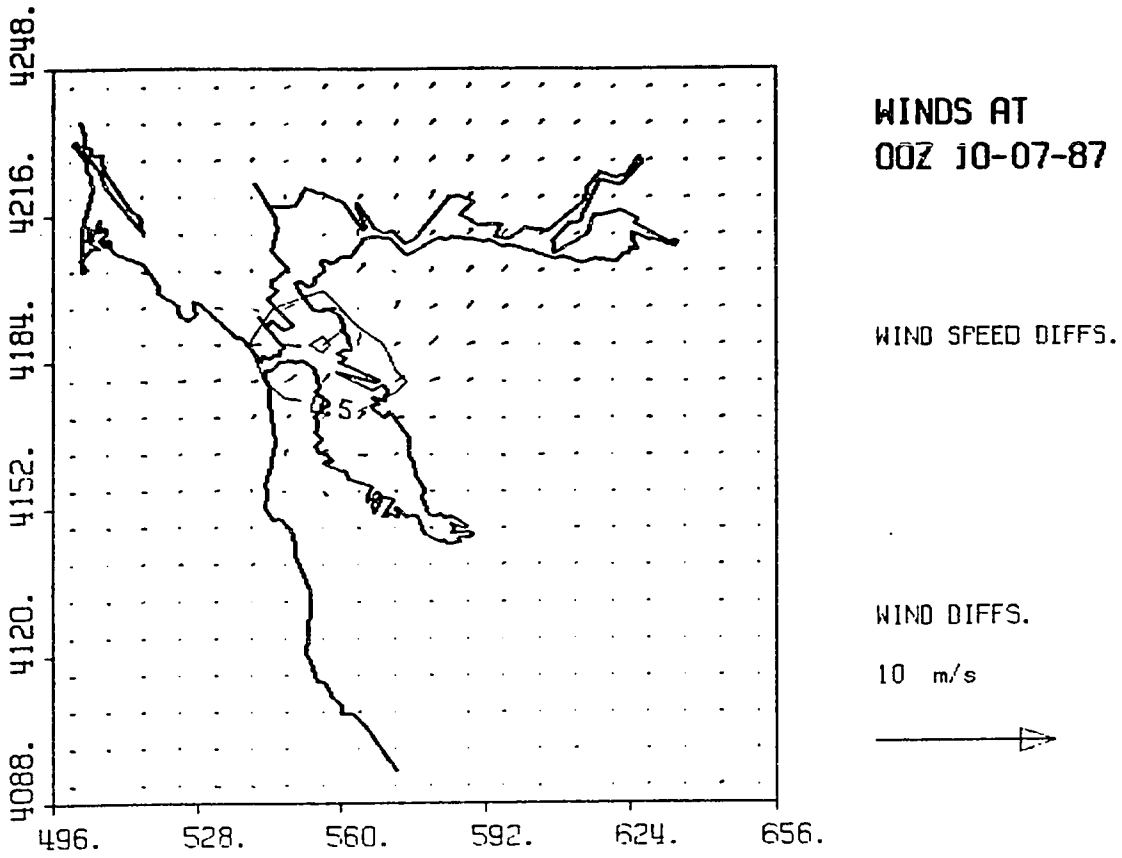

Figure 3-25 Vector difference plot of Figure 3-8 minus Figure 3-24.

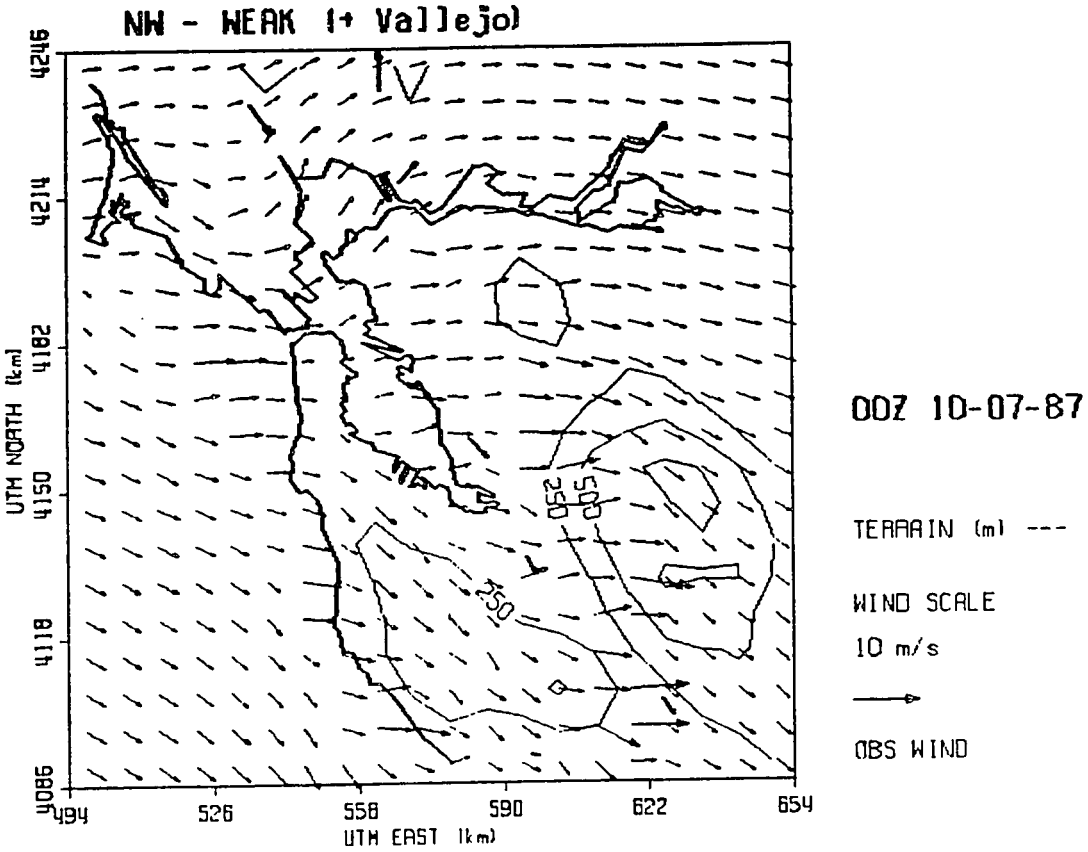

Figure 3-26 Same as Figure 3-18, but with Vallejo added.

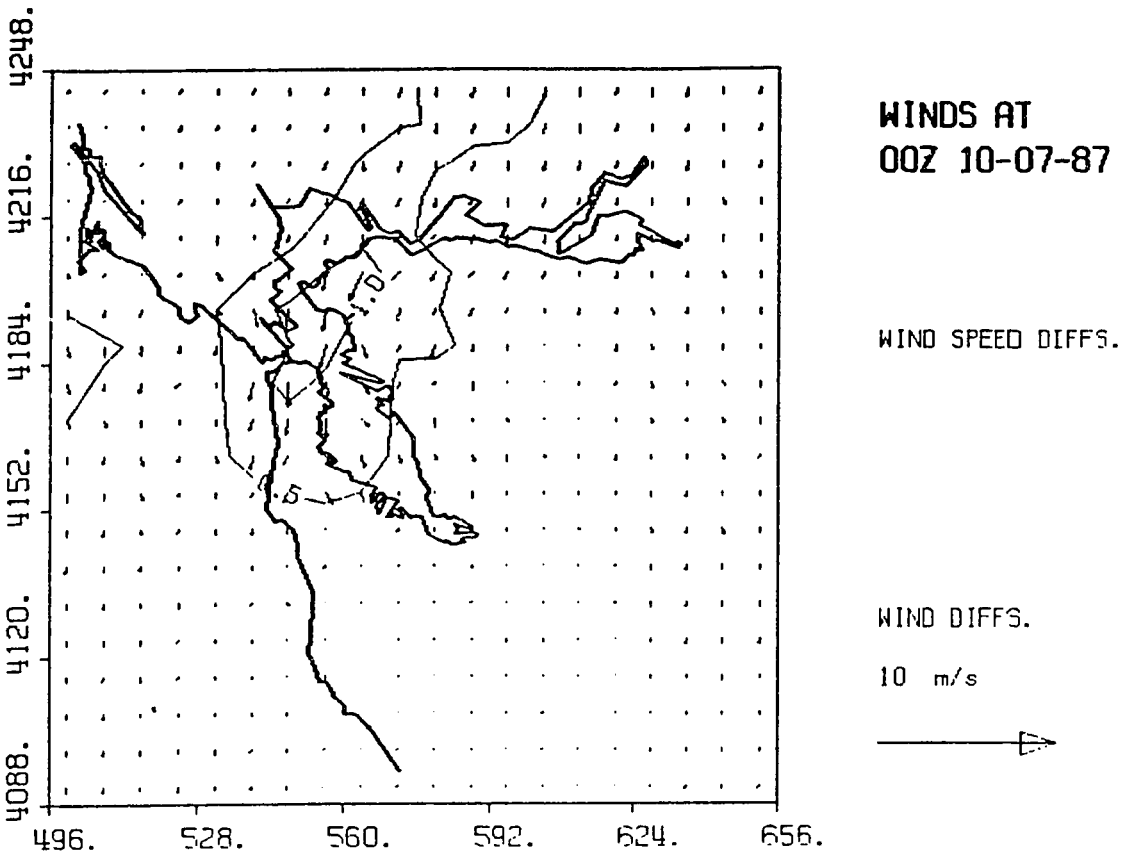

Figure 3-27 Vector difference plot of Figure 3-8 minus Figure 3-26.

distance-weighted interpolation. It is not surprising therefore that the addition of data showing relatively strong flow at a single site can influence flow across a large part of the domain. Tables 3-16 and 3-20 of Appendix C indicate results similar to the Benicia case, and thus comparable to the basic case.

Richmond added

In this test, wind data from Richmond (UTM coordinates 557,4200) were added to the standard data set. The resulting winds are shown in Fig. 3-28. The observed wind at Richmond was from 180°. The addition of this wind therefore causes model winds to be more southerly in the Richmond area (compare with Fig. 3-8). West of the Richmond area and the Golden Gate, winds back and slow considerably. The effect of adding Richmond is felt strongly particularly west of the Golden Gate (Fig. 3-29). Tables 3-17 and 3-20 of Appendix C indicate that the addition of Richmond has similar effects on model winds as adding Alameda NAS (with model speeds 24% slower than observed speeds). However, there is an improvement over the basic run with average directional error.

All six sites added (13 stations)

In this test, wind data from all six additional sites were added to the standard data set. The resulting winds are shown in Fig. 3-30. Differences between the resulting flow and that shown in Fig. 3-8 are due to a combination of

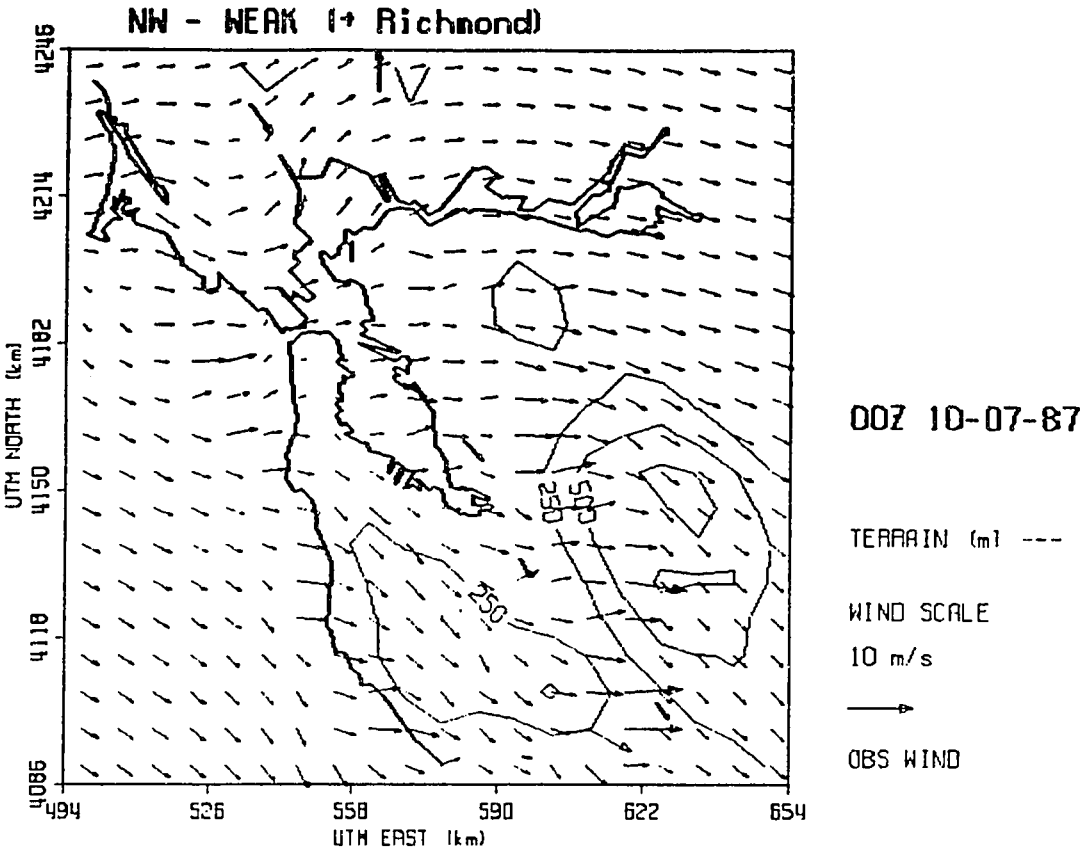

Figure 3-28 Same as Figure 3-18, but with Richmond added.

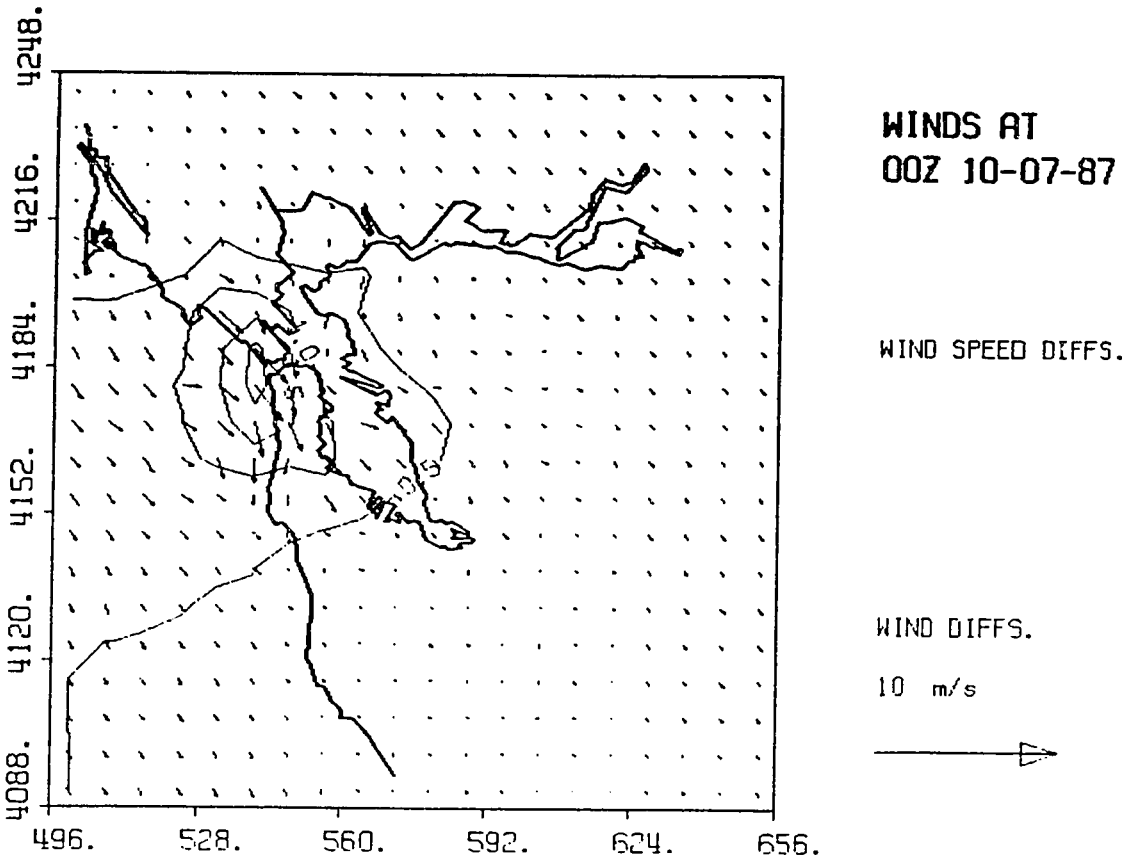

Figure 3-29 Vector difference plot of Figure 3-8 minus Figure 3-28.

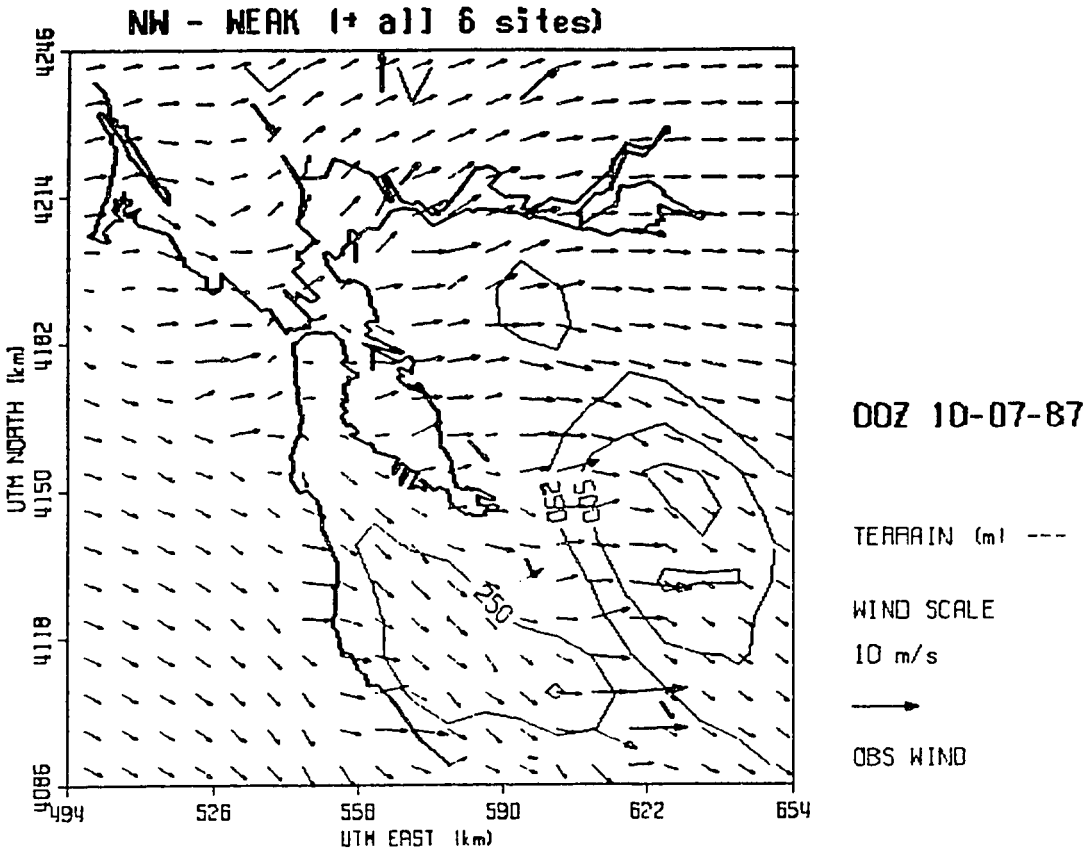

Figure 3-30 Same as Figure 3-18, but with all six sites added.

the effects discussed above. Fig. 3-31 shows that vector differences are felt over the entire domain (although to a lesser amount over the Diablo and Santa Cruz mountain ranges). Northward turning of the flow across the north bay region, and strong northeastward flow toward the delta are enhanced by the addition of data from the five north bay sites. Tables 3-18 and 3-20 in Appendix C indicate a significant improvement in model speeds throughout the area (only 1% slower than observed winds) in contrast to the basic run and the runs with individual stations added. On the other hand, model directions are slightly worse than the basic case (6.4% vs. 5.5%). The addition of an ensemble of carefully selected sites has greatly improved overall model performance.

All available data used (20 stations)

In this final test, wind data from seven more available sites were added to the previous run (i.e, normal eight plus twelve additional sites). The resulting winds are shown in Fig. 3-32. Comparing with Fig. 3-8, we see that once again flow turning toward the northeast is enhanced in the north bay (as in the preceding case). Modifications are also noted in many other areas. Flow is slightly stronger down the Santa Clara valley due to the incorporation of winds at the south bay sites. It may be that results here would be improved by extending the domain southward to include the Monterey Bay, thus capturing flow features induced by the

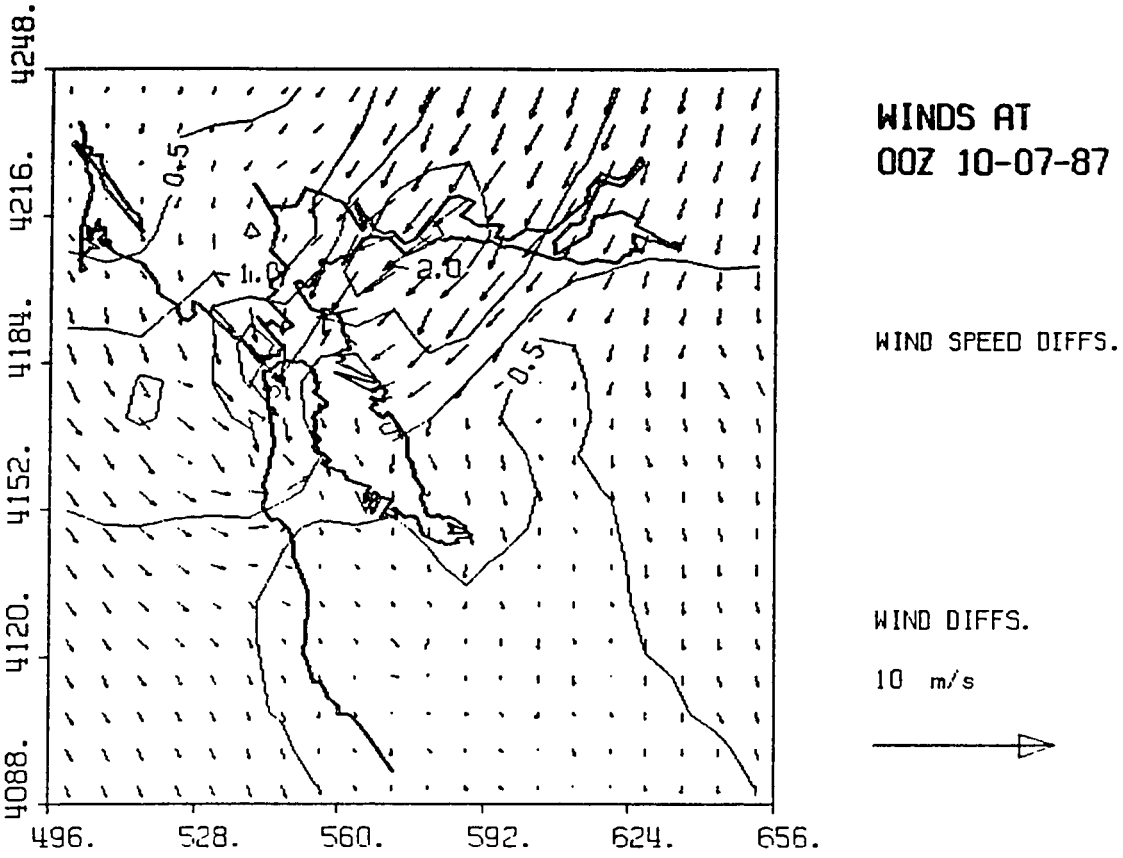

Figure 3-31 Vector difference plot of Figure 3-8 minus Figure 3-30.

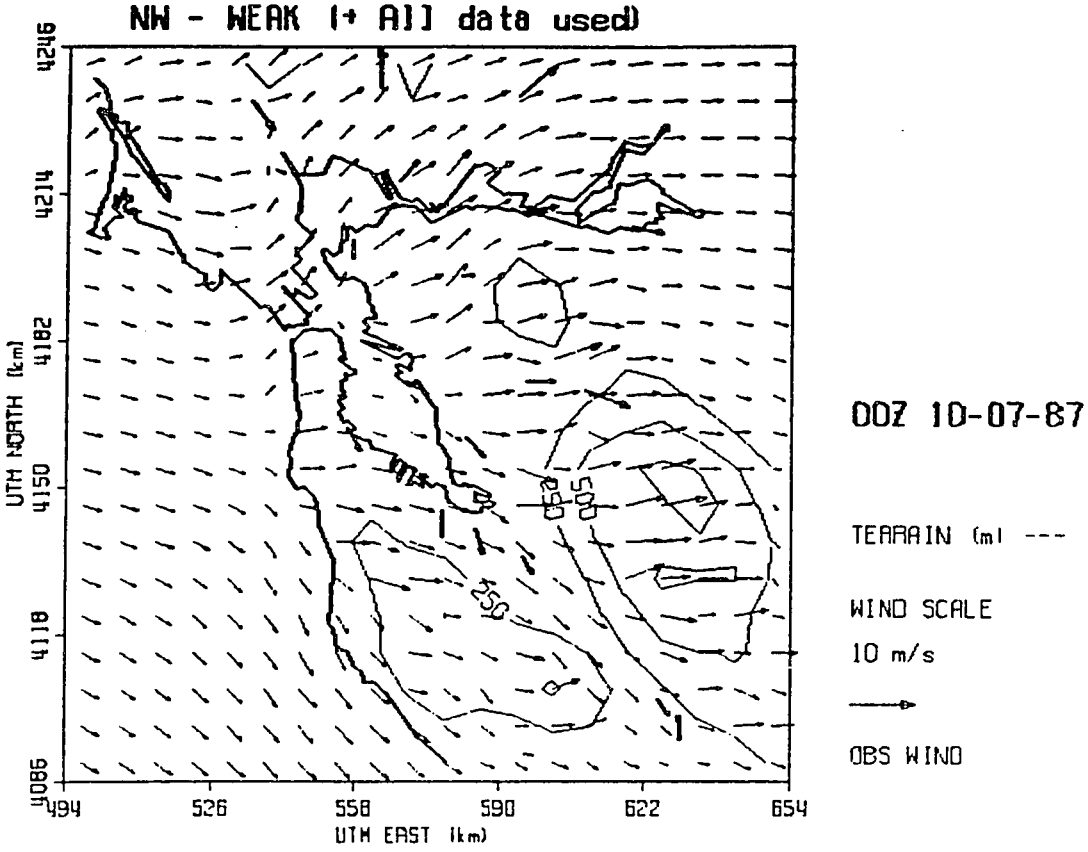

Figure 3-32 Same as Figure 3-18, but all available data used.

Bay. Flow from Half Moon Bay to Santa Cruz is more northerly and alongshore, and winds are generally weaker west of the Golden Gate. The addition of sites in these areas would likely improve model performance along the coast. Figure 3-33 shows that with the addition of all stations, vector differences are concentrated over the western delta, coastal areas, and in an area stretching from Mt. Hamilton to Gilroy. There are several lines of enhanced convergence (e.g., Marin coast to South Peninsula, Hamilton Range and East Bay hills) and divergence (Santa Clara Valley).

Table 3-19 in Appendix C shows results for this last case, and Table 3-20 summarizes all cases in this section. With twenty stations, model winds are only 3.3% faster than observed winds, while the directional deviation is slightly worse (6.8%) than in some of the other cases.

Summary

The last two cases above (with 13 and 20 total stations) indicate that with a high density of input data, model wind speeds are substantially improved. The inclusion of certain individual stations (e.g., Pittsburg) improves model performance, while other stations (Alameda NAS and Richmond) degrade model output. If both Alameda NAS and Richmond were added together, the split in the flow might be better defined and lead to substantial improvements in model output. This idea should be tested further.

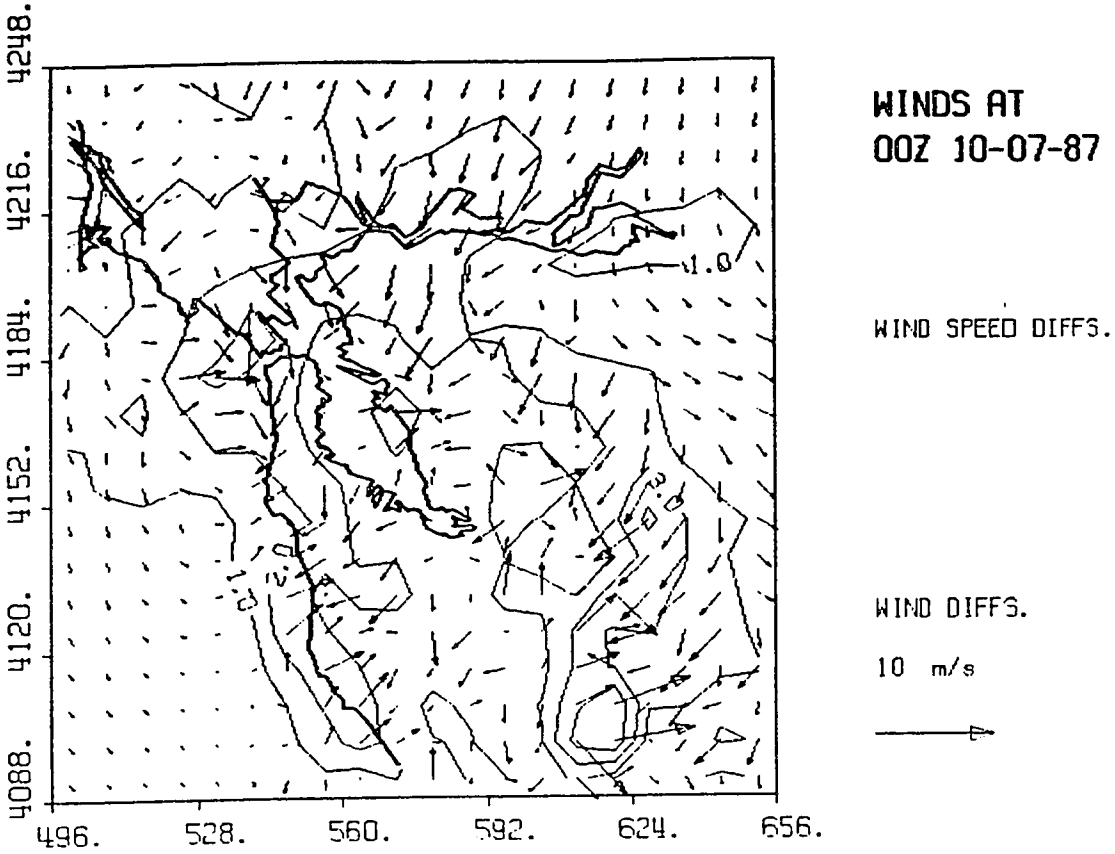

Figure 3-33 Vector difference plot of Figure 3-8 minus Figure 3-32.

e. Analysis of Model Performance with Missing Input Data

As mentioned above, the normal input data set used consisted of eight surface wind observations, and the Oakland sounding. The tests shown in Chapter 3d indicate that some improvement in model output can be expected when additional input data are provided. It is equally important to gauge the degradation in model output that may result from missing data. In this section therefore, model results when data from one (or more) of the standard sites are missing will be examined. Attention will again be focused on the October 1987 northwesterly flow case, since this flow pattern is so typical in the SFBA.

Bethel Island Deleted

In this test, wind data from Bethel Island (UTM coordinates 619,4207) were deleted from the standard data set. The resulting winds are shown in Fig. 3-34. Model winds with all standard data used (basic full set case) are shown in Fig. 3-8. A comparison of these figures shows that model flow is now much weaker in the northeastern SFBA, especially near Mt. Diablo (approximate UTM coordinates 595,4185). Fig. 3-35 shows that the vector difference winds are concentrated over Mt. Diablo and the southern delta region. Table 3-21 in Appendix C shows that model performance is diminished by deleting Bethel Island, most notably in the north bay. The ensemble directional error is

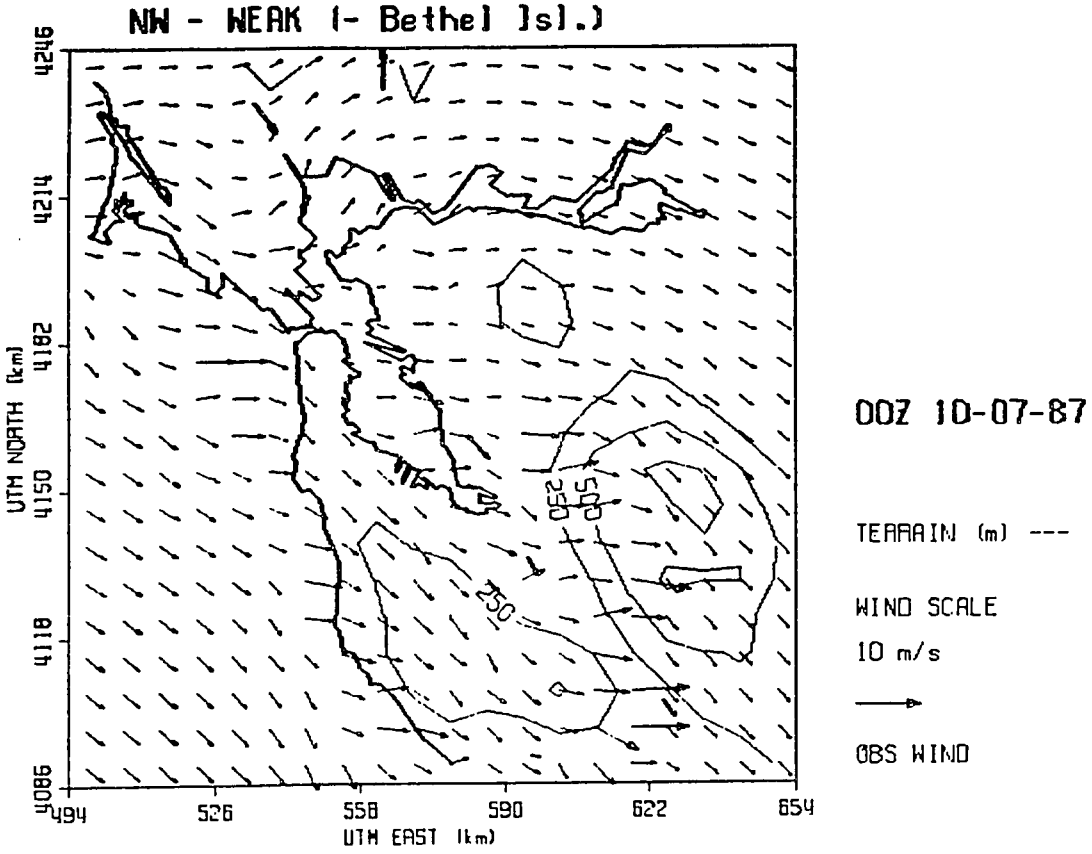

Figure 3-34 Plot of Weak Northwesterly case (as in Figure 3-8), but with Bethel Island deleted.

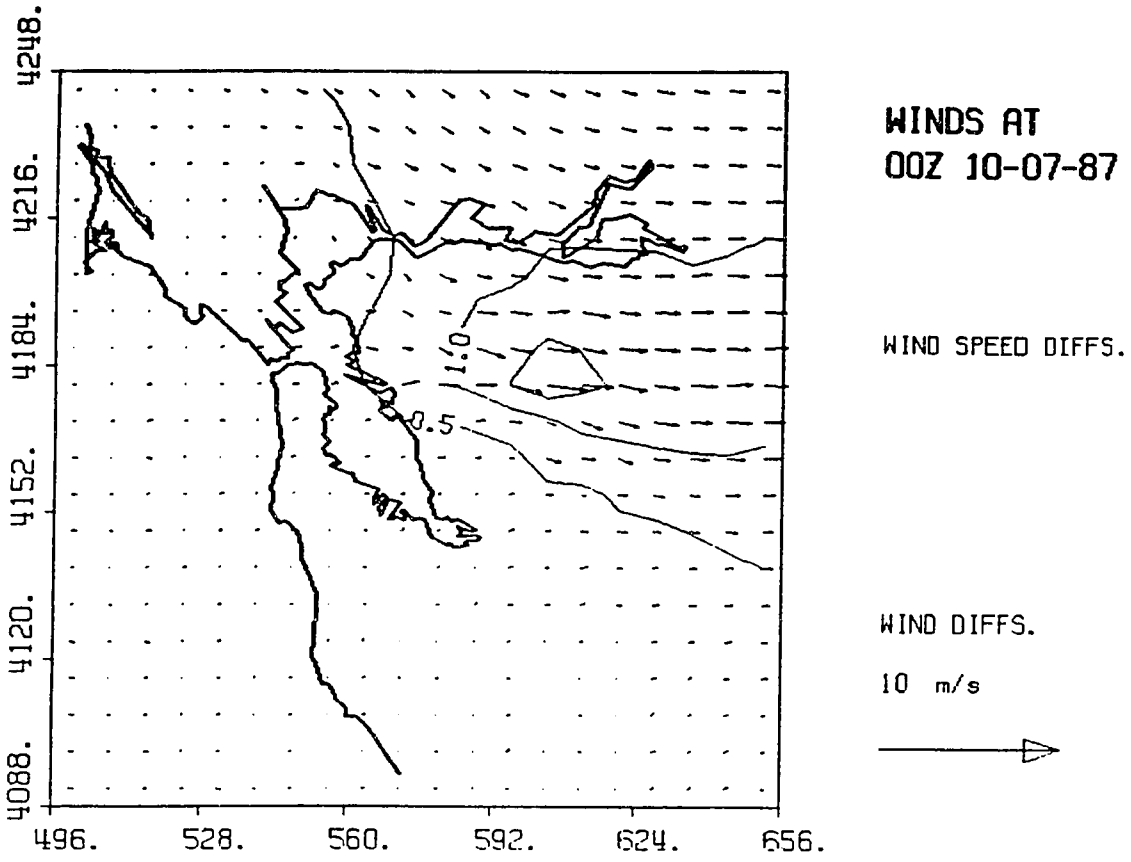

Figure 3-35 Vector difference plot of Figure 3-8 minus Figure 3-34.

7% (the worst of all runs in this section), while the speed ratio (76.3%) shows a similar degradation.

Napa Deleted

In this test, wind data from Napa (UTM coordinates 563,4237) were deleted from the standard data set. Winds at Napa were from 178° at 5.8 ms^{-1}. The resulting winds are shown in Fig. 3-36. Comparison of Figs. 3-8 and 3-36 shows that model flow has been turned to a more northerly direction from the eastern delta into the north-central SFBA. There is much less turning of the winds into the San Pablo Bay. Without Napa, the observed wind at Petaluma (northwesterly) dominates, increasing the westerly flow towards Mt. Diablo, and increasing the northerly flow into the San Pablo Bay. Fig. 3-37 shows dramatic differences over the north bay, and extending over much of the region. Table 3-22, Appendix C indicates that by deleting Napa, model speeds are dramatically improved to within 0.6% of observed speeds; the greatest improvements are seen at Bethel Island and Petaluma. This is likely due to the fact that Napa is on the edge of the domain and thus not representative of the flow over the greater SFBA, and also because of the observed directional variability over the North Bay (caused by complex terrain).

Santa Rosa Deleted

In this test, wind data from Santa Rosa (UTM coordinates 521,4250) were deleted from the standard data

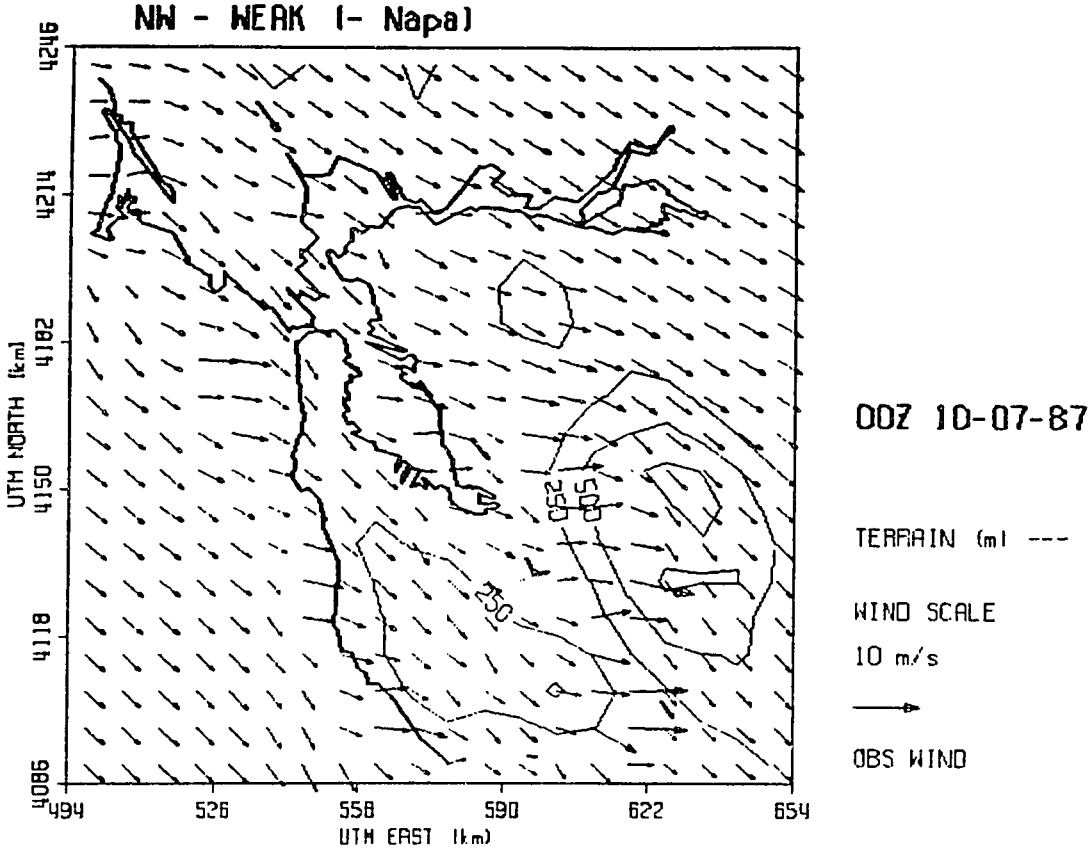

Figure 3-36 Same as Figure 3-34, but with Napa deleted.

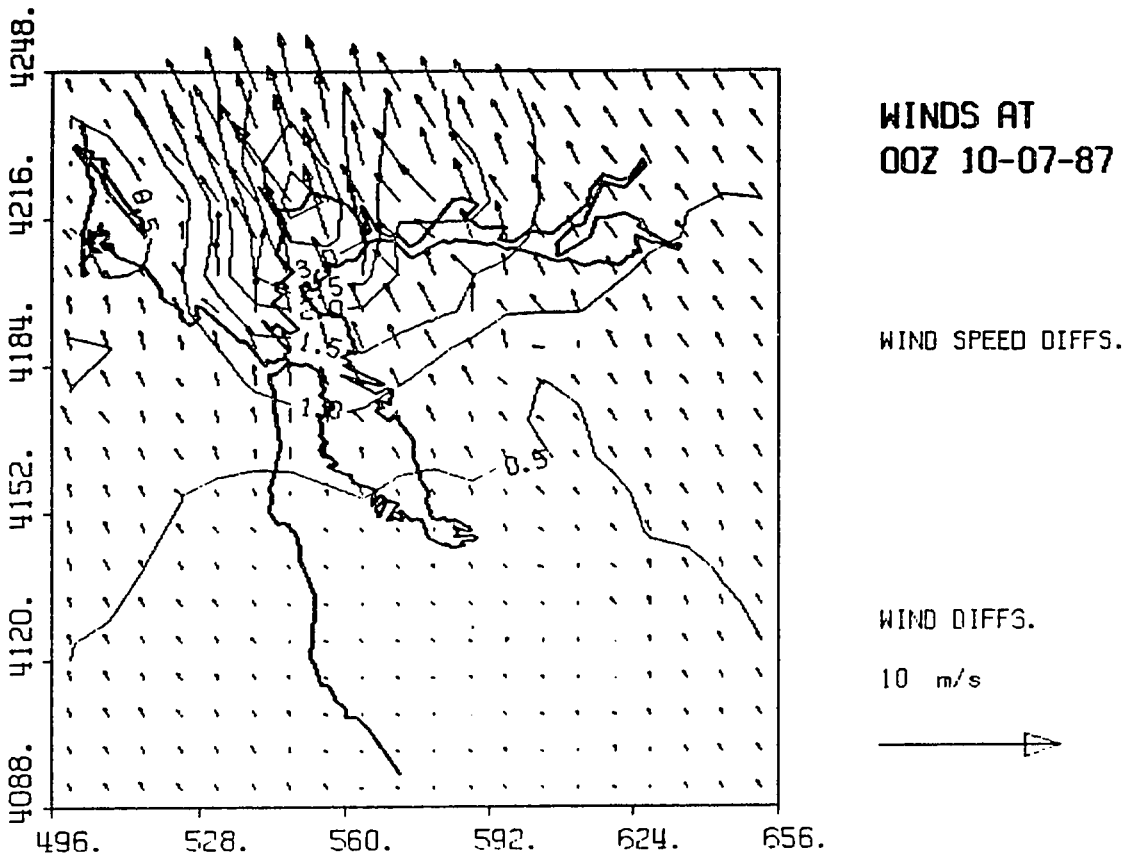

Figure 3-37 Vector difference plot of Figure 3-8 minus Figure 3-36.

set. The resulting winds are shown in Fig. 3-38. Comparison of Figs. 3-8 and 3-38 shows that the influence of this omission is limited to the extreme northwestern part of the region. Model winds in that region are now stronger and blow from a more northerly direction (see Fig. 3-39 for vector differences). Table 3-23, Appendix C indicates that deleting Santa Rosa improves model performance only slightly (and in the region of Petaluma), presumably because of its local influence, beyond the actual geographical domain of the model.

Petaluma deleted

In this test, wind data from Petaluma (UTM coordinates 534,4234) were deleted from the standard data set. Observed winds at Petaluma were from 321° at 5.4 ms^{-1}. The resulting winds are shown in Fig. 3-40. The influence of this omission is spread further than that due to missing Santa Rosa data (see Fig. 3-41 for vector differences). Winds west of the golden Gate gap are now more westerly, turning to southwesterly further north. A slight influence is seen throughout the western delta. Table 3-24, Appendix C indicates an improvement in both model speeds and directions, with closer model agreement at Napa, and worse agreement at Oakland.

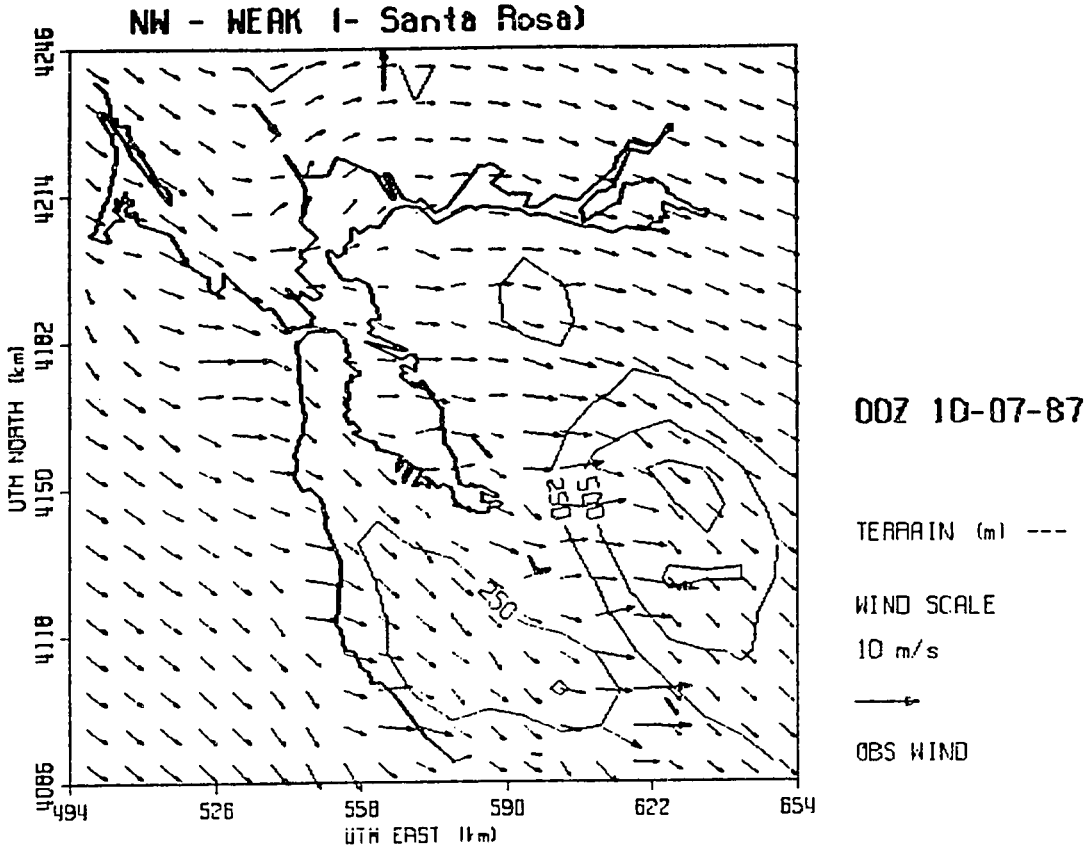

Figure 3-38 Same as Figure 3-34, but with Santa Rosa deleted.

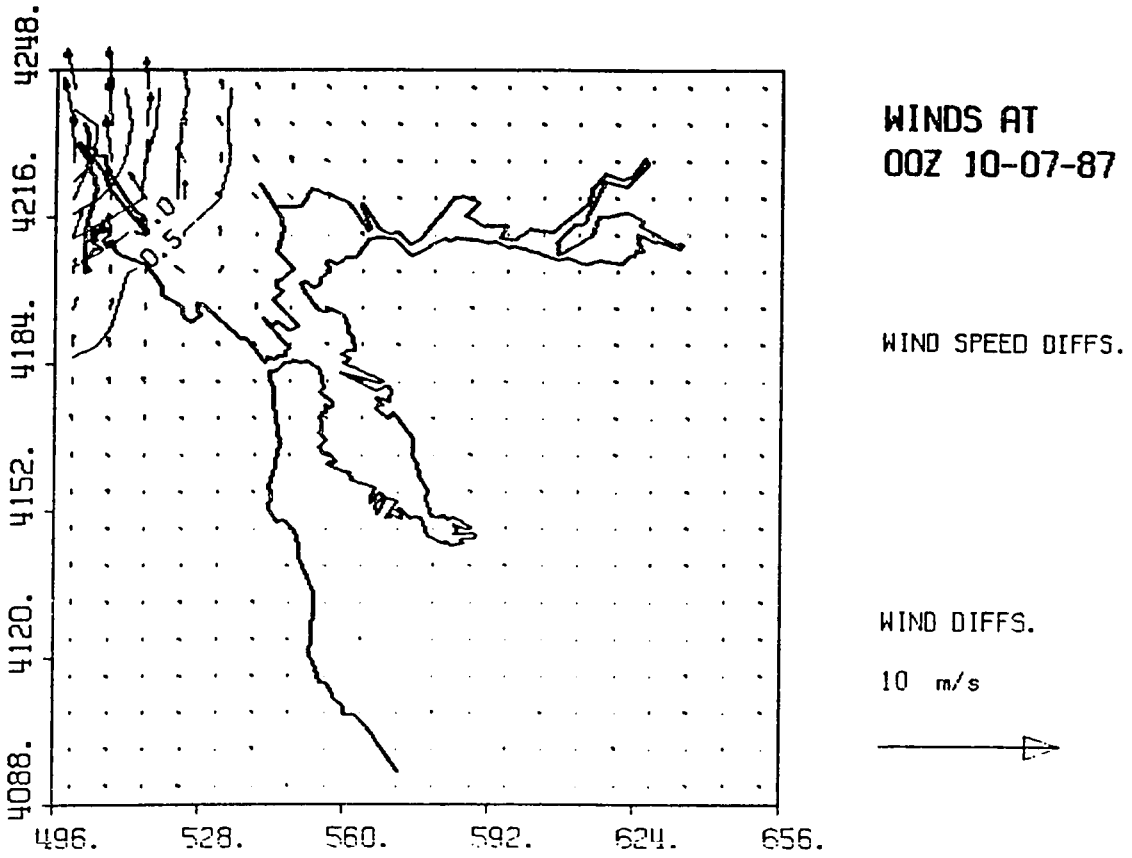

Figure 3-39 Vector difference plot of Figure 3-8 minus Figure 3-38.

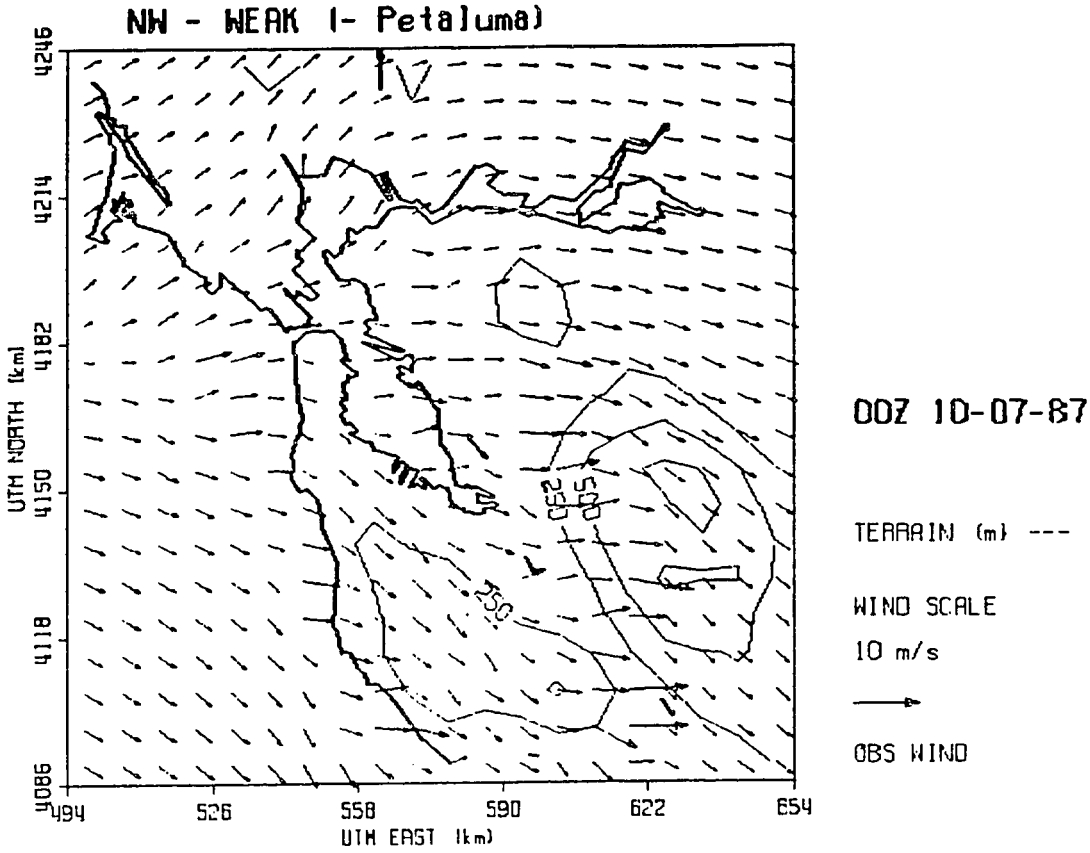

Figure 3-40 Same as Figure 3-34, but with Petaluma deleted.

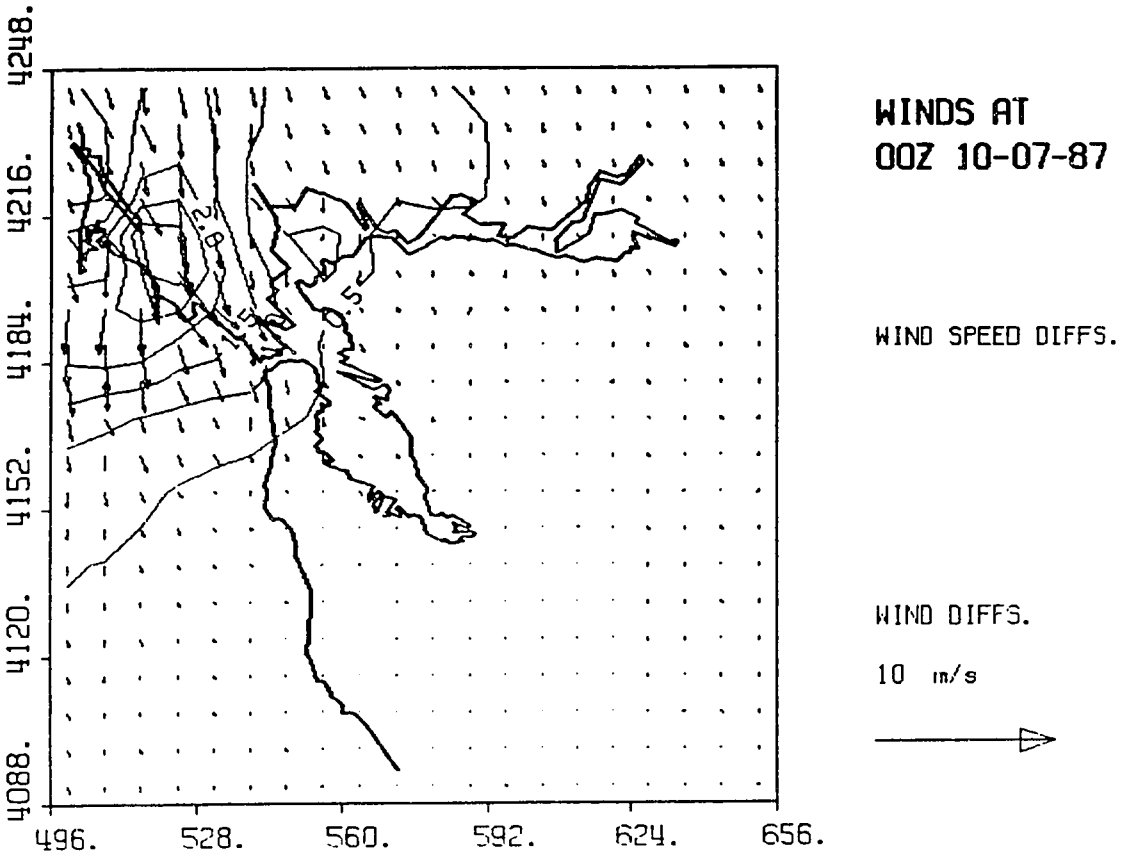

Figure 3-41 Vector difference plot of Figure 3-8 minus Figure 3-40.

Union City Deleted

In this test, wind data from Union City (UTM coordinates 582,4161) were deleted from the standard data set. Observed winds at Union City were 318° at 4.0 ms^{-1}. The resulting winds are shown in Fig. 3-42. The flow in the east bay is now determined by the northwesterly winds at Oakland and San Jose. Figure 3-43 shows that vector differences are slight, and are concentrated near the Santa Cruz gap. Table 3-25, Appendix C shows a slight decrease in model wind direction accuracy over the basic case, with a modest improvement in speed accuracy (81.3% vs. 81.9%).

San Jose Airport Deleted

In this test, wind data from San Jose Airport (UTM coordinates 595,4135) were deleted from the standard data set. Observed winds were 330° at 3.1 ms^{-1}. The resulting winds are shown in Fig. 3-44. As expected, the omission of this northwesterly observation leads to a slight increase in the westerly component over the Santa Cruz mountains, although the effects are slight (see Fig. 3-45). Table 3-26, Appendix C indicates only slight impact on model performance by the omission of data from San Jose Airport.

San Martin Deleted

In this test, wind data from San Martin (UTM coordinates 625,4104) were deleted from the standard data set. Observed winds were 324° at 3.1 ms^{-1}. The resulting winds are shown in Fig. 3-46. Figure 3-47 indicates that

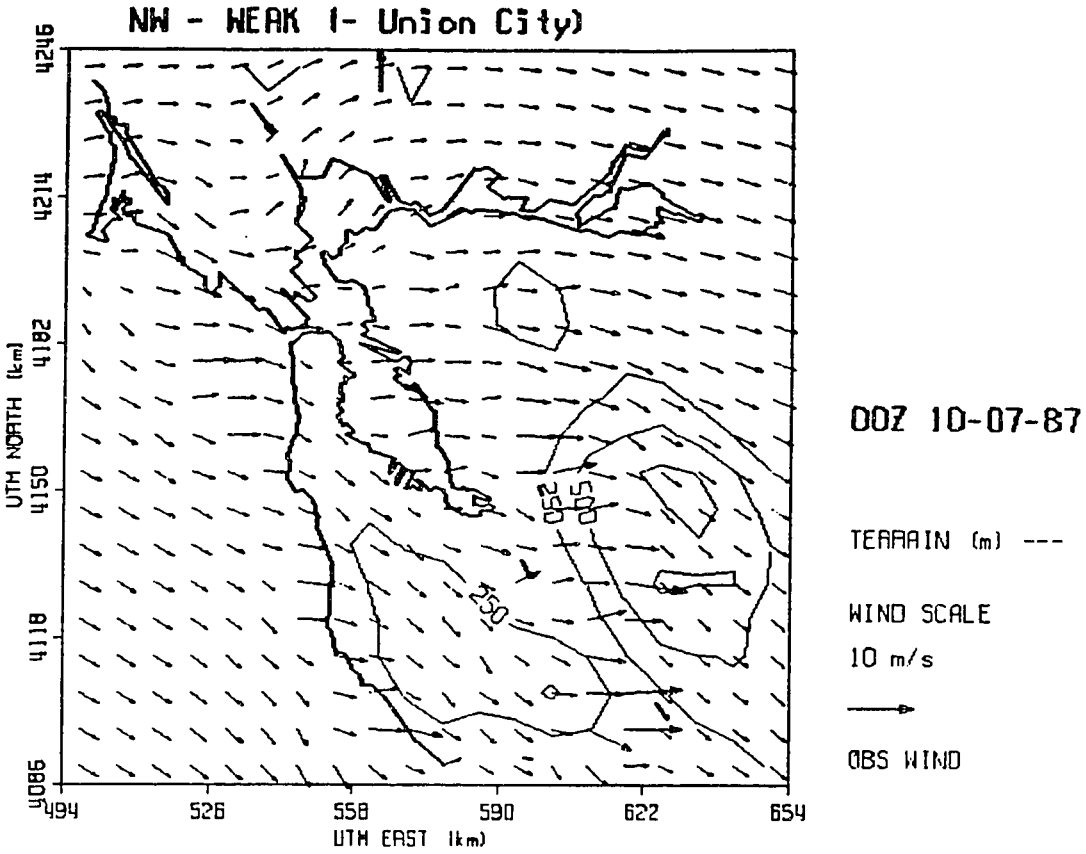

Figure 3-42 Same as Figure 3-34, but with Union City deleted.

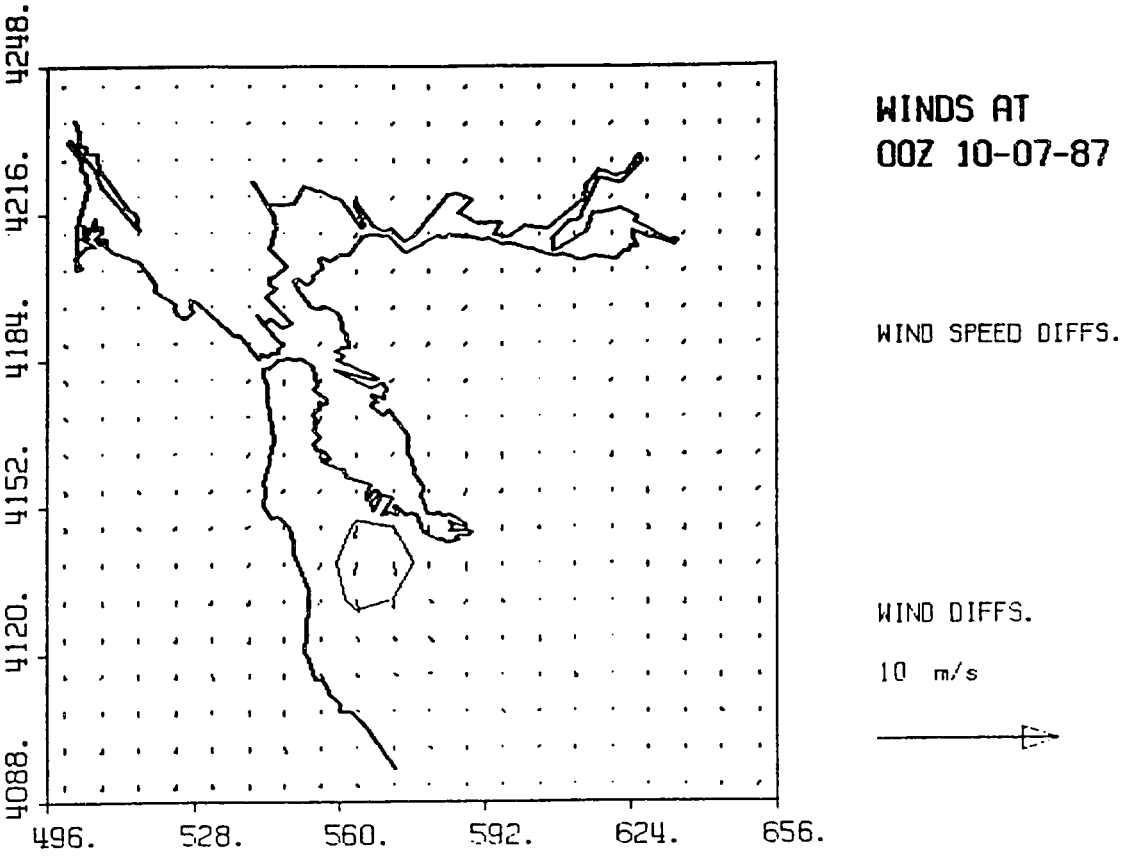

Figure 3-43 Vector difference plot of Figure 3-8 minus Figure 3-42.

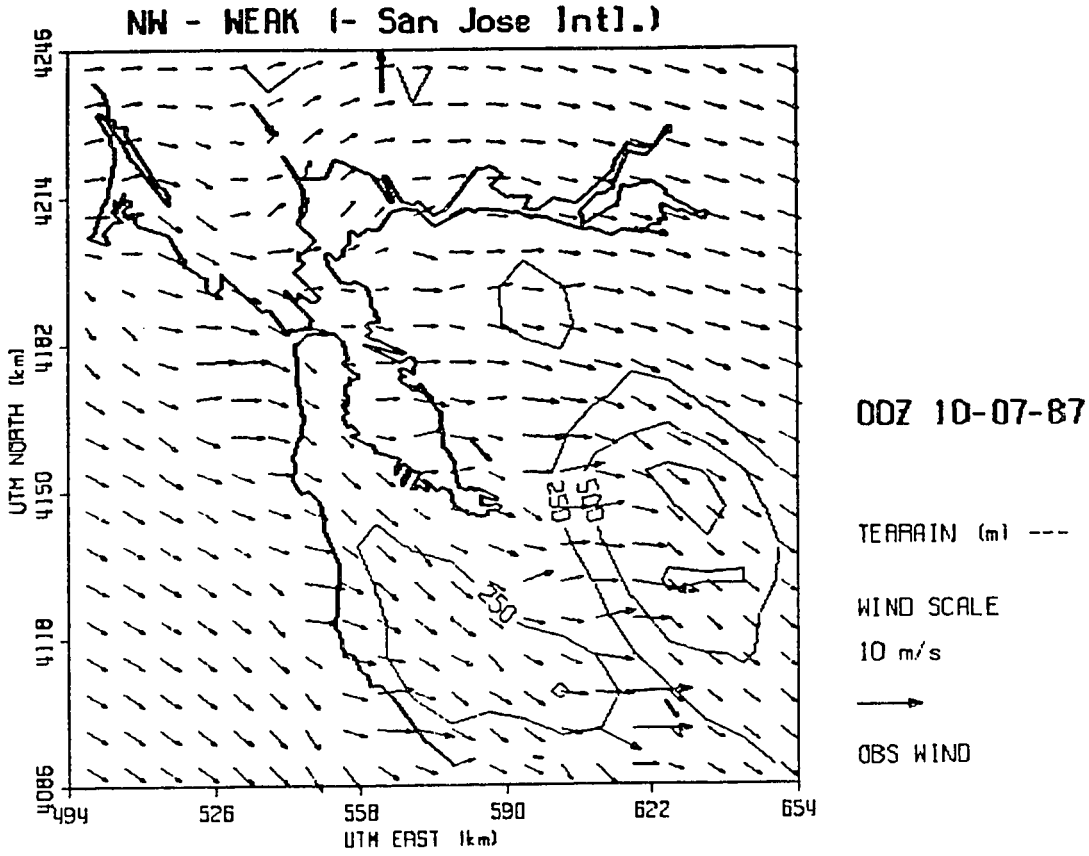

Figure 3-44 Same as Figure 3-34, but with San Jose Airport deleted.

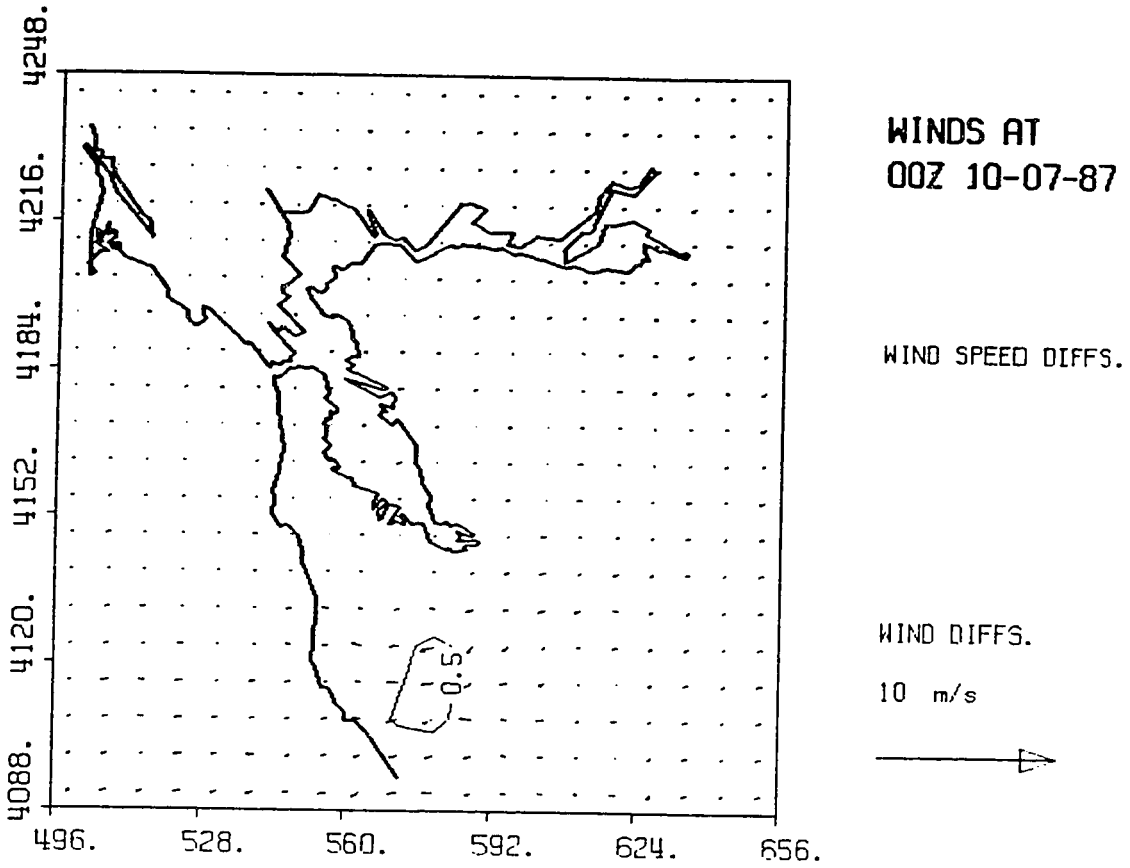

Figure 3-45 Vector difference plot of Figure 3-8 minus Figure 3-44.

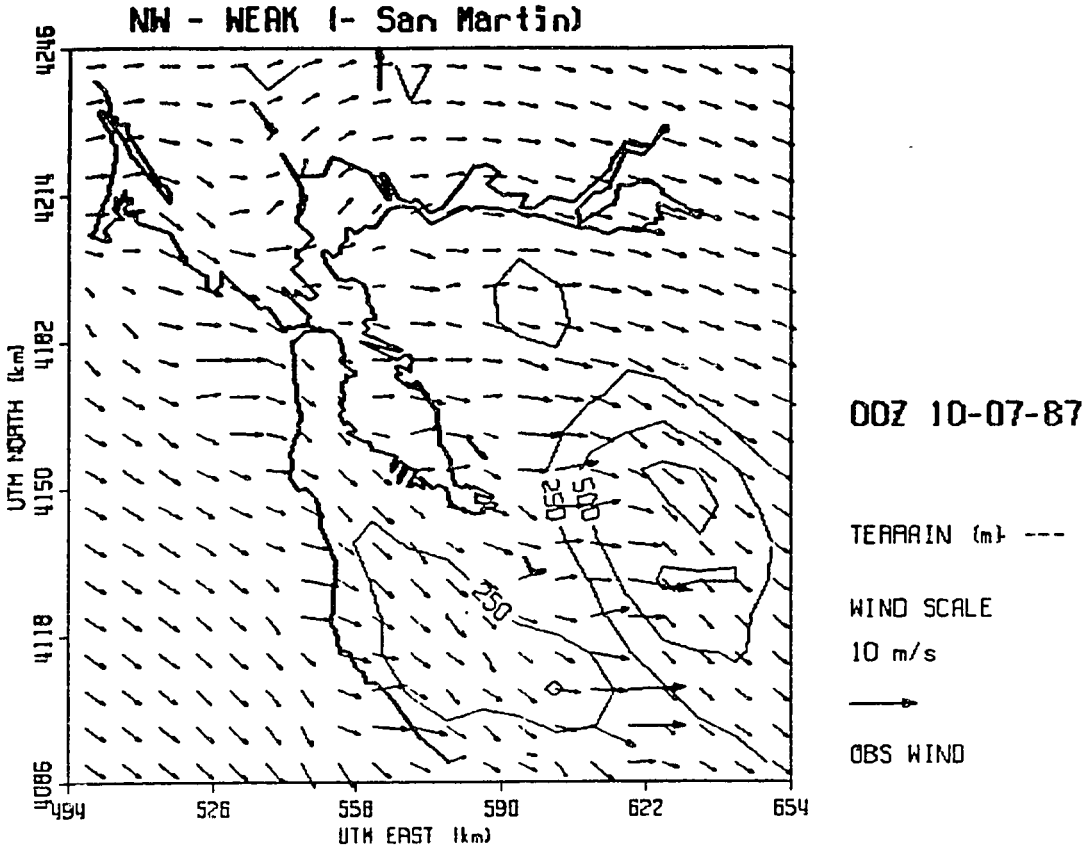

Figure 3-46 Same as Figure 3-34, but with San Martin deleted.

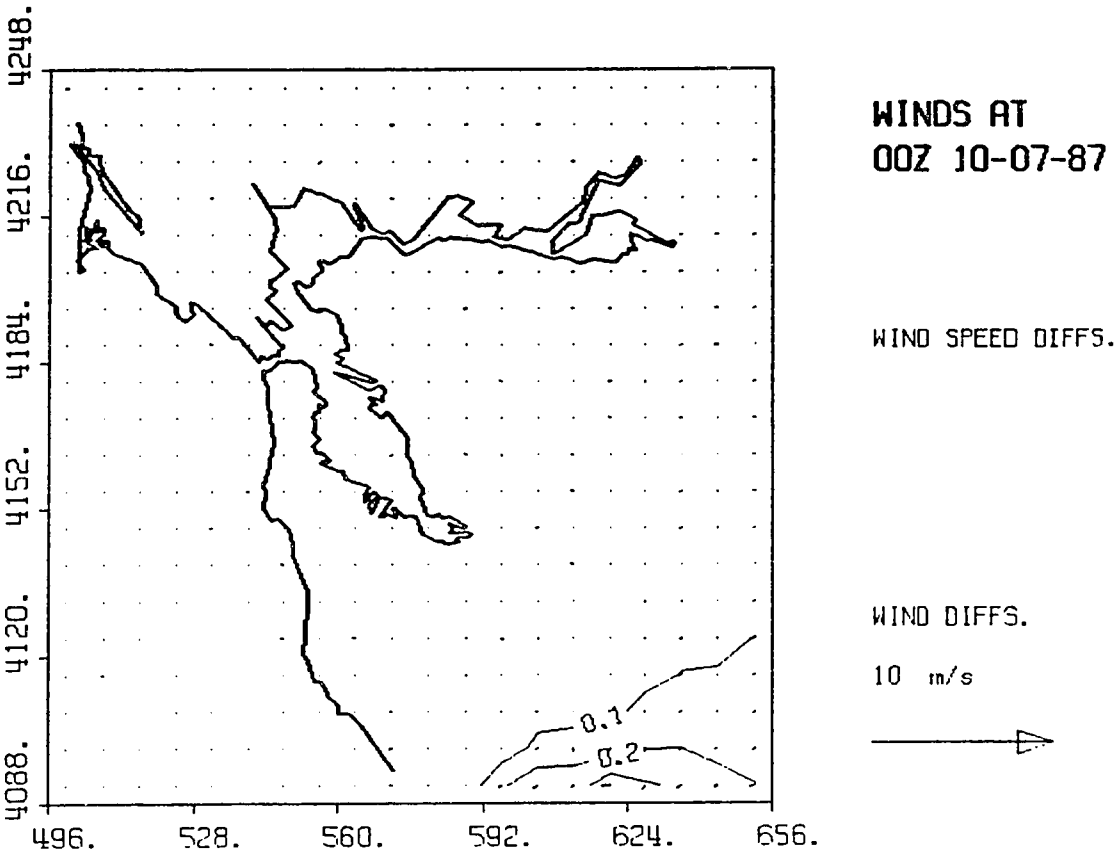

Figure 3-47 Vector difference plot of Figure 3-8 minus Figure 3-46.

vector differences between this run and the basic case are limited to the extreme southeast corner of the domain. The lack of change in the San Martin area is likely due to the fact that San Martin's winds are aligned with the Santa Clara valley, and thus provide no real impact to the mass balancing in this narrow valley region. Table 3-27, Appendix C shows a slight improvement in model direction accuracy (4.5% vs. 5.5%) over the basic case, but perhaps this is because the statistics lack San Martin, where model performance was particularly good.

Oakland Deleted

In this test, wind data from Oakland (UTM coordinates 569,4173) were deleted from the standard data set. Observed winds at Oakland were 300° at 3.6 ms^{-1}. The resulting winds are shown in Fig. 3-48. There is very little influence on the resulting flow on this occasion since the northwesterly flow toward the south bay is already defined by the Union City data. Changes are limited to the domain west of the southern SFBA (see Fig. 3-49). Table 3-28, Appendix C shows results similar to the San Martin case discussed above.

Oakland, Union City, and San Jose Airport Deleted

In this final test, wind data from Oakland, Union City and San Jose Airport were deleted from the standard data set. There are now no wind reports to guide the model in steering flow southeastward to the south bay. The resulting winds are shown in Fig. 3-50, and indicate that flow across

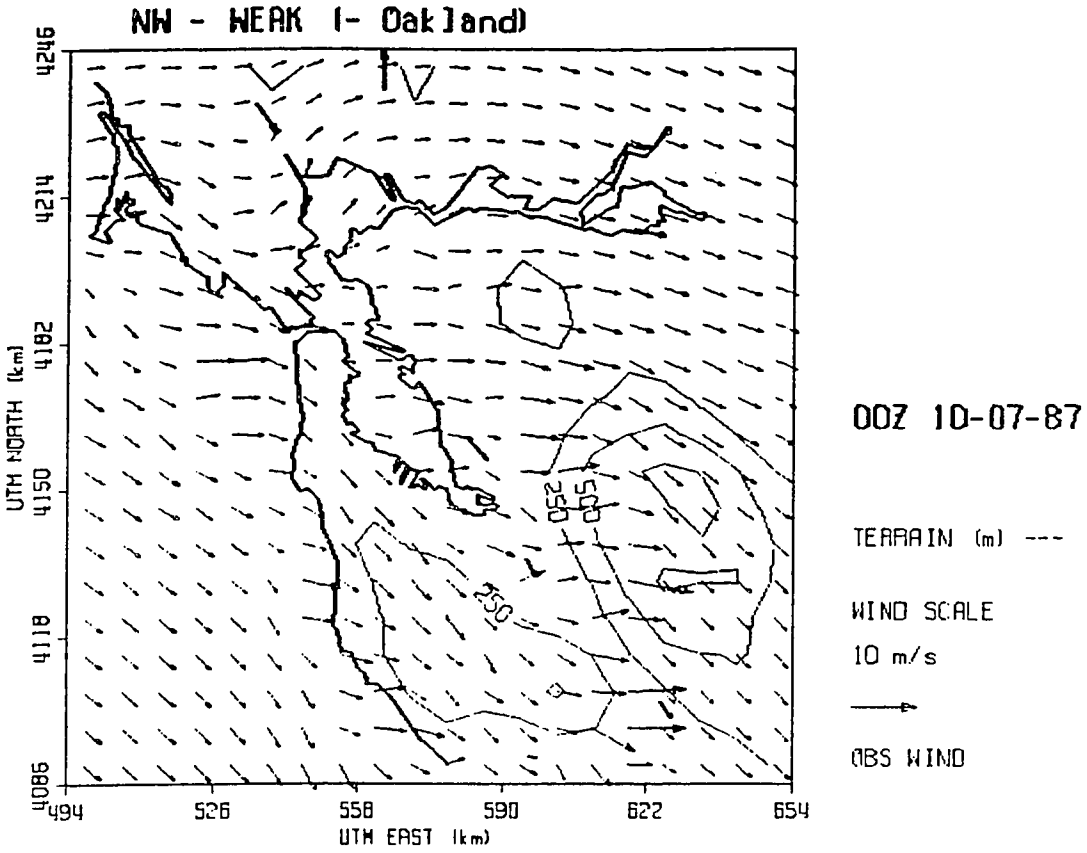

Figure 3-48 Same as Figure 3-34, but with Oakland deleted.

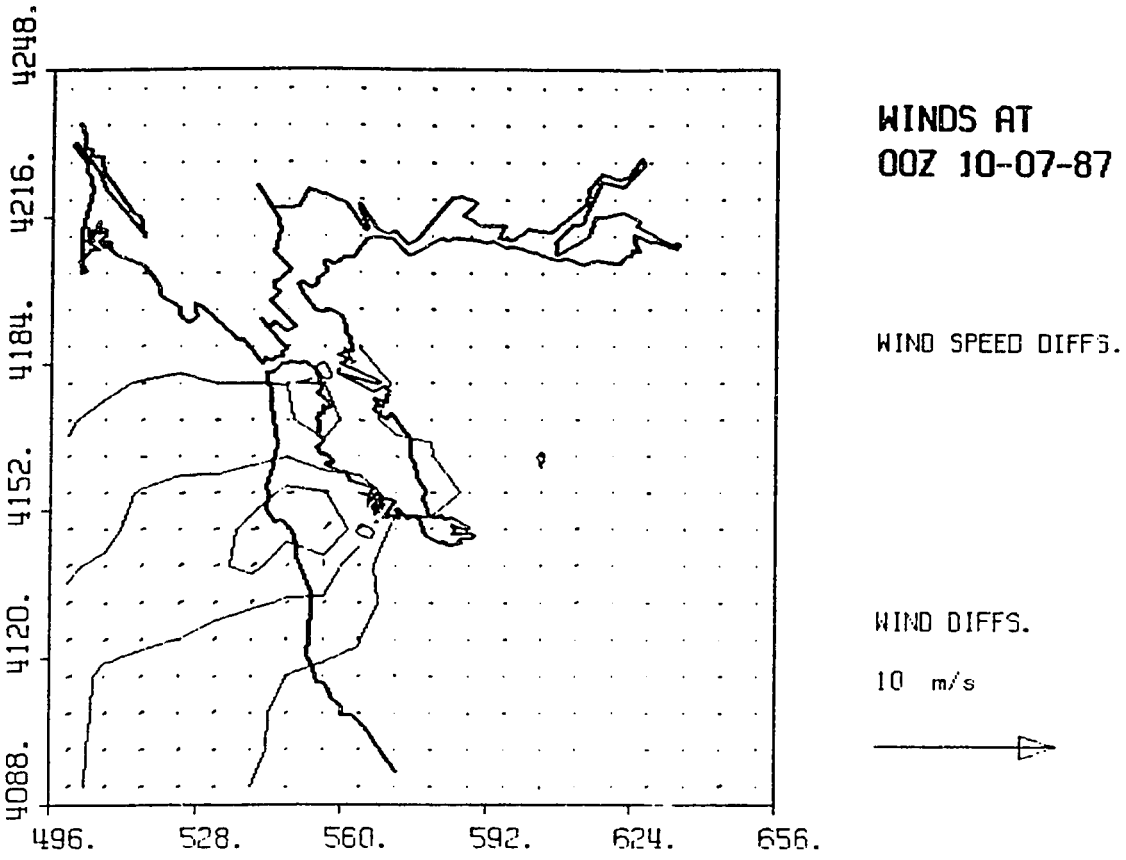

Figure 3-49 Vector difference plot of Figure 3-8 minus Figure 3-48.

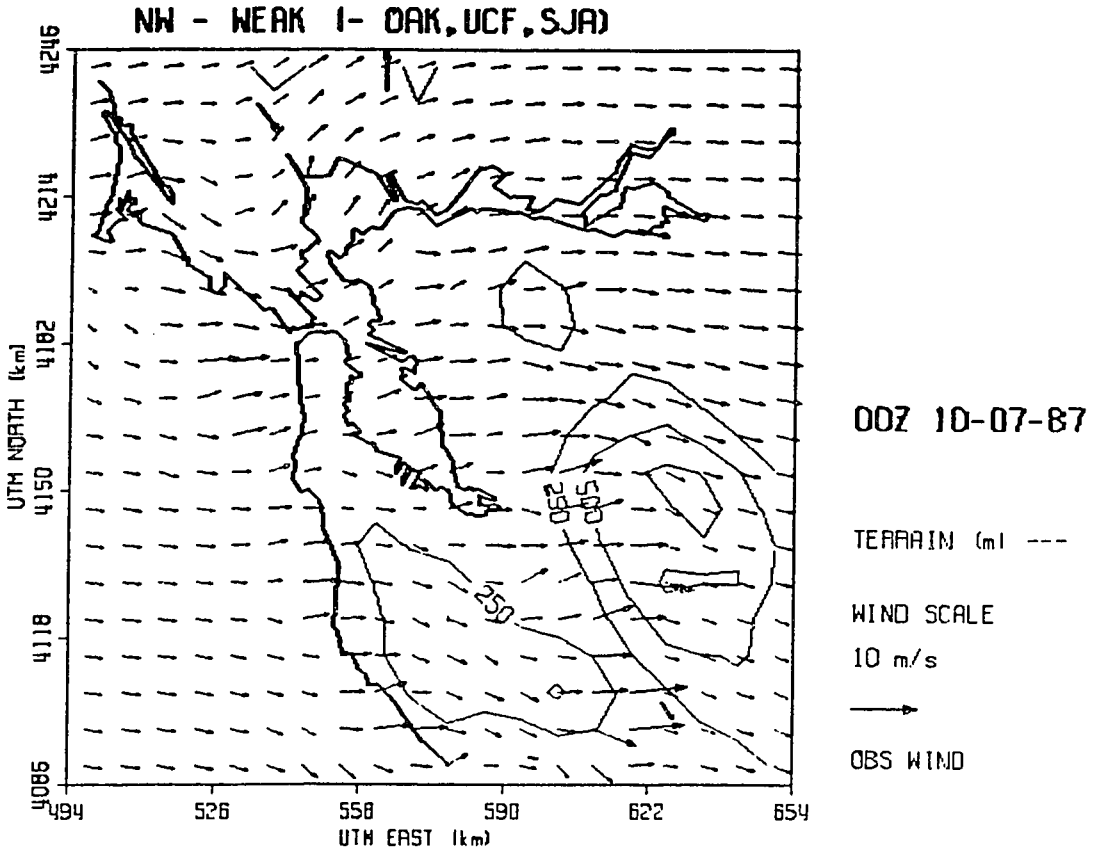

Figure 3-50 Same as Figure 3-34, but with Oakland, Union City, and San Jose Airport deleted.

much of the SFBA now has a more westerly component, especially in the region from Richmond to San Jose. Figure 3-51 shows that vector differences are observed throughout the region, but appear focused over the ocean, the peninsula hills and Santa Cruz mountains, and near the Mt. Hamilton range. Table 3-29, Appendix C indicates results rather similar to the Oakland and San Martin cases above. While directions were fairly good (-4.8%), the speed ratio (74.8%) was the worst of all cases.

Summary

In general, it is seen that in most cases, deletion of stations reduces model speed accuracy, affecting primarily upstream stations. The tabulated results indicate that Bethel Island, San Martin, Oakland, and, to a lesser extent, Union City and San Jose, are important stations to retain; their exclusion degrades model directional accuracy (see Table 3-30 for a summary of wind analyses). It appears that data from Napa, Santa Rosa, and Petaluma may best be deleted since their absence leads to a good model/observed speed ratio (even though directional accuracy is mildly degraded). These conclusions may only apply to this particular type of synoptic flow pattern; further testing with other flow situations is recommended. It may be that by extending the model domain northward, retaining the North Bay stations will lead to improved model performance.

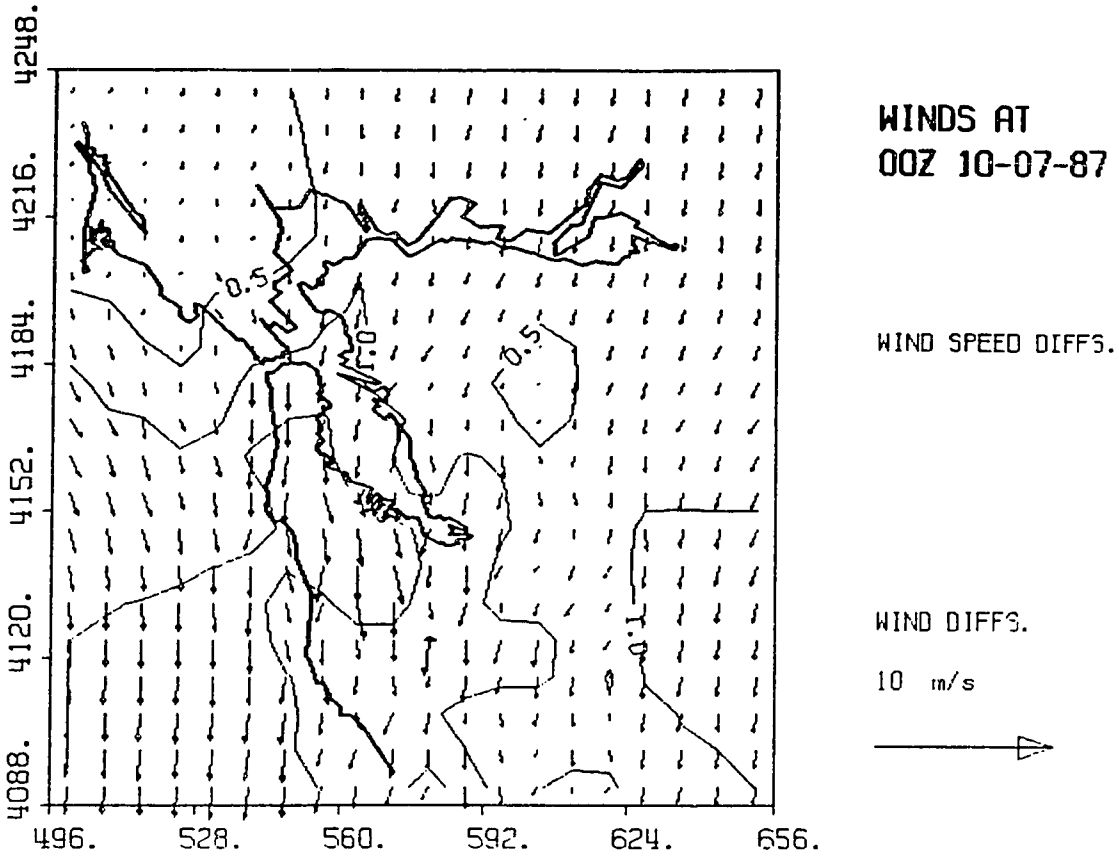

Figure 3-51 Vector difference plot of Figure 3-8 minus Figure 3-50.

f. **Effect of Resolution on Results**

In order to examine the effect that resolution has on model performance, WOCSS was run using the same data as in the previous tests (weak northwesterly), but with differing resolutions. Fig. 3-52 shows model output at 10 km resolution (compare to Fig. 3-8 at 8 km resolution), and Fig. 3-53 shows model output at 5 km resolution (but with every other vector in the domain plotted). Finally, Fig. 3-54 shows model output at 5 km resolution, but with all vectors plotted (in this run, vectors are scaled smaller for clarity).

A comparison of Figs. 3-52 and 3-53 indicates that the 5 km run is slightly superior to the 10 km run. This is verified by the results in Tables 3-31 and 3-32 (10 km and 5 km cases, respectively). The 5 km run shows an average directional error of -3.9%, while the corresponding result at 10 km resolution is -4.7%. The ratio of model/observed wind speeds is quite similar, with the 5 km run at 68.2% (slightly worse than the 10 km run at 72.8%). Note that while both runs show improved directional accuracy over the 8 km resolution run, the speed ratio is worsened in both cases. The real value of increased resolution on model output can be seen in the fine resolution plot (Fig. 3-54), where small directional details in the flow (which were not produced in the 10 km case) can be discerned. For example, flow acceleration over Mt. Umunhum (approximate UTM

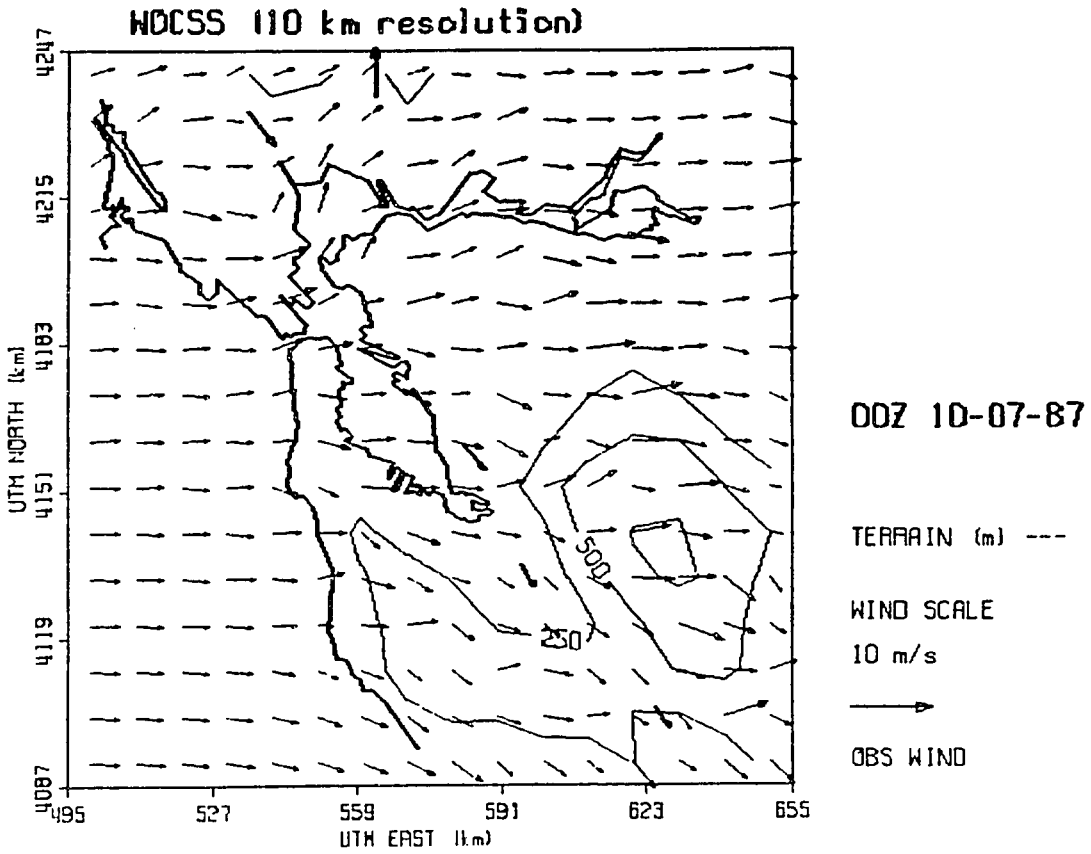

Figure 3-52 Plot of Weak Northwesterly case (October 7, 1987, 00 GMT), as in Figure 3-8, but at 10km resolution.

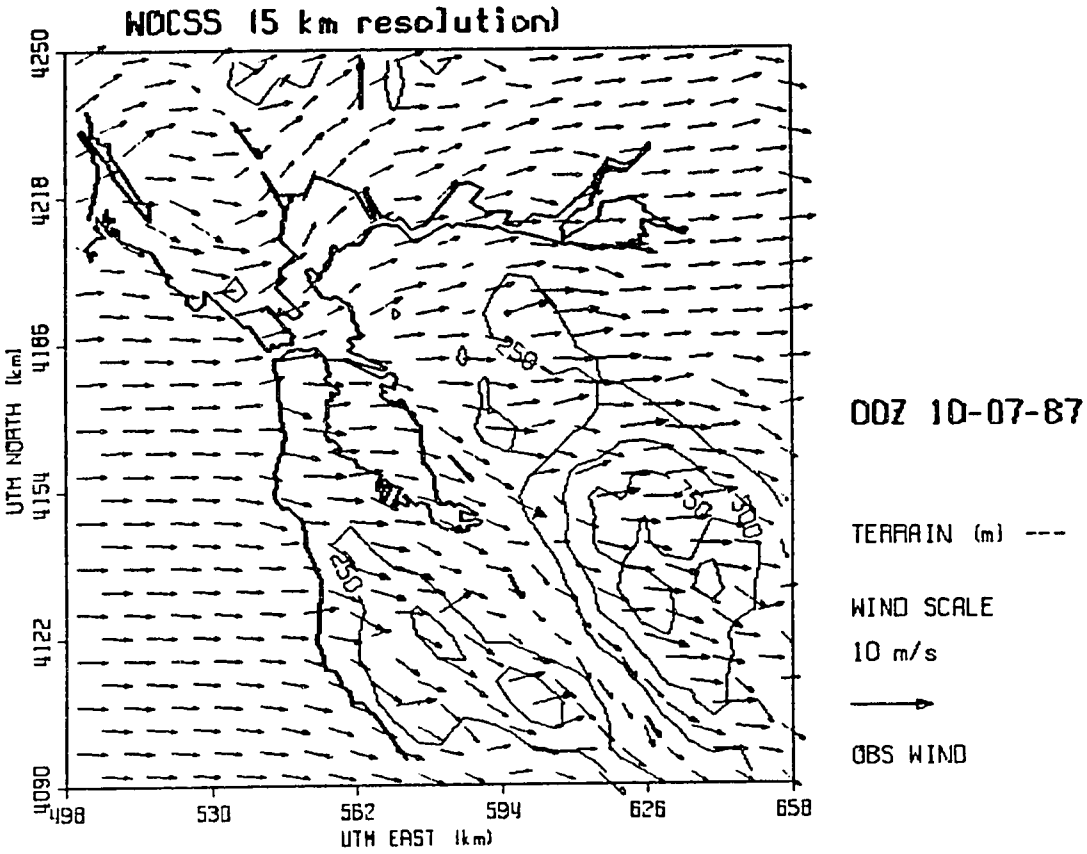

Figure 3-53 Same as Figure 3-52, but at 5km resolution (every other vector plotted).

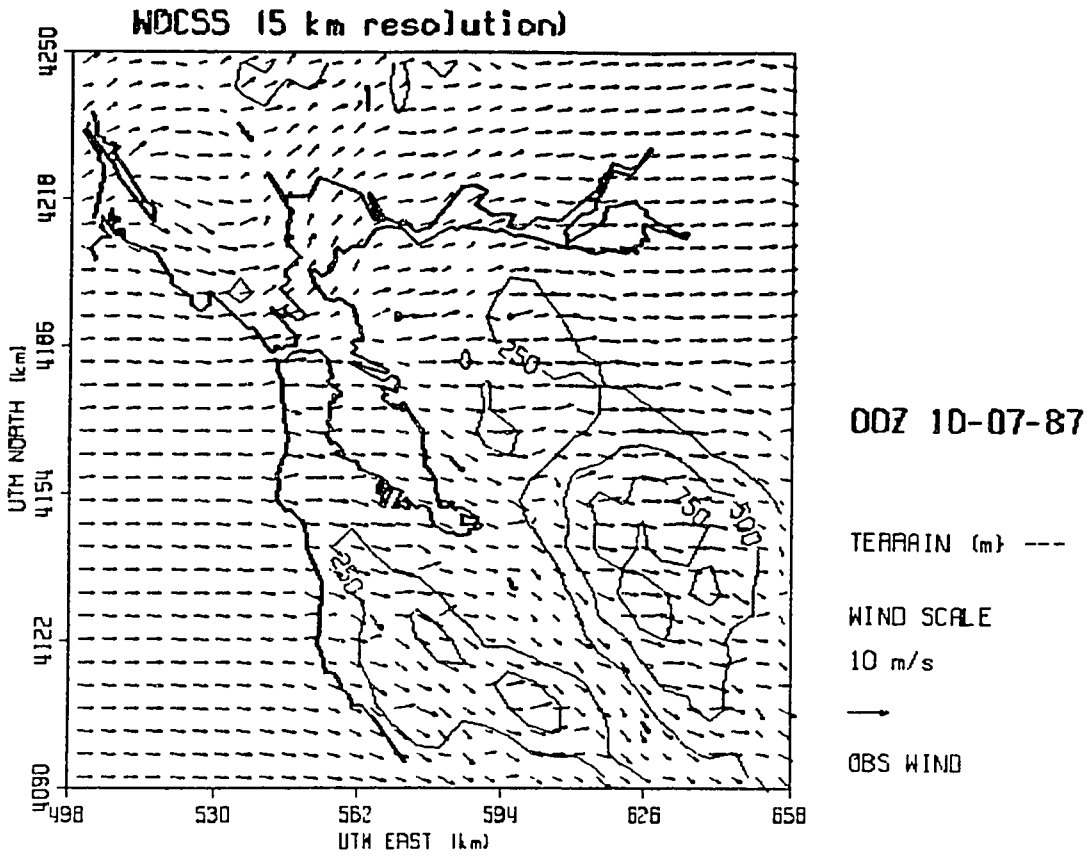

Figure 3-54 Same as Figure 3-53 (but all vectors plotted).

coordinates 580,4120) is seen in the 5 km case, as is channeling through the Carquinez gap (UTM 570,4210). The utility of the finer resolution model runs would be seen best in such applications as input to dispersion models, where the fine details would undoubtedly improve dispersion assessment. However, the user must weigh the relative merits of speed accuracy and directional accuracy at the different resolutions to achieve the best results from WOCSS model output.

g. Summary of San Francisco Bay Area cases

After extensive testing, we have seen WOCSS model output responds positively to carefully selected input data. WOCSS is able to closely reproduce many of the common SFBA flow types. By increasing data density in selected areas (e.g., in the southern SFBA), model accuracy in those areas can be improved. Generally, WOCSS performs best when using data from several stations throughout the domain. In a test of a limited data set, adding data from certain weather stations was seen to degrade or improve overall model performance. It was also found that deleting certain stations near the edge of the domain (e.g., Santa Rosa) generally enhanced overall model results. Further testing of the model under other synoptic conditions (especially at increased resolution) will identify those stations which are most crucial to optimum model performance.

4. MODEL IMPROVEMENTS

a. Inclusion of Inversion Topography into the Winds on Critical Streamline Surfaces (WOCSS) Model

Normally, boundary layer thicknesses are generated internally within WOCSS based on a single temperature sounding. However, it cannot generally be expected that one sounding can provide adequate representation of the complicated boundary layer structure known to exist over the SFBA. To address this problem, the model has been modified (by Ludwig and Endlich, 1988) to accept multiple temperature soundings. However, since adequate data of this type is not normally available in the SFBA, another approach is taken in the current research. Using detailed inversion topography data from the MABLES dataset boundary layer thicknesses over the domain are externally prescribed to WOCSS. This is done in order to explore the effect that boundary layer thickness and thickness variations may have on the accuracy of modeled surface winds in the SFBA. Model runs using the prescribed inversion topography (hereafter referred to as RDBLT runs) are compared with normal runs (those using a single temperature sounding to define flow surfaces).

Prior to running an actual case for the SFBA, preliminary tests have been performed using simple inversion topographies in order to examine and verify expected effects. The motivation for this approach stems from the fact that initial tests for the SFBA using MABLES inversion

topography data produced only slight differences in winds between normal runs and RDBLT runs. We therefore tested the effects that certain terrain and/or inversion features (i.e., those most likely to be encountered in the SFBA under normal circumstances) would have on model results. It should be recalled that Muranaka (1988) had achieved encouraging results with a similar approach, using a prescribed inversion topography (see Fig. 4-1) in his study of strong downslope windstorms. Muranaka found model wind speeds reasonably close to observed speeds, with the strongest winds directly below the lowest point of the inversion base trough.

Modification of WOCSS to accept inversion topography

The reading of inversion topography data by WOCSS is performed by the same subroutine which reads terrain data (TOPO). To enable reading of the inversion data, a few internal program settings are required: (1) the number of temperature soundings must be set to zero, and (2) an instruction to read the inversion data must be given (by setting RDBLT to "TRUE"). This then causes the program to skip the initial boundary layer thickness interpolation procedure (usually based on the temperature sounding). WOCSS thereafter continues with the normal iterative adjustments to boundary layer thickness (e.g., in the mass-balancing subroutine).

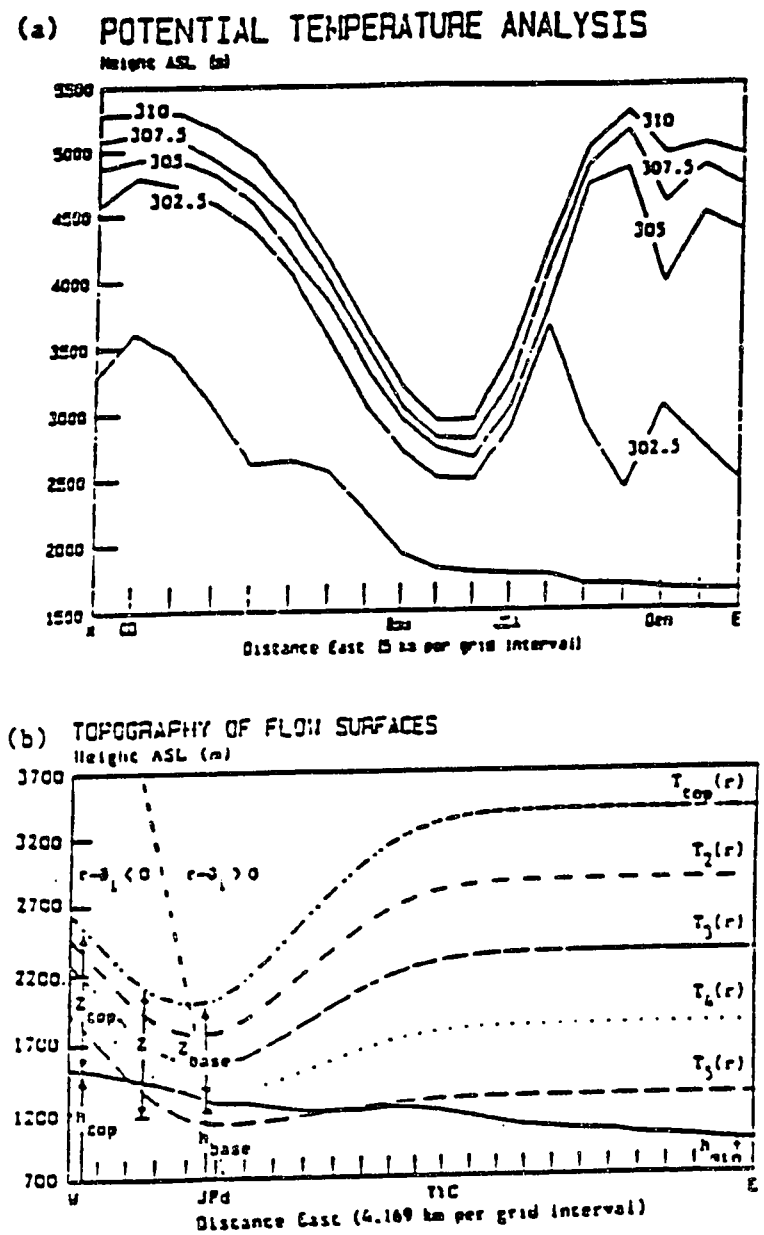

(a) Potential temperature analysis from Boulder windstorm of 11 January 1972 (after Lilly and Zipser, 1972). Potential temperature isopleths are drawn at 2.5 K intervals. The analysis extends from the Continental Divide (CD) through Boulder (Bou), Jefferson County Airport (JCA), and Denver (Den). (b) Schematic cross section of model flow surfaces illustrating terrain height and layer thickness parameters. The upstream tilt of the hydrostatic wave trough axis is represented by a thin dashed line.

Figure 4-1 Potential temperature analysis and topography of flow surfaces (from Muranaka, 1988).

Inversion Data

During the MABLES observation period (8-10 August 1978), extensive data from aircraft, tower, ship- and land-based SODAR (acoustic radar) were collected along the central coast of California (Lester, 1985). From this data, Erickson (1981) constructed topographies of the elevated marine inversion, using a conceptual model of the inversion suggested by many prior researchers (e.g., Miller, 1968; Russell and Uthe, 1978). Erickson merged MABLES WC data, accounting for the large variety of instrumentation and their respective biases. He prepared inversion topography maps for 1600 LST, 8-9 August 1978, and 0800 LST, 10 August 1978 in order to document diurnal variations and utilize maximum data density. The 1600 LST, 9 August 1978, data is used here. Erickson's analysis is shown in Fig. 4-2; height contours represent heights above sea level. The figure illustrates the structure of SFBA inversion topography, with low base heights over the San Francisco and San Pablo Bays and the Salinas valley. The inversion is higher over elevated terrain. The sparse analysis west of San Francisco is based on the limited aircraft data. The domain of Erickson's plots is a rectangular area from latitude 36°30'N to 38°15'N and from longitude 121°15'W to 125°W.

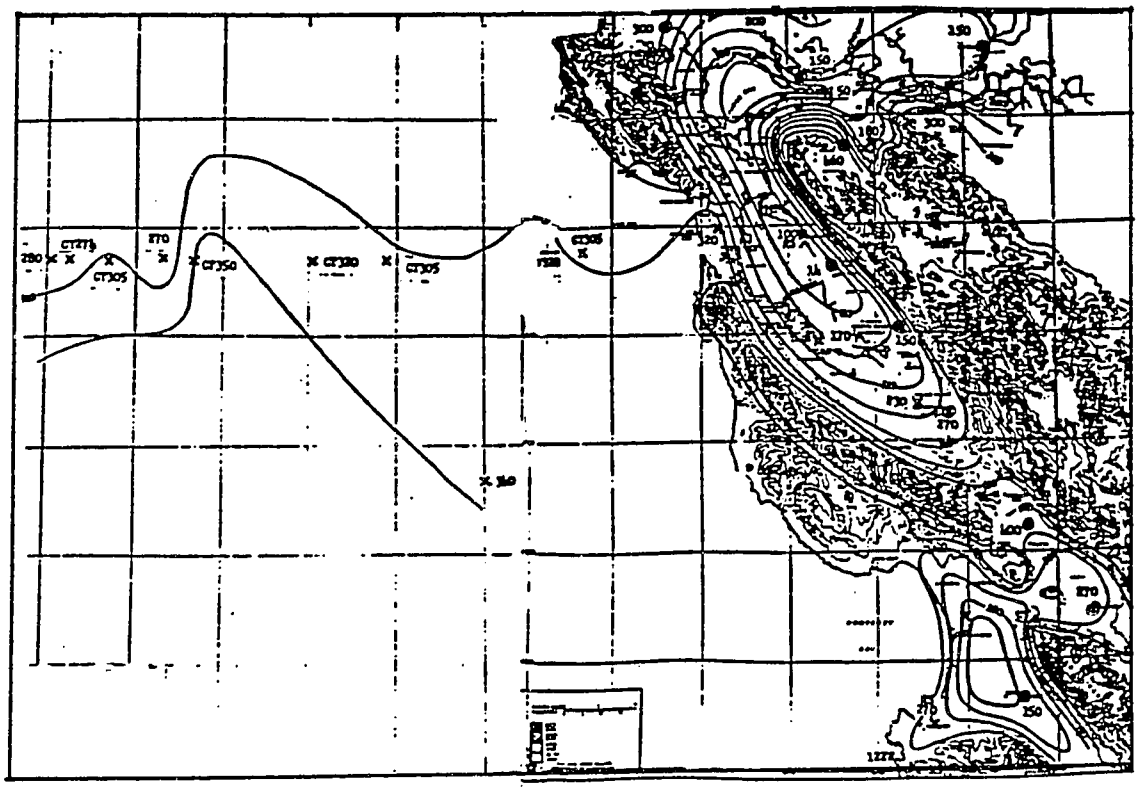

Figure 4-2 Plot of inversion topography for August 10, 1978, 00 GMT; heights ASL (from Erickson, 1981).

Erickson's analyses were based on the available data. In cases where there were discrepancies between data from different sources, the analysis was subjectively weighted in favor of the more reliable data (e.g., SODAR over aircraft data). Further modifications were guided by analyses prepared by Ahrens and Miller (1969) and Russell (1979), especially in data-sparse areas. Finally, isopleths were smoothed as a compromise between the data, the conceptual models, and temporal continuity between data sets.

The inversion plots of Erickson were digitized to obtain data at 4 km resolution. The southwest corner of the domain is at UTM coordinate 500,4072; the northeast corner is at UTM 632,4236. Also created were data for use with SURFER plotting software; the UTM coordinate of the southwest corner of this domain is at 500,4092. Fig. 4-3 is a SURFER plot of inversion topography (heights AGL); it is equivalent to Erickson's plot (Fig. 4-2), with missing data assumed to closely follow the higher terrain. Figure 4-4 is of the same data, but with heights MSL.

A program was devised to read the 4 km inversion data and convert it to 4, 5, and 8 km resolution for input to WOCSS. In cases of incomplete or missing data near the eastern edge of the SFBA, the boundary layer thickness was kept to at least 30 m AGL using the closest available data to establish local boundary layer slope trends, which were

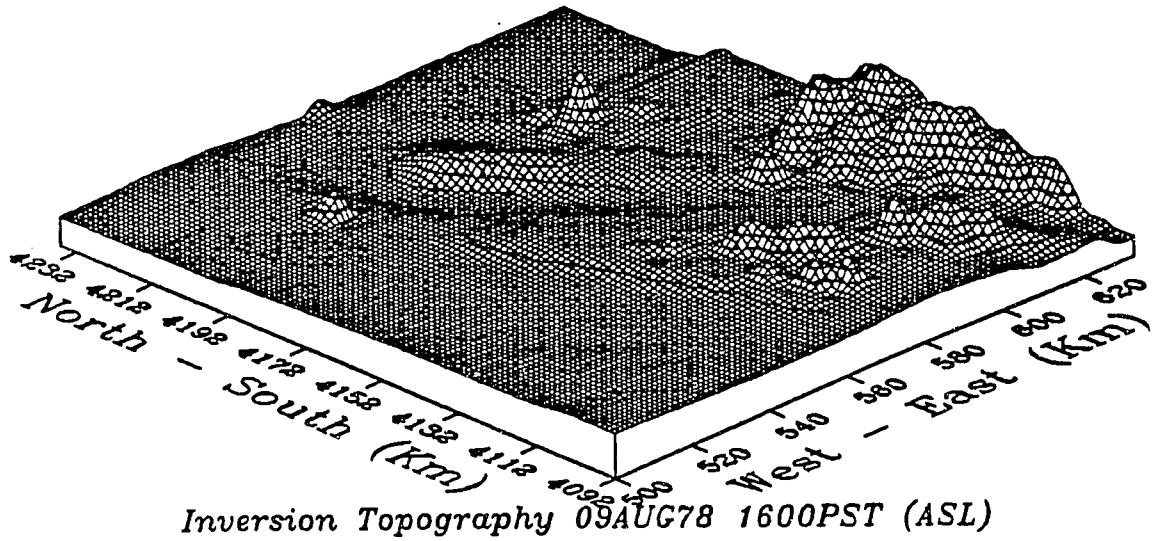

Figure 4-3 SURFER plot of inversion topography (heights, ASL) for August 10, 1978, 00 GMT.

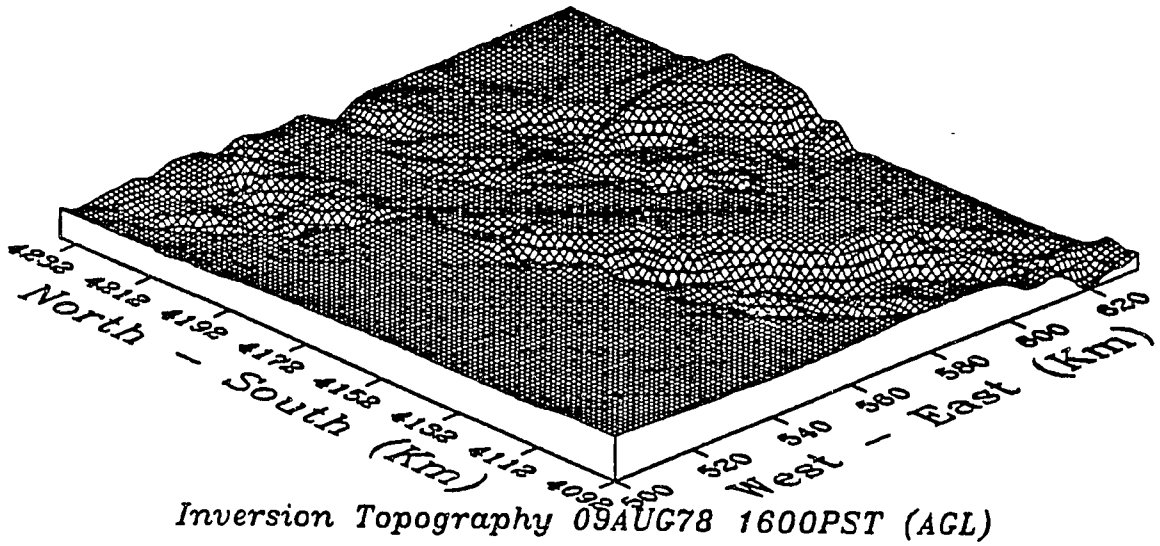

Inversion Topography 09AUG78 1600PST (AGL)

Figure 4-4 Same as Figure 4-3, but heights AGL.

then extrapolated to fill in data gaps. (See Appendix B-3 for code).

Experimental Procedures

An initial set of experiments was conducted with simple prescribed inversion data, and with westerly winds prescribed on the western edge of the domain as input. The terrain and inversion shapes used are detailed in each case below. Experiments with real flows were then conducted at 8 km resolution using the detailed inversion topography data available from the MABLES WC observation period. The output was compared to WOCSS runs that did not use prescribed inversion topography.

Discussion of simple cases

i. Cone Terrain, Squeezed Cone Inversion

In this case, a 250 meter hill is centered in the domain, with the inversion base "squeezed" over the hill (100 m thickness over the hilltop and 200 m over the surrounding flat terrain). Figure 4-5 shows the surface wind output for this test. Some speed decrease is seen upwind of the cone. It is also seen that some flow is forced around the obstacle. Fig. 4-6 shows a west-east cross section of this case, showing terrain (heavy curve) and flow surfaces (light curves). It should be noted that flow surface #1 coincides with sea level, and cannot be seen. Flow surface #5 represents the prescribed inversion topography. Surfaces #2, #3, #4, and #6 are determined in accordance with the

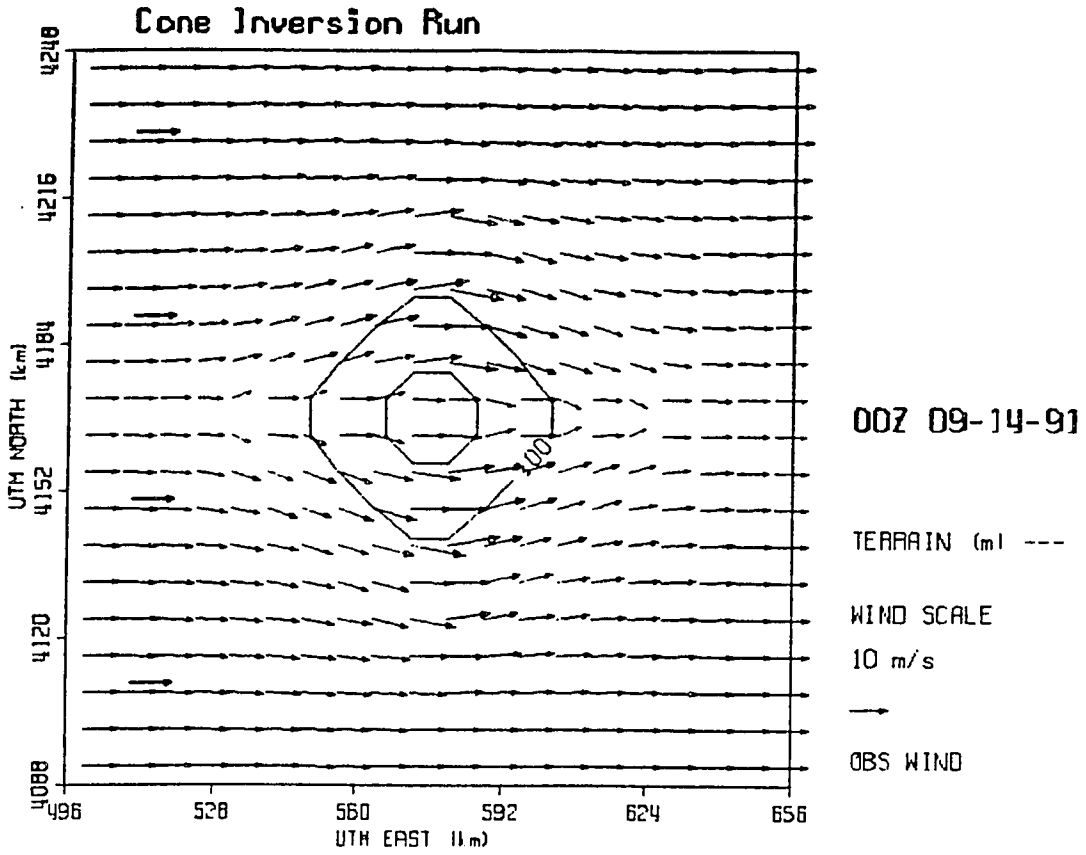

Figure 4-5 Plot of model winds for cone terrain case.

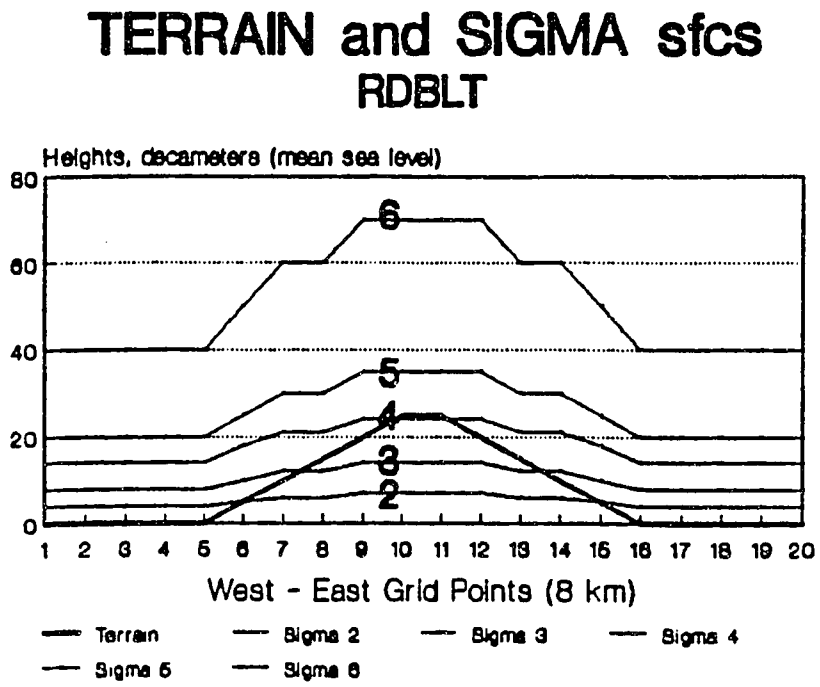

Figure 4-6 West-east cross section of sigma surfaces (light curves) and terrain (heavy curve) for cone terrain case.

critical streamline concept discussed in Chapter 2. Figure 4-7 shows that wind speeds decrease just upwind of the cone, but fluctuate as the top is approached. Speeds are constant over and in the lee of the top, but then fluctuate again downwind. This fluctuation is likely due to the method used for determining anemometer wind speeds (described in Chapter 2), which is sensitive to the separation distance between the ground and the flow surface immediately above. At upwind grid points where the flow surfaces intersect the topography, the anemometer speeds are seen to fluctuate. Downwind, the fluctuation is possibly due to the irregularly-converging flow. In general, the results are encouraging in that speeds increase over the high terrain, where flow surfaces are squeezed as they tend to ascend the terrain obstacle. In the lee of the cone, speeds drop as flow surfaces begin to spread further apart.

ii. Trough Terrain, Inverted Trough Inversion

In this case, a gently sloped north-south valley is placed down the center of the domain. A trough-shaped inversion is placed so that smaller thicknesses are over the valley and increasing thicknesses ascend the higher terrain to the west and east. Figure 4-8 shows the model output for this case. The model winds are mainly from the west, but there are some directional fluctuations along the northern and southern edges of the domain, caused by the mass-balancing routine. Figures 4-9 and 4-10 show the west-east

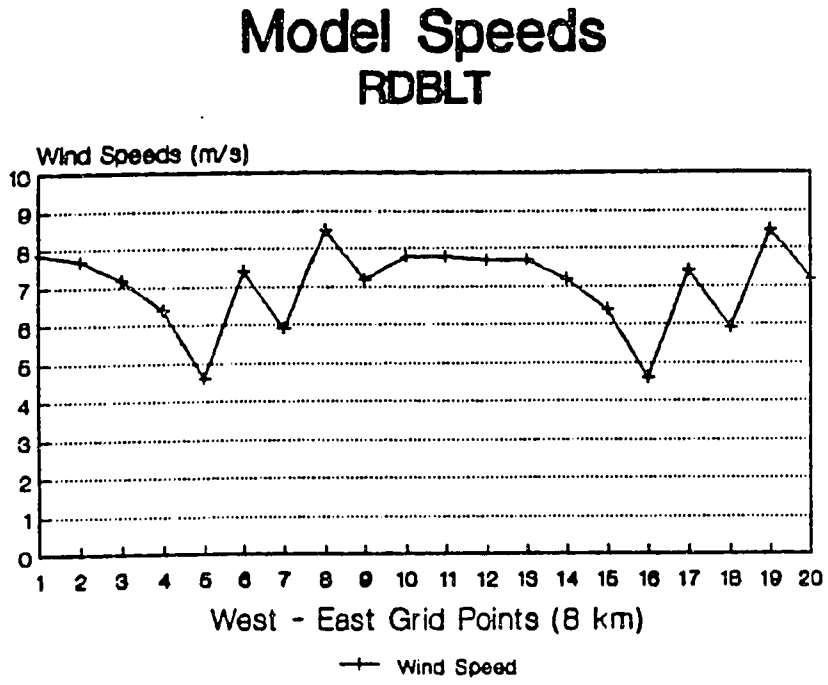

Figure 4-7 West-east cross section of model speeds for cone terrain case.

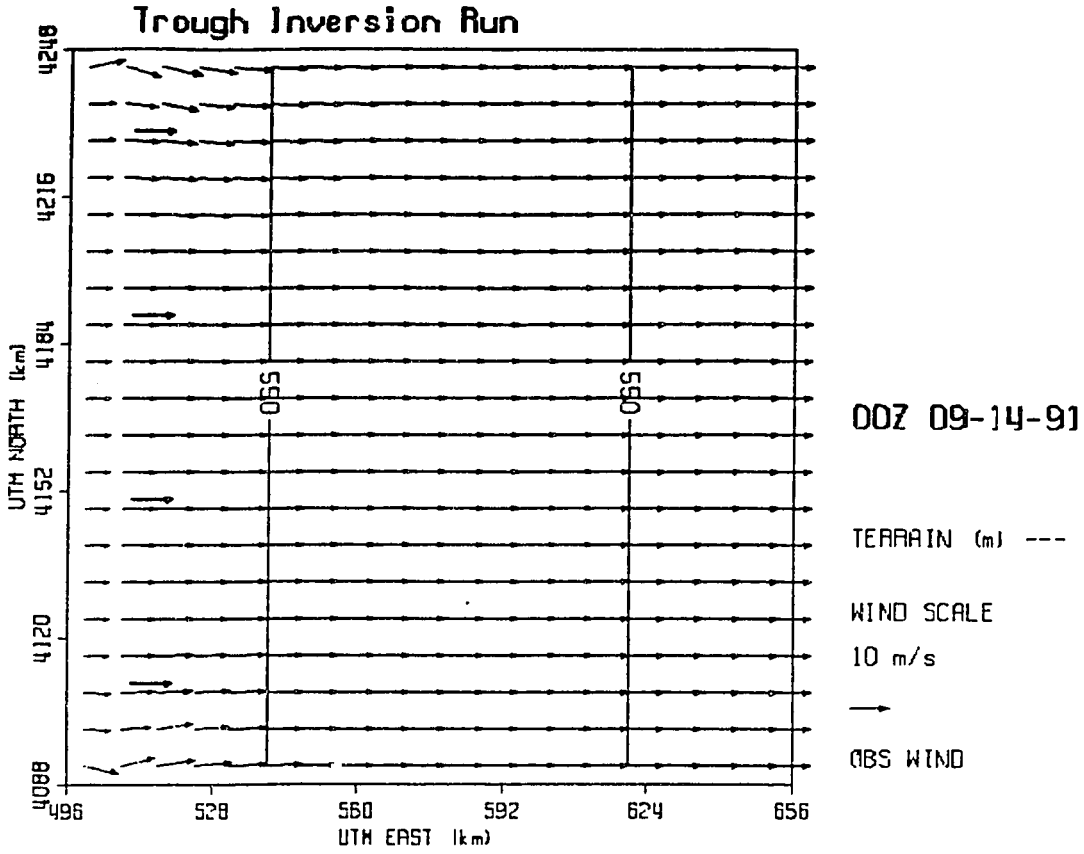

Figure 4-8 Plot of model winds for trough inversion case.

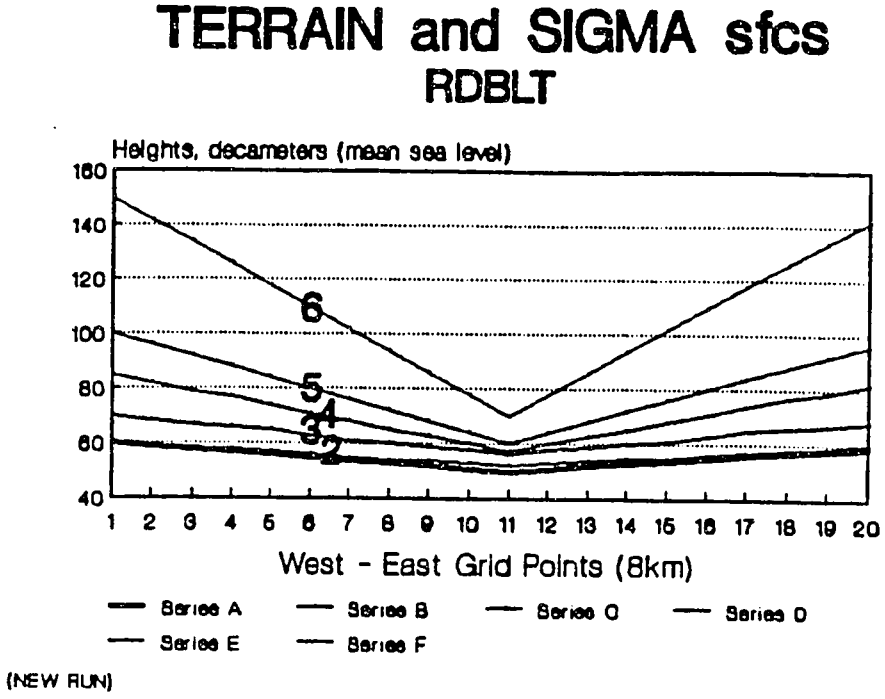

Figure 4-9 West-east cross section of sigma surfaces and terrain for trough inversion case.

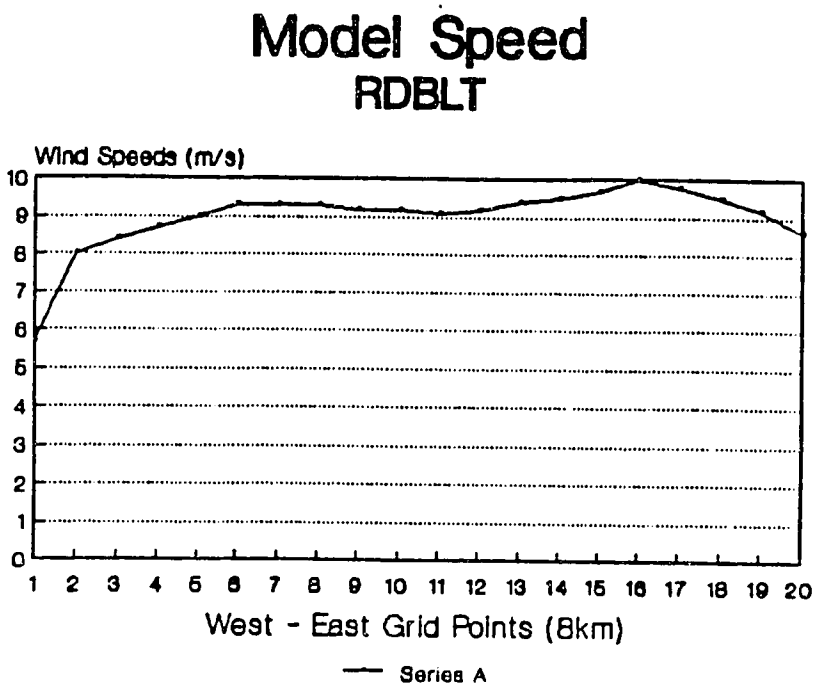

Figure 4-10 West-east cross section of model speeds for trough inversion case.

cross sections for this case. The inversion is generally low over the center of the valley, although the lowest thicknesses are located to either side of the center of the valley (see Fig. 4-9). Thus, the wind speeds (Fig. 4-10) are not at a maximum under the inversion trough axis. However, it is noted that speeds do increase where the flow surface separations are minimal (e.g., at grid points 6 and 16). Thus, flow is increased over sloping terrain, but not over the highest terrain.

iii. Flat Terrain, Sloping Inversion (10 iterations)

In this case, flat terrain is overlain by an inversion structure which slopes sharply downward from west to east, starting at 1000 MSL in the west, and lowering to 400 MSL in the east. For this test, the mass-balancing scheme was only allowed to operate for 10 iterations (the default value). Figure 4-11 shows the model output for this case; note that there is some acceleration of the winds from west to east, and that some winds are diverging through the northern and southern domain boundaries. However, Figs. 4-12 and 4-13 show that although the depth of the boundary layer decreases from 1000 m to 400 m, the anemometer wind speeds only increase from 6.3 ms^{-1} in the west to 8 ms^{-1} in the east. From mass continuity considerations, the wind speed would be expected to at least double across the domain. After conducting this test, it was therefore suspected that the model may not be balancing mass to within an acceptable

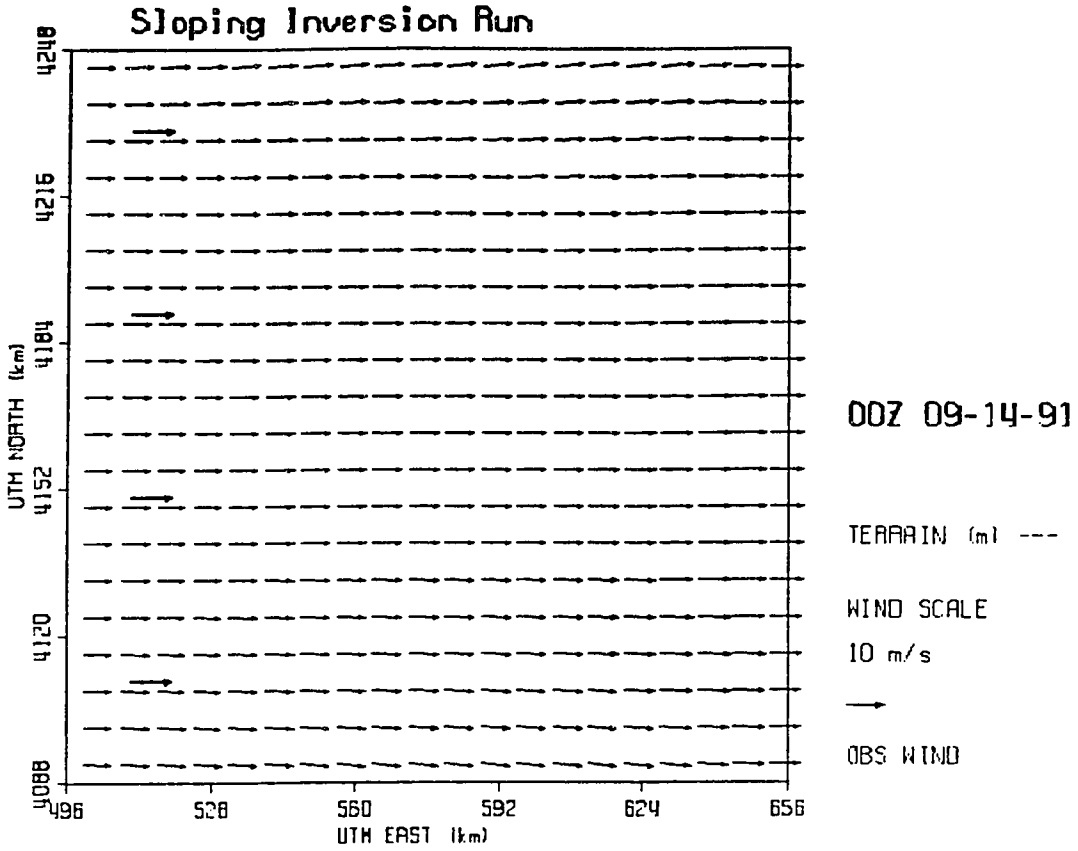

Figure 4-11 Plot of model winds for sloping inversion case (10 iterations in mass balancing routine).

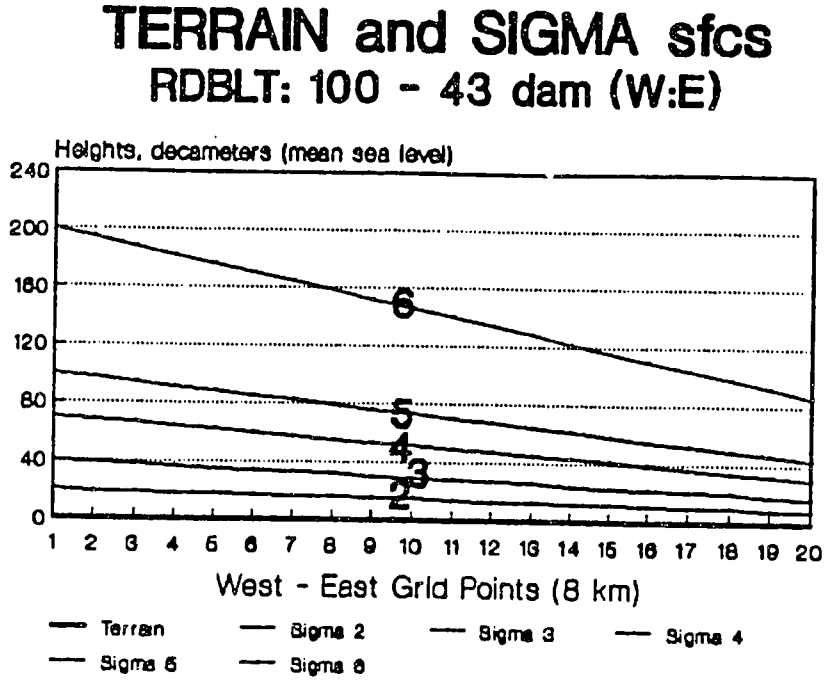

Figure 4-12 West-east cross section of sigma surfaces and terrain for sloping inversion case.

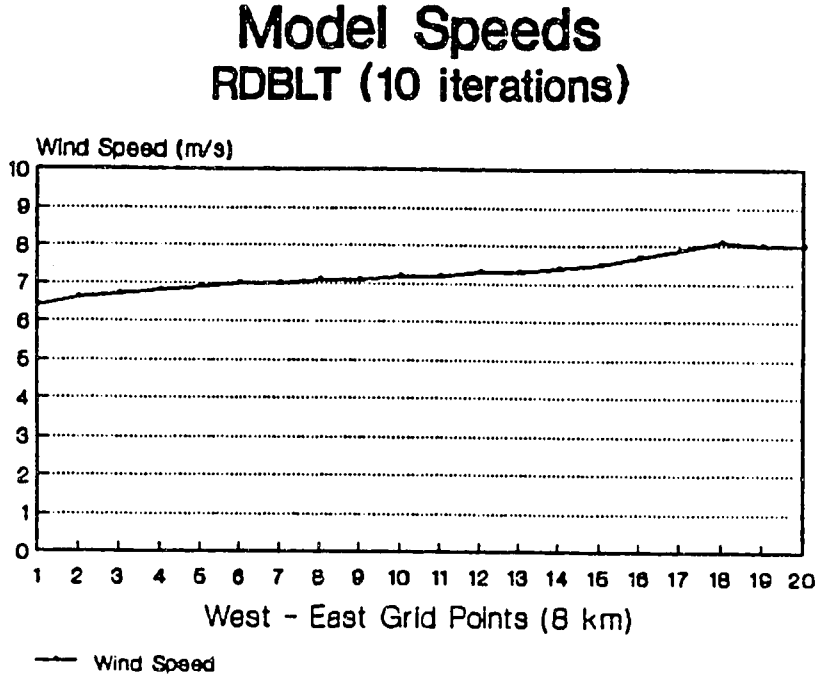

Figure 4-13 West-east cross section of model speeds for sloping inversion case.

level of accuracy. A program was developed to assess the model's ability to balance the mass in the wind field (BALANCE; see Appendix B-4 for code). The analysis scheme is based on the same method that WOCSS uses to balance mass (discussed in Chapter 2). For this slope case, the entire domain showed a 34% increase in mass. This corresponds well with the lack of wind speed increase on the eastern edge. The test was repeated, but with additional iterations allowed in the mass balancing procedure. Below we describe results when 100 iterations are allowed.

iv. Flat Terrain, Sloping Inversion (100 iterations)

As mentioned above, the inversion sloped from 1000 MSL in the west to 400 MSL in the east. Figures 4-14, 4-15, and 4-16 show that when the model is run with 100 iterations in BAL5, the wind speeds are closer to what would be expected from complete mass balancing, although still not quite doubling from west to east (now from 5.8 ms^{-1} to 9.9 ms^{-1}). When the mass balance analysis scheme mentioned above was applied to this test, the domain's mass only increases by 6%. The plot of model winds (Fig. 4-14) suggests that much of this mass discrepancy is accounted for by lateral flow out of the domain (i.e., to the north and south). Other tests (not shown here) were conducted with still more iterations. The western speeds were further reduced while eastern speeds were further increased. However, there appears to be a point beyond which additional iterations

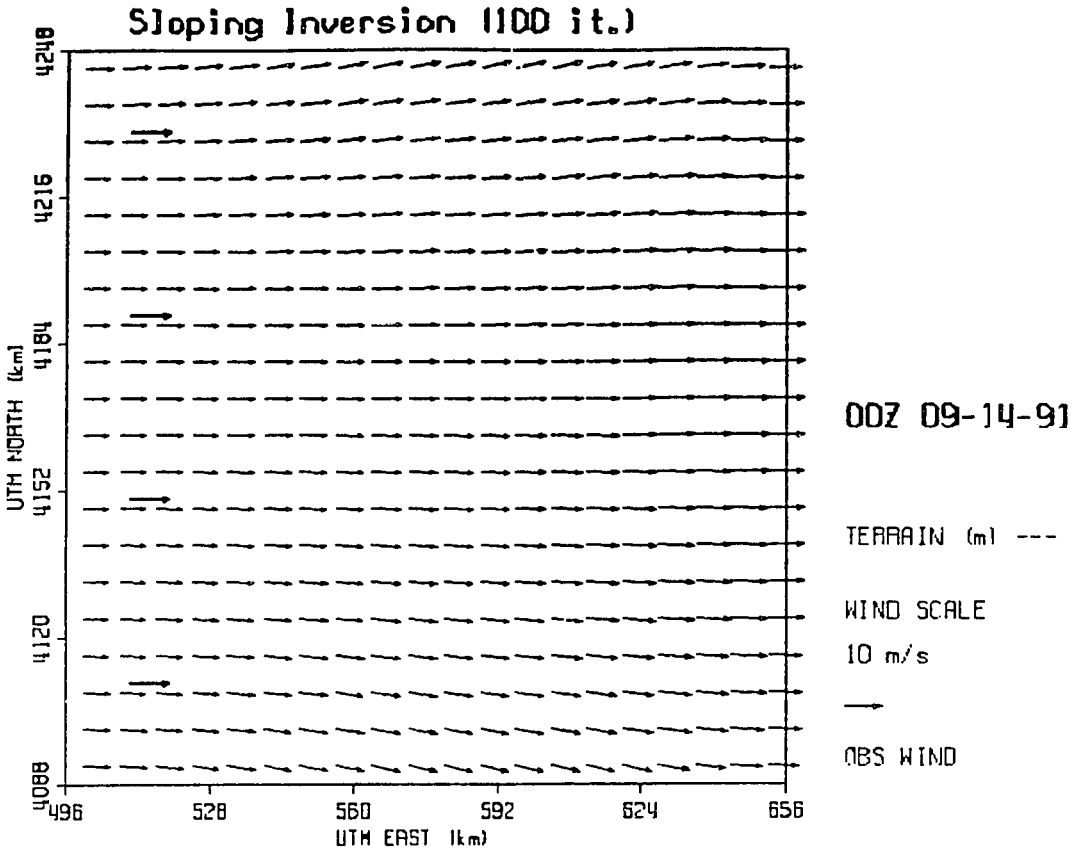

Figure 4-14 Plot of model winds, as in Figure 4-11, but with 100 iterations.

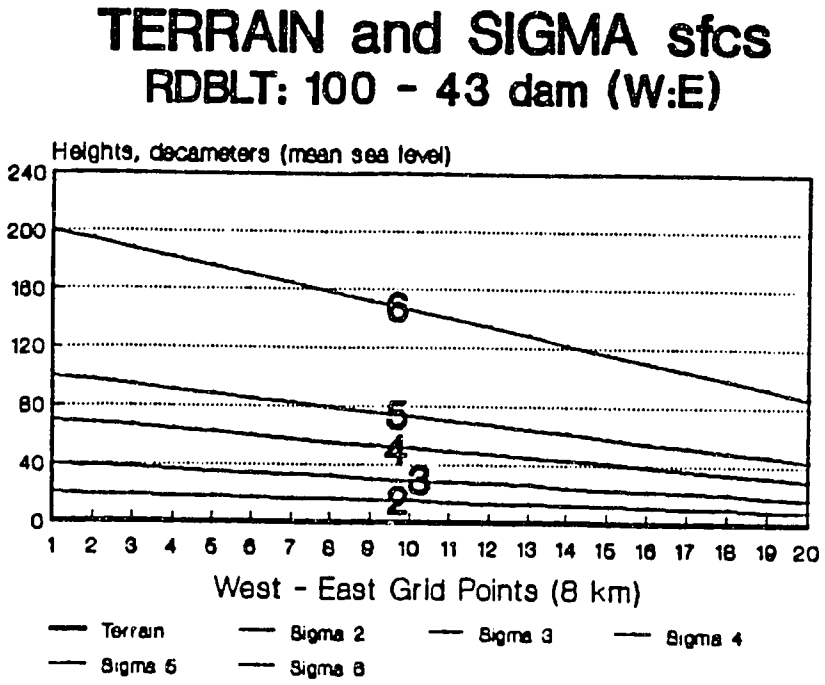

Figure 4-15 West-east cross section of sigma surfaces and terrain for sloping inversion case (100 iterations).

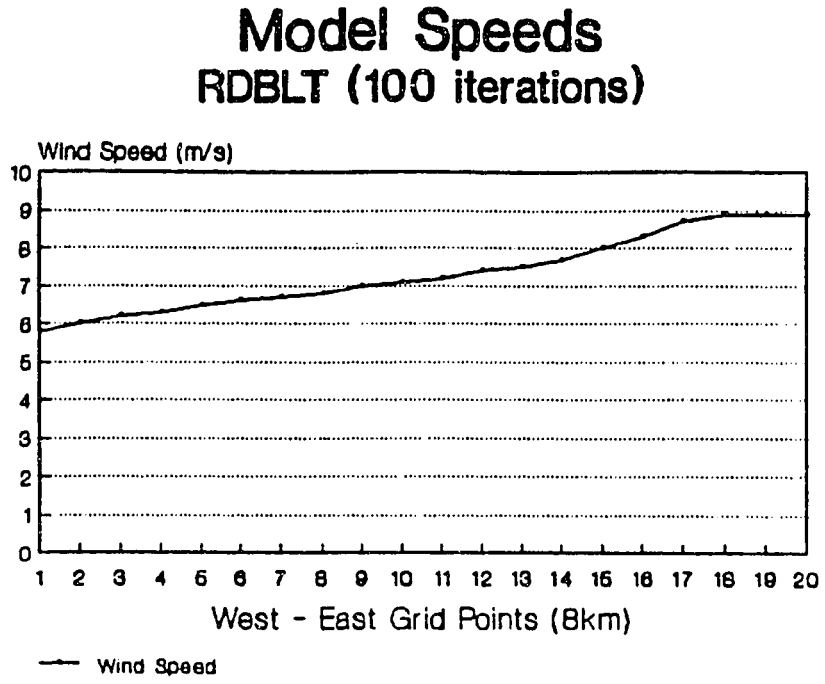

Figure 4-16 West-east cross section of model speeds for sloping inversion case (100 iterations).

do not improve the wind solution. It is likely that the intense slope of the inversion topography in this case is the cause of the problem, since other tests were conducted with much gentler slopes to the inversion topography and those produced very satisfactory correlations between boundary layer depth change and wind speed change. In these tests, mass was balanced throughout the domain. The inversion topography in the experiment discussed above was selected as being representative of the most extreme slopes found in the SFBA.

Summary

It is seen that model winds do respond in a realistic way to the depth and shape of the boundary layer. It must be remembered that the simple cases discussed above involve idealized shapes. In the SFBA we find a superposition of many terrain and inversion structures. Tests not shown here indicate that sufficient mass balance accuracy (even after only 10 iterations) is observed in the cases involving real MABLES inversion topography data to warrant confidence in proceeding to the next step, that of testing a case using real data.

Discussion of MABLES case

The WOCSS model was next run with data from the MABLES case (00Z, 10 August 1978). The flow at this time was a typical northwesterly flow, common during summer months in

the SFBA. Figure 4-17 shows the vector plot of the winds when we exclude specific inversion data (non-RDBLT case). The prevailing flow shows evidence of being channeled (e.g., through the Altamont Pass and Santa Clara Valley). Cross sections (west-east from the Golden Gate gap, across the Berkeley Hills, through Mt. Diablo and beyond, and northwest-southeast from the Golden Gate gap, down the SF Bay, through San Jose to the Gilroy area) were made and shown in Figures 4-18 through 4-21. The west-east cross section shows increased speeds just upwind of the east bay hills, and some acceleration west of Mt. Diablo. A similar feature is seen near grid points 10-11 in the northwest-southeast cross section. Generally, weak accelerations are seen upwind of hills, with weak decelerations downwind.

Figure 4-22 shows the vector plot of the case where inversion topography was explicitly included (RDBLT case). Again, cross sections were made in this case and are shown in Figs. 4-23 and 4-24 (for the west-east cross section), and Figs. 4-25 and 4-26 (for the northwest-southeast cross section). The cross sections indicate the wind speed/ terrain relationship is similar to the non-RDBLT case, with speeds increasing upwind of hills, and decreasing to the lee. The major difference between the two cases appears to be the increased wind speeds over higher terrain in the RDBLT case, closer to what is observed in the SFBA. A comparison between the vector plots and cross section data

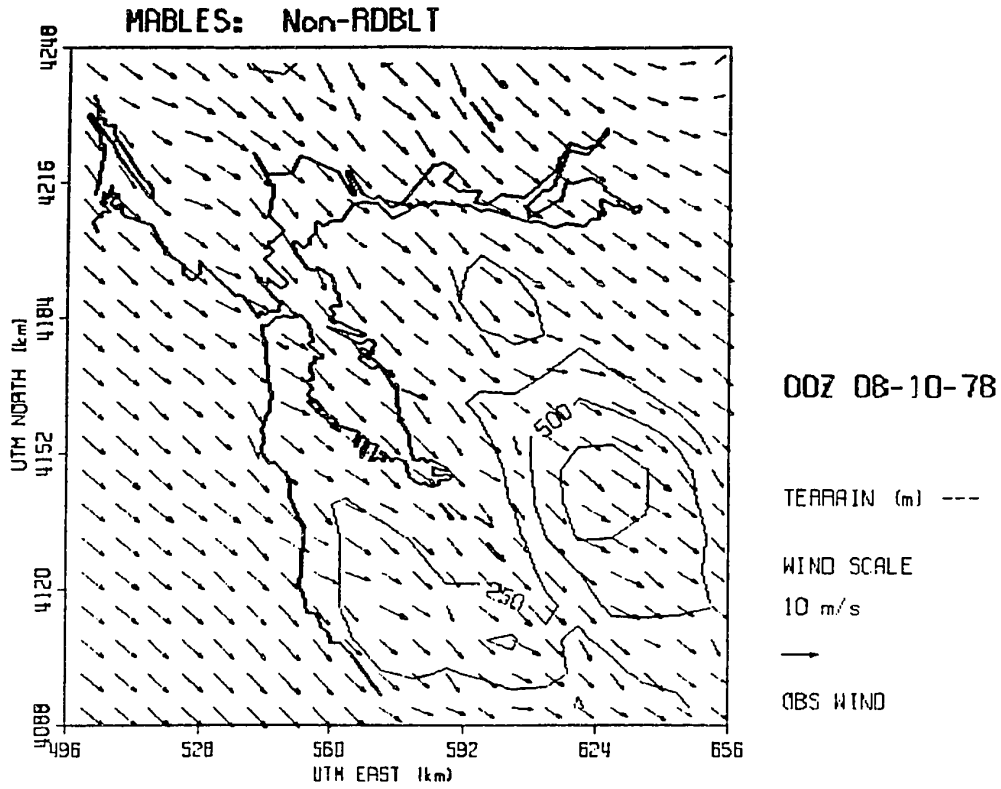

Figure 4-17 Plot of model winds for MABLES case (August 10, 1978, 00 GMT), using normal model settings (non-RDBLT run).

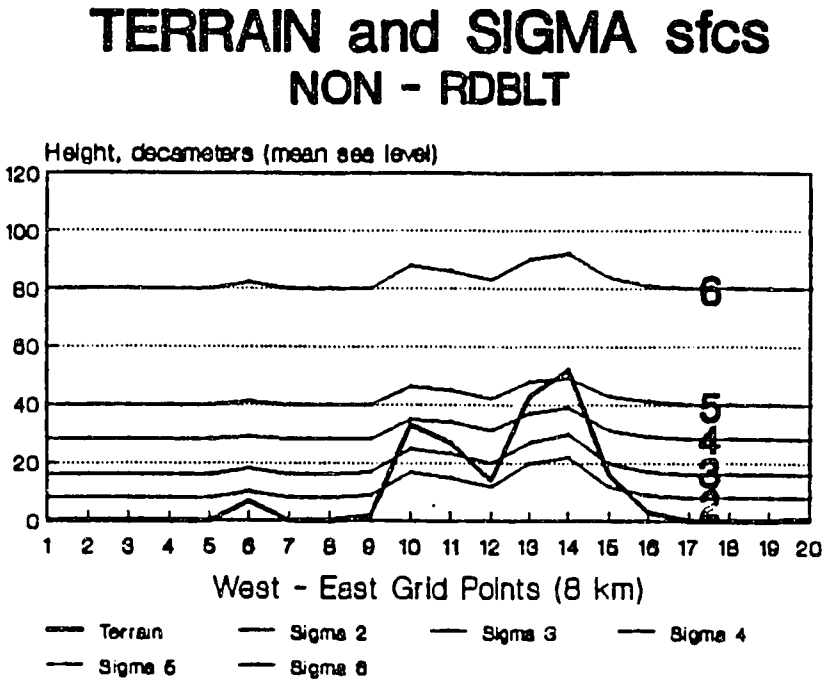

Figure 4-18 West-east cross section of sigma surfaces and terrain for MABLES case (non-RDBLT run).

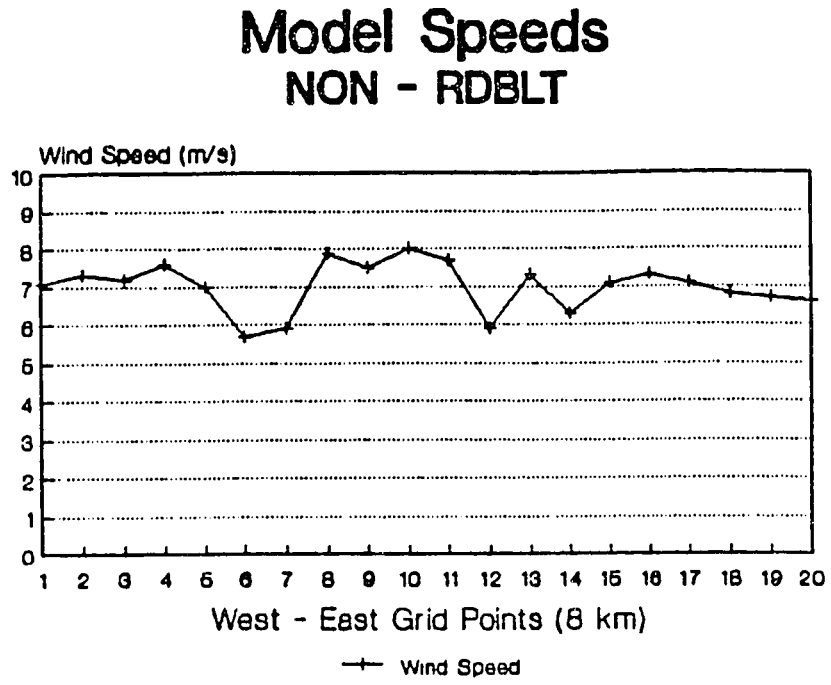

Figure 4-19 West-east cross section of model speeds for MABLES case (non-RDBLT).

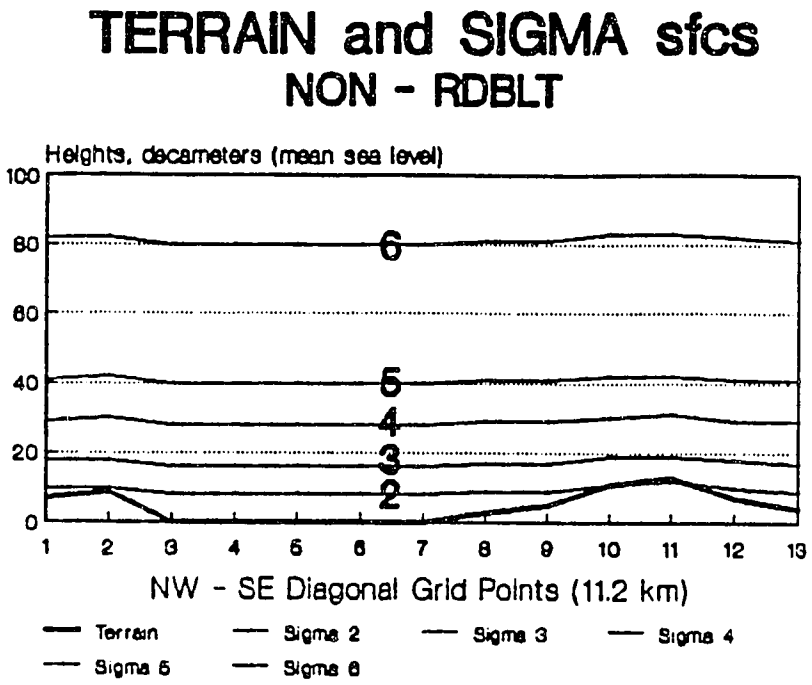

Figure 4-20 Northwest-southeast cross section of sigma surfaces and terrain for MABLES case (non-RDBLT run).

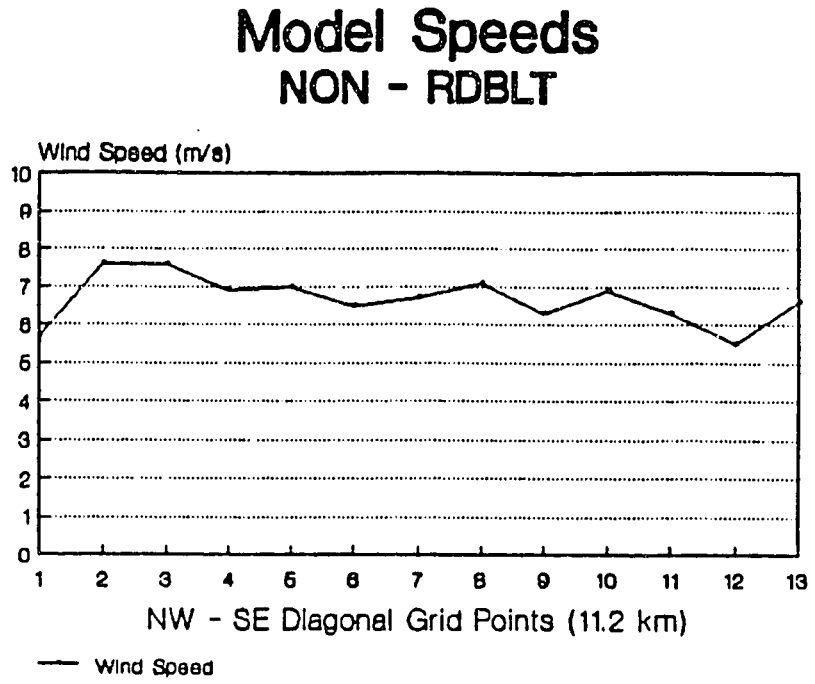

Figure 4-21 Northwest-southeast cross section of model speeds for MABLES case (non-RDBLT run).

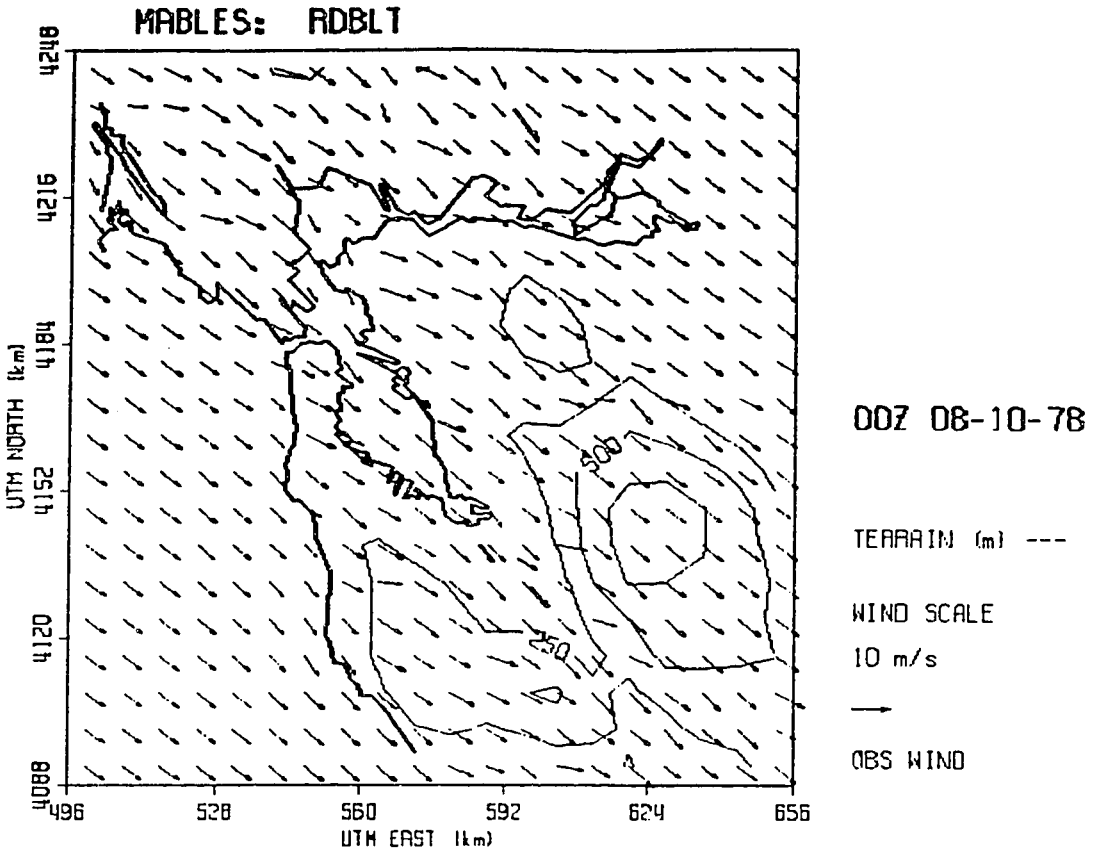

Figure 4-22 Plot of model winds for MABLES case (August 10, 1978, 00 GMT), using inversion topography reading module (RDBLT run).

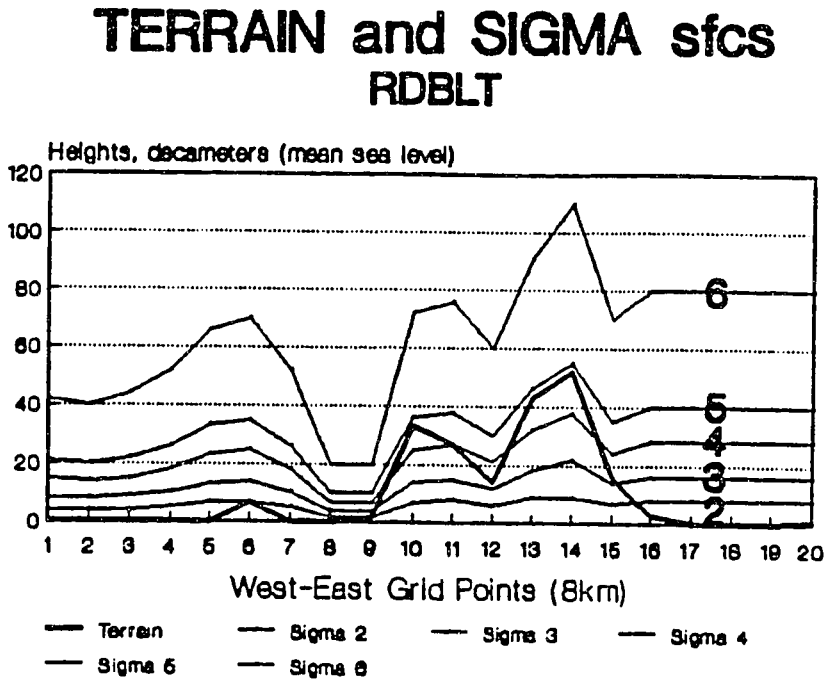

Figure 4-23 West-east cross section of sigma surfaces and terrain for MABLES case (RDBLT run).

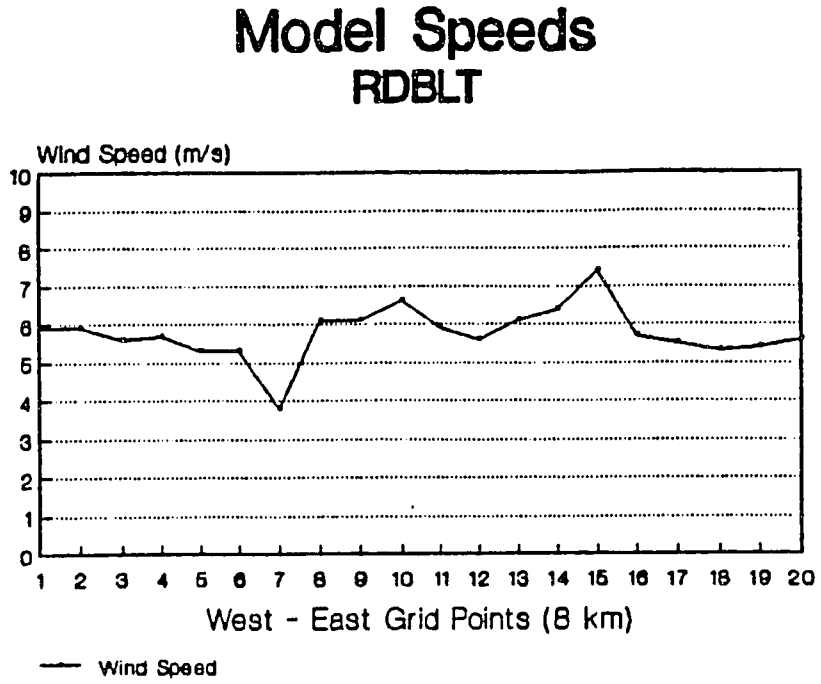

Figure 4-24 West-east cross section of model speeds for MABLES case (RDBLT run).

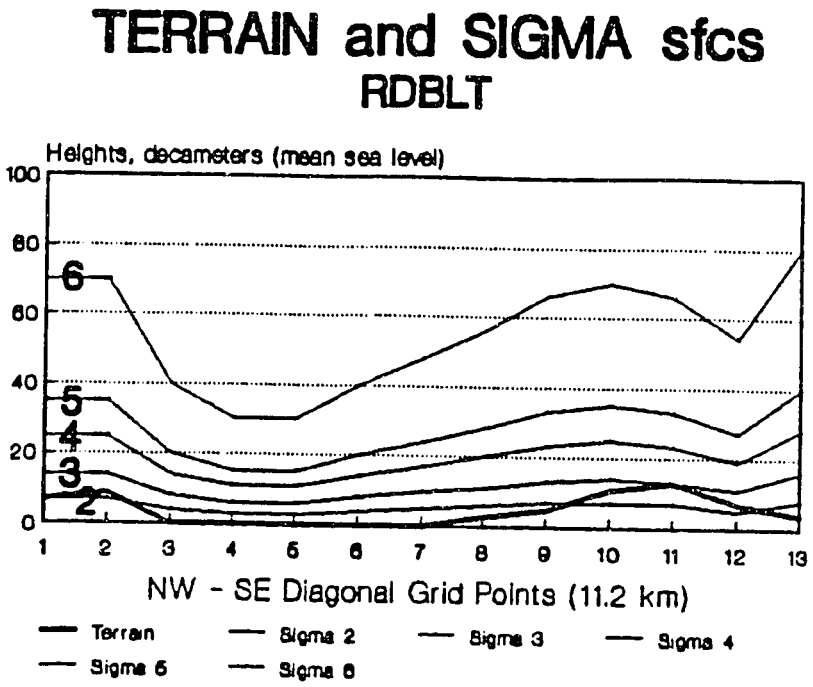

Figure 4-25 Northwest-southeast cross section of sigma surfaces and terrain for MABLES case (RDBLT run).

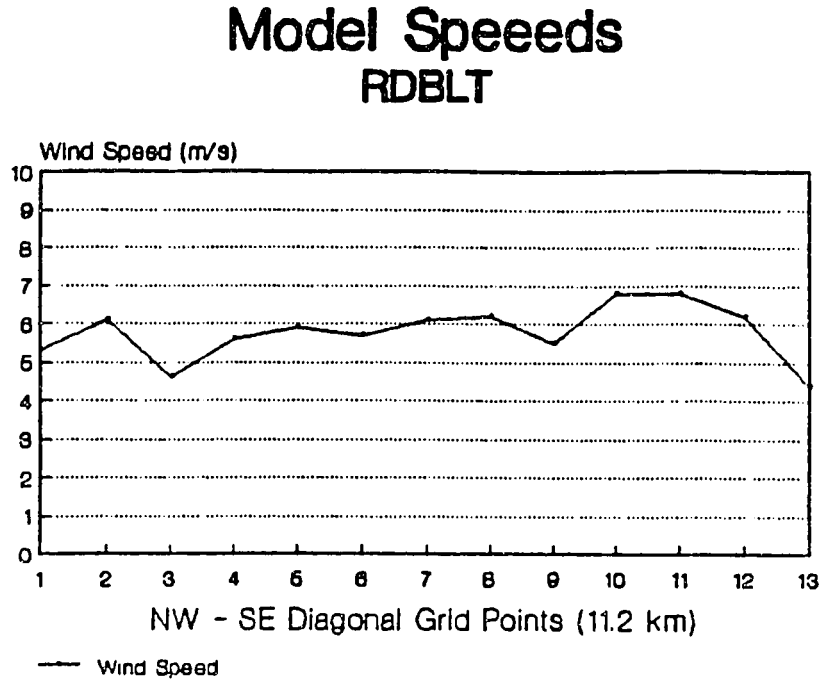

Figure 4-26 Northwest-southeast cross section of model speeds for MABLES case (RDBLT run).

shows that the inversion run (RDBLT) has slightly slower speeds overall (compare Fig. 4-24 with Fig. 4-19, and Fig. 4-26 with Fig. 21). In Tables 4-1 and 4-2 of Appendix C (non-RDBLT and RDBLT cases, respectively) we show a more detailed comparison at observation sites which verifies that the inclusion of the RDBLT feature slows the model winds, in closer agreement with overall observed speeds (even though winds at some stations are degraded).

Also notable are the differences in the way the model handles the placement of sigma surfaces. In the non-RDBLT case, the surfaces are fairly flat. Speeds appear to increase along the windward slopes of terrain (where the sigma surfaces impinge on the terrain). In the RDBLT run, speeds generally increase over the higher terrain, more in response to the squeezing of the sigma surfaces. A comparison of the vector differences between the RDBLT and non-RDBLT runs is shown in Fig. 4-27. The largest differences are focused over the Mt. Hamilton range, upwind of the Santa Cruz mountains, and near the delta.

The addition of inversion topography to WOCSS appears to have encouraging preliminary results. Wind speeds do increase over higher terrain, as is often observed. There is a small speed decrease in the lee of barriers, but a much larger one windward. Overall, the inversion runs best captured the observed effect of speed increases over the higher terrain.

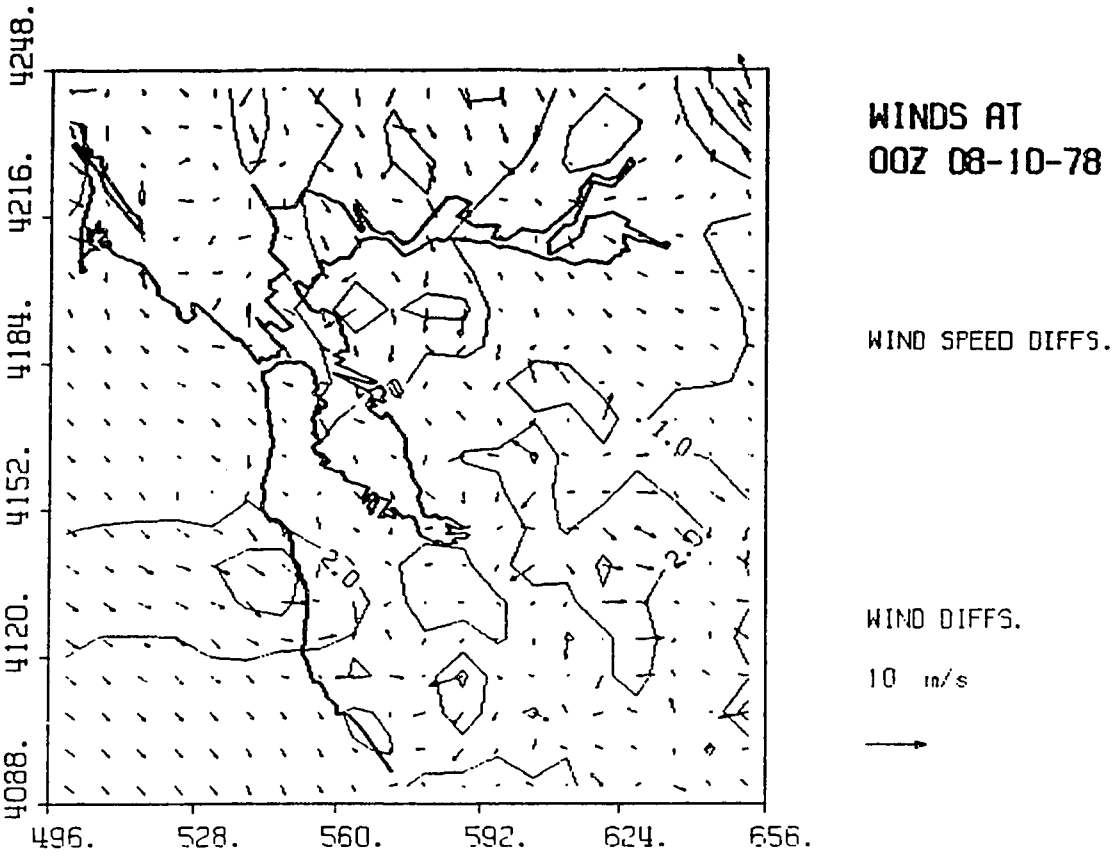

Figure 4-27 Vector difference plot of Figure 4-22 minus Figure 4-17 (RDBLT run minus non-RDBLT run).

It would be desirable to test WOCSS in more situations in which inversion topography data is available. In addition, results may be improved with finer resolution. The method used to extrapolate inversion height data along the edges of the domain could be improved. Also, it would be desirable to conduct tests under other synoptic situations. It would be worthwhile to explore the new model capability of using multiple temperature soundings, to see if selected soundings could better reproduce the observed inversion topography. Also, the values used for allowable separation between surfaces should be experimented with.

b. Nested Grids and Focused Grids

The model's nested grid capabilities have seldom been used. Usually it is desirable to use the available computer memory on a coarse grid with the best possible resolution. In the nested grid scenario, the model winds produced on the coarse grid are then used as first-guess winds for the medium grid, and so on (as many as 3 grids can be used: coarse-medium-fine). An anchor point must be specified in the model operation, that being the one grid point that is shared between the coarse grid and nested grid(s).

In this section, nested grid runs were performed for the Golden Gate gap area, and for the Morgan Hill area. The coarse grid resolution was 8 km, with a 2 km resolution nested grid. The Golden Gate gap was chosen for its unique

position in the regional flow pattern, and for its complex terrain. The Morgan Hill area was chosen to explore the recommendation made by Tredo. Additionally, a "focused grid" (i.e., a coarse grid run with high resolution terrain data) was performed over the Golden Gate gap area.

Figure 4-28 shows winds generated by WOCSS for the normal MABLES case. This is the coarse grid result. Figure 4-29 shows winds on the nested grid centered near the Golden Gate gap; Mt. Sutro is shown on the plot with a star. Nested grid winds are shown at each point, while coarse grid winds are available and shown at every 4th grid point. Observed winds are also shown (at UTM 547,4178). The vectors clearly show that the speeds over Mt. Tamalpais (the 300 m contour in the northwest corner), are higher on the nested grid. Also the flow is directed more through the Golden Gate and towards the South Bay, and model wind speeds are generally slower. Table 4-3 (Appendix C) shows good results for the coarse run; model winds are slowed at Mt. Sutro in the nested run (from 206% in the coarse grid, to 188% in the medium grid). Tabular output for the medium grid only includes the results from Mt. Sutro, and is not shown.

Figure 4-30 shows the winds produced by the medium grid centered in the Morgan Hill area (Morgan Hill is located at UTM 620,4110). The San Jose observation (UTM 598,4131) is visible near the upper left corner. Again, model winds from

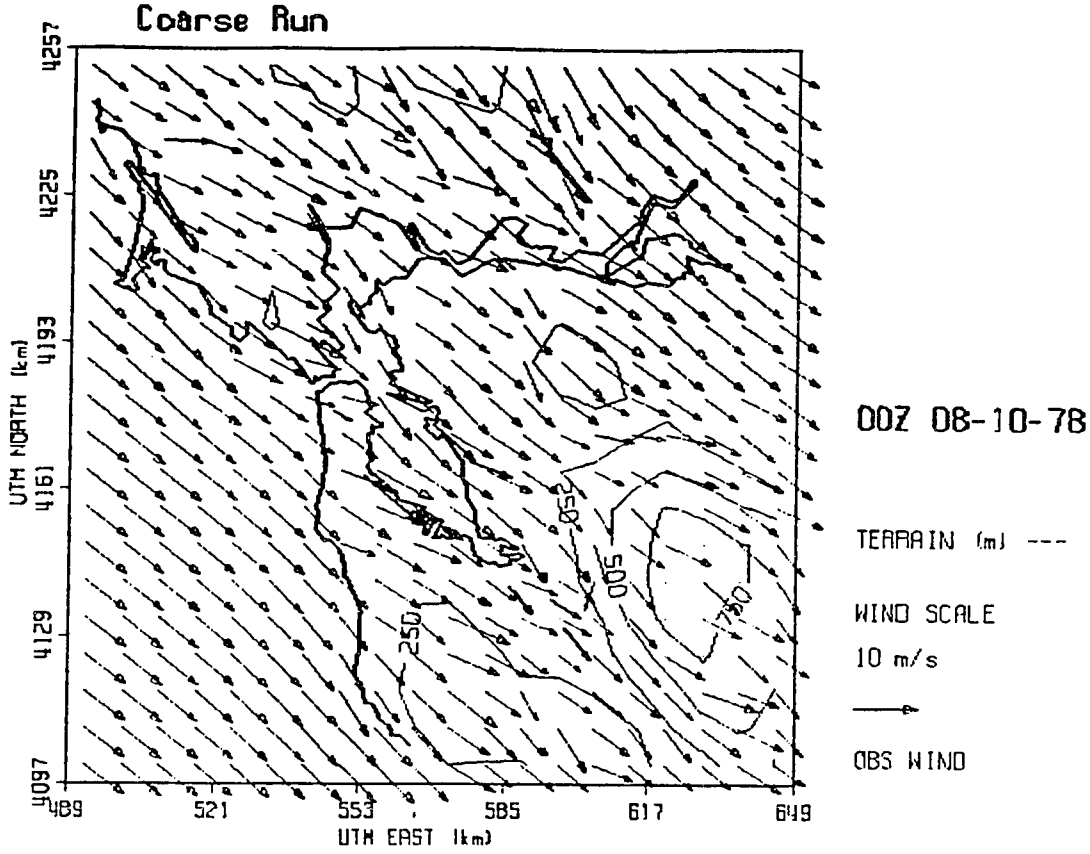

Figure 4-28 Plot of model winds for MABLES case (August 10, 1978, 00 GMT), using normal settings.

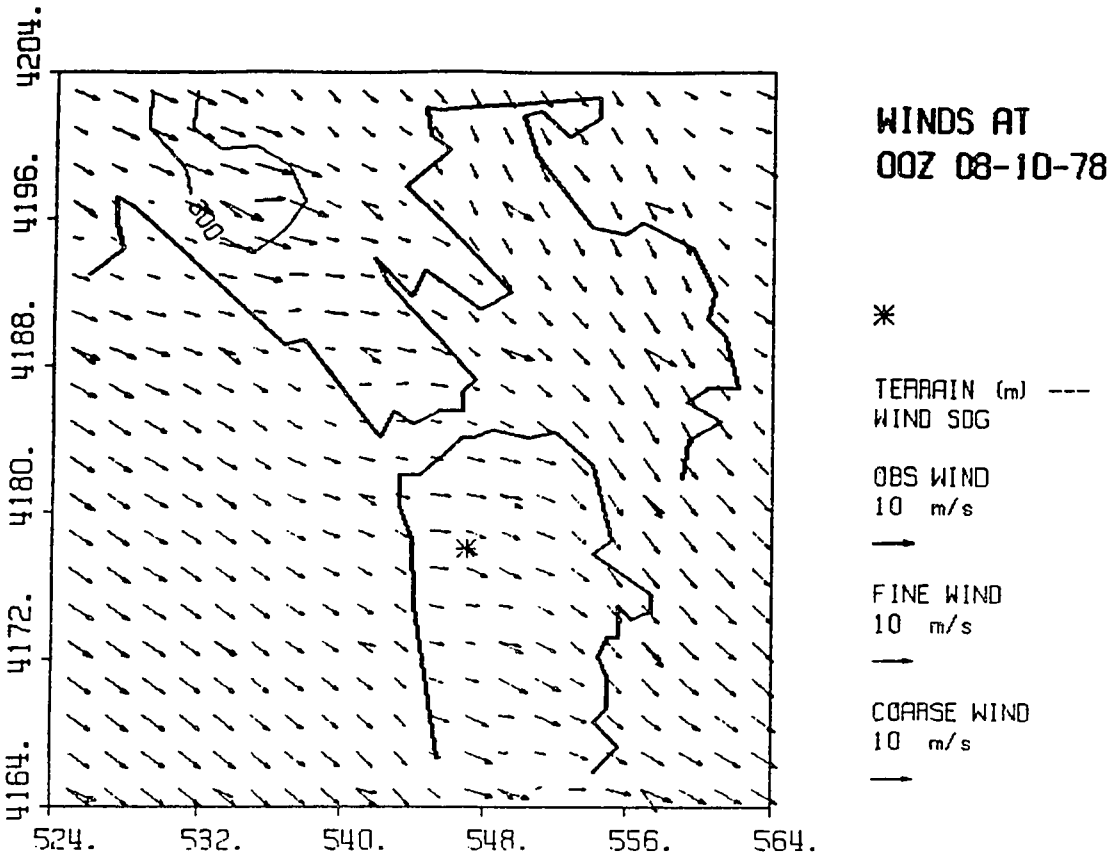

Figure 4-29 Plot of nested grid output for run of Figure 4-28 (focused on Golden Gate area).

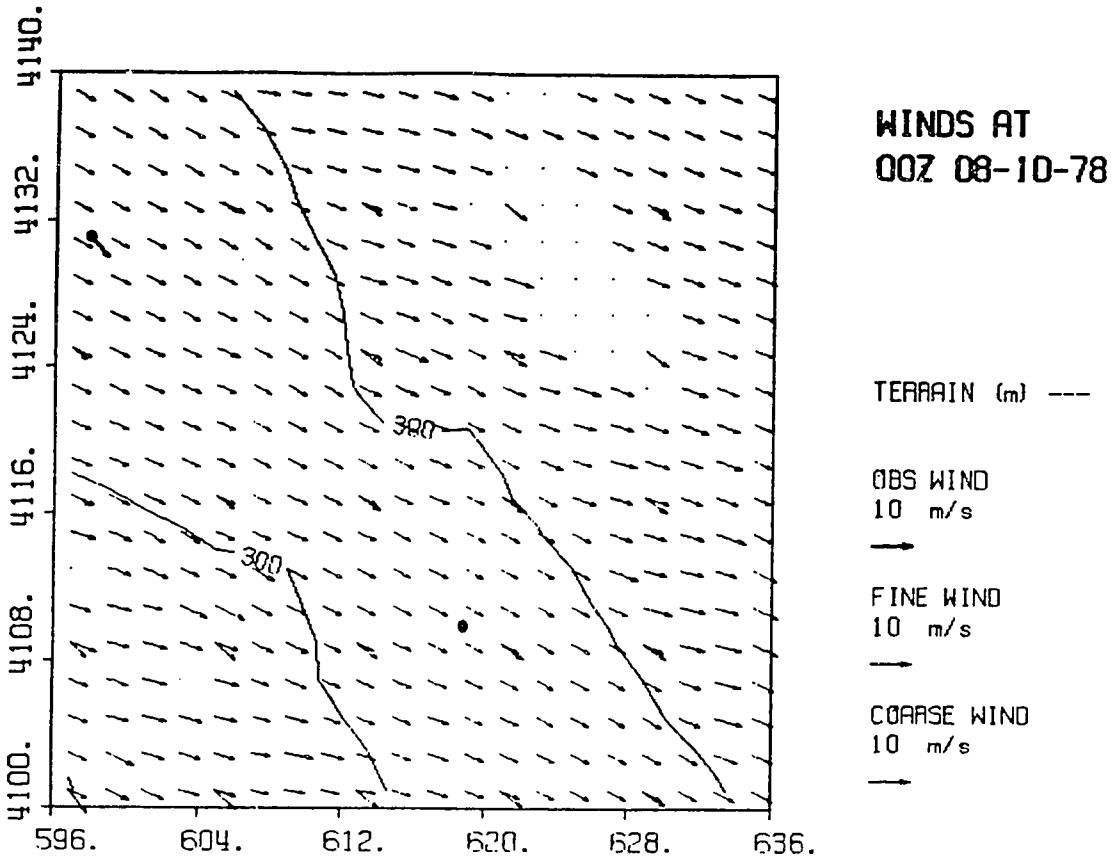

Figure 4-30 As in Figure 4-29, but for Morgan Hill area.

the coarse and medium grids are superimposed at those grid points which are shared. A comparison of the coarse and nested winds show that the most significant effect of the medium grid in this case is to increase the flow's avoidance of higher terrain (see the southwest corner of the plot, in particular). Table 4-4 shows good results for the coarse grid. For San Jose State, the medium grid slows model winds (from 96% to 82%), as with Mt. Sutro above. Tabular output for the medium grid (not shown) only includes the results from San Jose State.

Figure 4-31 shows the Golden Gate area, but with a focused grid. This is merely a coarse grid run of WOCSS applied to a small area of interest and with fine resolution of 2 km. An analysis of model results in this case shows that Mt. Sutro's winds veer by 2% with respect to observed winds, and are 170% of observed speeds (tabular data not shown here).

Summary

From the case above, it is suggested that a focused grid will perform better than a nested grid of the same domain. There may be times when a nested grid may be of use, but this would require large computing resources. The nested grid uses excessive memory, and our runs on the PC were restricted to undesirably small domains. Generally, the careful placing of focused grids will yield the best results. This should be tested further.

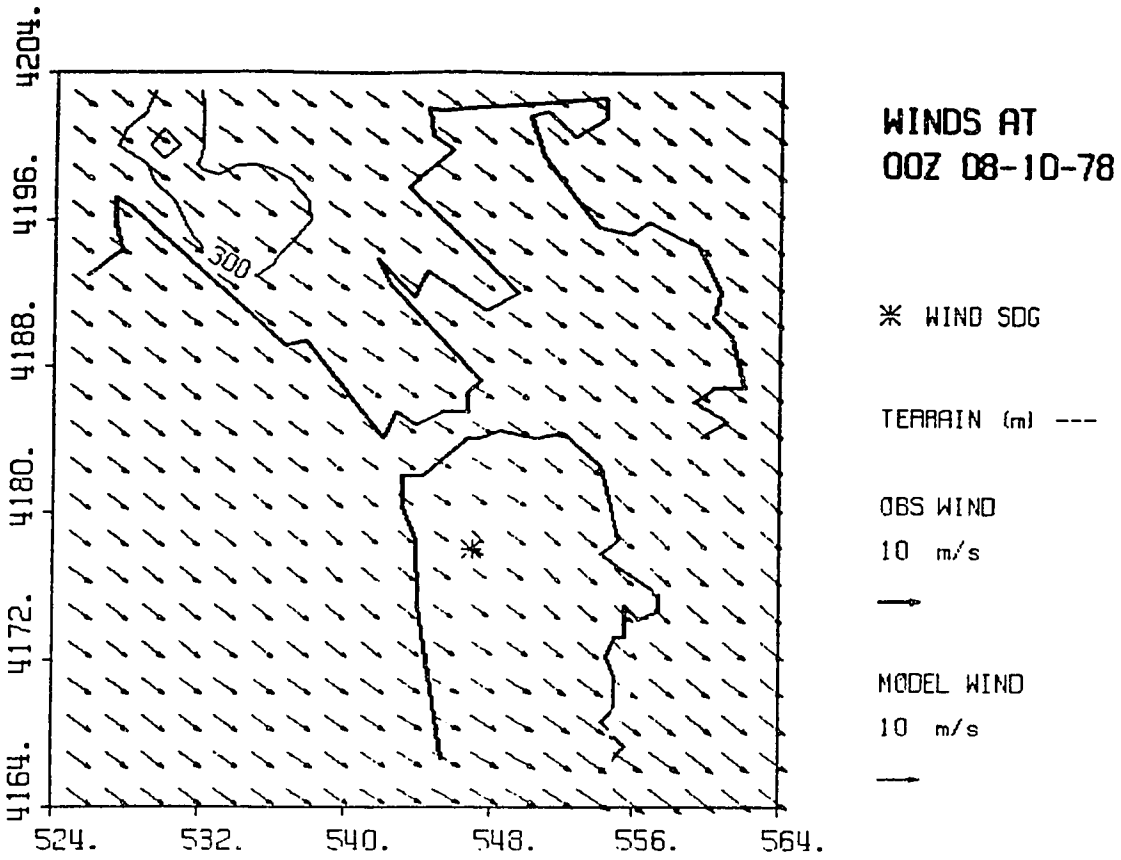

Figure 4-31 Plot of high resolution coarse grid for Golden Gate area.

c. Mass Balancing Modifications

Endlich (1990) has conducted experiments with the method by which WOCSS balances the flow around terrain obstacles. Currently, WOCSS balances the flow in an iterative manner until divergence is reduced below an acceptable level, usually after 10 iterations in the mass balancing subroutine. Endlich has revised the balancing routine (BALWND) to incorporate a "barrier effect" produced by higher terrain features. His modifications apply only to those grid points on any flow surface that are adjacent to a terrain barrier, and operate as follows: the flow is decomposed into a component parallel to the local terrain contours and a component perpendicular to terrain contours. The perpendicular component is set to zero. In this way, flow is effectively blocked from ascending the terrain, and flow is forced around the barrier. With this computation performed at each iteration, the barrier effect propagates away from the terrain obstacle, leading to a smoother flow around the elevated terrain. The effect is most notable in stable situations, and on the lower sigma surfaces.

Figure 4-32 shows the standard MABLES run (i.e., the normal run without Endlich's modifications). Figure 4-33 shows the same case but using the revised BALWND code. A comparison of the two figures reveals some striking differences. The large speed differences between the two runs is most notable. The BALWND run exhibits greatly

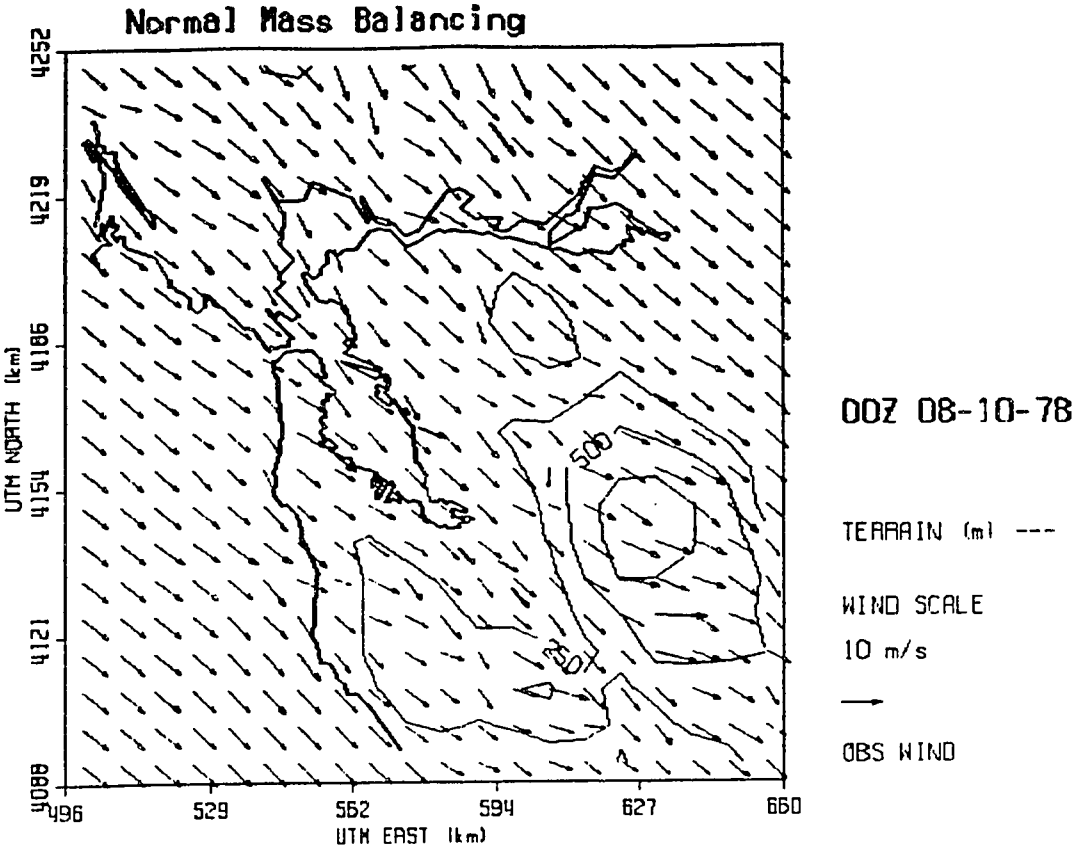

Figure 4-32 Same as Figure 4-28, but with different grid anchor point.

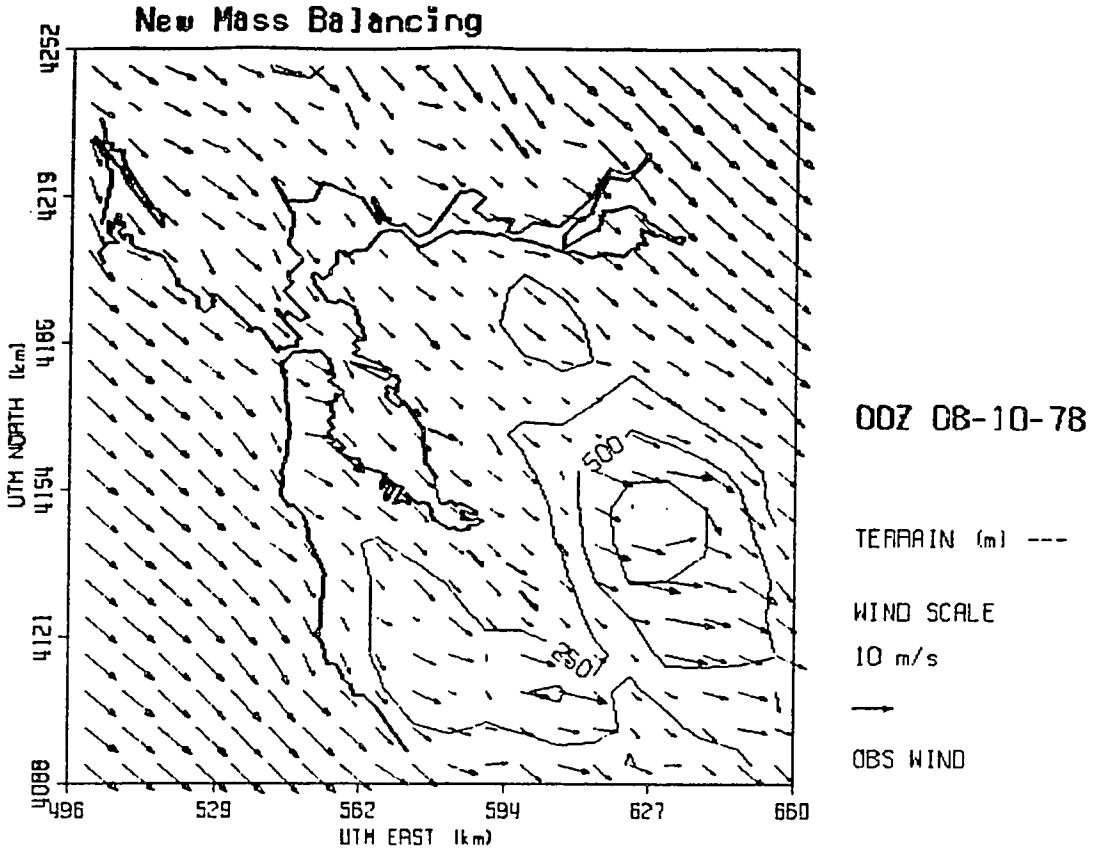

Figure 4-33 Same as Figure 4-32, but with barrier effect, wind normalization, and smoothing options in effect.

reduced wind speeds upwind of hilly terrain, with a corresponding speed increase found over the ocean and Sacramento delta regions.

Tables 4-5 and 4-6 (Appendix C) show that both the normal WOCSS and the BALWND versions produce excellent model wind directions. However, the BALWND version is seen to reduce model wind speeds to approximately 81% of observed values, while the normal WOCSS run increases speeds to 110%. This speed difference can be discerned in the vector plot (Fig. 4-34); the flow is slowed too much near barriers. The plot also confirms that the largest speed and direction differences are concentrated on the windward side of higher terrain features in the SFBA, as might be expected from the nature of the BALWND code. Further testing and adjusting of the mass balancing routine is recommended. For example, the degree to which flow is forced around barriers may need to be reduced.

d. Summary of Model Improvements

The WOCSS model is composed of many modules, which have been expanded as new ideas have been incorporated into the program. We have examined the inclusion of inversion topography into WOCSS, and have seen good model response to this feature, although further testing will determine its ultimate utility. The nested grid feature appears to have limited use, especially on computers with limited memory.

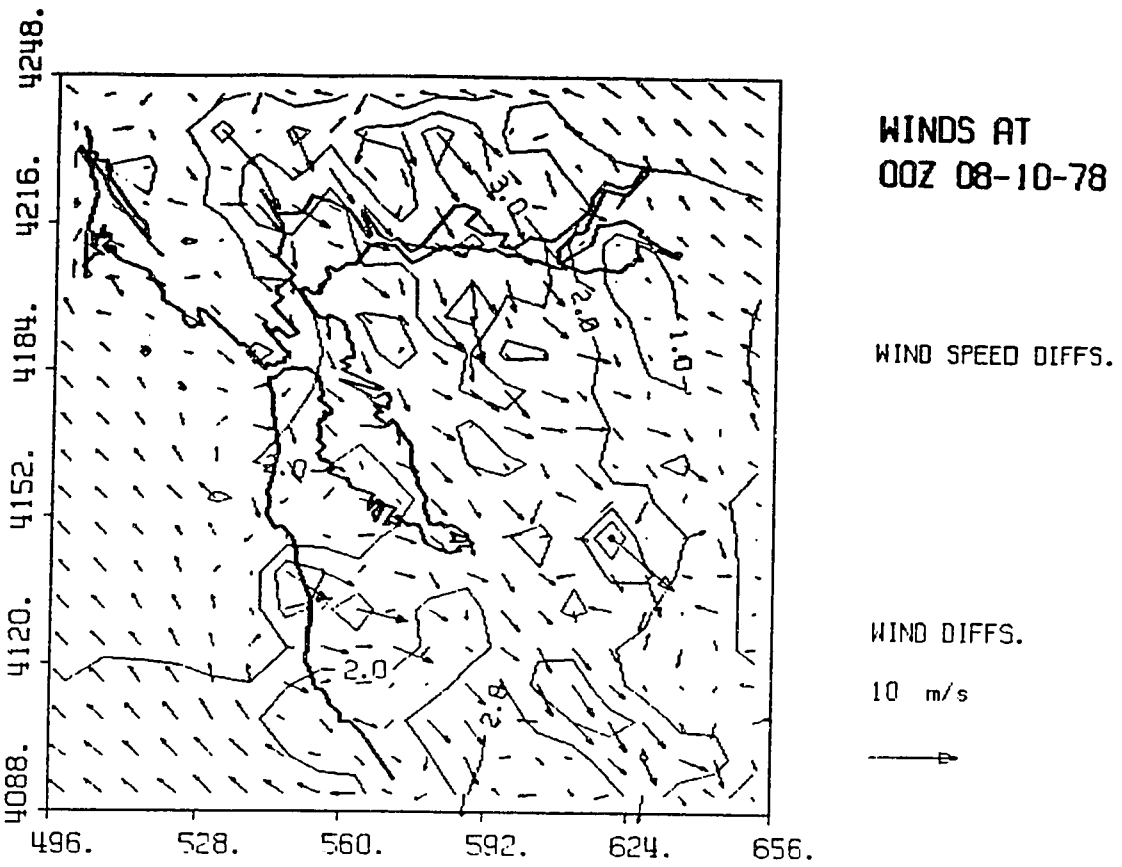

Figure 4-34 Vector difference plot of Figure 4-32 minus Figure 4-33 (normal settings minus all options).

It is better to increase resolution over a domain of interest. Finally, the manner in which the model balances mass is at the heart of the program. Further efforts to refine this module will likely improve overall model performance.

5. SUMMARY, CONCLUSIONS AND RECOMMENDATIONS

The Winds on Critical Streamline Surfaces model has been thoroughly tested using data from the San Francisco Bay Area in an effort to quantify and improve model performance. This mass-conserving wind flow model produces real-time wind analyses which have been tested against observations. Several tests of some of the model's newer features have been accomplished. These tests have incorporated real-time data, and have explored the model's nested grid and inversion topography-reading capabilities. Graphical output has been improved.

WOCSS model output was initially compared to output from its earlier version (CMPLX). These runs indicate that recent model developments have improved model output over high terrain. Further comparisons with earlier CMPLX runs point out the necessity of using additional observations in locations that are critical to shaping the overall flow pattern (e.g., Gilroy).

Tests were conducted with the model using observed data representing the range of synoptic situations common in the SFBA. It was found that the model reproduces observed speeds and directions best during episodes of strong flow; in weaker flow situations (e.g., weak-northwesterly), the model speeds are too low. Model wind directions appear best in flow patterns where the prevailing winds are aligned with the major SFBA terrain features (i.e., NW-SE). Additional

tests confirmed that some stations are more important than others in determining the regional flow pattern. Further research could be devoted to using the model in assessing the optimal placement of an ideal network of observation sites, factoring in model performance as well as the cost of operating the stations.

The extensive set of synoptic climatology tests have demonstrated the model's performance under many of the typical flows encountered in the SFBA. Possible improvements to modeling SFBA flows involve extending the computational domain to areas which may have a strong influence on the regional flow patterns. For example, the seabreeze from the Monterey Bay often reaches the southern SFBA, at times creating a convergence zone near Gilroy. The model's ability to resolve this feature should be tested.

The effect of resolution on model output was also examined. While the high resolution run produced slightly better directional results, the wind speeds appear unaffected by resolution changes. The high resolution run does enable the user to discern finer details in the flow than is possible in the low resolution run, due to the finer terrain data. The improved directional output may improve the accuracy of results from a dispersion model. The resolution effect should be tested more rigorously, since it is possible that more complicated flows (e.g., northeasterly) would be treated more accurately with

increased resolution. The run performed here is only twice the normal resolution (4 km vs. 8 km). With expanded computer memory (to handle larger domains), a 1 km run should be performed over the entire SFBA to more fully test the importance of model resolution on output wind fields.

The tests in which inversion topography was explicitly input showed that model winds do respond in a satisfactory manner to externally prescribed variations in the depth of the boundary layer. In the simple inversion runs, results for ideal terrain and inversion features (e.g., gently sloping inversions) indicate that the model can produce reasonable flow fields. Using observed inversion topography data, the addition of inversion data to WOCSS improved the modeled speeds over higher terrain features. As mentioned earlier, finer resolution inversion topography data is available and WOCSS should be tested with this in the future.

Nested and focused grid capabilities of the model were explored. The nested grids do not appear to be very useful in improving model accuracy in a limited area of interest. From the few tests performed here, we recommend that computer resources be devoted to the finest resolution possible over the largest domain to produce best results.

Finally, preliminary results from adjusting the mass balancing procedure indicate that more experimentation is needed. While the new flow directions were satisfactory,

speed accuracy was degraded upwind of higher terrain. Further work needs to be done with this module, perhaps modifying the extent to which flow is forced around terrain barriers.

The results above indicate the utility and flexibility of WOCSS. The model reproduces observed winds very well. Users may wish to adjust and test selected model features in order to further refine the model for their specific needs.

REFERENCES

Ahrens, D., and A. Miller, 1969: Variations of the Temperature Inversion over the San Francisco Bay Area. Report, San Jose State University Dept. of Meteorology, 51 pp.

Anderson, G.E., 1971: Mesoscale Influences on Wind Fields. J. Appl. Meteor., 10, 377-386.

Bhumralkar, C.M., R.L. Mancuso, F.L. Ludwig, and D.S. Renne, 1980: A Practical and Economic Method for Estimating Wind Characteristics at Potential Wind Energy Conversion Sites, Solar Energy, 25, 55-65.

Cionco, R.M., 1985: A Mesometeorological and Micrometeorological Windflow Modeling System for Variable Terrain. Proceedings of Seventh Annual EOSAEL/TWI Conferences, December 1986, 22 pp.

Cressman, G.P., 1959: An Operational Objective Analysis System. Mon. Wea. Rev., 87, 367-374.

Danard, M., 1977: A Simple Model for Mesoscale Effects of Topography on Surface Winds. Mon. Wea. Rev., 105, 572-580.

Dickerson, M.H., 1978: MASCON - A Mass Consistent Atmospheric Flux Model for Regions with Complex Terrain. J. Appl. Meteor., 17, 241-253.

Endlich, R.M., 1967: An Iterative Method for Altering the Kinematic Properties of Wind Fields. J. Appl. Meteor., 6, 837-844.

Endlich, R.M., and J.D. Lee, 1983: An improved diagnostic model for estimating wind energy. PNL-4526 UC-60. SRI International, 89 pp. [Under U.S.D.O.E. Subcontract No. B-D5789-A-E.]

Endlich, R.M., 1990: Model Description and User's Guide for Taimod (Boundary Layer Diagnostic Wind Model for Taiwan), prepared for TaiPower Company, Taiwan, 13 pp.

Erasmus, D.A., 1986a: A Model for Objective Simulation of Boundary-Layer Winds in an Area of Complex Terrain. J. Climate Appl. Meteor., 25, 1832-1841.

Erasmus, D.A., 1986b: **A Comparison of Simulated and Observed Boundary-Layer Winds in an Area of Complex Terrain.** J. Climate Appl. Meteor., 25, 1842-1852.

Erickson, N.A., 1981: **Variations of the Topography of the Marine Inversion over the Central California Coast.** Report, San Jose State University Dept. of Meteorology, 26 pp.

Estoque, M.A., 1973: **Numerical Modeling of the Planetary Boundary Layer, Workshop on Micrometeorology,** Boston, Amer. Meteor. Soc., 217-270.

Fosberg, M.A., and M.L. Sestak 1986: **KRISSY: user's guide to modeling three-dimensional wind flow in complex terrain.** USDA Forest Service General Technical Report PSW-92, 7 pp.

Hayes, T.P., Kinney, J.J.R., and N.J.M. Wheeler, 1984: **California Surface Wind Climatology.** Staff Rep., Aerometric Data Div., ARB, Rev. ARB/TSD Meteor., June 1989, 74 pp.

King, C., 1980: **SODAR observations of the marine boundary layer during MABLES-WC.** Preprints Second Conference on Coastal Meteorology, Los Angeles, American Meteorological Society, 258-261.

Lester, P.F., 1979: **Marine Atmospheric Boundary Layer Experiments - West Coast (MABLES WC); July 31-August 17, 1978,** Report, San Jose State University Dept. of Meteorology, 57 pp.

Lester, P.F., 1985: **Studies of the Marine Inversion Over the San Francisco Bay Area ... A Summary of the Work of Albert Miller, 1961-1978.** Bull. Amer. Meteor. Soc., 66, 1396-1402.

Ludwig, F.L., 1985: **Inclusion of Buoyancy Forces and Energy Considerations in Mass Consistent Interpolation Schemes.** Prepared for Stanford University Civil Engineering 299, (Prof. Robert Street), Stanford, CA. 26 pp. (Available from author).

Ludwig, F.L., 1986: **Behavior of Smokes and Agents During Variable Meteorological Conditions Over Complex Terrain.** Final Report, Army Research Office Contract DAAG29-83-K-0009, SRI International, Menlo Park, CA, 94025.

Ludwig, F.L., and R.M. Endlich, 1987a: **Improvement of a Mass-Conserving Airflow Scheme.** Proposal for Research, prepared for U.S. Army Atmospheric Sciences Laboratory, SRI International No. ESD 87-115, Menlo Park, CA., 94025.

Ludwig, F.L., and R.M. Endlich, 1987b: **Improvements to the WOCSS (Winds on Critical Streamline Surfaces) Airflow Analysis Code.** Research Brief RB-151, SRI International, Menlo Park, CA.,94025.

Ludwig, F.L., and R.M. Endlich, 1988: **User's Guide For The Winds on Critical Streamline Surfaces (WOCSS) Code.** SRI International Project No. 4354, Menlo Park, CA., 94025.

Mass, C.F. and D.P. Dempsey, 1985: **A One Level Mesoscale Model for Diagnosing Surface Winds in Mountainous and Coastal Regions.** Mon. Wea. Rev., 113, 1211-1227.

McGinley, J., 1986: **Nowcasting Mesoscale Phenomena.** Mesoscale Meteorology and Forecasting (ed. by P. S. Ray), American Meteorological Society, 657-658.

Miller, A., 1968: **Wind Profiles in West Coast Temperature Inversions.** Report, San Jose State Dept. of Meteorology, 57 pp.

Muranaka, Neil J., 1988: **Application of a Mass-Consistent Wind Model to Chinook Windstorms.** Master of Science Thesis, San Jose State Dept. of Meteorology, 92 pp.

Nitz, K.C., R.M. Endlich, and F.L. Ludwig, 1985a: **User's Guide for On-Line Software for Wind Field Analysis and Display.** Prepared for Pacific Gas & Electric Co., SRI International Project No. 7688, Menlo Park, CA., 94025.

Nitz, K.C., R.M. Endlich, and F.L. Ludwig, 1985b: **On-Line Wind Field Calculations for Routine and Emergency Response Applications.** Air Pollution Modeling and Its Applications V (ed. by C. DeWispelaere, F.A. Schiermeier, and N.V. Gillani), Plenum Press, New York, 123-131.

Pielke, R., 1974: **A three-dimensional numerical model of the sea breeze over south Florida,** Mon. Wea. Rev., 102, 115-139.

Pielke, R., 1984: Mesoscale Meteorological Modeling. Academic Press, Inc., 612 pp.

Roope, G.W., 1980: Aircraft observations of the marine inversion during MABLES-WC. Preprints Second AMS Conference on Coastal Meteorology, Los Angeles, 254-257.

Russell, P.B., 1979: Sodar Network Support for LIRAQ Utilization in Conjunction with Project MABLES. Project 8052, SRI International, 39 pp.

Russell, P.B., and E.E. Uthe, 1978: Regional Patterns of Mixing Depth and Stability: SODAR Network Measurements for Input to Air Quality Models. Bull. Amer. Meteor. Soc., 59, 1275-1287.

Sherman, C.A., 1978: A Mass-Consistent Model for Wind Fields over Complex Terrain. J. Appl. Meteor., 17, 312-319.

Thuillier, R.H., 1987: Real-Time Analysis of Local Wind Patterns for Application to Nuclear-Emergency Response. Bull. Amer. Meteor. Soc., 68, 1111-1115.

Tredo, D.C., 1987: Application of a Diagnostic Boundary Layer Wind Model to the San Francisco Bay Area. Master of Science Thesis, San Jose State Dept. of Meteorology, 119 pp.

APPENDIX A

DATA FILES

STATION	UTME	UTMN
ALAMEDA NAS	560.0	4180.0
BETHEL ISLAND	619.4	4207.4
CHABOT	579.4	4175.0
CONCORD	585.4	4199.4
DANVILLE	588.7	4185.0
FORT FUNSTON	544.1	4174.1
FORT ORD	598.0	4061.0
FREMONT	589.2	4155.6
GILROY	630.7	4095.5
HAYWARD	577.0	4167.0
HIGHLAND	605.0	4185.7
KREGOR	597.5	4199.9
LIVERMORE	608.9	4171.4
MOFFETT NAS	586.0	4140.0
MONTEREY	602.0	4050.0
MORGAN HILL	620.0	4110.0
MOSS LANDING	609.2	4145.0
MT. HAMILTON	621.5	4134.0
MT. PISE	558.5	4144.9
MT. TAMALPAIS	534.6	4196.9
NAPA	563.0	4237.5
NOVATO	540.1	4219.2
OAKLAND ARPT	569.0	4173.0
PALO ALTO	576.7	4144.9
PETALUMA	534.1	4234.5
PIDGEON PT	553.0	4115.0
PILLAR POINT	544.4	4150.8
PITTSBURG	595.0	4210.0
PLEASANTON	595.9	4172.9
REID-HILLVIEW	604.0	4130.0
RIO VISTA	613.5	4227.4
SALINAS	625.0	4056.0
SAN CARLOS	566.4	4152.4
SAN FRAN ARPT	556.2	4163.2
SAN MARTIN	625.0	4104.4
SAN JOSE	595.2	4134.7
SANTA CLARA	592.7	4143.4
SANTA ROSA	521.0	4252.0
SONOMA MARINA	546.1	4220.4
STOCKTON	652.1	4201.6
TESLA	626.5	4174.8
TRAVIS AFB	594.4	4235.4
UNION CITY	581.9	4160.9
VALLEY FORD	509.1	4239.9
VOLLMER PEAK	568.5	4193.0
WALNUT CREEK	580.7	4196.4

APPENDIX A-1 UTM Coordinates of Stations

```
871007 00

8 0 0 0 0

8 0 0 0 0

619. 4207.  -999.0 88.     283.0 4.9  'Bethel Island'
563. 4237.  -999.0 78.     178.0 5.8  'Napa'
521. 4250.  -999.0 77.     238.0 2.7  'Santa Rosa'
534. 4234.  -999.0 81.     321.0 5.4  'Petaluma'
582. 4161.  -999.0 83.     318.0 4.0  'Union City'
595. 4135.  -999.0 85.     330.0 3.1  'San Jose Airport'
625. 4104.  -999.0 87.     324.0 3.1  'San Martin'
569. 4173.  -999.0 81.     300.0 3.6  'Oakland RAOB'
561. 4181.  -999.0 -999.0 -999.0 -999.0  Alameda NAS
584. 4141.  -999.0 -999.0 -999.0 -999.0  Moffett NAS
596. 4173.  -999.0 -999.0 -999.0 -999.0  Pleasanton
594. 4235.  -999.0 -999.0 -999.0 -999.0  Travis AFB
581. 4196.  -999.0 -999.0 -999.0 -999.0  Walnut Creek
652. 4202.  -999.0 -999.0 -999.0 -999.0  Stockton
540. 4219.  -999.0 -999.0 -999.0 -999.0  Novato
556. 4163.  1012.2 -999.0 -999.0 -999.0  San Francisco Airport
566. 4152.  -999.0 -999.0 -999.0 -999.0  San Carlos
577. 4145.  -999.0 -999.0 -999.0 -999.0  Palo Alto
577. 4167.  -999.0 -999.0 -999.0 -999.0  Hayward
609. 4171.  -999.0 -999.0 -999.0 -999.0  Livermore
595. 4210.  -999.0 -999.0 -999.0 -999.0  Pittsburg
630. 4095.  -999.0 -999.0 -999.0 -999.0  Gilroy
593. 4143.  -999.0 -999.0 -999.0 -999.0  Santa Clara

569. 4173.
8
6.     300. 3.6
111.   295. 4.0
305.   280. 4.5
610.   245. 6.7
915.   240. 8.0
1220.  240. 6.3
1524.  240. 4.5
1829.  215. 4.5
```

The above lines of data include:

- date (yymmdd hh)
- values of array IDOP (explained below*)
- values of array ITMP (explained below*)
- list of NUMNWS sites (the value of NUMNWS is given in w7.for) at which wind & temperature data is available:
  UTME, UTMN, sfc. pressure, sfc. temperature, dd, ff.
- for those sites at which doppler data is available (as defined by the values of array IDOP), the following data:
  UTME, UTMN (coords of stn)
  NHTS (number of data levels)
  Nhts lines of: elevation(m), dd, ff.

* Example: IDOP(1)=8, IDOP(2)=IDOP(3)=IDOP(4)=IDOP(5)=0 means that the 2nd station in the list above contain doppler data (other array elements are set to zero). This information is needed deep in the heart of the program! Ditto for ITMP. The sizes of arrays IDOP and ITMP are set in GRIDS.PAR and NTSITES.PAR (currently, IDOP(5) and ITMP(5) allow for wind data from up to 5 doppler sites and sounding data from up to 5 sites).

APPENDIX A-2 Sample Wind data input file

```
569. 4173.
18  3
020.     27.2     1012.0
364.     25.6     1000.0
500.     25.0      996.0
827.     24.4      987.0
1000.    25.6      980.0
1299.    27.2      968.0
1500.    27.2      961.0
2000.    26.7      945.0
2500.    26.7      929.0
2520.    26.7      928.0
3000.    25.6      914.0
3500.    24.4      898.0
4000.    23.3      883.0
4500.    22.2      868.0
5000.    21.1      852.0
5033.    21.1      850.0
5500.    20.0      835.0
6000.    18.9      821.0
```

The above lines of data include:

- For each temperature sounding site (separated by a space):
  UTME, UTMN
  NHTS, ITYP
  Nhts lines of:
    height(M--MSL), temperature (°C), potential temp lapse rate(°K/M)
    (IF ITYP=1)
    height(M--MSL), temperature (°C), pressure (mb)
    (IF ITYP=2)
    height(in FT, MSL), temperature(°C), pressure(mb)
    (IF ITYP=3)

APPENDIX A-3 Sample Temperature Sounding data input file

10.	8.	8.	3.	19.	26.	36.	14.	3.	31.	25.	6.	2.	1.	0.	0.	0.	0.	1.
0.	3.	6.	8.	3.	28.	2.	11.	2.	20.	3.	1.	1.	0.	0.	0.	0.	0.	1.
0.	9.	14.	11.	9.	2.	7.	0.	1.	14.	0.	2.	0.	3.	1.	0.	0.	0.	1.
0.	8.	15.	25.	13.	2.	0.	0.	0.	14.	0.	0.	0.	6.	3.	0.	0.	0.	1.
0.	6.	8.	21.	23.	10.	0.	0.	0.	1.	0.	1.	0.	0.	0.	0.	0.	0.	0.
0.	0.	1.	24.	31.	7.	0.	0.	10.	21.	5.	4.	17.	4.	3.	0.	0.	0.	0.
0.	0.	0.	5.	35.	10.	0.	0.	19.	22.	13.	9.	44.	20.	5.	1.	0.	0.	0.
0.	0.	0.	0.	0.	7.	0.	0.	2.	33.	27.	14.	43.	52.	16.	3.	0.	0.	0.
0.	0.	0.	0.	0.	0.	9.	0.	0.	2.	18.	26.	18.	28.	29.	20.	4.	1.	1.
0.	0.	0.	0.	0.	0.	11.	0.	0.	0.	7.	26.	10.	12.	17.	41.	23.	7.	3.
0.	0.	0.	0.	0.	0.	20.	0.	0.	0.	1.	25.	40.	26.	28.	60.	45.	30.	11.
0.	0.	0.	0.	0.	0.	33.	14.	0.	0.	1.	1.	20.	37.	76.	70.	76.	63.	48.
0.	0.	0.	0.	0.	0.	0.	31.	12.	1.	0.	0.	5.	25.	71.	95.	105.	79.	72.
0.	0.	0.	0.	0.	0.	0.	25.	40.	9.	2.	0.	1.	23.	74.	89.	77.	82.	56.
0.	0.	0.	0.	0.	0.	0.	12.	23.	52.	19.	5.	3.	4.	53.	92.	72.	71.	83.
0.	0.	0.	0.	0.	0.	0.	7.	32.	34.	52.	13.	6.	5.	29.	43.	85.	61.	64.
0.	0.	0.	0.	0.	0.	0.	11.	31.	46.	49.	36.	68.	21.	11.	25.	70.	52.	48.
0.	0.	0.	0.	0.	0.	0.	0.	17.	58.	25.	30.	54.	80.	22.	13.	30.	45.	51.
0.	0.	0.	0.	0.	0.	0.	0.	0.	24.	37.	23.	25.	41.	48.	16.	7.	37.	49.
0.	0.	0.	0.	0.	0.	0.	0.	0.	0.	9.	2.	1.	11.	6.	35.	10.	4.	11.

This data file is extracted from the original 1km x 1km dataset.
The resolution is 8km, the lower left hand corner of the domain
has UTM coordinates 500.,4092. and the upper right hand corner
of the domain has UTM coordinates 652.,4244.

APPENDIX A-4 Sample Terrain data input file (heights are in decameters, ASL)

APPENDIX B

CODE LISTINGS

```
      PROGRAM TOPO
c
c  Reads topography data from the TOPO data file, and creates
c  the desired array for PLOT88 (1, 2, 4, or 8 km. resolution.)
c    Original by: AFC Bridger          (Rev. by Becker, 12/1/90)
c
c       NOTE that 20 x 20, for example, is 152km x 152km (not 160)
c
      dimension z(490:660,4090:4286),ztemp(8)
      integer resol,blok,Beg,End
c
      open (7,file='topo.dat')
      open (4,file='terr.dat')
c
      print*,'Enter desired resolution (km, integer) >'
      read*,resol
c
      print*
      print*,'Enter western and eastern limits (UTM coordinates)'
      print*
      print*,'   min/max available:    490 and 660'
      print*,'      suggest 500,652 for a 20x20 at 8km resol'
      print*,'              or 500,656       40x40 at 4km resol'
      print*,'              or 500,658       80x80    2km resol'
      read (*,*) utxw,utxe
c
      print*
      print*,'Enter southern and northern limits (UTM coordinates)'
      print*
      print*,'   min/max available:     4090 and 4286'
      print*,'      suggest 4092,4244 for a 20x20 at 8km resol'
      print*,'              or 4092,4248       40x40 at 4km resol'
      print*,'              or 4092,4250       80x80    2km resol'
      read (*,*) utys,utyn
c-----------------------------------------------------------------------
c       Read entire topo.dat file and create huge 1 km array:
c
      Do 5 K = 1,197
         Do 6 J = 1,21
              Read(7,*) utx,uty,(ztemp(i),i=1,8)
                     Do 7 I = 1,8
                          L = I-1
                          z(utx + L,uty) = ztemp(I)
   7                 Continue
   6     Continue
              Read(7,*) utx,uty,(ztemp(i),i=1,3)
                     Do 8 I = 1,3
                          L = I-1
                          z(utx + L,uty) = ztemp(I)
   8                 Continue
   5  Continue
c
      do 10 i=utxw,utxe
      do 10 j=utys,utyn
          z(i,j)=z(i,j)/10.
   10 Continue
```

APPENDIX B-1 TOPO program listing

```
c-----------------------------------------------------------------------
c                      Create output:
c
      kx= (utxe-utxw)/resol
      ky= (utyn-utys)/resol
c
      IF(kx.LE.20) THEN
      blok = 1
      ELSE IF(kx.GT.20.and.kx.LE.40) THEN
      blok = 2
      ELSE IF(kx.GT.41.and.kx.LE.60) THEN
      blok = 3
      ELSE IF(kx.GT.61.and.kx.LE.80) THEN
      blok = 4
      END IF
c
      DO 30   L = 1,blok
c
             M = L-1
             N = 19*resol
             NN= 20*resol
             Beg =  INT(utxw) + (M*NN)
             End =  INT(utxw) + N+(NN*M)
             iutxe = INT(utxe)
c
      DO 31  J= utyn, utys, (-resol)
               IF((L*N)+utxw.GE.utxe) THEN
      write(4,35) (z(I,J),I = Beg,iutxe,resol)
               ELSE
      write(4,35) (z(I,J),I = Beg,End,resol)
               END IF
  31  CONTINUE
  30  CONTINUE
c
  35  format (20f4.0)
c
      write (4,36) resol,utxw,utys,utxe,utyn
  36  format (//,1x,'This data file is extracted from the original 1km x
     . 1km dataset.',/,1x,'The resolution is',i3,'km, the lower left han
     .d corner of the domain ',/,1x,'has UTM coordinates ',f5.0,',',f5.0
     .,' and the upper right hand corner ',/,1x,'of the domain has UTM c
     .oordinates ',f5.0,',',f5.0)
c
      close(4)
      close(7)
c
      stop
      end
```

APPENDIX B-1 TOPO program listing (continued)

```
      PROGRAM     ANAL
C     Version:          INVERSE SQUARED              {created: 12/1/90}
C                                                    {latest:  8/18/91}
C
C         *  up to 21 weather stations  (user-selected, on line)
C         *  up to 5 nearby grid points (sqrt(resol**2 + resol**2)
C         *  20 x 20 grid point domain
B
B     **  * * * * * * Revision Notes:* * * * * * * * * * * * * * * * **
B     **                                                               **
B     **               REVISED on March 24, 1991:                      **
B     **  1)   Elimated tower height                                   **
B     **  2)   Edited the explanatory text on output page bottom       **
B     **  3)   Fixed the calculation of %err between speeds           **
B     **         (now: %err = model winds are X% of observed winds)    **
B     **               REVISED on August 19, 1991:                     **
B     **  4)   Eliminated station height                               **
B     **  5)   Fixed left margin for missing stations                  **
B     **  6)   miscellaneous edits suggested by AFCB, May 1991         **
B     * * * * * * * * * * * * * * * * * * * * * * * * * * * * * * * * * *
B
C   * * * * * * * * * * * * * * * * * * * * * * * * * * * * * * * * * * *
C   Reads WOCSS output: DIR1.1 and SPD1.1 files, and WOCSS input:
C   WINDS.DAT and TERRAIN.DAT.  Program assesses how well the WOCSS
C   model output compares to the observed winds at each of the Nstns
C   reporting stations.  Note that there is a problem when observed
C   winds are calm, as this creates an infinite % difference in speed
C   (currently handled by not including calm winds into stats).
C-----------------------------------------------------------------------
      Parameter (Maxwx=21, NN=20)
      REAL UTMX(Maxwx), UTMY(Maxwx)
      REAL UTx(NN), UTy(NN)
      REAL LLx, LLy, URx, URy
      INTEGER NNx(Maxwx), NNy(Maxwx)
      REAL Uavg(Maxwx), Vavg(Maxwx), DIRavg(Maxwx), SPDavg(Maxwx)
      REAL DIR(NN,NN), SPD(NN,NN), U(NN,NN), V(NN,NN)
      REAL DD(Maxwx), FF(Maxwx)
      REAL DelDD(Maxwx), DelFF(Maxwx)
      REAL DDerr(Maxwx),FFerr(Maxwx), DDoff, FFoff
      INTEGER DATE, RESOL, Nstns
      CHARACTER NAME(Maxwx)*27,BV(Maxwx)*4,STN(23)*27,temp1*9,temp2*9
C
      Open(5,file='info.txt')
      Open(6,file='terrain.dat')
      Open(7,file='winds.dat')
      Open(8,file='dir1.1')
      Open(9,file='spd1.1')
      Open(10,file='anal.out')
b
      print*,'how many stations to be read? '
      read*,Nstns
C***********************************************************************
C Read INFO.TXT for list of stations
c
       DO 5 I = 1,23
       print*,'I = ',I
```

APPENDIX B-2 **ANAL program listing**

```
           Read(5,*) Stn(I)
         print*,'stn = ',stn(I)
 5       CONTINUE
*************************************************************************
C-- Read TERRAIN.DAT file for Resolution, LL and UR corner of domain:
         DO 10 I = 1,(NN+3)
       Read(6,*)
 10      CONTINUE
       Read(6,600) RESOL
       Read(6,601) LLx, LLy
       Read(6,602) URx, URy
 600     Format (19x,I2)
 601     Format (22x,F4.0,1x,F5.0)
 602     Format (36x,F4.0,1x,F5.0)
C*************************************************************************
C---- Read the WINDS.DAT file for Date of Run, and Weather Stn. Data:
c
       Read(7,700) DATE
 700     Format(I9)
       Write(10,780) DATE, RESOL
         DO 20 I = 1,5
       Read(7,*)
 20      CONTINUE
C
         DO 21 I = 1, Nstns
       Read(7,*) UTMX(I),UTMY(I),Gunk1,Gunk2,DD(I),FF(I),NAME(I)
       XX=UTMX(I)
       YY=UTMY(I)
       IF (XX.LT.LLx.OR.XX.GT.URx) Write(10,790) Name(I)
       IF (YY.LT.LLy.OR.YY.GT.URy) Write(10,791) Name(I)
       IF (DD(I).LT.0.0) Write(10,792) Name(I)
c
       temp1=name(I)
         DO 111 J = 1,23
       temp2=stn(J)
         print*,temp1(1:9), temp2(1:9)
         IF (temp1(1:9).eq.temp2(1:9)) THEN
       NAME(I) = STN(J)
         ENDIF
 111     CONTINUE
c
 21      CONTINUE
C*************************************************************************
C---------------- Read the DIRECTION and SPEED files (DIR1.1, SPD1.1)
         DO 30 J = NN,1,-1
       Read(8,*) (DIR(I,J), I=1,NN)
 30      CONTINUE
         DO 31 J = NN,1,-1
       Read(9,*) (SPD(I,J), I=1,NN)
 31      CONTINUE
c
         DO 32 J = 1,NN
         DO 32 I = 1,NN
       SPD(I,J) = SPD(I,J)*0.1
 32      CONTINUE
```

APPENDIX B-2 ANAL program listing (continued)

```
C-------------------------Transfer all DIR's and SPD's to U's & V's:
          DO 33 J = NN,1,-1
          DO 33 I = 1,NN
       U(I,J) = -SPD(I,J)*SIN(DIR(I,J)/57.295)
       V(I,J) = -SPD(I,J)*COS(DIR(I,J)/57.295)
 33       CONTINUE
C
C*****************************************************************************
C------ Find each weather station's NEAREST NEIGHBOR grid point (x,y)
          DO 35 M = 1, Nstns
       NNx(M) =  1 + NINT((UTMX(M)-LLx)/RESOL)
       NNy(M) =  1 + NINT((UTMY(M)-LLy)/RESOL)
 35       CONTINUE
C
C*****************************************************************************
C----------------------------- Assign UTM values to every grid point:
          DO 41 J = 1, NN
          DO 41 I = 1, NN
             UTx(I) = LLx + (I-1)*Resol
             UTy(J) = LLy + (J-1)*Resol
 41       CONTINUE
C*****************************************************************************
C             Calculate the inverse-square average of the four or five
C                      grid points nearest to the observation station:
C
        DIAG = SQRT(resol**2 + resol**2)
C
C                                                        For each station:
        DO 45 M = 1, Nstns
        SUM = 0.0
        SUMU = 0.0
        SUMV = 0.0
        DIST = 0.0
          XX=UTMX(M)
          YY=UTMY(M)
        print*,'Station # ',M
      IF (XX.LT.LLx.OR.XX.GT.URx) GOTO 45
      IF (YY.LT.LLy.OR.YY.GT.URy) GOTO 45
C
      IF (FF(M).LE.0.00) GOTO 45
C
           DO 46 J = NN,1,-1
           DO 46 I = 1,NN
C--------------------------- for a station exactly on a grid point:
      IF(UTMX(M).EQ.UTx(I).and.UTMY(M).EQ.UTy(J))  THEN
             Uavg(M) = U(I,J)
             Vavg(M) = V(I,J)
             print*,'exactly on a grid point'
             GOTO 45
      ENDIF
C---------------------------------------otherwise, find nearby points:
      IF(ABS(UTMX(M)-UTX(I)).LT.DIAG.AND.ABS(UTMY(M)-UTY(J)).LT.DIAG)
     & THEN
             DIST = SQRT((UTMX(M)-UTX(I))**2 +
     &                   (UTMX(M)-UTY(J))**2)
             DIST = DIST**2
```

APPENDIX B-2 ANAL program listing (continued)

```
            IF(DIST.LT.0.01) DIST = 0.01
            RSEPSQ = 1.0/DIST
            Utemp = U(I,J)
            Vtemp = V(I,J)
            SUM = SUM + RSEPSQ
            SUMU = SUMU + RSEPSQ*Utemp
            SUMV = SUMV + RSEPSQ*Vtemp
      ENDIF
C
  46    CONTINUE
C
          IF(SUM.LE.0.0) THEN
             Uavg(M) = 0.0
             Vavg(M) = 0.0
          ELSE
             Uavg(M) = sumu/sum
             Vavg(M) = sumv/sum
          ENDIF
C
C----------------------convert Uavg and Vagv into DIRavg and SPDavg:

          IF(Uavg(M).eq.0.00 .AND. Vavg(M).eq.0.00) THEN
           DIRavg(M) = 0.00
           SPDavg(M) = 0.00
      print*,'uavg(m) and vavg(m) are: ', uavg(M), vavg(M)
           GOTO 45
          ENDIF
      DIRavg(M) = AMOD(540.+ATAN2(Uavg(M),Vavg(M))*57.295,360.)
      SPDavg(M) = SQRT(Uavg(M)**2+Vavg(M)**2)
      print*,' Station # ',M, Name(M)
      print*,'uavg(m) and vavg(m) are: ', uavg(M), vavg(M)
      print*,'diravg(m) and spdavg(m) are: ', diravg(M), spdavg(M)
 45   CONTINUE
C
C*************************************************************************
C---- Calculate the difference between obs. wind and NEARBY grid pts.
         DO 50 I = 1, Nstns
      DelDD(I) = DIRavg(I) - DD(I)
      DelFF(I) =  SPDavg(I) - FF(I)
 50      CONTINUE
C*************************************************************************
C---- Calculate the PERCENT difference between obs & model winds, and
C------------------------------ determine backing and veering winds:
         DO 60 I = 1, Nstns
      DDerr(I) =   100*ABS(DelDD(I)/360.)
      IF(DDerr(I).GT.50.) DDerr(I)=100.-DDerr(I)
           IF (FF(I).eq.0.) GOTO 60
           IF (SPDavg(I).eq.0.) GOTO 60
      FFerr(I) =   100*(SPDavg(I)/FF(I))
C
      IF(DelDD(I).LT.0.AND.DelDD(I).GT.-180.) bv(I)='back'
      IF(DelDD(I).GT.0.AND.DelDD(I).LT.180.)  bv(I)='veer'
      IF(DelDD(I).LT.-180.)                   bv(I)='veer'
      IF(DelDD(I).GT.180.)                    bv(I)='back'
 60      CONTINUE
C
```

APPENDIX B-2 ANAL program listing (continued)

```
C*********************************************************************
C-------- Calculate the average of all percentage errors (DD and FF):
      FFoff = 0.
      DDoff = 0.
      Nout = 0.
         DO 70 I = 1, Nstns
                IF (FF(I).LE.0.) THEN
                  Nout = Nout + 1
                  GOTO 70
                ENDIF
                       XX=UTMX(I)
                       YY=UTMY(I)
                     IF (XX.LT.LLx.OR.XX.GT.URx) THEN
                       Nout = Nout + 1
                       GOTO 70
                     ENDIF
                     IF (YY.LT.LLy.OR.YY.GT.URy) THEN
                       Nout = Nout + 1
                       GOTO 70
                     ENDIF
C
        IF(bv(I).eq.'back') THEN
        DDerr(I) = -DDerr(I)
        ENDIF
C
      FFoff = FFoff + FFerr(I)
      DDoff = DDoff + DDerr(I)
 70      CONTINUE
      FFoff = FFoff/(Nstns-Nout)
      DDoff = DDoff/(Nstns-Nout)
C*********************************************************************
C---- Output:
C
      Write(10,781) FFoff
      Write(10,782) DDoff
      Write(10,799)
      Write(10,801)
      Write(10,802)
      Write(10,800)
         DO 80 I = 1, Nstns
             IF (FF(I).eq.0.) THEN
             WRITE(10,8000) NAME(I)
             GOTO 80
             ENDIF
             IF (FF(I).lt.0.) THEN
             WRITE(10,8001) NAME(I)
             GOTO 80
             ENDIF
           XX=UTMX(I)
           YY=UTMY(I)
           IF (XX.LT.LLx.OR.XX.GT.URx) GOTO 80
           IF (YY.LT.LLy.OR.YY.GT.URy) GOTO 80
     Write(10,803) Name(I),Nint(DD(I)),Nint(DIRavg(I)),Nint(DDerr(I)),
    +bv(I),FF(I),SPDavg(I),FFerr(I)
 80      CONTINUE
```

APPENDIX B-2 ANAL program listing (continued)

```
      Write(10,800)
      Write(10,804)
      Write(10,805)
      Write(10,806)
      Write(10,807)
      Write(10,808)
  780 FORMAT(4(/),2x,' RESULTS FOR ',I9, ' (yymmddhh) :',I2,' km resol')
  781 FORMAT(/,15x,' AVERAGE SPEED RATIO (model/obs) = ', F5.1,'%')
  782 FORMAT(15x,' AVERAGE DIRECTIONAL ERROR =        ', F5.1,'%')
  790 FORMAT(/,16x,A14,' lies BEYOND the DOMAIN(x))',
     $/,16x,'not listed below; NOT included in the following stats')
  791 FORMAT(/,15x,A14,' lies BEYOND the DOMAIN(y))',
     $/,16x,'not listed below; NOT included in the following stats')
  792 FORMAT(/,16x,A14,' is NOT AVAILABLE',
     $/,16x,'not listed below; NOT included in the following stats')
  799     FORMAT(/,2x,75('='))
  800     FORMAT(2x,75('='))
  801     FORMAT(2x,'STATION',15x,'DIRECTION',4x,'%err*',15x,'SPEED',
     +7x,'ratio**')
  802     FORMAT(23x,'(obs)',1x,'(model)',20x,'(obs)',1x,'(model)')
 8000     format(/,2x,A13,1x,13x,'CALM winds--no stats.')
 8001     format(/,2x,A13,1x,13x,'MISSING-----no stats.')
  803     FORMAT(/2x,A17,4x,I3,'''',2x,I3,'''',2x,I3,
     +'%',1x,A4,11x,F5.1,1x,F5.1,2x,F5.0,'%')
  804     FORMAT(2x,'LEGEND:')
  805     FORMAT(/,2x,'*  %err uses the smallest angle between model and
     +obs, div. by 360°.')
  806     FORMAT('     %err is the % difference between model-obs, and do
     +es not exceed 50%.')
  807     FORMAT(/,2x,'   ("backing & veering" means how the model has ch
     +anged the observed winds).')
  808     FORMAT(/,2x,'** (Column represents model/observed wind ratio)')
C
        DO 90 I = 1,5
      Close(I+5)
   90   CONTINUE
       END
```

APPENDIX B-2 ANAL program listing (continued)

```
      PROGRAM BLTOP
c                                                                       **
c * * Reads Logie's inversion data file (09Aug78.16p),                  **
c          (UTMS:  500-632,  4072-4236)                                 **
c          (with top 2 and bottom 5 rows trimmed off: 34 x 37)          **
c * * Produces an inversion layer height data file (BLTOP.DAT),         **
c           at 4km or 8 km resolution:  40 x 40 or 20 x 20)             **
c * * Reads TERR4KM.DAT so that inversion data can be related           **
c          to terrain height.                                           **
c * * Lower left corner is UTM 500,4092.                                **
c                                                                       **
c       --------------- Becker:  October 27, 1990 ---revision---       **
c***********************************************************************
      Parameter(nx=34, ny=37)
      Real Terr(40,40)
      Real Blt(40,40)
      integer resol
c
      Open(11,file='09aug78.16p')
      Open(12,file='bltop.dat')
      Open(13,file='terr4km.dat')
c
c------------------------------------------- Choose 4km or 8km output
      Print*,'enter desired output, 4 or 8 km'
      Read(*,*) resol
c
c********************************************** Read TERR4KM.DAT (4km)
      Do 10 J=40,1,-1
         Read(13,7) (terr(I,J), I=1,20)
  10  Continue
      Do 11 J=40,1,-1
         Read(13,7) (terr(I,J), I=21,40)
  11  Continue
c
c**************** Read Inversion data (09AUG78.16P) (4km) (data in dam)
         Read(11,*)
      Do 12 J=ny,1,-1
         Read(11,*) (Blt(I,J), I=1,nx)
  12  Continue
c***********************************************************************
c---------  For missing data points ("99"), let Bltop = terr + adj, **
c---------  where the adjustment has been carefully determined from **
c---------  Logie's plotted data of terrain & inversion topography, **
c---------  using two "best fit" lines to describe the data trends. **
c---------  Also, ensure that the Bltop is at least 30 meters AGL.  **
c
      Do 13 J=ny,1,-1
      Do 13 I=1,nx
         IF(Blt(I,J).NE.99.) GO TO 130
            IF(terr(I,J).GE.0.AND.terr(I,J).LE.30.) THEN
              Blt(I,J) = terr(I,J) + (terr(I,J) - 40.)/(-6/5)
            ELSEIF(terr(I,J).GT.30.AND.terr(I,J).LT.90.) THEN
              Blt(I,J) = terr(I,J) + (terr(I,J) - 105.)/(-4.)
            ENDIF
 130  continue
c
```

APPENDIX B-3 BLTOP program listing

```
      IF(Blt(I,J).LE.(terr(I,J)+3.))   Blt(I,J) = Terr(I,J) + 3.
c
  13  CONTINUE
c
c-----  NOTE that Logie's data is 34 x 37, and I need 40 x 40 data. **
c-----  Therefore, fill in unavailable edges of inversion data by   **
c-----  using the above method.                                     **
c
      Do 14 J=38,40
      Do 14 I=1,34
c
            IF(terr(I,J).GE.0.AND.terr(I,J).LE.30.) THEN
              Blt(I,J) = terr(I,J) + (terr(I,J) - 40.)/(-6/5)
            ELSEIF(terr(I,J).GT.30.AND.terr(I,J).LT.90.) THEN
              Blt(I,J) = terr(I,J) + (terr(I,J) - 105.)/(-4.)
            ENDIF
c
      IF(Blt(I,J).LE.(terr(I,J)+3.))   Blt(I,J) = Terr(I,J) + 3.
c
  14  CONTINUE
c
      Do 15 J=1,40
      Do 15 I=35,40
c
            IF(terr(I,J).GE.0.AND.terr(I,J).LE.30.) THEN
              Blt(I,J) = terr(I,J) + (terr(I,J) - 40.)/(-6/5)
            ELSEIF(terr(I,J).GT.30.AND.terr(I,J).LT.90.) THEN
              Blt(I,J) = terr(I,J) + (terr(I,J) - 105.)/(-4.)
            ENDIF
c
      IF(Blt(I,J).LE.(terr(I,J)+3.))   Blt(I,J) = Terr(I,J) + 3.
c
  15  Continue
c*************************************************************************
c-----------------------------------------WRITE TO WOCSS INPUT FILES:
      IF(resol.eq.4) THEN
c--------------------------------------- Write to 4km BLTOP.DAT file
      Do 20 J=40,1,-1
         Write(12,7) (Blt(I,J),I=1,20)
  20  Continue
      Do 21 J=40,1,-1
         Write(12,7) (Blt(I,J),I=21,40)
  21  Continue
   7  Format(20f4.0)
      ELSE
c-----------------------------------------Write to 8km BLTOP.DAT file
      Do 30 J=39,1,-2
         Write(12,7) (Blt(I,J),I=1,39,2)
  30  Continue
      END IF
c-------------------------------------------------------------------
      close(11)
      close(12)
      close(13)
c
      end
```

APPENDIX B-3 BLTOP program listing (continued)

```
      PROGRAM NEWBAL
C                              (10/20/90)
C     Program designed to read u and v components from COARSE.OUT
C     (levels 2 - 5), and sig level heights from SIG1.N (N=1,6).
C     It calculates mass balance along 4 edges of entire domain.
N
N     The method attempts to emulate the BAL5 method of WOCSS, wherein
N     the flow components on sig. surfaces are multiplied by layer thk,
N     defined as spanning from halfway above and below each flow surface,
N     except for the bottom and top layers:  Layer 5 is only halfthick,
N     while Layer 1 is 1.5 thick.
N
      Integer U(6,20,20), V(6,20,20), W(6,20,20)
      Integer SIGZ(6,20,20)
      Character Junk*30, input*30
C           The domain sides have 5 face levels & 19 hor. faces,
C           and, four total sides (N, E, S, and W)
      Real Nmass(20,20)
      Real Emass(20,20)
      Real Smass(20,20)
      Real Wmass(20,20)
      Real Nlayer(6), Elayer(6), Slayer(6), Wlayer(6)
      Real North, East, South, West
C
      Real InMass(4), OutMass(4), AllIn, AllOut, Net
      Real TotMASS
      Real LossR
C
C*************************************************************************
C****           EXPLANATION OF VARIABLES ABOVE:                          ***
c****                                                                     ***
C     U, V, W are from coarse.out.                                         **
C     Z are sigma sfc heights from sig1.N.                                 **
C     (nMass, e.g., is the mass entering domain through north face)        **
C     InMass(4) is the contribution to incoming mass from 4 faces.         **
C     OutMass(4) is for outgoing mass, LossR = rate of loss.               **
C*************************************************************************
C***                                                                       ***
                Open(1,file='sig1.1')
                Open(2,file='sig1.2')
                Open(3,file='sig1.3')
                Open(4,file='sig1.4')
                Open(5,file='sig1.5')
                Open(6,file='sig1.6')
                Open(10,file='coarse.out')
                Open(11,file='newbal.out')
                Open(12,file='BUGS.OUT')
C*************************************************************************
C   Enter information desired to appear on output file:                   **
C                                                                         **
      print*,'*********************************************************'
      print*,' enter the desired information for the output file   **'
      print*,'*********************************************************'
      Read(*,801) input
      Write(11,689) input
 689  FORMAT(' RUN RESULTS:   ',A30)
```

APPENDIX B-4 BALANCE program listing

```
C*********************************************************************
C                                                          Read all files:
C
C        (NOTE that I have fixed Coarse.out to have north row first)
C
                READ(10,801) junk
        DO 20 M = 2, 6
              DO 21 J = 20,1,-1
                 READ(10,800) (U(M,I,J), I = 1, 20)
 21           CONTINUE
        print*, junk
                READ(10,801) junk
              DO 22 J = 20,1,-1
                 READ(10,800) (V(M,I,J), I = 1, 20)
 22           CONTINUE
                READ(10,801) junk
              DO 23 J = 20,1,-1
                 READ(10,800) (W(M,I,J), I = 1, 20)
 23           CONTINUE
                IF(M.eq.6) GO TO 20
                READ(10,801) junk
 20     CONTINUE
C
        DO 30 M = 1, 6
                DO 31 J = 20, 1, -1
                        READ(M,800) (SIGZ(M,I,J), I = 1, 20)
 31             CONTINUE
 30     CONTINUE
 800    FORMAT(1x,20I4)
C*********************************************************************
C*********************************************************************
C      Mass balance calculations, for 4 sides, 19 horiz. box faces,
C      and 5 "flow levels" (actually, spanning between box faces).
C      (for a total of 4*5*19 = 380 box faces):
C
      DO 200 I = 2,6
         Nlayer(I) = 0.
         Elayer(I) = 0.
         Slayer(I) = 0.
         Wlayer(I) = 0.
 200  CONTINUE
C
      DO 201 I = 1,4
         InMass(I) = 0.
         OutMass(I)= 0.
 201  CONTINUE
C
         AllIn=0.
         AllOut=0.
C*********************************************************************
C-----------Check BOTTOM layer first (1.5 times thick)----------
        M = 2
        write(12,*) M
```

APPENDIX B-4 BALANCE program listing (continued)

```
C--------------------------------------- Check along north edge:
         DO 210 I = 1, 19
                J = 20
      ABOVE = .5*5.*((SIGZ(M+1,I,J)-SIGZ(M,I,J))+
     $(SIGZ(M+1,I+1,J)-SIGZ(M,I+1,J)))
      BOTTOM  =  5.*((SIGZ(M,I,J)-SIGZ(M-1,I,J))+
     $(SIGZ(M,I+1,J)-SIGZ(M-1,I+1,J)))
      THK = ABOVE + BOTTOM
      TEMP = .05*(V(M,I,J)+V(M,I+1,J))
        Nmass(I,J) = -TEMP*THK*8000.
        Nlayer(M)  = Nlayer(M) + Nmass(I,J)
         write(12,*) THK
 210     CONTINUE
C
C--------------------------------------- Check along east edge:
         DO 220 J = 1, 19
                I = 20
      ABOVE = .5*5.*((SIGZ(M+1,I,J)-SIGZ(M,I,J))+
     $(SIGZ(M+1,I,J+1)-SIGZ(M,I,J+1)))
      BOTTOM  =  5.*((SIGZ(M,I,J)-SIGZ(M-1,I,J))+
     $(SIGZ(M,I,J+1)-SIGZ(M-1,I,J+1)))
      THK = ABOVE + BOTTOM
      TEMP = .05*(U(M,I,J)+U(M,I,J+1))
        Emass(I,J) = -TEMP*THK*8000.
        Elayer(M)  = Elayer(M) + Emass(I,J)
         write(12,*) THK
 220     CONTINUE

C--------------------------------------- Check along south edge:
         DO 230 I = 1, 19
                J = 1
      ABOVE = .5*5.*((SIGZ(M+1,I,J)-SIGZ(M,I,J))+
     $(SIGZ(M+1,I+1,J)-SIGZ(M,I+1,J)))
      BOTTOM  =  5.*((SIGZ(M,I,J)-SIGZ(M-1,I,J))+
     $(SIGZ(M,I+1,J)-SIGZ(M-1,I+1,J)))
      THK = ABOVE + BOTTOM
      TEMP = .05*(V(M,I,J)+V(M,I+1,J))
        Smass(I,J) = TEMP*THK*8000.
        Slayer(M)  = Slayer(M) + Smass(I,J)
         write(12,*) THK
 230     CONTINUE
C
C--------------------------------------- Check along west edge:
         DO 240 J = 1, 19
                I = 1
      ABOVE = .5*5.*((SIGZ(M+1,I,J)-SIGZ(M,I,J))+
     $(SIGZ(M+1,I,J+1)-SIGZ(M,I,J+1)))
      BOTTOM  =  5.*((SIGZ(M,I,J)-SIGZ(M-1,I,J))+
     $(SIGZ(M,I,J+1)-SIGZ(M-1,I,J+1)))
      THK = ABOVE + BOTTOM
      TEMP = .05*(U(M,I,J)+U(M,I,J+1))
        Wmass(I,J) =  TEMP*THK*8000.
        Wlayer(M)  =  Wlayer(M) + Wmass(I,J)
         write(12,*) THK
 240     CONTINUE
C
```

APPENDIX B-4 BALANCE program listing (continued)

```
        write(12,1100) Nlayer(M), Elayer(M), Slayer(M), Wlayer(M)
 1100    format(/,' N,E,S,W sides for bottom are :',4(1x,F12.0))

C*****************************************************************
C----------Check TOP layer next (only 0.5 times thick)---------
        M = 6
        write(12,*) M
C-------------------------------------- Check along north edge:
         DO 310 I = 1, 19
                J = 20
      THK  = .5*5.*((SIGZ(M,I,J)-SIGZ(M-1,I,J))+
     $(SIGZ(M,I+1,J)-SIGZ(M-1,I+1,J)))
      TEMP = .05*(V(M,I,J)+V(M,I+1,J))
        Nmass(I,J) = -TEMP*THK*8000.
        Nlayer(M)  = Nlayer(M) + Nmass(I,J)
         write(12,*) THK
 310     CONTINUE
C
C-------------------------------------- Check along east edge:
         DO 320 J = 1, 19
                I = 20
      THK  = .5*5.*((SIGZ(M,I,J)-SIGZ(M-1,I,J))+
     $(SIGZ(M,I,J+1)-SIGZ(M-1,I,J+1)))
      TEMP = .05*(U(M,I,J)+U(M,I,J+1))
        Emass(I,J) = -TEMP*THK*8000.
        Elayer(M)  = Elayer(M) + Emass(I,J)
         write(12,*) THK
 320     CONTINUE

C-------------------------------------- Check along south edge:
         DO 330 I = 1, 19
                J = 1
      THK  =  .5*5.*((SIGZ(M,I,J)-SIGZ(M-1,I,J))+
     $(SIGZ(M,I+1,J)-SIGZ(M-1,I+1,J)))
      TEMP = .05*(V(M,I,J)+V(M,I+1,J))
        Smass(I,J) = TEMP*THK*8000.
        Slayer(M)  = Slayer(M) + Smass(I,J)
         write(12,*) THK
 330     CONTINUE
C
C-------------------------------------- Check along west edge:
         DO 340 J = 1, 19
                I = 1
      THK  =  .5*5.*((SIGZ(M,I,J)-SIGZ(M-1,I,J))+
     $(SIGZ(M,I,J+1)-SIGZ(M-1,I,J+1)))
      TEMP = .05*(U(M,I,J)+U(M,I,J+1))
        Wmass(I,J) =  TEMP*THK*8000.
        Wlayer(M)  =  Wlayer(M) + Wmass(I,J)
         write(12,*) THK
 340     CONTINUE
C
        write(12,1101) Nlayer(M), Elayer(M), Slayer(M), Wlayer(M)
 1101    format(/,' N,E,S,W sides, top layer are :',4(1x,F12.0))
C
```

APPENDIX B-4 BALANCE program listing (continued)

```
C*****************************************************************
C--------------- Check IN-BETWEEN layers (3-5)-------------------
      DO 402 M = 3, 5
        write(12,*) M
C--------------------------------------- Check along north edge:
         DO 410 I = 1, 19
                J = 20
       ABOVE  = .5*5.*((SIGZ(M+1,I,J)-SIGZ(M,I,J))+
     $(SIGZ(M+1,I+1,J)-SIGZ(M,I+1,J)))
       BELOW  = .5*5.*((SIGZ(M,I,J)-SIGZ(M-1,I,J))+
     $(SIGZ(M,I+1,J)-SIGZ(M-1,I+1,J)))
       THK = ABOVE + BELOW
       TEMP = .05*(V(M,I,J)+V(M,I+1,J))
         Nmass(I,J) = -TEMP*THK*8000.
         Nlayer(M)  = Nlayer(M) + Nmass(I,J)
          write(12,*) THK
 410     CONTINUE
C
C--------------------------------------- Check along east edge:
         DO 420 J = 1, 19
                I = 20
       ABOVE  = .5*5.*((SIGZ(M+1,I,J)-SIGZ(M,I,J))+
     $(SIGZ(M+1,I,J+1)-SIGZ(M,I,J+1)))
       BELOW  = .5*5.*((SIGZ(M,I,J)-SIGZ(M-1,I,J))+
     $(SIGZ(M,I,J+1)-SIGZ(M-1,I,J+1)))
       THK = ABOVE + BELOW
       TEMP = .05*(U(M,I,J)+U(M,I,J+1))
         Emass(I,J) = -TEMP*THK*8000.
         Elayer(M)  = Elayer(M) + Emass(I,J)
          write(12,*) THK
 420     CONTINUE

C--------------------------------------- Check along south edge:
         DO 430 I = 1, 19
                J = 1
       ABOVE  = .5*5.*((SIGZ(M+1,I,J)-SIGZ(M,I,J))+
     $(SIGZ(M+1,I+1,J)-SIGZ(M,I+1,J)))
       BELOW  = .5*5.*((SIGZ(M,I,J)-SIGZ(M-1,I,J))+
     $(SIGZ(M,I+1,J)-SIGZ(M-1,I+1,J)))
       THK = ABOVE + BELOW
       TEMP = .05*(V(M,I,J)+V(M,I+1,J))
         Smass(I,J) = TEMP*THK*8000.
         Slayer(M)  = Slayer(M) + Smass(I,J)
          write(12,*) THK
 430     CONTINUE
C
C--------------------------------------- Check along west edge:
         DO 440 J = 1, 19
                I = 1
       ABOVE  = .5*5.*((SIGZ(M+1,I,J)-SIGZ(M,I,J))+
     $(SIGZ(M+1,I,J+1)-SIGZ(M,I,J+1)))
       BELOW  = .5*5.*((SIGZ(M,I,J)-SIGZ(M-1,I,J))+
     $(SIGZ(M,I,J+1)-SIGZ(M-1,I,J+1)))
       THK = ABOVE + BELOW
       TEMP = .05*(U(M,I,J)+U(M,I,J+1))
         Wmass(I,J) =  TEMP*THK*8000.
```

APPENDIX B-4 BALANCE program listing (continued)

```
        Wlayer(M)  = Wlayer(M) + Wmass(I,J)
         write(12,*) THK
 440     CONTINUE
C
C
C
        write(12,1102) M, Nlayer(M), Elayer(M), Slayer(M), Wlayer(M)
 1102    format(/,' N,E,S,W sides for',I3,'layer are:',4(1x,F12.0))
C
 402  CONTINUE
*********************************************************************
        North = 0.
        East  = 0.
        South = 0.
        West  = 0.
C
      DO 500 M = 2, 6
        North = North + Nlayer(M)
        East  = East  + Elayer(M)
        South = South + Slayer(M)
        West  = West  + Wlayer(M)
 500  CONTINUE
        Write(12,1104) North, East, South, West
 1104    Format(/,'N,E,S,W TOTALS are           : ', 4(1x,F12.0))
C
      IF(North.GE.0.) InMass(1)  = North
      IF(East.GE.0.)  InMass(2)  = East
      IF(South.GE.0.) InMass(3)  = South
      IF(West.GE.0.)  InMass(4)  = West
      IF(North.LE.0.) OutMass(1) = North
      IF(East.LE.0.)  OutMass(2) = East
      IF(South.LE.0.) OutMass(3) = South
      IF(West.LE.0.)  OutMass(4) = West
C
        DO 600 I = 1,4
            AllIn = AllIn + InMass(I)
            AllOut= AllOut + OutMass(I)
 600    CONTINUE
C
      Net = AllIn + AllOut
      LossR = Net/AllIn
C
      TOTMASS = North + East + South + West
      IF(TOTMASS.eq.0.) print*,'TOTMASS = 0. !! '
C
      Write(11,899)
      Write(11,*) TOTMASS
      Write(11,900)
      Write(11,*) North, East, South, West
      Write(11,901)
      Write(11,*) InMass(1), InMass(2), InMass(3), InMass(4)
      Write(11,902)
      Write(11,*) OutMass(1), OutMass(2), OutMass(3), OutMass(4)
      Write(11,903)
      Write(11,*) Net, AllIn, AllOut
      Write(11,904)  LossR
```

APPENDIX B-4 BALANCE program listing (continued)

```
C
      DO 1500 M = 2, 6
        Write(12,1501) M
        Write(12,*) Nlayer(M)
        Write(12,*) Elayer(M)
        Write(12,*) Slayer(M)
        Write(12,*) Wlayer(M)
 1500  CONTINUE
 1501  FORMAT(/,'LEVEL ', I3 , ' Layers (N, E, S, W) : ')
C
 801   FORMAT(A30)
 899   FORMAT(/,'    TOTAL mass')
 900   FORMAT(/,8x,'N side',10x,'E side',9x,'S side',10x,'W side')
 901   FORMAT(/,8x,'North In',8x,'East In',8x,'South In',8x,'West In')
 902   FORMAT(8x,'North Out',7x,'East Out',7x,'South Out',7x,'West Out')
 903   FORMAT(/,8x,'Net Mass',8x,'Allin',9x,'AllOut  ')
 904   FORMAT(/,'  The RATIO of NETLOSS to Total Mass IN is:  ', F7.5)
C
 300    CONTINUE
            DO 301 N = 1,6
                Close(N)
 301        CONTINUE
                Close(10)
                Close(11)
        END
```

APPENDIX B-4 BALANCE program listing (continued)

APPENDIX C

TABULATED WIND ANALYSIS RESULTS

LEGEND:

* %err uses the smallest angle between model and obs, div. by 360°.
%err is the % difference between model-obs, and does not exceed 50%.

("backing & veering" means how the model has changed the observed winds).

** (Column represents model/observed wind ratio)

Table 3-1 Tabulated analysis for NW-Weak climatology case.

RESULTS FOR 87100700 (yymmddhh) : 8 km resol

Santa Rosa lies BEYOND the DOMAIN(y))
not listed below; NOT included in the following stats

AVERAGE SPEED RATIO (model/obs) = 81.9%
AVERAGE DIRECTIONAL ERROR = -5.5%

STATION	DIRECTION (obs)	DIRECTION (model)	%err*	SPEED (obs)	SPEED (model)	ratio**
Bethel Island	283°	286°	1% veer	4.9	3.5	70.%
Napa	178°	257°	22% veer	5.8	2.6	45.%
Petaluma	321°	260°	-17% back	5.4	2.1	39.%
Union City	318°	274°	-12% back	4.0	3.3	82.%
San Jose	330°	280°	-14% back	3.1	3.2	103.%
San Martin	324°	284°	-11% back	3.1	4.3	137.%
Oakland RAOB	300°	273°	-8% back	3.6	3.5	97.%

LEGEND:

* %err uses the smallest angle between model and obs, div. by 360°.
%err is the % difference between model-obs, and does not exceed 50%.

("backing & veering" means how the model has changed the observed winds).

** (Column represents model/observed wind ratio)

Table 3-2 Tabulated analysis for NW-Weak climatology case, but with erroneous Oakland sounding.

RESULTS FOR 87100700 (yymmddhh) : 8 km resol

Santa Rosa lies BEYOND the DOMAIN(y))
not listed below; NOT included in the following stats

AVERAGE SPEED RATIO (model/obs) = 70.4%
AVERAGE DIRECTIONAL ERROR = -2.3%

STATION	DIRECTION (obs)	DIRECTION (model)	%err*	SPEED (obs)	SPEED (model)	ratio**
Bethel Island	283°	285°	1% veer	4.9	3.4	69.%
Napa	178°	252°	21% veer	5.8	2.6	45.%
Petaluma	321°	261°	-17% back	5.4	2.1	39.%
Union City	318°	297°	-6% back	4.0	3.3	82.%
San Jose	330°	304°	-7% back	3.1	2.8	91.%
San Martin	324°	303°	-6% back	3.1	3.0	95.%
Oakland RAOB	300°	294°	-2% back	3.6	2.6	72.%

LEGEND:

* %err uses the smallest angle between model and obs, div. by 360°.
%err is the % difference between model-obs, and does not exceed 50%.

("backing & veering" means how the model has changed the observed winds).

** (Column represents model/observed wind ratio)

Table 3-3 Tabulated analysis for NW-Moderate climatology case.

RESULTS FOR 88042100 (yymmddhh) : 8 km resol

Santa Rosa lies BEYOND the DOMAIN(y))
not listed below; NOT included in the following stats

AVERAGE SPEED RATIO (model/obs) = 66.9%
AVERAGE DIRECTIONAL ERROR = .6%

STATION	DIRECTION (obs)	DIRECTION (model)	%err*	SPEED (obs)	SPEED (model)	ratio**
Bethel Island	322°	298°	-7% back	3.7	3.4	92.%
Napa	222°	271°	14% veer	3.6	2.1	59.%
Petaluma	339°	283°	-15% back	4.8	2.0	41.%
Union City	286°	301°	4% veer	4.9	3.0	61.%
San Jose	328°	305°	-6% back	3.8	2.7	71.%
San Martin	234°	279°	13% veer	4.2	2.4	57.%
Oakland RAOB	290°	297°	2% veer	3.1	2.7	87.%

LEGEND:

* %err uses the smallest angle between model and obs, div. by 360°.
%err is the % difference between model-obs, and does not exceed 50%.

("backing & veering" means how the model has changed the observed winds).

** (Column represents model/observed wind ratio)

Table 3-4 Tabulated analysis for NW-Strong climatology case.

RESULTS FOR 88111800 (yymmddhh) : 8 km resol

Santa Rosa lies BEYOND the DOMAIN(y))
not listed below; NOT included in the following stats

AVERAGE SPEED RATIO (model/obs) = 100.5%
AVERAGE DIRECTIONAL ERROR = -.2%

STATION	DIRECTION (obs)	DIRECTION (model)	%err*	SPEED (obs)	SPEED (model)	ratio**
Bethel Island	286°	288°	1% veer	5.2	4.7	90.%
Napa	281°	290°	2% veer	3.0	4.2	138.%
Petaluma	288°	293°	1% veer	5.1	3.7	72.%
Union City	289°	289°	0% back	5.8	4.8	84.%
San Jose	294°	292°	-1% back	4.4	4.9	111.%
San Martin	317°	299°	-5% back	4.2	4.4	106.%
Oakland RAOB	290°	289°	0% back	4.6	4.7	103.%

LEGEND:

* %err uses the smallest angle between model and obs, div. by 360°.
%err is the % difference between model-obs, and does not exceed 50%.

("backing & veering" means how the model has changed the observed winds).

** (Column represents model/observed wind ratio)

Table 3-5 Tabulated analysis for Northeast climatology case.

RESULTS FOR 89112900 (yymmddhh) : 8 km resol

Santa Rosa lies BEYOND the DOMAIN(y))
not listed below; NOT included in the following stats

AVERAGE SPEED RATIO (model/obs) = 116.4%
AVERAGE DIRECTIONAL ERROR = 1.5%

STATION	DIRECTION (obs)	(model)	%err*	SPEED (obs)	(model)	ratio**
Ft. Funston	65°	97°	9% veer	5.3	.8	16.%
Union City	206°	82°	-35% back	1.6	2.8	171.%
Mt. Pisc	75°	80°	2% veer	2.9	2.8	94.%
Chabot	68°	90°	6% veer	4.8	3.5	74.%
Napa	89°	87°	0% back	5.2	3.3	63.%
Fremont	60°	86°	7% veer	5.4	3.0	55.%
Valley Ford	110°	136°	7% veer	6.1	3.7	60.%
Petaluma	120°	114°	-2% back	5.3	3.6	68.%
San Jose	268°	84°	49% veer	2.1	1.9	92.%
Vollmer Peak	266°	102°	-45% back	5.9	3.2	54.%
Kregor	87°	67°	-6% back	8.4	2.5	30.%
Rio Vista	35°	80°	12% veer	2.2	2.7	125.%
San Martin	6°	58°	14% veer	2.2	1.6	73.%
Sonoma Marina	110°	94°	-4% back	5.2	4.0	78.%
Gilroy	60°	55°	-1% back	4.1	1.8	45.%
Bethel Island	89°	78°	-3% back	1.2	2.3	186.%
Highland	99°	74°	-7% back	6.9	2.6	38.%
Mt. Hamilton	126°	90°	-10% back	.3	1.9	729.%
Mt. Tamalpais	114°	100°	-4% back	4.4	3.9	88.%
Danville	298°	86°	41% veer	1.8	3.3	190.%

Table 3-6 Tabulated analysis for Northeast climatology case, but without Vollmer Peak data.

RESULTS FOR 89112900 (yymmddhh) : 8 Km resol

Santa Rosa lies BEYOND the DOMAIN(y))
not listed below; NOT included in the following stats

Vollmer Peak is NOT AVAILABLE
not listed below; NOT included in the following stats

AVERAGE SPEED RATIO (model/obs) = 138.1%
AVERAGE DIRECTIONAL ERROR = 4.1%

STATION	DIRECTION (obs)	(model)	%err*	SPEED (obs)	(model)	ratio**
Ft. Funston	65°	87°	6% veer	5.3	3.8	73.%
Union City	206°	87°	-33% back	1.6	3.4	207.%
Mt. Pise	75°	79°	1% veer	2.9	3.1	107.%
Chabot	68°	92°	7% veer	4.8	4.3	90.%
Napa	89°	87°	0% back	5.2	3.7	70.%
Fremont	60°	87°	8% veer	5.4	3.3	61.%
Valley Ford	110°	135°	7% veer	6.1	3.8	62.%
Petaluma	120°	113°	-2% back	5.3	3.8	72.%
San Jose	268°	84°	49% veer	2.1	2.2	104.%
Vollmer Peak	MISSING-----no stats.					
Kregor	87°	68°	-5% back	8.4	2.9	34.%
Rio Vista	35°	81°	13% veer	2.2	3.1	143.%
San Martin	6°	59°	15% veer	2.2	1.7	79.%
Sonoma Marina	110°	94°	-4% back	5.2	4.2	81.%
Gilroy	60°	56°	-1% back	4.1	2.0	48.%
Bethel Island	89°	79°	-3% back	1.2	2.6	208.%
Highland	99°	76°	-7% back	6.9	2.9	42.%
Mt. Hamilton	126°	89°	-10% back	.3	2.1	819.%
Mt. Tamalpais	114°	103°	-3% back	4.4	4.5	101.%
Danville	298°	87°	41% veer	1.8	3.9	222.%

Table 3-7 Tabulated analysis for South climatology case.

RESULTS FOR 88042000 {yymmddhh} : 8 km resol

Santa Rosa lies BEYOND the DOMAIN(y))
not listed below; NOT included in the following stats

AVERAGE SPEED RATIO (model/obs) = 107.7%
AVERAGE DIRECTIONAL ERROR = 1.4%

STATION	DIRECTION (obs)	(model)	%err*	SPEED (obs)	(model)	ratio**
Bethel Island	190°	167°	-6% back	3.4	3.6	106.%
Napa	186°	172°	-4% back	3.3	3.9	117.%
Petaluma	115°	150°	10% veer	2.9	3.3	116.%
Union City	165°	166°	0% veer	5.6	4.3	77.%
San Jose	147°	162°	4% veer	2.7	3.8	142.%
San Martin	141°	158°	5% veer	3.4	3.8	112.%
Oakland RAOB	160°	165°	1% veer	5.2	4.3	84.%

LEGEND:

* %err uses the smallest angle between model and obs, div. by 360°.
%err is the % difference between model-obs, and does not exceed 50%.

("backing & veering" means how the model has changed the observed winds).

** (Column represents model/observed wind ratio)

Table 3-8 Tabulated analysis for Southeast climatology case.

RESULTS FOR 88042012 (yymmddhh) : 8 km resol

Santa Rosa lies BEYOND the DOMAIN(y))
not listed below; NOT included in the following stats

AVERAGE SPEED RATIO (model/obs) = 100.9%
AVERAGE DIRECTIONAL ERROR = 6.1%

STATION	DIRECTION (obs)	DIRECTION (model)	%err*	SPEED (obs)	SPEED (model)	ratio**
Bethel Island	156°	143°	-4% back	3.4	3.0	89.%
Napa	353°	144°	42% veer	1.4	1.5	105.%
Petaluma	93°	125°	9% veer	2.7	1.6	58.%
Union City	138°	149°	3% veer	3.8	3.2	86.%
San Jose	174°	154°	-6% back	1.9	2.8	147.%
San Martin	168°	155°	-4% back	1.3	2.2	172.%
Oakland RAOB	140°	147°	2% veer	6.2	3.1	50.%

LEGEND:

* %err uses the smallest angle between model and obs, div. by 360°.
%err is the % difference between model-obs, and does not exceed 50%.

("backing & veering" means how the model has changed the observed winds).

** (Column represents model/observed wind ratio)

Table 3-9 Tabulated analysis for Weak Outflow climatology case.

RESULTS FOR 88120100 (yymmddhh) : 8 km resol

Santa Rosa lies BEYOND the DOMAIN(y))
not listed below; NOT included in the following stats

AVERAGE SPEED RATIO (model/obs) = 36.1%
AVERAGE DIRECTIONAL ERROR = -7.7%

STATION	DIRECTION (obs)	(model)	%err*	SPEED (obs)	(model)	ratio**
Bethel Island	145°	132°	-4% back	2.3	1.1	48.%
Napa	213°	167°	-13% back	1.9	1.1	60.%
Petaluma	143°	148°	1% veer	4.5	1.7	39.%
Union City	238°	106°	-37% back	1.1	.6	53.%
San Jose	278°	242°	-10% back	2.4	.3	13.%
San Martin	338°	324°	-4% back	2.8	.6	22.%
Oakland RAOB	50°	92°	12% veer	5.2	1.0	19.%

LEGEND:

* %err uses the smallest angle between model and obs, div. by 360°.
%err is the % difference between model-obs, and does not exceed 50%.

("backing & veering" means how the model has changed the observed winds).

** (Column represents model/observed wind ratio)

Table 3-10 Tabulated analysis for Weak Inflow climatology case.

RESULTS FOR 88120112 (yymmddhh) : 8 km resol

Santa Rosa lies BEYOND the DOMAIN(y))
not listed below; NOT included in the following stats

AVERAGE SPEED RATIO (model/obs) = 59.6%
AVERAGE DIRECTIONAL ERROR = 1.0%

STATION	DIRECTION (obs)	DIRECTION (model)	%err*	SPEED (obs)	SPEED (model)	ratio**
Bethel Island	230°	177°	-15% back	1.0	.7	73.%
Napa	65°	164°	28% veer	1.2	.7	54.%
Petaluma	130°	151°	6% veer	6.8	1.7	25.%
Union City	102°	196°	26% veer	1.3	.8	61.%
San Jose	161°	190°	8% veer	.8	1.0	122.%
San Martin	323°	224°	-28% back	1.8	.5	27.%
Oakland RAOB	240°	174°	-18% back	1.5	.8	55.%

LEGEND:

* %err uses the smallest angle between model and obs, div. by 360°.
%err is the % difference between model-obs, and does not exceed 50%.

("backing & veering" means how the model has changed the observed winds).

** (Column represents model/observed wind ratio)

Table 3-11 Summary of analysis results for climatology cases.

SUMMARY OF BAY AREA CLIMATOLOGY RUNS

NAME OF RUN	# STATIONS	WINDANAL DIR (%)	SPD RATIO (%)
NW - WEAK	7	-5.5	81.9
NW - MODERATE	7	0.6	66.9
NW - STRONG	7	-0.2	100.9
NE	20	1.5	116.4
NE (-Vollmer)	19	4.1	138.1
SOUTH	7	1.4	107.7
SOUTHEAST	7	6.1	100.9
BAY - OUT	7	-7.7	36.1
BAY - IN	7	1.0	59.6

Table 3-12 Tabulated analysis for NW-Weak case, with Travis AFB added.

RESULTS FOR 87100700 (yymmddhh) : 8 km resol

Santa Rosa lies BEYOND the DOMAIN(y))
not listed below; NOT included in the following stats

AVERAGE SPEED RATIO (model/obs) = 84.2%
AVERAGE DIRECTIONAL ERROR = -5.4%

STATION	DIRECTION (obs)	DIRECTION (model)	%err*	SPEED (obs)	SPEED (model)	ratio**
Bethel Island	283°	276°	-2% back	4.9	3.8	78.%
Napa	178°	248°	20% veer	5.8	3.4	59.%
Petaluma	321°	257°	-18% back	5.4	2.5	45.%
Union City	318°	267°	-14% back	4.0	3.4	86.%
San Jose	330°	277°	-15% back	3.1	3.3	105.%
San Martin	324°	281°	-12% back	3.1	4.3	137.%
Oakland RAOB	300°	264°	-10% back	3.6	3.9	108.%
Travis AFB	230°	258°	8% veer	7.1	3.9	55.%

LEGEND:

* %err uses the smallest angle between model and obs, div. by 360°.
%err is the % difference between model-obs, and does not exceed 50%.

("backing & veering" means how the model has changed the observed winds).

** (Column represents model/observed wind ratio)

Table 3-13 Tabulated analysis for NW-Weak case, with Pittsburg added.

RESULTS FOR 87100700 {yymmddhh} : 8 km resol

Santa Rosa lies BEYOND the DOMAIN(y))
not listed below; NOT included in the following stats

AVERAGE SPEED RATIO (model/obs) = 86.7%
AVERAGE DIRECTIONAL ERROR = -5.2%

STATION	DIRECTION (obs)	DIRECTION (model)	%err*	SPEED (obs)	SPEED (model)	ratio**
Bethel Island	283°	282°	0% back	4.9	3.9	79.%
Napa	178°	259°	22% veer	5.8	3.1	53.%
Petaluma	321°	260°	-17% back	5.4	2.3	43.%
Union City	318°	269°	-14% back	4.0	3.6	90.%
San Jose	330°	277°	-15% back	3.1	3.3	107.%
San Martin	324°	282°	-12% back	3.1	4.3	139.%
Oakland RAOB	300°	265°	-10% back	3.6	4.2	118.%
Pittsburg	260°	271°	3% veer	5.4	3.5	65.%

LEGEND:

* %err uses the smallest angle between model and obs, div. by 360°.
%err is the % difference between model-obs, and does not exceed 50%.

("backing & veering" means how the model has changed the observed winds).

** (Column represents model/observed wind ratio)

Table 3-14 Tabulated analysis for NW-Weak case, with Alameda NAS added.

RESULTS FOR 87100700 (yymmddhh) : 8 km resol

Santa Rosa lies BEYOND the DOMAIN(y))
not listed below; NOT included in the following stats

AVERAGE SPEED RATIO (model/obs) = 75.2%
AVERAGE DIRECTIONAL ERROR = -6.7%

STATION	DIRECTION (obs)	(model)	%err*	SPEED (obs)	(model)	ratio**
Bethel Island	283°	290°	2% veer	4.9	3.2	66.%
Napa	178°	260°	23% veer	5.8	2.3	40.%
Petaluma	321°	262°	-16% back	5.4	1.9	35.%
Union City	318°	277°	-11% back	4.0	3.0	74.%
San Jose	330°	282°	-13% back	3.1	3.0	98.%
San Martin	324°	286°	-11% back	3.1	4.2	134.%
Oakland RAOB	300°	278°	-6% back	3.6	2.9	81.%
Alameda NAS	360°	287°	-20% back	3.1	2.3	74.%

LEGEND:

* %err uses the smallest angle between model and obs, div. by 360°.
%err is the % difference between model-obs, and does not exceed 50%.

("backing & veering" means how the model has changed the observed winds).

** (Column represents model/observed wind ratio)

Table 3-15 Tabulated analysis for NW-Weak case, with Benicia added.

RESULTS FOR 87100700 (yymmddhh) : 8 km resol

Santa Rosa lies BEYOND the DOMAIN(y))
not listed below; NOT included in the following stats

AVERAGE SPEED RATIO (model/obs) = 82.2%
AVERAGE DIRECTIONAL ERROR = -6.2%

STATION	DIRECTION (obs)	(model)	%err*	SPEED (obs)	(model)	ratio**
Bethel Island	283°	288°	2% veer	4.9	3.2	66.%
Napa	178°	261°	23% veer	5.8	2.3	41.%
Petaluma	321°	261°	-17% back	5.4	1.9	36.%
Union City	318°	275°	-12% back	4.0	3.1	77.%
San Jose	330°	280°	-14% back	3.1	3.1	100.%
San Martin	324°	284°	-11% back	3.1	4.2	135.%
Oakland RAOB	300°	276°	-7% back	3.6	3.1	86.%
Benicia	315°	266°	-14% back	1.8	2.1	117.%

LEGEND:

* %err uses the smallest angle between model and obs, div. by 360°.
%err is the % difference between model-obs, and does not exceed 50%.

("backing & veering" means how the model has changed the observed winds).

** (Column represents model/observed wind ratio)

Table 3-16 Tabulated analysis for NW-Weak case, with Vallejo added.

RESULTS FOR 87100700 (yymmddhh) : 8 km resol

Santa Rosa lies BEYOND the DOMAIN(y))
not listed below; NOT included in the following stats

AVERAGE SPEED RATIO (model/obs) = 80.0%
AVERAGE DIRECTIONAL ERROR = -6.0%

STATION	DIRECTION (obs)	DIRECTION (model)	%err*	SPEED (obs)	SPEED (model)	ratio**
Bethel Island	283°	280°	-1% back	4.9	3.4	69.%
Napa	178°	248°	19% veer	5.8	2.8	48.%
Petaluma	321°	252°	-19% back	5.4	2.2	41.%
Union City	318°	268°	-14% back	4.0	3.2	81.%
San Jose	330°	277°	-15% back	3.1	3.2	102.%
San Martin	324°	281°	-12% back	3.1	4.2	135.%
Oakland RAOB	300°	264°	-10% back	3.6	3.4	95.%
Vallejo	225°	237°	3% veer	4.0	2.8	70.%

LEGEND:

* %err uses the smallest angle between model and obs, div. by 360°.
%err is the % difference between model-obs, and does not exceed 50%.

("backing & veering" means how the model has changed the observed winds).

** (Column represents model/observed wind ratio)

Table 3-17 Tabulated analysis for NW-Weak case, with Richmond added.

RESULTS FOR 87100700 (yymmddhh) : 8 km resol

Santa Rosa lies BEYOND the DOMAIN(y))
not listed below; NOT included in the following stats

AVERAGE SPEED RATIO (model/obs) = 76.5%
AVERAGE DIRECTIONAL ERROR = -4.3%

STATION	DIRECTION (obs)	(model)	%err*		SPEED (obs)	(model)	ratio**
Bethel Island	283°	282°	0%	back	4.9	3.1	63.%
Napa	178°	247°	19%	veer	5.8	2.4	42.%
Petaluma	321°	251°	-20%	back	5.4	1.9	36.%
Union City	318°	267°	-14%	back	4.0	2.9	73.%
San Jose	330°	277°	-15%	back	3.1	3.1	98.%
San Martin	324°	282°	-12%	back	3.1	4.1	132.%
Oakland RAOB	300°	265°	-10%	back	3.6	2.9	81.%
Richmond	180°	240°	17%	veer	2.7	2.3	86.%

LEGEND:

* %err uses the smallest angle between model and obs, div. by 360°.
%err is the % difference between model-obs, and does not exceed 50%.

("backing & veering" means how the model has changed the observed winds).

** (Column represents model/observed wind ratio)

Table 3-18 Tabulated analysis for NW-Weak case, with Travis AFB, Pittsburg, Alameda NAS, Benicia, Vallejo, and Richmond added.

RESULTS FOR 87100700 (yymmddhh) : 8 km resol

Santa Rosa lies BEYOND the DOMAIN(y))
not listed below; NOT included in the following stats

AVERAGE SPEED RATIO (model/obs) = 99.0%
AVERAGE DIRECTIONAL ERROR = -6.4%

STATION	DIRECTION (obs)	DIRECTION (model)	%err*	SPEED (obs)	SPEED (model)	ratio**
Bethel Island	283°	270°	-4% back	4.9	3.7	76.%
Napa	178°	245°	18% veer	5.8	3.4	58.%
Petaluma	321°	249°	-20% back	5.4	2.4	44.%
Union City	318°	259°	-16% back	4.0	3.2	80.%
San Jose	330°	272°	-16% back	3.1	3.1	101.%
San Martin	324°	278°	-13% back	3.1	4.1	133.%
Oakland RAOB	300°	260°	-11% back	3.6	3.7	103.%
Vallejo	225°	238°	3% veer	4.0	3.8	96.%
Richmond	180°	236°	15% veer	2.7	3.4	126.%
Benicia	315°	243°	-20% back	1.8	4.4	244.%
Alameda	360°	269°	-25% back	3.1	3.0	97.%
Pittsburg	260°	254°	-2% back	5.4	4.1	76.%
Travis AFB	230°	253°	6% veer	7.1	3.8	53.%

LEGEND:

* %err uses the smallest angle between model and obs, div. by 360°.
%err is the % difference between model-obs, and does not exceed 50%.

("backing & veering" means how the model has changed the observed winds).

** (Column represents model/observed wind ratio)

Table 3-19 Tabulated analysis for NW-Weak case, with all available data added.

RESULTS FOR 87100700 (yymmddhh) : 8 km resol

Santa Rosa lies BEYOND the DOMAIN(y))
not listed below; NOT included in the following stats

AVERAGE SPEED RATIO (model/obs) = 103.3%
AVERAGE DIRECTIONAL ERROR = -6.8%

STATION	DIRECTION (obs)	DIRECTION (model)	%err*	SPEED (obs)	SPEED (model)	ratio**
Bethel Island	283°	269°	-4% back	4.9	3.1	64.%
Napa	178°	238°	17% veer	5.8	3.3	57.%
Petaluma	321°	248°	-20% back	5.4	2.2	41.%
Union City	318°	281°	-10% back	4.0	2.9	74.%
San Jose	330°	297°	-9% back	3.1	3.2	102.%
San Martin	324°	291°	-9% back	3.1	2.5	80.%
Oakland RAOB	300°	274°	-7% back	3.6	2.1	58.%
Benicia	315°	239°	-21% back	1.8	4.2	233.%
Moffett NAS	340°	292°	-13% back	4.0	3.4	85.%
Pleasanton	269°	262°	-2% back	4.5	4.3	95.%
Travis AFB	230°	250°	6% veer	7.1	3.8	53.%
Walnut Creek	261°	241°	-6% back	1.8	4.0	223.%
Stockton	299°	276°	-6% back	1.3	2.7	209.%
Novato	289°	221°	-19% back	1.3	2.3	180.%
San Francisco Air	330°	269°	-17% back	4.0	2.7	68.%
Vallejo	225°	240°	4% veer	4.0	3.4	86.%
Palo Alto	360°	289°	-20% back	4.1	3.6	89.%
Richmond	180°	219°	11% veer	2.7	3.5	131.%
Livermore	290°	262°	-8% back	7.1	4.4	62.%
Pittsburg	260°	256°	-1% back	5.4	4.1	75.%

Table 3-20 Summary of analysis results for NW-Weak case with selected stations added.

SUMMARY OF BAY AREA RUNS (STATIONS ADDED)

NAME OF RUN	WINDANAL # STATIONS	DIR (%)	SPD RATIO (%)
NW - WEAK (basic run)	7	-5.5	81.9
TRAVIS added	8	-5.4	84.2
PITTSBURG added	8	-5.2	86.7
ALAMEDA NAS added	8	-6.7	75.2
BENICIA added	8	-6.2	82.2
VALLEJO added	8	-6.0	80.0
RICHMOND added	8	-4.3	76.5
ALL 6 SITES added	13	-6.4	99.0
ALL AVAILABLE DATA used	20	-6.8	103.3

Table 3-21 Tabulated analysis for NW-Weak case, with Bethel Island deleted.

RESULTS FOR 87100700 (yymmddhh) : 8 km resol

Bethel Island is NOT AVAILABLE
not listed below; NOT included in the following stats

Santa Rosa lies BEYOND the DOMAIN(y))
not listed below; NOT included in the following stats

AVERAGE SPEED RATIO (model/obs) = 76.3%
AVERAGE DIRECTIONAL ERROR = -7.0%

STATION	DIRECTION (obs)	DIRECTION (model)	%err*	SPEED (obs)	SPEED (model)	ratio**
Bethel Island	MISSING-----no stats.					
Napa	178°	246°	19% veer	5.8	2.2	38.%
Petaluma	321°	257°	-18% back	5.4	1.9	35.%
Union City	318°	275°	-12% back	4.0	2.9	74.%
San Jose	330°	282°	-13% back	3.1	3.0	97.%
San Martin	324°	285°	-11% back	3.1	4.1	133.%
Oakland RAOB	300°	274°	-7% back	3.8	3.0	82.%

LEGEND:

* %err uses the smallest angle between model and obs, div. by 360°.
%err is the % difference between model-obs, and does not exceed 50%.

("backing & veering" means how the model has changed the observed winds).

** (Column represents model/observed wind ratio)

Table 3-22 Tabulated analysis for NW-Weak case, with Napa deleted.

RESULTS FOR 87100700 (yymmddhh) : 8 km resol

Napa is NOT AVAILABLE
not listed below; NOT included in the following stats

Santa Rosa lies BEYOND the DOMAIN(y))
not listed below; NOT included in the following stats

AVERAGE SPEED RATIO (model/obs) = 100.6%
AVERAGE DIRECTIONAL ERROR = -6.6%

STATION	DIRECTION (obs)	DIRECTION (model)	%err*	SPEED (obs)	SPEED (model)	ratio**
Bethel Island	283°	297°	4% veer	4.9	4.3	87.%
Napa		MISSING-----no stats.				
Petaluma	321°	301°	-6% back	5.4	3.7	69.%
Union City	318°	283°	-10% back	4.0	3.6	90.%
San Jose	330°	283°	-13% back	3.1	3.3	106.%
San Martin	324°	287°	-10% back	3.1	4.4	142.%
Oakland RAOB	300°	283°	-5% back	3.6	3.9	110.%

LEGEND:

* %err uses the smallest angle between model and obs, div. by 360°.
%err is the % difference between model-obs, and does not exceed 50%.

("backing & veering" means how the model has changed the observed winds).

** (Column represents model/observed wind ratio)

Table 3-23 Tabulated analysis for NW-Weak case, with Santa Rosa deleted.

RESULTS FOR 87100700 (yymmddhh) : 8 km resol

Santa Rosa lies BEYOND the DOMAIN(y))
not listed below; NOT included in the following stats

Santa Rosa is NOT AVAILABLE
not listed below; NOT included in the following stats

AVERAGE SPEED RATIO (model/obs) = 83.0%
AVERAGE DIRECTIONAL ERROR = -4.5%

STATION	DIRECTION (obs)	DIRECTION (model)	%err*	SPEED (obs)	SPEED (model)	ratio**
Bethel Island	283°	288°	1% veer	4.9	3.5	72.%
Napa	178°	262°	23% veer	5.8	2.7	46.%
Santa Rosa		MISSING-----no stats.				
Petaluma	321°	277°	-12% back	5.4	2.2	41.%
Union City	318°	275°	-12% back	4.0	3.3	83.%
San Jose	330°	281°	-14% back	3.1	3.2	104.%
San Martin	324°	285°	-11% back	3.1	4.3	138.%
Oakland RAOB	300°	274°	-7% back	3.6	3.5	98.%

LEGEND:

* %err uses the smallest angle between model and obs, div. by 360°.
%err is the % difference between model-obs, and does not exceed 50%.

("backing & veering" means how the model has changed the observed winds).

** (Column represents model/observed wind ratio)

Table 3-24 Tabulated analysis for NW-Weak case, with Petaluma deleted.

RESULTS FOR 87100700 (yymmddhh) : 8 km resol

Santa Rosa lies BEYOND the DOMAIN(y))
not listed below; NOT included in the following stats

Petaluma is NOT AVAILABLE
not listed below; NOT included in the following stats

AVERAGE SPEED RATIO (model/obs) = 87.2%
AVERAGE DIRECTIONAL ERROR = -5.0%

STATION	DIRECTION (obs)	DIRECTION (model)	%err*	SPEED (obs)	SPEED (model)	ratio**
Bethel Island	283°	281°	-1% back	4.9	3.3	67.%
Napa	178°	242°	18% veer	5.8	2.6	44.%
Petaluma		MISSING-----no stats.				
Union City	318°	271°	-13% back	4.0	3.2	80.%
San Jose	330°	279°	-14% back	3.1	3.2	102.%
San Martin	324°	283°	-12% back	3.1	4.2	136.%
Oakland RAOB	300°	269°	-9% back	3.6	3.4	94.%

LEGEND:

* %err uses the smallest angle between model and obs, div. by 360°.
%err is the % difference between model-obs, and does not exceed 50%.

("backing & veering" means how the model has changed the observed winds).

** (Column represents model/observed wind ratio)

Table 3-25 Tabulated analysis for NW-Weak case, with Union City deleted.

RESULTS FOR 87100700 {yymmddhh} : 8 km resol

Santa Rosa lies BEYOND the DOMAIN(y))
not listed below; NOT included in the following stats

Union City is NOT AVAILABLE
not listed below; NOT included in the following stats

AVERAGE SPEED RATIO (model/obs) = 81.3%
AVERAGE DIRECTIONAL ERROR = -5.4%

STATION	DIRECTION (obs)	DIRECTION (model)	%err*	SPEED (obs)	SPEED (model)	ratio**
Bethel Island	283°	282°	0% back	4.9	3.4	70.%
Napa	178°	254°	21% veer	5.8	2.6	45.%
Petaluma	321°	258°	-17% back	5.4	2.1	39.%
Union City		MISSING-----no stats.				
San Jose	330°	275°	-15% back	3.1	3.1	101.%
San Martin	324°	281°	-12% back	3.1	4.2	135.%
Oakland RAOB	300°	268°	-9% back	3.6	3.5	98.%

LEGEND:

* %err uses the smallest angle between model and obs, div. by 360°.
%err is the % difference between model-obs, and does not exceed 50%.

("backing & veering" means how the model has changed the observed winds).

** (Column represents model/observed wind ratio)

Table 3-26 Tabulated analysis for NW-Weak case, with San Jose Airport deleted.

RESULTS FOR 87100700 (yymmddhh) : 8 km resol

Santa Rosa lies BEYOND the DOMAIN(y))
not listed below; NOT included in the following stats

San Jose Airpo is NOT AVAILABLE
not listed below; NOT included in the following stats

AVERAGE SPEED RATIO (model/obs) = 81.0%
AVERAGE DIRECTIONAL ERROR = -4.5%

STATION	DIRECTION (obs)	DIRECTION (model)	%err*	SPEED (obs)	SPEED (model)	ratio**
Bethel Island	283°	284°	0% veer	4.9	3.6	73.%
Napa	178°	257°	22% veer	5.8	2.7	46.%
Petaluma	321°	260°	-17% back	5.4	2.2	40.%
Union City	318°	273°	-12% back	4.0	3.4	85.%
San Jose		MISSING-----no stats.				
San Martin	324°	282°	-12% back	3.1	4.4	142.%
Oakland RAOB	300°	272°	-8% back	3.6	3.6	100.%

LEGEND:

* %err uses the smallest angle between model and obs, div. by 360°.
%err is the % difference between model-obs, and does not exceed 50%.

("backing & veering" means how the model has changed the observed winds).

** (Column represents model/observed wind ratio)

Table 3-27 Tabulated analysis for NW-Weak case, with San Martin deleted.

RESULTS FOR 87100700 (yymmddhh) : 8 km resol

Santa Rosa lies BEYOND the DOMAIN(y))
not listed below; NOT included in the following stats

San Martin is NOT AVAILABLE
not listed below; NOT included in the following stats

AVERAGE SPEED RATIO (model/obs) = 73.2%
AVERAGE DIRECTIONAL ERROR = -4.7%

STATION	DIRECTION (obs)	DIRECTION (model)	%err*	SPEED (obs)	SPEED (model)	ratio**
Bethel Island	283°	285°	1% veer	4.9	3.5	71.%
Napa	178°	257°	22% veer	5.8	2.6	45.%
Petaluma	321°	260°	-17% back	5.4	2.1	39.%
Union City	318°	274°	-12% back	4.0	3.3	83.%
San Jose	330°	279°	-14% back	3.1	3.2	103.%
San Martin	MISSING-----no stats.					
Oakland RAOB	300°	272°	-8% back	3.6	3.5	97.%

LEGEND:

* %err uses the smallest angle between model and obs, div. by 360°.
%err is the % difference between model-obs, and does not exceed 50%.

("backing & veering" means how the model has changed the observed winds).

** (Column represents model/observed wind ratio)

Table 3-28 Tabulated analysis for NW-Weak case, with Oakland deleted.

RESULTS FOR 87100700 (yymmddhh) : 8 km resol

Santa Rosa lies BEYOND the DOMAIN(y))
not listed below; NOT included in the following stats

Oakland RAOB is NOT AVAILABLE
not listed below; NOT included in the following stats

AVERAGE SPEED RATIO (model/obs) = 77.5%
AVERAGE DIRECTIONAL ERROR = -5.3%

STATION	DIRECTION (obs)	DIRECTION (model)	%err*	SPEED (obs)	SPEED (model)	ratio**
Bethel Island	283°	286°	1% veer	4.9	3.4	69.%
Napa	178°	255°	22% veer	5.8	2.5	43.%
Petaluma	321°	260°	-17% back	5.4	2.0	37.%
Union City	318°	274°	-12% back	4.0	3.2	79.%
San Jose	330°	281°	-14% back	3.1	3.1	101.%
San Martin	324°	284°	-11% back	3.1	4.2	136.%
Oakland RAOB	MISSING-----no stats.					

LEGEND:

* %err uses the smallest angle between model and obs, div. by 360°.
%err is the % difference between model-obs, and does not exceed 50%.

("backing & veering" means how the model has changed the observed winds).

** (Column represents model/observed wind ratio)

Table 3-29 Tabulated analysis for NW-Weak case, with Oakland, Union City, and San Jose Airport deleted.

RESULTS FOR 87100700 (yymmddhh) : 8 km resol

Santa Rosa lies BEYOND the DOMAIN(y))
not listed below; NOT included in the following stats

Union City is NOT AVAILABLE
not listed below; NOT included in the following stats

San Jose Airpo is NOT AVAILABLE
not listed below; NOT included in the following stats

Oakland RAOB is NOT AVAILABLE
not listed below; NOT included in the following stats

AVERAGE SPEED RATIO (model/obs) = 74.1%
AVERAGE DIRECTIONAL ERROR = -4.8%

STATION	DIRECTION (obs)	DIRECTION (model)	%err*	SPEED (obs)	SPEED (model)	ratio**
Bethel Island	283°	272°	-3% back	4.9	3.5	71.%
Napa	178°	244°	18% veer	5.8	2.8	49.%
Petaluma	321°	249°	-20% back	5.4	2.3	42.%
Union City	MISSING-----no stats.					
San Jose	MISSING-----no stats.					
San Martin	324°	272°	-15% back	3.1	4.2	135.%
Oakland RAOB	MISSING-----no stats.					

LEGEND:

* %err uses the smallest angle between model and obs, div. by 360°.
%err is the % difference between model-obs, and does not exceed 50%.

("backing & veering" means how the model has changed the observed winds).

** (Column represents model/observed wind ratio)

Table 3-30 Summary of analysis results for NW-Weak case with selected stations deleted.

SUMMARY OF BAY AREA RUNS (STATIONS DELETED)

NAME OF RUN		WINDANAL # STATIONS	DIR (%)	SPD RATIO (%)
NW - WEAK (basic run)		7	-5.5	81.9
BETHEL ISLAND	deleted	6	-7.0	76.3
NAPA	deleted	6	-6.6	100.6
SANTA ROSA	deleted	6	-4.5	83.0
PETALUMA	deleted	6	-5.0	87.2
UNION CITY	deleted	6	-5.4	81.3
SAN JOSE	deleted	6	-4.5	81.0
SAN MARTIN	deleted	6	-4.7	73.2
OAKLAND	deleted	6	-5.3	77.5
OAKLAND, UNION CITY, SAN JOSE	deleted	4	-4.8	74.1

Table 3-31 Tabulated analysis for 10 km resolution case.

RESULTS FOR 87100700 (yymmddhh) :10 km resol

Santa Rosa lies BEYOND the DOMAIN(y))
not listed below; NOT included in the following stats

AVERAGE SPEED RATIO (model/obs) = 72.8%
AVERAGE DIRECTIONAL ERROR = -4.7%

STATION	DIRECTION (obs)	DIRECTION (model)	%err*	SPEED (obs)	SPEED (model)	ratio**
Bethel Island	283°	272°	-3% back	4.9	3.4	69.%
Napa	178°	[illegible]°	19% veer	5.8	2.9	50.%
Petaluma	321°	265°	-16% back	5.4	2.6	49.%
Union City	318°	278°	-11% back	4.0	3.4	86.%
San Jose	330°	296°	-9% back	3.1	2.5	80.%
San Martin	324°	307°	-5% back	3.1	2.7	87.%
Oakland RAOB	300°	272°	-8% back	3.6	3.2	89.%

LEGEND:

* %err uses the smallest angle between model and obs, div. by 360°.
%err is the % difference between model-obs, and does not exceed 50%.

("backing & veering" means how the model has changed the observed winds).

** (Column represents model/observed wind ratio)

Table 3-32 Tabulated analysis for 5 km resolution case.

RESULTS FOR 87100700 (yymmddhh) : 5 km resol

Santa Rosa lies BEYOND the DOMAIN(y))
not listed below; NOT included in the following stats

AVERAGE SPEED RATIO (model/obs) = 68.2%
AVERAGE DIRECTIONAL ERROR = -3.9%

STATION	DIRECTION (obs)	DIRECTION (model)	%err*	SPEED (obs)	SPEED (model)	ratio**
Bethel Island	283°	272°	-3% back	4.9	3.3	68.%
Napa	178°	248°	19% veer	5.8	2.8	47.%
Petaluma	321°	265°	-16% back	5.4	2.2	41.%
Union City	318°	289°	-8% back	4.0	3.0	74.%
San Jose	330°	290°	-11% back	3.1	2.6	84.%
San Martin	324°	315°	-3% back	3.1	2.8	91.%
Oakland RAOB	300°	278°	-6% back	3.6	2.6	72.%

LEGEND:

* %err uses the smallest angle between model and obs, div. by 360°.
%err is the % difference between model-obs, and does not exceed 50%.

("backing & veering" means how the model has changed the observed winds).

** (Column represents model/observed wind ratio)

Table 4-1 Tabulated analysis for MABLES case, without RDBLT provision.

RESULTS FOR 78081000 (yymmddhh) : 8 km resol

Salinas Airp. lies BEYOND the DOMAIN(y))
not listed below; NOT included in the following stats

Sacramento lies BEYOND the DOMAIN(x))
not listed below; NOT included in the following stats

Sacramento lies BEYOND the DOMAIN(y))
not listed below; NOT included in the following stats

AVERAGE SPEED RATIO (model/obs) = 111.7%
AVERAGE DIRECTIONAL ERROR = .8%

STATION	DIRECTION (obs)	(model)	%err*	SPEED (obs)	(model)	ratio**
Travis AFB	320°	317°	-1% back	9.8	7.6	78.%
Moffett NAS	320°	309°	-3% back	5.2	6.3	123.%
Oakland Intl	310°	313°	1% veer	8.3	6.8	82.%
Hayward Airp.	290°	314°	7% veer	6.7	6.8	101.%
San Fran. Airp.	310°	305°	-1% back	11.3	7.3	64.%
San Jose Airp.	300°	311°	3% veer	5.2	5.6	110.%
San Jose State	320°	315°	-1% back	6.2	5.8	93.%
Mt Sutro Tower	300°	307°	2% veer	2.8	6.8	242.%

LEGEND:

* %err uses the smallest angle between model and obs, div. by 360°.
%err is the % difference between model-obs, and does not exceed 50%.

("backing & veering" means how the model has changed the observed winds).

** (Column represents model/observed wind ratio)

Table 4-2 Tabulated analysis for MABLES case, with RDBLT provision.

RESULTS FOR 78081000 {yymmddhh} : 8 km resol

Salinas Airp. lies BEYOND the DOMAIN(y))
not listed below; NOT included in the following stats

Sacramento lies BEYOND the DOMAIN(x))
not listed below; NOT included in the following stats

Sacramento lies BEYOND the DOMAIN(y))
not listed below; NOT included in the following stats

AVERAGE SPEED RATIO (model/obs) = 96.4%
AVERAGE DIRECTIONAL ERROR = -.8%

STATION	DIRECTION (obs)	DIRECTION (model)	%err*	SPEED (obs)	SPEED (model)	ratio**
Travis AFB	320°	305°	-4% back	9.8	5.4	56.%
Moffett NAS	320°	310°	-3% back	5.2	5.9	114.%
Oakland Intl	310°	307°	-1% back	8.3	5.5	67.%
Hayward Airp.	290°	308°	5% veer	6.7	6.2	92.%
San Fran. Airp.	310°	301°	-2% back	11.3	6.0	53.%
San Jose Airp.	300°	305°	1% veer	5.2	5.7	112.%
San Jose State	320°	305°	-4% back	6.2	5.7	92.%
Mt Sutro Tower	300°	305°	1% veer	2.8	5.2	186.%

LEGEND:

* %err uses the smallest angle between model and obs, div. by 360°.
%err is the % difference between model-obs, and does not exceed 50%.

("backing & veering" means how the model has changed the observed winds).

** (Column represents model/observed wind ratio)

Table 4-3 Tabulated analysis for nested grid run for Golden Gate area.

RESULTS FOR 78081000 (yymmddhh) : 8 km resol

Salinas Airp. lies BEYOND the DOMAIN(y))
not listed below; NOT included in the following stats

Sacramento lies BEYOND the DOMAIN(x))
not listed below; NOT included in the following stats

Sacramento lies BEYOND the DOMAIN(y))
not listed below; NOT included in the following stats

AVERAGE SPEED RATIO (model/obs) = 103.0%
AVERAGE DIRECTIONAL ERROR = -.6%

STATION	DIRECTION (obs)	DIRECTION (model)	%err*	SPEED (obs)	SPEED (model)	ratio**
Travis AFB	320°	323°	1% veer	9.8	6.8	69.%
Moffett AFB	320°	303°	-5% back	5.2	6.0	116.%
Oakland Intl	310°	307°	-1% back	8.3	7.4	89.%
Hayward Airp.	290°	301°	3% veer	6.7	7.3	108.%
San Fran. Intl	310°	301°	-2% back	11.3	7.8	69.%
San Jose Intl	300°	305°	1% veer	5.2	4.6	89.%
San Jose State	320°	306°	-4% back	6.2	4.7	76.%
Mt. Sutro	300°	305°	1% veer	2.8	5.7	206.%

LEGEND:

* %err uses the smallest angle between model and obs, div. by 360°.
%err is the % difference between model-obs, and does not exceed 50%.

("backing & veering" means how the model has changed the observed winds).

** (Column represents model/observed wind ratio)

Table 4-4 Tabulated analysis for nested grid run for Morgan Hill area.

RESULTS FOR 78081000 (yymmddhh) : 8 km resol

Salinas Airp. lies BEYOND the DOMAIN(y))
not listed below; NOT included in the following stats

Sacramento lies BEYOND the DOMAIN(x))
not listed below; NOT included in the following stats

Sacramento lies BEYOND the DOMAIN(y))
not listed below; NOT included in the following stats

AVERAGE SPEED RATIO (model/obs) = 100.4%
AVERAGE DIRECTIONAL ERROR = -.8%

STATION	DIRECTION (obs)	(model)	%err*	SPEED (obs)	(model)	ratio**
Travis AFB	320°	307°	-4% back	9.8	5.1	52.%
Moffett AFB	320°	305°	-4% back	5.2	6.1	118.%
Oakland Intl	310°	309°	0% back	8.3	6.4	77.%
Hayward Arpr.	290°	306°	4% veer	6.7	6.3	94.%
San Fran. Intl	310°	300°	-3% back	11.3	6.3	56.%
San Jose Intl	300°	307°	2% veer	5.2	6.2	120.%
San Jose State	320°	307°	-4% back	6.2	5.9	96.%
Mt. Sutro	300°	306°	2% veer	2.8	5.3	190.%

LEGEND:

* %err uses the smallest angle between model and obs, div. by 360°.
%err is the % difference between model-obs, and does not exceed 50%.

("backing & veering" means how the model has changed the observed winds).

** (Column represents model/observed wind ratio)

Table 4-5 Tabulated analysis for normal WOCSS run, without BALWND code.

RESULTS FOR 78081000 (yymmddhh) : 8 km resol

Salinas Airp. lies BEYOND the DOMAIN(y))
not listed below; NOT included in the following stats

AVERAGE SPEED RATIO (model/obs) = 110.3%
AVERAGE DIRECTIONAL ERROR = .6%

STATION	DIRECTION (obs)	DIRECTION (model)	%err*	SPEED (obs)	SPEED (model)	ratio**
Travis AFB	320°	318°	-1% back	9.8	7.7	78.%
Moffett NAS	320°	309°	-3% back	5.2	6.3	122.%
Oakland Intl	310°	313°	1% veer	8.3	6.7	82.%
Hayward Airp	290°	313°	6% veer	6.7	6.9	103.%
San Fran. Intl	310°	305°	-1% back	11.3	6.9	61.%
San Jose Intl	300°	309°	2% veer	5.2	5.7	111.%
San Jose State	320°	312°	-2% back	6.2	5.8	94.%
Sutro Tower	300°	310°	3% veer	2.8	6.4	231.%

LEGEND:

* %err uses the smallest angle between model and obs, div. by 360°.
%err is the % difference between model-obs, and does not exceed 50%.

("backing & veering" means how the model has changed the observed winds).

** (Column represents model/observed wind ratio)

Table 4-6 Tabulated analysis for WOCSS run, with BALWND code.

RESULTS FOR 78081000 {yymmddhh} : 8 km resol

Salinas Airp. lies BEYOND the DOMAIN(y))
not listed below; NOT included in the following stats

AVERAGE SPEED RATIO (model/obs) = 81.0%
AVERAGE DIRECTIONAL ERROR = .3%

STATION	DIRECTION (obs)	DIRECTION (model)	%err*	SPEED (obs)	SPEED (model)	ratio**
Travis AFB	320°	313°	-2% back	9.8	6.9	71.%
Moffett NAS	320°	307°	-4% back	5.2	4.3	83.%
Oakland Intl	310°	314°	1% veer	8.3	4.4	53.%
Hayward Airp	290°	312°	6% veer	6.7	4.9	73.%
San Fran. Intl	310°	305°	-1% back	11.3	5.4	48.%
San Jose Intl	300°	308°	2% veer	5.2	3.9	75.%
San Jose State	320°	310°	-3% back	6.2	3.7	60.%
Sutro Tower	300°	308°	2% veer	2.8	5.2	186.%

LEGEND:

* %err uses the smallest angle between model and obs, div. by 360°.
%err is the % difference between model-obs, and does not exceed 50%.

("backing & veering" means how the model has changed the observed winds).

** (Column represents model/observed wind ratio)